

THESIS ON CIVIL ENGINEERING F43

Optimising Fairways in the Gulf of Finland Using Patterns of Surface Currents

BERT VIKMÄE

TUT
PRESS

TALLINN UNIVERSITY OF TECHNOLOGY
Institute of Cybernetics
Laboratory of Wave Engineering

The dissertation was accepted for the defence of the degree of Doctor of Philosophy in Engineering on 21 January 2014

Supervisors: Prof. Dr. Tarmo Soomere
Institute of Cybernetics, Tallinn University of Technology, Estonia

Dr. Tomas Torsvik
Institute of Cybernetics, Tallinn University of Technology, Estonia

Opponents: Prof. Dr. Pentti Kujala
School of Engineering, Aalto University, Espoo, Finland

Dr. Bjørn Ådlandsvik
Institute of Marine Research and Bjerknes Centre for Climate
Research, Bergen, Norway

Defence of the thesis: 03 March 2014

Declaration:

Hereby I declare that this doctoral thesis, my original investigation and achievement, submitted for the doctoral degree at Tallinn University of Technology, has not been submitted for a doctoral or an equivalent academic degree.



European Union
Regional Development Fund



Investing in your future

/Bert Viikmäe/

Copyright: Bert Viikmäe, 2014
ISSN 1406-4766
ISBN 978-9949-23-586-5 (publication)
ISBN 978-9949-23-587-2 (PDF)

EHITUS F43

Laevateede optimeerimine Soome lahel pinnahoovuste mustrite põhjal

BERT VIKMÄE

Contents

List of publications constituting the thesis	6
List of figures	7
Introduction	10
Shipping activities and related environmental impact in the Baltic Sea	11
The challenge of current-driven transport.....	13
Semi-persistent patterns and eddies as building blocks of transport.....	15
Objective and outline of the thesis	17
Approbation of the results.....	20
1. In search for favourable patterns of currents	23
1.1. Circulation in the Gulf of Finland	24
1.2. Numerical modelling of circulation.....	29
1.3. Circulation models RCO and OAAS.....	32
1.4. Lagrangian particle tracking.....	36
2. Analysis of the structure of surface currents.....	39
2.1. Favourable patterns reducing environmental risks	40
2.2. Patterns in strain and vorticity fields	42
2.3. Methods for automatic detection of eddy structures	45
2.4. Coherent structures in the Gulf of Finland	46
3. Modelling the equiprobability line	49
3.1. Model parameters	49
3.2. Quantifying the nearshore and time scale for coastal hit.....	52
3.3. Time scales for transport patterns.....	55
3.4. Counting hits to the opposite coasts	56
3.5. Sensitivity studies.....	59
4. Preventive methods for coastal protection.....	61
4.1. Probability and particle age	61
4.2. Optimum fairways and safe corridors	63
4.3. Frequently hit coastal sections.....	67
4.4. Frequent sources of nearshore pollution.....	71
4.5. Impact of horizontal eddy diffusivity on Lagrangian statistics	73
Conclusions	77
Summary of the results	77
Main conclusions proposed to defend.....	79
Recommendations for further work	80
Bibliography.....	82
Acknowledgements.....	96
Abstract	97
Resümee.....	98
Appendix A: Curriculum Vitae.....	99
Appendix B: Elulookirjeldus.....	104

List of publications constituting the thesis

The thesis is based on seven academic publications which are referred to in the text as Paper A, Paper B, Paper C, Paper D, Paper E, Paper F and Paper G. Papers A, D, E, F and G are indexed by the ISI Web of Science:

- Paper A Soomere T., **Viikmäe B.**, Delpeche N. and Myrberg K. 2010. Towards identification of areas of reduced risk in the Gulf of Finland. *Proceedings of the Estonian Academy of Sciences*, 59(2), 156–165.
- Paper B **Viikmäe B.**, Soomere T., Viidebaum M. and Berezovski M. 2010. Temporal scales for transport patterns in the Gulf of Finland. *Estonian Journal of Engineering*, 16(3), 211–227.
- Paper C **Viikmäe B.**, Torsvik T. and Soomere T. 2012. Analysis of the structure of currents in the Gulf of Finland using the Okubo–Weiss parameter. In: *IEEE/OES Baltic 2012 International Symposium*, May 8–11, 2012, Klaipeda, Lithuania, Proceedings. IEEE, 7 pp.
- Paper D **Viikmäe B.** and Torsvik T. 2013. Quantification and characterization of mesoscale eddies with different automatic identification algorithms. *Journal of Coastal Research*, Special Issue 65, 2077–2082.
- Paper E Soomere T., Berezovski M., Quak E. and **Viikmäe B.** 2011. Modelling environmentally friendly fairways using Lagrangian trajectories: a case study for the Gulf of Finland, the Baltic Sea. *Ocean Dynamics*, 61(10), 1669–1680.
- Paper F **Viikmäe B.** and Soomere T. 2014. Spatial pattern of current-driven hits to the nearshore from a major marine highway in the Gulf of Finland. *Journal of Marine Systems*, 129, 106–117.
- Paper G **Viikmäe B.**, Torsvik T. and Soomere T. 2013. Impact of horizontal eddy-diffusivity on Lagrangian statistics for coastal pollution from a major marine fairway. *Ocean Dynamics*, 63(5), 589–597.

Author's contribution

The author set up and configured the Lagrangian particle tracking model TRACMASS in the Institute of Cybernetics. Moreover, the author was responsible for making changes to the diffusion scheme parameterisation in that model. His contribution to writing papers A, B, C, D, E, F and G is as follows:

Paper	Contribution of the author
A	Data extraction, processing, implementing the necessary algorithms, visualisation of results and writing several parts.
B	Data extraction, processing, implementing the necessary algorithms, visualisation, writing the first draft of the paper and contribution to polishing the final version.

C, D, F	Data extraction, processing, implementing the necessary algorithms, visualisation and writing the first draft of the paper.
E	Data extraction, processing, implementing the necessary algorithms, visualisation and a small part of writing.
G	Data extraction, processing, implementing the necessary algorithms, visualisation and writing the first draft of the paper; modification of the diffusion scheme in the Lagrangian particle tracking model TRACMASS.

List of figures

Figure 1.	Shipping activities in the Gulf of Finland.	11
Figure 2.	Main fairways in the Baltic Sea. Map by M. Viška.....	23
Figure 3.	Average meridional transport (cm/s) for March to April in 1987 (left) and for September to October in 1988 (right) by Soomere et al. (2011).....	42
Figure 4.	The Okubo–Weiss parameter averaged over the entire computational domain for each 3-h period. Results are presented for the year 1987. Red circles indicate time instants corresponding to panels shown in Figure 5.	43
Figure 5.	Spatial distribution of the Okubo–Weiss parameter in the Gulf of Finland during the windy (top and bottom pairs of panels) and calm (middle pair of panels) seasons. The panels on the left correspond to time instants with large peaks in average W (Figure 4), while the panels on the right correspond to time instants with relatively low average W . Red colour indicates strain-dominated and blue colour vorticity-dominated areas.	44
Figure 6.	The winding angle (WA) method for a segmented streamline....	46
Figure 7.	Detection of flow structures in the Gulf of Finland for 1 nautical mile surface velocity data on 17 December 1987 at 18:00. Panels show results for (a) the Okubo–Weiss and (b) the hybrid winding angle method.....	48
Figure 8.	Splitting the simulation period into time windows.....	51
Figure 9.	Starting points of trajectories (grey circles located approximately along the centreline of the Gulf of Finland) in simulations of coastal hits. Dark grid points indicate the nearshore area of alert zone 3. The entrance line to the gulf (bold line) is set along 59° N and $21^\circ 48'$ E.	53
Figure 10.	Monthly mean percentage of coastal hits (filled parts of bars) and the parcels leaving the gulf (white parts of bars) in 1987 for $t_w = 15$ days. The left, middle and right bars show the results for alert zones 1, 2 and 3, respectively.	53

Figure 11. Percentage of hits to the nearshore for $t_w = 15$ days for different starting instants of trajectory calculations in 1987. The dashed line shows the total percentage of parcels that have either hit the coast or drifted out of the gulf.....54

Figure 12. Monthly mean percentage of parcels hitting the coast (black) and leaving the gulf (white) for different lengths of the time window for alert zone 3 in 1987. For each month, columns from left to right show the percentage for $t_w = 3, 5, 7, 10, 13$ and 15 days.....55

Figure 13. Probabilities of parcels to hit the nearshore of the northern or the southern coast for the years 1987–1991 calculated with the use of Method I (left panel) and Method II (right panel). The red colour indicates high probability of transport to the southern coast and the blue colour – to the northern coast. The green colour marks the location of the equiprobability line (black line) and the areas from which transport to either of the coasts is unlikely (Paper E).58

Figure 14. Probabilities of parcels hitting the coast (% , left panel) and particle age (days, right panel) for the years 1987–1991 calculated with the time window of 20 days (Paper E). Although a few islands with a size up to 10 km are located in the eastern Gulf of Finland, their nearshore is ignored in the calculations and only hits to the mainland coasts are accounted for.62

Figure 15. Examples of cross-sections of probabilities for coastal hits (green), particle age (Method IVa, red; Method IVb, magenta) and for the quantity characterising the probability of a hit to the opposite coasts (Method I, black; Method II, cyan; both shown as $(\hat{p}+1)/2$, where $\hat{p} \approx 1$ and $\hat{p} \approx -1$ mean a high probability of a hit to the southern and the northern coasts, respectively): for the gulf entrance (a), western narrow part (b), middle of the gulf (c) and for the wider eastern part of the gulf (d). Circles indicate the location of the optimum fairway. The location of the cross-section is shown in Figure 16.63

Figure 16. The location of the optimum fairways based on Methods I–IV calculated for the years 1987–1991 with the time window of 20 days. The centreline (the axis of the gulf, zero line in the lower panel) is determined based on sea points of the 2 nautical mile grid of the RCO model and thus does not necessarily exactly follow the geographical centreline of the gulf.....65

Figure 17. Initial location of selected parcels and the border of the nearshore in the Gulf of Finland. The double arrow indicates the separation point of the ‘southern’ and ‘northern’ parts of the nearshore in Figure 21.....68

Figure 18. Annual average map of the most frequent hits to the nearshore in 1989 and 1992, and the 5-year average map of nearshore hits. Grey sections – areas with no hits, blue – sections that received <7 hits/yr (20% of the maximum, about twice as large as the average), green – 7–17.5 hits/yr (20–50% of the maximum), red – areas where the hit count is >17.5 ($>50\%$ of the maximum).....69

Figure 19. Upper left panel: most frequently hit nearshore areas (red; >60% of the annual maximum number of hits at least in three model years out of 1987–1991 or 1992–1996); other panels: interconnections between the above most frequently hit areas and the origin of the parcels. The link between the nearshore areas and the origin is shown by the same colour.72

Figure 20. Four patches of selected parcels (a) and the maximum parcel separation for each four-parcel cluster seeded within a grid cell for the three different methods: (b) no eddy-diffusivity (pure advection); (c) eddy-diffusivity with a constant diffusion coefficient; (d) eddy-diffusivity with a time- and space-variable diffusion coefficient. The grid cell colour corresponds to a distance (km) as shown by the colour bar.74

Figure 21. The most frequently hit nearshore areas averaged for the period 1982–2001 for the northern (upper panel) and southern (lower panel) coast of the Gulf of Finland (see Figure 17). The *x*-axis is the distance along the coast (in nautical miles), from the west of the gulf, near Hanko in the north and Hiiumaa in the south, to the eastern end of the gulf.76

Introduction

The traditional approach to marine and coastal management has to a large extent relied on a sectoral concept, dividing the coastal and sea areas into zones designated for specific use. This approach has led to fragmentation of jurisdiction and decision-making. For example, fisheries' managers focus on the exploitation of fish stock, shipping authorities address safety of navigation, watershed managers focus on freshwater discharge and coastal planners consider mostly land-side impacts. In a congested marine environment these interests are often conflicting, which has highlighted the need for new approaches in marine and coastal management (Agardy et al., 2011). A fundamental problem with the sectoral management approach is that water, and any substance immersed in water, is constantly being exchanged between sea areas. While atmospheric modelling systems have reached a stage where short-term weather forecasts are reasonably reliable, the same cannot be said for the present state of ocean modelling systems with respect to predictions of current velocities.

This thesis is focused on certain options towards better protection of coastal and nearshore areas. Such areas are among the most productive ecosystems on the planet, a vital source of food for many communities, while being under increasing anthropogenic pressure due to commercial, transport and recreational activities. The importance and challenges of maintaining a healthy coastal environment is recognised globally, and has been addressed by major international organisations such as United Nations through the United Nations Environment Program, European Union through the Water Framework Directive and the Marine Strategy Framework Directive, as well as regional organisations such as the Baltic Environment Protection Commission (HELCOM). Such organisations promote management strategies based on monitoring programmes, maritime spatial planning, and establishment of marine protected areas to preserve important and sensitive habitats. A stated goal of the Water Framework Directive is to achieve a good ecological and chemical status for all surface water areas within the European Union region. Likewise, the HELCOM Baltic Sea Action Plan is a programme to restore a good ecological status of the Baltic marine environment by 2021.

The coastal impact of harmful substances originating from offshore sources is one of the topics where the mismatch between marine and coastal management becomes an issue. This topic includes, but is not limited to, pollution from shipping accidents and spillage of oil or other harmful substances under certain circumstances. There is a general interest in minimising the number and severity of shipping accidents, but conflicts of interests may arise as to what kind of risk should be minimised. Shipping authorities are primarily concerned with safety of navigation, where minimising risk of ships' grounding or collision as well as possibilities for rescue operations are the main factors to consider. Institutions responsible for a good ecological status emphasise the risk related to the environmental impact of various harmful substances, especially pollution in economically valuable or ecologically vulnerable coastal areas.

Shipping activities and related environmental impact in the Baltic Sea

A large part of accidents associated with the release of harmful substances (oil or chemical pollution) or undesired items (for example, lost containers) into the marine environment occur along shipping routes (Burgherr, 2007). Although relatively small, the Baltic Sea is the host to heavy ship traffic, with up to 15% of the world's international maritime cargo (HELCOM, 2009). The number and size of ships have grown in recent years. The largest environmental threat to this vulnerable brackish, high-latitude environment is oil transportation. Its volume has increased by more than a factor of two in 2000–2008 and a further 40% increase is expected by the year 2015 (HELCOM, 2009; Brunila and Storgard, 2013). One of the major marine highways in the European waters enters the Baltic Sea through the Danish straits, crosses the Baltic Proper¹ and stretches through the Gulf of Finland (Figure 1) to Saint Petersburg, a major population and industrial centre in this area, and to a number of new harbours in its vicinity. Sustainable management of this traffic flow is a great challenge in the Baltic Sea, which is designated as a Particularly Sensitive Sea Area by the International Maritime Organisation (IMO, 2007; Kachel, 2008).

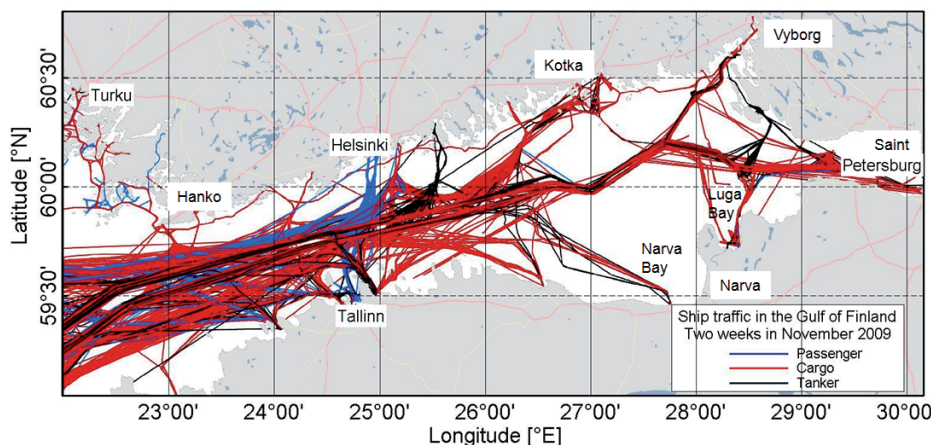


Figure 1. Shipping activities in the Gulf of Finland.

A commonly used approach to manage adverse impacts in the marine environment (including potential maritime pollution) is to develop quick remedial action plans in the event of an accident (e.g., Keramitsoglou et al., 2003; Kostianoy et al., 2008). This approach includes (but is not limited to) the development of

¹ This notion is used here to denote the Eastern, Northern and Western Gotland Basin, Bornholm Basin and Gdańsk Bay (Leppäranta and Myrberg, 2009).

operational oil spill drift and fate models, increasing the capacity of oil-combating services and raising awareness of the potential involvement of people in coastal countries (HELCOM, 2009).

The problem of detection, modelling and forecast of the fate of oil spills in the Baltic Sea has been addressed in numerous publications since the mid-1990s (Ambjörn, 2000; Tufte et al., 2004; Kostianoy et al., 2005; Lavrova et al., 2006; Uiboupin et al., 2008), including the related economic issues (Gottinger, 2001; Aps et al., 2009; Elofsson, 2010), statistical models of collision and grounding probability (Gucma, 2008), optimum allocation of the available monitoring resources (Deissenberg et al., 2001) and propagation of pollution under the ice cover (Alhimenko et al., 1997; Wang et al., 2007). The official HELCOM oil spill forecast system *Seatrack Web*, launched at the turn of the millennium (Ambjörn, 2000; Gästgifvars et al., 2002) and regularly updated (Ambjörn, 2007), has become an important part of operational oceanography in the region (Kostianoy et al., 2005, 2008; Lavrova et al., 2006; Ambjörn, 2008; Uiboupin et al., 2008).

In addition to oil pollution, a variety of different, possibly dangerous, adverse impacts (substances, objects, etc.) can potentially be released from ships. They may be carried to a substantial distance along trajectories governed by the complex interaction of different metocean drivers (currents, turbulence, wind and waves etc.) and/or modified by a number of physical and chemical processes (e.g., weathering of the oil pollution, dispersion of chemicals, change in the radioactivity level for nuclear waste). Even the very best models for the propagation and fate of adverse impacts of different kinds still suffer certain limitations that result in imperfect predictions (e.g., Ambjörn, 2007). Such models are also demanding in terms of computational power and long simulation times.

Another, rapidly developing approach is the preventive maritime planning and decision-making strategy. The primary focus of such efforts is to account for the effect that an accident would incur before it actually happens. The relevant efforts range from the optimisation of the location of tugboats along a major tanker fairway to aid ships that suffer loss of steering or propulsion (Eide et al., 2007) and optimisation of shipping routes (Schwehr and McGillivray, 2007; Soomere and Quak, 2013) over a proper designation of marine protected areas and Particularly Sensitive Sea Areas and development of possible policies and regulations (Lefebvre-Chalain, 2007; Ko and Chang, 2010) to the theoretical research of the relevant issues (Hassler, 2011; Rusli, 2012). A large part of the work in this thesis contributes to one of the foci of this approach, namely, to the development of preventive methods for coastal protection.

The developments in physical and biological oceanography in the last decades have demonstrated the richness of the internal structure of various sea properties. The perception that different sea areas may have different value and/or vulnerability has led to the designation of many marine protected areas. The marine protected areas of the Baltic Sea are mostly located in the nearshore, with the only exceptions to the south and north of the island of Gotland and in the northern part of Pomeranian Bay. It is a common practice to treat the coastal zone and the open

sea areas differently. This practice reflects the major differences in their ecosystems (e.g., the coastal areas are generally the main life reproduction areas and thus play a great role in restoring the fish stock) and also a policy dimension of their management. The coastal zone is, as a rule, the responsibility of a specific state, whereas open sea areas customarily are managed as a shared resource between many states. Whereas pollution in the open sea can have strong short-term impact on marine life, pollution in the nearshore has potential to destroy habitats vital for the reproduction of marine life, with possibly severe long-term consequences. Combating oil pollution is generally much more effective and less expensive in the open sea than in shallow coastal areas. Damage due to pollution in a major spawning area, a nesting or wintering region of birds, a beach of a national park or a large tourist industry at the coast is highly undesirable from both an environmental and economic point of view.

Hence the nearshore areas are considered as ‘high-value’ regions in this thesis. A simple measure to reduce the risk of danger to the coast from the release of adverse impacts associated with shipping activities is to shift the fairways further away from the coast. In large water bodies such as the Atlantic Ocean in principle the fairways could be moved so far offshore that any adverse impact released from ships would have minor chances to reach the coast. This solution does not suit for smaller seas such as the Black Sea, the Baltic Sea or the Mediterranean Sea.

The challenge of current-driven transport

With the ever growing size of ships and the volume of cargo, potential pollution released through an accident, careless operation or human error is no more concentrated in a small area around the ship (Soomere, 2013). Instead, in case of larger releases of adverse impacts, various substances are often carried a large distance from the point of origin, first of all by currents in the surface layer, but also by wind and waves.

The impact of wind and surface waves on the propagation of water parcels and various substances in the surface layer of the sea has been relatively well understood (Ardhuin et al., 2009; Breivik et al., 2011). The present-day forecasts of wind and wave conditions in open sea areas are usually acceptable (Ardhuin et al., 2009) and relevant parameterisations have been implemented into operational models decades ago. The probability of purely wind- or wave-driven Lagrangian parcels to hit a certain area is, to a first approximation, a function of the wind or wave direction. The time until the hit occurs is roughly proportional to the combined downwind/downwave distance of the release location from this area. Hence, the location and time of a shipping accident determine not only which remote areas are exposed to adverse impacts (and thus the cost of the consequences of a ship accident) but also the time available to handle such hazards. The solution to the problem of the management of ship traffic is straightforward: the optimal location for the sailing line is just as far in the combined upwind/upwave direction from the susceptible spots as possible.

The situation with the forecast of currents and especially current-driven transport of various objects is less satisfactory (Vandenbulcke et al., 2009). The typical spatial scales of sea currents are considerably smaller than the usual dimensions of air flow patterns (Cushman-Roisin and Beckers, 2011) and thus more complicated to replicate. The system of currents exhibits large spatial and temporal variations even for practically stationary and spatially homogeneous wind fields. Although global circulation models are now able to provide improved forecasts compared to climatological (daily average) current fields (Blockley et al., 2012) and successful attempts have been made to replicate the three-dimensional (3D) propagation of oil spills (Chang et al., 2011), it is extremely hard to track the pathways of even single drifters (Vandenbulcke et al., 2009; Fingas, 2011). A deterministic method capable of adequately reproducing the floating object drift is still lacking (Vandenbulcke et al., 2009) and even small errors in its estimates can drastically change the calculated trajectories of parcels (Griffa et al., 2004).

The situation is even more difficult in shallow basins with complicated geometry such as the Baltic Sea (Verjovkina et al., 2010; Kjelsson and Döös, 2012) where the currents are frequently even in antiphase with wave- and wind-induced transport features (Andrejev et al., 2004b; Gästgifvars et al., 2006). Even with state-of-the-art circulation models and high-quality forcing data it is challenging to provide drift prediction in a dependable way, especially in areas with complex topography and a high degree of small-scale variability.

Hence, on the one hand, the probability of a vulnerable area being hit by an adverse impact (for example, by an oil spill) carried by currents may vary largely for areas located at an equal distance from the source. As mentioned above, the forecast of current-induced transport is usually much less reliable than the description of wind- and wave-induced transport. This means, on the other hand, that a better understanding and description of current-driven transport has the largest unused potential for the quantification of pollution propagation in the marine environment (Soomere and Quak, 2013).

In order to gain a solid understanding of the properties of current-driven transport and propagation of various adverse impacts in the surface layer, it is reasonable to consider the problem under slightly idealised conditions, by ignoring the direct impact of wind and waves on substances in the uppermost layer of the sea (Soomere and Quak, 2013). Following this idea, in this thesis the focus is on the impact the surface currents may have on the pathways of various objects and substances in the surface layer. Progress in this area is an important contribution to smart use of currents, more generally, to the challenge of the practical use of intrinsic features of marine dynamics for environmental management, for example, preventive reduction of the costs of accidents on sea.

An adverse impact from harmful human activity may happen at any depth. For example, large quantities of oil may be released into near-bottom waters after failures of offshore oil platforms (Burgherr, 2007) and an accident with a nuclear submarine may pollute any layer in the sea. The material presented above suggests that systematic analysis of the transport of adverse impacts by a 3D current field is

far too complicated today even for relatively small sea domains. For this reason, the work presented in this thesis is limited to the analysis of substances released to the surface layer and further transported by surface currents.

This framework has an obvious potential for the quantification of the role of surface currents in the dynamics of any objects or substances in the surface layer, for example, for search-and-rescue purposes (e.g., Melsom et al., 2012). However, strictly speaking, it is only directly applicable to persistent substances that are dissolved in strongly stratified environments under calm conditions when the contaminants (e.g., dissolved radioactive substances) largely remain in the uppermost layer and are mostly carried by surface currents (e.g., Periañez, 2004). It is only conditionally valid for the drift of floating objects that extend over sea surface or are exposed to wave action.

It is still a suitable approximation for a large portion of releases of adverse substances to the marine environment of the strongly stratified Baltic Sea. For example, during a large part of the spring and early summer when the wind speed is below 5 m/s (Mietus, 1998), favourable conditions for this approximation exist in the entire Baltic Sea: surface waves are very low and a very thin and stable uppermost mixed layer overlies a sharp pycnocline (Leppäranta and Myrberg, 2009). In such occasions current-driven transport apparently is responsible for a large fraction of the fate of the lighter components of oil that are usually thought to pose great danger to valuable areas. The field of currents also largely governs the transport of objects and substances in the surface layer during the ice season when the wave motion is absent and wind impact only becomes evident through the ice drift. This framework is still only conditionally valid for oil pollution because other metocean drivers, chemical processes and buoyancy effects are not accounted for (Murawski and Woge Nielsen, 2013). It may, however, be useful in many occasions to obtain a first approximation of the drift of oil pollution (Lončar et al., 2012; Meier and Höglund, 2012).

Semi-persistent patterns and eddies as building blocks of transport

Once some marine or coastal areas are agreed to be more valuable than others, the cost of the consequences of any marine accident that leads to the release of some potentially harmful substances or items into the marine environment (that are further transported by various met-ocean drivers) will depend on when and where the accident happens. Even if some of the costs are distant, remote or delayed, tagging some areas with a price label naturally yields an associated distribution of costs of otherwise similar accidents but occurring at different locations or at different time instants. Several ways of quantification of this distribution (equivalently, the damaging potential of accidents involving release of long-living harmful substances into the marine environment) and of its practical use were recently addressed in the BalticWay project. A large part of the research presented in this thesis was conducted within this project that was funded by the joint Baltic Sea research and development programme BONUS in 2009–2011.

The distribution of costs is often largely governed by the current-driven propagation of released substances from the accident site to vulnerable areas. It is assumed in this thesis that the transport of released substances by surface currents fully defines this distribution. As discussed in the previous section, this assumption is applicable in many occasions in the Baltic Sea.

A key requirement for the practical use of the distribution in question, for example, for reduction of risks associated with ship traffic, is the existence of certain favourable patterns. For example, the presence of such a pattern in the density of the likelihood to meet a whale was used to shift the fairway to Boston Harbour into an area infrequently visited by whales (Stokstad, 2009). Any favourable pattern may be used for some purpose. For example, sailing along jet currents reduces fuel consumption (Calvert et al., 1991), the use of areas with lower waves decreases the risk of wave damage and persistent currents can be used for transporting potential pollution to less vulnerable sea areas (Soomere and Quak, 2007)

It is natural to expect that the most distinct features in the distribution of current-driven costs of accidents are created by the presence of various persistent or semi-persistent patterns of surface currents. The problems of identification and analysis of such patterns are the central objects of the studies presented below. As there exist hardly any persistent jet-like currents in the Baltic Sea or in the Gulf of Finland (Andrejev et al., 2004a, 2004b; Leppäranta and Myrberg, 2009), the focus is on semi-persistent patterns extending from mesoscale features up to basin-scale transport pathways. If such features of currents or current-induced transport exist, it is very likely that, for example, the probability of coastal hits will also have a distinct pattern.

The problem of highlighting such (normally hidden) patterns in the mesoscale and basin-scale current-induced transport has been addressed in Soomere et al. (2011) and Andrejev et al. (2010). The transport properties have been analysed by statistical methods applied to realisations of Lagrangian trajectories of test parcels driven by simulated velocity data. Such an analysis allows the identification of several flow features that cannot easily be extracted from the Eulerian velocity fields. This technique is widely used below for the quantification of the distribution of environmental costs of releases of such dangerous substances that are further carried by surface currents.

As motions in the sea are extremely complicated, it is usually not clear whether the field of currents contains isolated, long-living eddies (that are able to transport water masses to large distances) or whether the instantaneous velocity patterns just resemble eddy-like structures. The presence of eddies over longer time in a specific location evidently has a strong impact also on the long-term statistical properties (including the usually hidden features) of the long-term transport.

It is fairly easy to visually distinguish eddy-like roughly circular features from two-dimensional (2D) satellite images, but it is difficult to single out a particular long-living eddy and/or to track its motion even from a sequence of remotely sensed or numerically simulated velocity fields. The problem of automatic

detection of eddies, their characteristic dimensions and evolution has been studied during more than 40 years (Isern-Fontanet et al., 2003). This research area has greatly benefited from several technological advances such as surface or subsurface drifters or satellite and remote sensing imagery. Similarly to the transport of pollution, the Lagrangian framework and methods constitute an important tool in the field of eddy detection (Davis, 1991). Eddy detection by Lagrangian methods requires that the eddies must be stable. If this is the case, drifters (either a real passive parcel or device, or a simulated parcel) move along a roughly circular track. The detection is more difficult if the eddy meanders, the swirling motion is slow, or the eddy does not live long enough to exert a full rotation. In such cases a larger number of drifters is required to obtain a reasonable portrayal of the eddy. In this thesis, both Eulerian and Lagrangian methods are employed to detect short-term dominant features in the flow field and transport created by semi-persistent patterns.

A generic property affecting the presence of semi-persistent patterns of transport is that realistic motions in the ocean are turbulent. This is commonly reflected in surface currents that are normally characterised by a complex field of eddies or vortices interspersed by meanders, fronts, filaments and other features, and only in exceptional cases are rectilinear or laminar. A part of this thesis addresses certain options for the quantification of such complicated flow patterns. The goal is to determine to what extent the patterns of Lagrangian surface transport (identified using Lagrangian trajectories) are reflected in the spatial structure of widely used and easily computable parameters of the flow such as strain or relative vorticity. These features are analysed using Eulerian velocity fields.

Objective and outline of the thesis

As shipping, and especially oil transport in the Baltic Sea, is a serious threat to vulnerable coastal regions, there is a clear incentive to explore novel methods to reduce environmental risks. The economically best way is to use, if possible, certain intrinsic properties of sea dynamics to mitigate these risks. The material presented above suggests that smart use of surface currents may have great potential for such mitigation. In this thesis I attempt to apply this line of thinking to development of certain components of a preventive method for environmental management of shipping in the northern Baltic Sea. Methods of this type focus on adjusting the potential accident site (equivalently, the sailing line) beforehand, not waiting until an accident happens (Eide et al., 2007; Soomere and Quak, 2013). If an accident does not happen, nothing is lost except maybe a certain amount of time due to the lengthening of the sailing line, but in case of an accident, the related environmental costs are minimised. The main idea is to make use of the properties of Lagrangian transport induced by surface currents to either minimise the probability of the transport of pollution to vulnerable areas or to prolong the drift time in open sea before the harmful substances reach such areas.

The particular objectives are as follows:

- to demonstrate the presence of various potentially favourable flow patterns in the Gulf of Finland and to develop express methods for their detection;
- to develop a method for the specification of a sailing line, the use of which would correspond to sensible sharing of environmental risks;
- to generalise this method towards the design of sailing lines that would preventively minimise the probability of coastal pollution.

This problem generally involves the specification of the ‘price’ for different sea or coastal areas. Similarly to Soomere and Quak (2013), it is assumed that the nearshore is the most vulnerable and valuable area.

Chapter 1 gives a short overview of the existing knowledge of these features of the hydrography and dynamics of the Baltic Sea and the Gulf of Finland that are essential for the research in this thesis (Section 1.1) and provides a short insight into the efforts of numerical replication of these features (Section 1.2).

In an ideal case, information about flow dynamics may be gathered by direct measurements. The available *in situ* or remote sensing data sets do not provide adequate coverage in space and time, and this is likely to remain the case for the foreseeable future. A realistic way to create the necessary data is to simulate the fluid motion with a General Circulation Model (GCM, for simplicity called ocean model in this thesis), velocity data from which provide a basis for the calculation of the transport (over time) of substances immersed in the fluid. Section 1.3 describes the main features of these ocean models, the output of which has been used in this thesis.

A major technical problem is how to extract rational information from the vast amount of numerically simulated data and how to build a reasonable implementation for the shipping industry with its specific needs and restrictions. A feasible way is to use Lagrangian trajectories of very small but persistent parcels that are passively advected by surface currents. These parcels can be associated, for example, with certain fractions of oil pollution (Murawski and Woge Nielsen, 2013). Section 1.4 shortly describes the method and code for the construction of such trajectories from the simulated velocity fields.

The entire concept only has a practical value if the field of currents contains some (usually hidden) features or patterns. The relevant questions are discussed in Chapter 2. Although the currents in the key study area, the Gulf of Finland, are extremely complex, they often contain certain favourable patterns, which can be used for the reduction of environmental risks (Soomere and Quak, 2007) and are essential for the design of optimum ship routes (Murawski and Woge Nielsen, 2013). Several examples of such patterns, for example, highly persistent almost basin-scale motions in certain layers (Andrejev et al., 2004b) and semi-persistent systems of surface currents and rapid pathways of Lagrangian transport (Soomere et al., 2011) are presented in Section 2.1. This description is followed by examples of applications of automatic detection of their smaller siblings from simulated or observed velocity fields. For this purpose the areas with pronounced strain or vorticity (Section 2.2, Paper C) are compared with the outcome of a hybrid method,

based on some physical and geometrical properties of relatively small-scale persistent eddies (Section 2.3, Paper D).

To identify the ‘best’ location of the possible release of pollution, its propagation has to be tracked backwards in time. No straightforward solution exists to such inverse problems; moreover, no universal method exists for their treatment. A feasible way forward, towards an approximate solution to this ‘inverse’ problem, is to extract information from statistical properties of large ensembles of particular solutions to the direct problem of current-driven propagation of single passive persistent pollution parcels released to the sea at different time instants and locations (Soomere and Quak, 2013). Lagrangian trajectories of pollution parcels, constructed using modelled velocity fields, provide the required solutions for the direct problem. In essence, this approach is a variation of the ‘trial and error’ method, to some extent resembling the Monte Carlo approach, in which 2D trajectories of selected parcels are considered as individual samples or trails, and has been applied in many applications, e.g., for studies of transport of larvae and migration of fish (e.g., Ådlandsvik et al., 2007). The least dangerous offshore areas for a particular example of oil spill released at different locations can be estimated based on a large enough number of trials. The potential of the use of this method for ‘ideal’ persistent pollution parcels will be demonstrated in the context of the optimisation of ship routes in the Gulf of Finland in terms of minimising the risk of coastal pollution.

Research presented in Chapter 3 (Papers A, B and E) contributed to the development of a novel method for preventive coastal protection (Soomere and Quak, 2013). This method contains four components: (i) a high-resolution circulation model, (ii) a scheme for tracking Lagrangian trajectories of pollution parcels, (iii) a technique for the calculation of quantities characterising the potential of different sea areas to serve as a starting point of propagation of such adverse impacts that may affect the coast and (iv) decision-making routines. The underlying calculations involved evaluation of the transport of substances by means of tracing individual passive parcels by surface currents over time spans of several weeks. Such simulations were repeated for subsequent time intervals spanning over several years with the same set of pollution parcels but with slightly shifted release instants, and thus involved several crucial parameters. Section 3.1 describes the overall scheme of such calculations, Section 3.2 analyses the problem of adequate representation of the nearshore area in such models and Section 3.3 provides an insight into the sensible time scales to be used in the calculations. This also involves research towards justification of this method (Paper B). Section 3.4 introduces the concept of the equiprobability line, the use of which as a possible sailing line provides an option for sharing the risk of coastal pollution between the opposite coasts (Paper A). Section 3.5 presents a short overview of sensitivity studies of the applied method, performed in parallel with the work in this thesis.

Chapter 4 demonstrates some possibilities of the application of the above-described preventive method for coastal protection. Following Andrejev et al. (2011), the probability for a coastal hit and the time it takes for parcels to reach

the coast (called particle age in this thesis) are taken as the decisive parameters (Section 4.1, Paper E) to calculate the optimum fairways and ‘safe corridors’ (Section 4.2). Using the same technology, connections between the most frequently affected nearshore areas and the most probable starting points of pollution along the major fairway in the Gulf of Finland are analysed in Sections 4.3 and 4.4. Finally, the reliability of the results with respect to the way of treating the dispersion of pollution (which is one of the processes that were parameterised in the ocean model) is evaluated in Section 4.5 (Paper G) based on the Lagrangian particle modelling with several options of spatially variable dispersion coefficients.

Approbation of the results

The basic results described in this thesis have been presented by the author at the following international conferences:

Viikmäe B. and Torsvik T. 2013. Analysis and comparison of automatic eddy detection methods. Poster presentation at the *9th Baltic Sea Science Congress* (26–30 August 2013, Klaipeda, Lithuania).

Torsvik T., Soomere T., Kalda J. and **Viikmäe B.** 2013. Improving the forecast of coastal pollution using surface drifter trajectories. Poster presentation at the *9th Baltic Sea Science Congress* (26–30 August 2013, Klaipeda, Lithuania).

Viikmäe B., Torsvik T. and Soomere T. 2013. In search for hidden transport patterns governing the coastal pollution. Oral presentation at the *International Coastal Symposium 2013* (8–12 April 2013, Plymouth, UK).

Viikmäe B., Torsvik T. and Soomere T. 2012. Analysis of the structure of currents in the Gulf of Finland using the Okubo–Weiss parameter. Poster presentation at the *6th European Postgraduate Fluid Dynamics Conference* (10–12 July 2012, London, UK).

Viikmäe B. and Soomere T. 2012. Spatial pattern of hits to the nearshore from a major marine highway in the Gulf of Finland. Oral presentation at the *Joint Numerical Modelling Group 16th Biennial Conference* (21–23 May 2012, Brest, France).

Viikmäe B., Torsvik T. and Soomere T. 2012. Analysis of the structure of currents in the Gulf of Finland using the Okubo–Weiss parameter. Oral presentation at the *IEEE/OES Baltic International Symposium* (08–11 May 2012, Klaipeda, Lithuania).

Viikmäe B. and Soomere T. 2012. Patterns of hits to the nearshore from a major fairway in the Gulf of Finland. Poster presentation at the *European Geosciences Union General Assembly* (22–27 April 2012, Vienna, Austria).

Viikmäe B., Soomere T. and Delpeche-Ellmann N. 2011. Optimizing fairways to reduce environmental risks in the Baltic Sea. Oral presentation at the *8th Baltic Sea Science Congress* (22–26 August 2011, St. Petersburg, Russian Federation).

Viikmäe B., Soomere T. and Delpeche-Ellmann N. 2011. Optimizing fairways for environmental management in the Baltic Sea. Oral presentation at the *3rd International Workshop on Modeling the Ocean* (06–09 June 2011, Qingdao, China).

Viikmäe B., Soomere T. and Delpeche N. 2011. Technology for finding optimum fairways for environmental management in the Baltic Sea. Oral presentation at the *International Conference "Particles in Turbulence 2011" on Fundamentals, Experiments, Numeric and Applications* (16–18 March 2011, Potsdam, Germany).

Viikmäe B., Soomere T. and Delpeche N. 2010. Using Lagrangian trajectories to find areas of reduced risk of coastal pollution in the Gulf of Finland. Oral presentation at the *5th International Student Conference on "Biodiversity and Functioning of Aquatic Ecosystems in the Baltic Sea Region"* (06–08 October 2010, Palanga, Lithuania).

Viidebaum M., **Viikmäe B.** and Delpeche N. 2010. Sensitivity study of the Lagrangian trajectory model TRACMASS. Oral presentation at the *5th International Student Conference on "Biodiversity and Functioning of Aquatic Ecosystems in the Baltic Sea Region"* (06–08 October 2010, Palanga, Lithuania).

Viikmäe B., Soomere T. and Delpeche-Ellmann N. 2010. Potential of using Lagrangian trajectories for environmental management in the Gulf of Finland. Oral presentation at the *10th International Marine Geological Conference* (24–28 August 2010, St. Petersburg, Russian Federation).

Delpeche N., Soomere T. and **Viikmäe B.** 2010. Towards a quantification of areas of high and low risk of pollution in the Gulf of Finland, with the application to ecologically sensitive areas. Poster presentation at the *6th Study Conference on BALTEX* (14–18 June 2010, Międzyzdroje, Island of Wolin, Poland).

Andrejev O., Sokolov A., Soomere T., Myrberg K. and **Viikmäe B.** 2010. Using multi-year circulation simulations to identify areas of reduced risk for marine transport. Application to the Gulf of Finland. Oral presentation at the *6th Study Conference on BALTEX* (14–18 June 2010, Międzyzdroje, Island of Wolin, Poland).

Viikmäe B., Soomere T., Delpeche N., Meier H.E.M and Döös K. 2010. Utilizing Lagrangian trajectories for reducing environmental risks. Oral presentation at the *6th Study Conference on BALTEX* (14–18 June 2010, Międzyzdroje, Island of Wolin, Poland).

Viikmäe B., Soomere T. and Delpeche N. 2010. The use of Lagrangian trajectories for minimisation of the risk of coastal pollution. Oral presentation at the *Joint Numerical Modelling Group 15th Biennial Conference* (10–12 May 2010, Delft, The Netherlands).

Soomere T., Delpeche N. and **Viikmäe B.** 2010. The use of current-induced transport for coastal protection in the Gulf of Finland, the Baltic Sea. Poster

presentation at the *European Geosciences Union General Assembly* (2–7 May 2010, Vienna, Austria).

Viikmäe B., Isotamm R. and Delpeche N. 2010. An empirical method to determine patterns of the risk of coastal pollution in the Gulf of Finland. Oral presentation at the *Joint Baltic Sea Research Programme* (19–21 January 2010, Vilnius, Lithuania).

Soomere T., Delpeche N. and **Viikmäe B.** 2010. Semi-persistent patterns of transport in surface layers of the Gulf of Finland. Oral presentation at the *Joint Baltic Sea Research Programme* (19–21 January 2010, Vilnius, Lithuania).

Isotamm R., **Viikmäe B.** and Delpeche N. 2009. An empirical method to determine a low-risk fairway in the Gulf of Finland. Oral presentation at the *Coping with Uncertainty: A Multidisciplinary Research Conference on Risk Governance in the Baltic Sea Region* (15–17 November 2009, Sigtuna, Sweden).

Delpeche N., Isotamm R., **Viikmäe B.** and Soomere T. 2009. Application of a trajectory model to select areas of high risk of pollution. Oral presentation at the *Coping with Uncertainty: A Multidisciplinary Research Conference on Risk Governance in the Baltic Sea Region* (15–17 November 2009, Sigtuna, Sweden).

1. In search for favourable patterns of currents

The Baltic Sea (Figure 2), which is sometimes called a small intra-continental sea (Leppäranta and Myrberg, 2009), belongs to the shelf seas connected to the Atlantic Ocean. The outermost part of the Baltic Sea is located in the narrow region between the mainland of Denmark and Sweden. The traditional definition places its boundary between the Kattegat and the Danish straits. Although the Kattegat is customarily not considered as a part of the Baltic Sea, many circulation models of the Baltic Sea include this basin in the model domain.

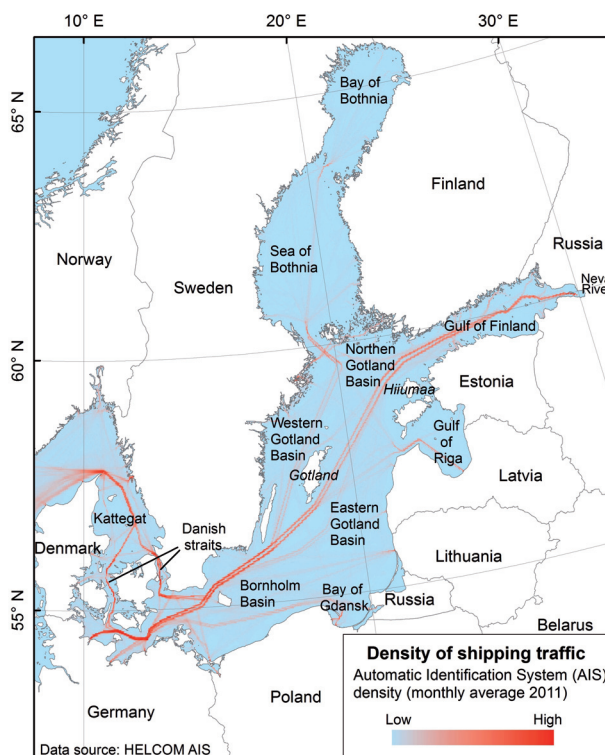


Figure 2. Main fairways in the Baltic Sea. Map by M. Viška.

The Baltic Sea is relatively shallow (mean depth 54 m and the deepest part, 459 m) and small (392 978 km²), with a total volume of 21 205 km³. Only about 12% of its total area has a depth of more than 100 m, and only 2.7% is deeper than 150 m. Consequently, a large part of the Baltic Sea can be characterised as a shallow, coastal-like area. The sea consists of several sub-basins of different depths and volumes (Leppäranta and Myrberg, 2009). The largest basin is the Gotland Sea with an area of 151 920 km² or 39% of the total area of the Baltic Sea. The Gulf of Finland covers an area of 29 498 km² and has a volume of 1098 km³ (5% of the

Baltic Sea). Its mean depth is only 37 m, clearly less than that of the entire Baltic Sea. The Danish straits, the Arkona Basin and the Gulf of Riga have relatively small volumes.

The research in this thesis concerns mostly the Gulf of Finland. A small part of the results comes from the area of Vattlestraumen (Norway, not shown in figures). The possibilities of the use of a similar technology for preventive optimisation of fairways have been analysed for the south-western Baltic Sea and Danish straits (Lu et al., 2012), for the northern Baltic Proper (Viikmäe et al., 2011) and for the entire Baltic Sea using Lagrangian transport (Lehmann et al., 2014) and Eulerian tracers (Höglund and Meier, 2012; Meier and Höglund, 2013). The impact of wind- and wave-driven transport on the results obtained from the analysis of current-driven transport is presented in Murawski and Woge Nielsen (2013). The main message from this work is that inclusion of wind drift renders the climatologically valid solution discussed in this study and in Andrejev et al. (2011) into two branches, one of which is valid for summer and winter months and another for transitional seasons (spring and autumn).

1.1. Circulation in the Gulf of Finland

The motion of water masses in the Gulf of Finland is tightly connected with the overall circulation in the central Baltic Sea. The mean circulation in the Gulf of Finland, similarly to the Gotland Sea, Gulf of Riga, Sea of Bothnia and Bay of Bothnia, is cyclonic (Leppäranta and Myrberg, 2009). As a result, the water is warmer and saltier in the eastern sides of all these basins than in the western parts. In the narrow, west–east oriented Gulf of Finland such a difference induced by mean circulation is observed between the northern and southern sides.

Although the long-term mean current in the Baltic Sea is weak, with an average speed of 5–10 cm/s, the circulation system is in some areas relatively persistent (Andrejev et al., 2004b). During storms the surface drift currents can reach 50 cm/s, in straits up to 100 cm/s.

Water masses in the Baltic Sea and in the Gulf of Finland are strongly stratified. As a result, motions in the upper layer (above the main pycnocline) are only weakly connected with the motions in the lower layer. This feature is most vividly evident in the Gulf of Finland. To characterise interactions between the layers and vertical fluxes, Döös et al. (2004) introduced the term ‘haline conveyor belt’ in analogy to the deep-water conveyor belt of the World Ocean. This term denotes the combination of many factors (such as bottom currents of the denser inflowing waters from the North Sea, the entrainment of ambient surface waters, mixing due to diffusion, interleaving of the inflowing water at a depth corresponding to the level of neutral buoyancy, vertical advection and upward entrainment of deep water into moving surface water in the Northern Gotland Basin) that are responsible for the overturning circulation of the Baltic Sea.

Water masses in the Gulf of Finland are diverse and rich in fronts due to the estuarine character of the gulf. This diversity is enhanced by the voluminous river

runoff, vigorous modulation of currents by bathymetry and frequently occurring upwelling events. Systematic studies of circulation in the Gulf of Finland have been performed already at the beginning of the 1900s (Leppäranta and Myrberg, 2009). These observations were collected onboard lightships using simple instrumentation but they still provided a fair understanding of the surface circulation for the northern Baltic Sea.

One of the key properties of sea dynamics from the viewpoint of this thesis is the existence of (semi-)persistent patterns of transport. The above-mentioned classical studies highlighted the marked horizontal variability of the entire field of currents and demonstrated that the mean circulation is a statistical property rather than a permanent feature. Palmén (Leppäranta and Myrberg, 2009) defined the persistency R of the direction of the current as the ratio

$$R = \frac{\langle |\mathbf{U}| \rangle}{\langle U \rangle} \times 100\%, \quad (1.1)$$

where \mathbf{U} is the current velocity², $|\langle \mathbf{U} \rangle|$ is the length of a vector consisting of mean values of velocity components and $\langle U \rangle$ is the mean current speed. If the direction of the current is constant, the persistency is 100%. The long-term persistency of surface currents in the Gulf of Finland was between 6% and 26% (Leppäranta and Myrberg, 2009), whereas it was much larger during some seasons.

The early analyses and observations revealed some other important details of the behaviour of the entire surface layer, including local drift currents. The surface flow (equivalently, the transport in the surface layer, including the Ekman current) has a speed of about 1.4% of the wind speed and is deflected by 19° to the right of the wind direction (Leppäranta and Myrberg, 2009).

A major improvement of this picture was achieved in the 1970s when the existence of mesoscale features was discovered. The numerical values in Eq. (1.1) did not change much. The persistency R of the surface circulation is usually well below 20% in the central part of the gulf but up to 50% in the coastal areas and can be even higher in specific locations of the Gulf of Finland (Andrejev et al., 2004a). Due to the impact of local topographic and hydrographic features, the persistency of the currents is smaller along the northern nearshore than along the southern coast (Andrejev et al., 2004a).

The nature of the residual (mean) circulation is crucial for long-term estimates of the drift of substances. The presence of an overall cyclonic pattern does not mean the existence of a permanent stream-like circulation type (Myrberg and Soomere, 2013). The instantaneous field of mesoscale currents almost totally masks the mean circulation and even an anticyclonic gyre may exist in the eastern part of the Gulf of Finland in selected years (Soomere et al., 2011). The current system is additionally complicated by periodic processes like inertial oscillations,

² Below I interpret velocity as a vector and speed as its length (scalar).

‘harbour oscillations’ in the gulf and seiches of the combined Gulf of Finland–Northern Gotland Basin system (Jönsson et al., 2008).

The search for the background residual current revealed one detail that is important from the viewpoint of this thesis. This current was quantified using linear regression between the easterly and northerly wind components and the easterly component of the current at a depth of 5 m off Kotka in the northern Gulf of Finland (Myrberg and Soomere, 2013). The difference between the classical results for the surface flow (1–3 cm/s) and for the residual flow at a depth of 5 m (4.8 cm/s) signals the presence of a layered structure of velocity fields and the necessity of using a sufficiently high vertical resolution in circulation models of the Gulf of Finland. Andrejev et al. (2004a) suggest that in terms of instantaneous velocities, persistency and the overall structure of the flow, the uppermost 2–3 m thick layer may be almost completely decoupled from the subsurface layer. The results of Suursaar (2010) also confirm that the sea currents are highly variable over the first metres of depth, at least for some seasons.

The patterns of long-term (Lagrangian) transport are quite complicated in the Gulf of Finland. The long-term mean flow (of a couple of cm/s) towards the west was indirectly derived from the time difference between the annual minimum of the surface salinity near the island of Utö and the maximal river runoff (Myrberg and Soomere, 2013). These estimates match the typical east–west net transport speed in relatively coarse numerical models (Soomere et al., 2011).

A random transport model demonstrated that after a one-year period from a starting point at Helsinki, as expected, the probability distribution of the transport had a maximum in the west. However, the probability density was non-zero in the east, signalling that the eastward net transport does occur in some cases even if the direct impact of mesoscale features is filtered out (Leppäranta and Peltola, 1986).

The understanding of the circulation in the Gulf of Finland has considerably improved during the last decades based on numerical investigations of spatio-temporal variability of the currents and extensive *in situ* measurements (Alenius et al., 1998; Soomere et al., 2008). Mean surface current velocities were westwards (3–5 cm/s in summer and 4–6 cm/s in autumn) off the Hanko Peninsula (Laakkonen et al., 1981; Haapala et al., 1990) and near Kotka (Alenius, 1986) at the northern (Finnish) coast, supporting the concept of cyclonic circulation. Strong westerly winds turned these currents to the east even for several weeks at a time, indicating the possibility of an anticyclonic gyre for some seasons (Soomere et al., 2011). The largest flow speeds were recorded in summer. This feature probably reflects the strongly layered structure of the flow and signals that the energy of wind-driven motions is concentrated in a relatively thin upper layer. Interestingly, these features are consistent with the analysis of Murawski and Woge Nielsen (2013) who found that the same optimum fairway is valid for summer and winter.

Measurements with moored current meters revealed that current speeds near the Estonian coast (up to about 20–30 cm/s in coastal jets) were generally higher than on the Finnish side (Talpsepp, 1986; Talpsepp et al., 1994): the long-term mean current speed off Helsinki was only about 10 cm/s. The most prominent variability

of the currents occurred on time scales of about 18–20 days. The presence of unidirectional currents over several days (Laakkonen et al., 1981; Talpsepp et al., 1994) was further analysed by Soomere et al. (2011) in terms of semi-persistent transport patterns.

The Finnish Institute of Marine Research conducted measurements at five stations across the entrance region of the Gulf of Finland in summer and autumn 1994–1995 (Leppäranta and Myrberg, 2009; Myrberg and Soomere, 2013). The surface-layer flow had a typical velocity of 10–20 cm/s. Its direction varied across the gulf mostly consistently with a cyclonic circulation. The persistency of the outflowing current near the Finnish coast was about 50%. The current direction was highly variable in the middle of the gulf and inflow occurred near the Estonian coast. The regions of oppositely flowing currents were at times separated only by about 10 km. A long period of inflow along the Finnish coast was observed in autumn, possibly an evidence of surface water masses being pushed into the gulf by stronger south-western winds, associated with the export of saltier water at larger depths (Elken et al., 2003).

Remarkable seiche-driven currents with periods of 31, 24, 19.5, 16 and 11 h have been identified near the island of Naissaar (Lilover et al., 2011), despite a widespread opinion that tidal flows and especially seiches (Jönsson et al., 2008) are relatively weak in the entire gulf. The current was deflected by 35° to the right from the wind (Lilover et al., 2011), that is, slightly more than in the classical estimates (Alenius et al., 1998; Elken et al., 2011). On certain occasions the average speed of tidal flows was close to 10 cm/s (Lilover, 2012).

The currents in deep semi-enclosed bays at the southern coast of the gulf are apparently often multi-layered, with an anticyclonic flow in the upper layer and the cyclonic flow in the lower layer steered by the local topography (Raudsepp, 1998).

Although the Gulf of Finland evidently hosts a large number of mesoscale and submesoscale phenomena, observational evidence of such features is quite limited. Pavelson (2005) reported observations of a mesoscale eddy with a diameter of 15–20 km at the entrance to the gulf. The maximum velocities in its core reached 35 cm/s. Observations of fronts and upwelling events are more frequent. These features occurring in the uppermost layer can be easily tracked and quantified by remote sensing. A classical example is the quasi-permanent multi-layered salinity front at the entrance of the gulf (Kononen et al., 1996; Pavelson et al., 1997), supported by the interplay of waters of different salinity and/or temperature flowing into and out of the gulf. Several quasi-stationary patterns (e.g., certain features of stratification) persist for 4–15 days in the gulf (Liblik and Lips, 2012). The variability of hydrophysical forcing drives similar heterogeneity in phytoplankton distribution (e.g., Lips et al., 2014; Laas et al., 2014).

The system of currents in the eastern end of the Gulf of Finland (that is dynamically similar to an estuarine domain) is largely decoupled from the circulation in the rest of the gulf (Alenius et al., 1998). The mean flow is to the west with a speed ~10 cm/s. The flow direction is highly variable, while relatively persistent ‘streams’ can exist in this part of the gulf, in Neva Bay and in the

vicinity of the Saint Petersburg flood barrier where the influence of the Neva River is most clearly manifested.

Drifter experiments also indicate that the dynamics of currents in the gulf is extremely complicated. In May 2003, *Current Spy* surface buoys with a drogue depth of 0.7 m (Gästgifvars et al., 2006) moved with a speed of about 2% of the wind speed and with a deviation angle of 0–10° to the right in moderate wind conditions. In weak wind conditions the buoys drifted to ~60° to the left of the wind. A feasible explanation is that currents are strongly layered and that the dynamics of the lower layers has overridden the wind-induced drift of the upper layer (Gästgifvars et al., 2006; Myrberg and Soomere, 2013). The relevant observational evidence is presented, e.g., in (Liblik and Lips, 2012). The idea that the dynamics of deeper layers may play a great role in the drift of various substances in the uppermost layer has been further developed in Soomere and Quak (2007).

The presented material demonstrates that the system of currents in the Gulf of Finland hosts motions with a large range of spatial and temporal scales, from basinwide circulation down to synoptic vortices and submesoscale processes. In order to numerically resolve the diversity of processes and scales, partially caused by small values of the internal Rossby radius in some regions of the gulf (Nekrasov and Lebedeva, 2002; Alenius et al., 2003), extremely high-resolution models, down to 0.25 nautical miles are needed (Andrejev et al., 2010).

From the viewpoint of this thesis, an important aspect is the exchange of water masses between the Gulf of Finland and the rest of the Baltic Proper, with no sill in between (see Methods IVa and IVb in Section 4.1). Early estimates of the exchange were based on sparse field measurements, from which short-term variability has been filtered out. The classical Knudsen's formula predicts annual water in- and outflows of 480 and 600 km³/yr, respectively (Leppäranta and Myrberg, 2009). Although the excess of water (mainly owing to input of river water) to the Gulf of Finland, around 115 km³/yr, was recovered adequately, the corresponding mean current speed ~1 cm/s was clearly underestimated.

Although internal wave activity is only scarcely reflected in recent studies (Kurkina et al., 2011; Lilover and Stips, 2011), it is apparently high in this area. According to Pavelson (2005), the production of eddies, topographically controlled currents and fronts is frequent and therefore diapycnal mixing is intense in the entire entrance region. The forming of specific features of the vertical structure of water at the entrance to the gulf also stems from the anisotropic wind wave regime in the Baltic, with frequent occurrence of very high waves in the north-eastern part of the Northern Gotland Basin (Feistel et al., 2008).

Below (and in Paper E) I extensively use the concept of particle age. Its introduction in Andrejev et al. (2010, 2011) was motivated by a similar concept of water age that is a helpful tool to study water renewal rates and water quality. According to the classical definition, the age of a water parcel is the time elapsed since the parcel left the sea surface (Deleersnijder et al., 2001). This definition is particularly relevant in the Gulf of Finland, where the water is supplied either

through near-surface currents from the Northern Gotland Basin, precipitation or river discharge. The oldest water (about 8.3 years) is located at the bottom of the gulf (Meier, 2005). Another definition of water age accounts for both horizontal and vertical displacements (Bolin and Rodhe, 1973) and characterises the residence time of water parcels in a selected area.

Particular values of water age largely depend on the definition of the ‘outer’ basin. For example, Meier (2007) estimated the average age of the Gulf of Finland water in terms of water exchange between the North Sea and the entire Baltic Sea to be ~ 20 years. The same value for the Gulf of Finland with respect to water exchange with the Northern Gotland Basin is about two years. This indicates intense interaction between the gulf and the rest of the Baltic Sea. The water age shows a pronounced spatial and temporal variability in the Gulf of Finland (Andrejev et al., 2004b), with the smallest values in the inflow regions and at river mouths and the highest values in the outflow regions.

1.2. Numerical modelling of circulation

Numerical models are widely used in studying geophysical phenomena, including hindcasting or forecasting surface currents. Due to the vital role of mesoscale variability for transport by surface currents, it is important that the simulated current field contains dominant features similar to real current fields in the ocean.

A common opinion is that an eddy-permitting circulation model (that is, a model in which the largest eddies present in reality can be replicated) should have a spatial resolution not less than $\frac{1}{2}$ of the internal (baroclinic) Rossby radius R_1 (see, e.g., Cushman-Roisin and Beckers, 2011 for the relevant theory). As the typical values of R_1 in the Baltic Proper are about 10 km (Fennel et al., 1991), models with a grid step of about 5 km (3 nautical miles) can reproduce some of the effects driven by such eddies. A model is called eddy-resolving if it is able to resolve typical mesoscale motions in the given area, that is, vortices and other features with a typical scale somewhat below the internal Rossby radius (Cushman-Roisin and Beckers, 2011). It is commonly accepted that models with a spatial resolution of 2 nautical miles (about 3.5 km) are usually sufficient for eddy-resolving runs in the Baltic Proper (Lehmann, 1995) but are barely eddy-permitting in the Gulf of Finland (Myrberg et al., 2010).

Attempts at numerical modelling of the Baltic Sea dynamics started already in the 1970s (Leppäranta and Myrberg, 2009). At the time it was not possible to properly describe the complete 3D flow field in this basin with realistic bottom topography and forcing. It was common to use a flat bottom in the relevant studies in the 1970s, while sensible (albeit strongly generalised) bottom topography was introduced in the 1980s (Leppäranta and Myrberg, 2009).

The first realistic simulations of 3D dynamics of the Baltic Sea (that included both wind-driven and baroclinic circulation under realistic climatological forcing) using an eddy-permitting model resolution and adequate bottom topography were performed in the mid-1990s (Lehmann, 1995). Since then, 3D circulation

modelling has become an important tool that has substantially improved our understanding of the dynamics of the Baltic Sea. The number and variety of present models and applications for the Baltic Sea are rapidly increasing (Omstedt et al., 2004; Feistel et al., 2008; BACC, 2008; Leppäranta and Myrberg, 2009).

The 3D numerical modelling of today in the Baltic Sea is typically based on the horizontal resolution of 1–5 km and a vertical structure described by 20–100 layers. Even higher resolutions are often needed in local applications (Zhurbas et al., 2008a, 2008b; Andrejev et al., 2010; Lu et al., 2012). Properly adjusted geostrophic wind data (e.g., the gridded meteorological data by the Swedish Meteorological and Hydrological Institute) are often used for relatively low-resolution simulations, model validation and intercomparisons (Myrberg et al., 2010) and for the identification of long-term changes (e.g., Myrberg and Andrejev, 2006; Meier, 2006, 2007; Lehmann et al., 2011). The output of local atmospheric models such as different versions of the High Resolution Limited Area Model (HIRLAM) (www.hirlam.org) or the DWD model (www.dwd.de), ERA-40 reanalysis (Uppala et al., 2005) or its downscalings (Höglund et al., 2009; Samuelsson et al., 2011) are typically used as meteorological forcing for higher-resolution simulations. Several systematic features of air flow in the Gulf of Finland are still not captured by even the best atmospheric models (Keevallik and Soomere, 2010), hence new high-resolution reanalyses are urgently needed.

One of the most important inputs in the Baltic Sea modelling is the voluminous river discharge. The relevant data in terms of monthly mean values (Bergström and Carlsson, 1994) are available, e.g., from the BALTEX Hydrological Data Centre. The initial conditions for hydrographic parameters are available, e.g., from the Baltic Environment Database, which can be used through the Data Assimilation System (Sokolov et al., 1997). Observations from buoys and tide gauges provide useful information for model verification and data assimilation (Myrberg et al., 2010). The availability and accurate description of the open boundary conditions in the Danish straits is still a challenge, because only a limited number of data are available (Meier and Höglund, 2013).

Simulations of the mean circulation of the entire Baltic Sea confirm the main characteristics of the early findings (described above) about the general cyclonic circulation (Lehmann and Hinrichsen, 2000; Lehmann et al., 2002) but also indicate that the mean circulation is likely variable over longer periods, with changes in the character of wind forcing, heat fluxes and ice extent, freshwater budget and inflow activity (Meier, 2007). A hindcast for the period of 1958–2001 showed an increase in the yearly averaged surface velocities (mean over the entire sea area) by 0.21 cm/s per decade (Jeřdrasik et al., 2008). There is evidence that over shorter periods (months), the water movements may take alternative paths as compared to the regular spreading patterns.

High-resolution modelling has added many fascinating details to the above-discussed properties of the dynamics of the Gulf of Finland that were captured in the historical studies. The gulf hosts a manifold of mesoscale features such as persistent eddies with a typical size exceeding the internal Rossby radius (Andrejev

et al., 2004a, 2004b). Eddies are relatively small in the eastern part of the central gulf. The cyclonic mean circulation does exist in the Gulf of Finland but the patterns and the persistency of the currents deviate to some extent from the classical analyses. Voluminous runoff from the Neva River drives strong and persistent, mostly west to north-west directed but still strongly meandering currents in Neva Bay and the easternmost narrow part of the Gulf of Finland. These are important for commercial ship routing (Murawski and Woge Nielsen, 2013).

Modelling results confirm the observations that the Finnish side is primarily dominated by offshore outflow down to a depth of 40–50 m and with a mean speed of 8 cm/s (Meier, 1999; Andrejev et al., 2004a). According to Andrejev et al. (2004a), a persistent (up to 50%) inflow near the southern coast is visible at all depths with typical speeds of 1–4 cm/s, whereas the most intense flow (7–10 cm/s) occurs near the surface. A compensating and highly persistent (up to 80%) outflow exists in the rest of the gulf in the subsurface layer (2.5–7.5 m). The uppermost 2.5 m thick layer is characterised mainly by an Ekman-type drift (whereas an intense transport with a speed \sim 8 cm/s goes into the gulf on the Finnish side in this layer, Andrejev et al., 2004a). The layer just below it (2.5–7.5 m) may have clearly different dynamics. This once more confirms the different dynamics of the surface and sub-surface layers and signals that for the reconstruction of trajectories of parcels of pollutants and floating objects at the sea surface, very high vertical resolution is required for the ocean models.

The basic pathways of the water cycle in the gulf (Alenius et al., 1998) mirrored the infrequent one-way salt water inflow through the Danish straits (e.g., Lass and Matthäus, 1996; Elken and Matthäus, 2008) into the deeper layers of the Baltic Sea. According to Elken et al. (2003, 2014), a two-way exchange (involving the possibility of an almost total export of saline bottom water from the gulf), accompanied by drastic variations in the halocline's position (even almost its complete disappearance), may take place at the entrance to the gulf. Differently from the classical estuarine dynamics, the strongly anisotropic wind forcing (Soomere and Keevallik, 2003) plays an important role in the water exchange and formation of the vertical structure of the water masses in the Gulf of Finland. Namely, strong south-western winds occasionally push a large amount of fresher surface water back into the gulf. The increased hydrostatic pressure may lead to a gradual export of the salt wedge in the bottom layer of the gulf (Elken et al., 2003, 2014) or may cause a weakening of the stratification of water masses at the entrance to the gulf and intensification of vertical mixing (Elken et al., 2006) if the mean wind speed exceeds 4–5.5 m/s. This knowledge has led to a substantial revision of the traditional concept of mostly decoupled lower layer dynamics and reveals that both the surface and near-bottom layers respond rather actively to wind forcing. The layers are mostly decoupled on local scales, but here the coupling occurs on the scale of the entire basin (Myrberg and Soomere, 2013).

Although baroclinic instability usually leads to disintegration of the flow (Cushman-Roisin and Beckers, 2011), a gently sloping bottom at the Finnish coast may cause an internal adjustment of the flow to a quasi-stable state (Stipa, 2004).

The flow can thus be interpreted as an analogue to large-scale nearly zonal ocean currents where the impact of the beta-effect is mimicked by an equivalent impact of the sloping bottom (Cushman-Roisin and Beckers, 2011). Such baroclinic currents are generally more pronounced than barotropic ones (Soomere, 1995).

The importance of mesoscale motions in the transport becomes vividly evident from numerical simulations of the water exchange between the Gulf of Finland and the Northern Gotland Basin. Lehmann and Hinrichsen (2000) obtained the same long-term net outflow ($\sim 130 \text{ km}^3/\text{yr}$) as the classical sources. The volumes of short-time in- and outflow are not only much higher but also strongly depend on the spatio-temporal resolution of the processes (Andrejev et al., 2004a). The reason is that relatively persistent or quasi-periodic, mesoscale features (local jets, synoptic eddies, inertial oscillations) create comparatively short-term transport of water across the entrance line. This water is usually not transported far from its original location and does not affect the interior of the gulf. If the mesoscale circulation was accounted for, the average in- and outflows were 3154 and 3273 km^3/yr , respectively, for 1987–1992 (Andrejev et al., 2004a). A similar estimate only accounting for the quasi-stationary circulation pattern gave 1417 and 1532 km^3/yr .

1.3. Circulation models RCO and OAAS

A General Circulation Model (GCM) is a mathematical model that describes the large-scale fluid dynamics in the atmosphere and ocean. The basis of the commonly used models for ocean currents are the so-called primitive equations for incompressible and isotropic Newtonian fluid: (i) a continuity equation representing the conservation of mass, (ii) the Navier–Stokes equations (or, more commonly, certain equations derived from the Navier–Stokes equations) representing the conservation of momentum and (iii) thermodynamical equation(s). An ocean GCM also includes a budget equation for salinity and an equation of state relating water density with temperature, salinity and pressure (Cushman-Roisin and Beckers, 2011).

A large number of numerical ocean models are available (e.g., Haidvogel and Beckmann, 1999; Torsvik, 2013). This variety is largely due to design choices in the model construction, e.g., discretisation techniques, horizontal and vertical grid configurations, turbulence schemes and subgrid-scale parameterisation, parameterisation of boundary layer processes and boundary conditions. The optimal design usually depends on the intended use of the model, for instance whether it is designed for global-scale or regional-scale simulations, or used in a short-term forecast system, long-term climate study or intermediate-duration (multi-)seasonal study.

As discussed in Section 1.2, numerical replication of circulation patterns in the Baltic Sea, and especially in its sub-basins such as the Gulf of Finland, is a major challenge. Even the very best existing circulation models only partially reproduce the actual motions in these water bodies (Myrberg et al., 2010), whereas even reproduction of certain common statistical properties of transport is not always

perfect (Kjellsson and Döös, 2012; Kjellsson et al., 2013). The models, the output of which is used in this study, are expected to reproduce, at least, the core statistical features of currents, from which long-term statistical properties of Lagrangian transport can be extracted. For the purposes of this work it is critical that the patterns of surface motions should be reproduced as accurately as possible.

The material presented in Sections 1.1 and 1.2 shows that the Baltic Sea is relatively shallow, usually very strongly stratified (Leppäranta and Myrberg, 2009) and subject to the impact of extremely variable (both in space and time) wind patterns (Soomere, 2003). Typically, the stratification has a multi-layered structure (Alenius et al., 2003), whereas motions in the lower layer (below the main thermocline) are often almost disconnected from the motions in the upper layer (Leppäranta and Myrberg, 2009). This peculiarity is particularly strong in the Gulf of Finland (Alenius et al., 1998; Myrberg and Soomere, 2013). In relatively shallow areas the Ekman spiral evidently ‘feels’ the bottom (Leppäranta and Myrberg, 2009). It is thus likely that the horizontal velocity components are highly variable between different vertical layers and certain features of the surface circulation (such as an anticyclonic gyre in the eastern part of the gulf, Soomere et al., 2011) may not match the depth-integrated cyclonic circulation. Thus, for an adequate replication of the statistics of surface velocity fields in the Gulf of Finland the circulation model has to have very good resolution in both horizontal and vertical directions. A specific additional requirement is imposed by the relatively large sea-ice coverage during the winter season (SMHI and FIMR, 1982).

Several contemporary circulation models of the Baltic Sea match these requirements and are able to resolve the dynamics of at least the largest mesoscale features such as synoptic vortices: Rossby Centre Ocean (RCO) model (Meier, 1999; Meier et al., 2003) developed in the Swedish Hydrological and Meteorological Institute (SMHI), Nucleus of European Modelling (NEMO; Madec, 2008), High Resolution Oceanographic Model of the Baltic Sea (HIROMB; Funkquist and Kleine, 2007), the Kiel Baltic Sea Ice Ocean Model (BSIOM; Lehmann et al., 2002) or the family of DMI/BSHcmod circulation models (Kleine, 1994; Dick et al., 2001), originally developed in the Bundesamt für Seeschifffahrt and Hydrographie (Germany) and further improved in the Danish Meteorological Institute. They have been designed for different purposes. For example, the RCO model has been designed for long-term climate studies and has a moderate spatial resolution and the HIROMB model has been developed for operational forecast.

Most of the studies described in this thesis rely on the 3D velocity fields simulated for 1982–2001 using the RCO model and kindly provided by the SMHI in the framework of the BONUS BalticWay cooperation. This data set was one of the few that, technically, could have been used for the described studies due to: (i) a well-tested model, (ii) long, homogeneous timeseries of hindcast data and (iii) a sensible resolution in space and time. Calculations similar to those presented in this thesis have been performed for the south-western Baltic Sea using the DMI/BSHcmod model (Lu et al., 2012), for the entire Baltic Sea with the Kiel Baltic Sea Ice Ocean Model (Lehmann et al., 2014), for the Gulf of Finland using a

higher-resolution model OAAS (Andrejev et al., 2010, 2011) and by coupling current and wind drift for the Gulf of Finland by Murawski and Woge Nielsen (2013) who employed a further development of the DMI/BSHcmod.

The RCO model has been designed for simulations of long time intervals necessary for investigation of ocean climate. The underlying equations and details of the implementation are described in many papers (e.g., Meier, 1999; Meier et al., 2003; Meier, 2007; Meier and Höglund, 2013) and also shortly provided in Paper A and Paper B. The model equations are solved using a regular rectangular grid in the horizontal direction and z -coordinates in the vertical direction. The horizontal resolution (2 nautical miles) is considered acceptable with regard to mesoscale dynamics in the open part of the Baltic Sea (Meier et al., 2003; Meier, 2007) but is only eddy-permitting in the Gulf of Finland. The model uses up to 41 vertical levels (depending on the local water depth), the thickness of which varies between 3 m close to the surface and 12 m at 250 m depth. Winter conditions are resolved using a Hibler-type sea ice model (Hibler, 1979).

The motions in the sea depend on different forcing factors (e.g., direct wind impact, wave generation, mass and heat exchange) and on what happens at certain points or along specific sections of the water mass (e.g., river mouths, borders with adjacent sea domains). The RCO model accounts for inflow of fresh water from the major rivers along the Baltic Sea coasts and water exchange through the Danish straits. The model uses wind speed and direction at the standard height of 10 m above sea level, air temperature and specific humidity at a height of 2 m, precipitation, total cloudiness and sea level pressure. The relevant forcing fields were derived as a specific regionalisation of the ERA-40 re-analysis (for 1957–2002, Uppala et al., 2005) over Europe. The input for the RCO model was constructed using a regional atmospheric model with a horizontal resolution of 25 km (Samuelsson et al., 2011). As the atmospheric model tends to underestimate wind speed extremes, the wind was adjusted using simulated gustiness (Höglund et al., 2009). A comprehensive comparison of the performance of the RCO model in the Gulf of Finland against several other state-of-the-art circulation models is provided by Myrberg et al. (2010).

Although the RCO model has shown very good performance in the Baltic Sea conditions, it still has several shortcomings similarly to other models of this generation, especially if applied to the Gulf of Finland (Myrberg et al., 2010). From the viewpoint of my work, the statistics of the spreading of modelled trajectories and the typical Lagrangian transport speed to some extent deviate from the values evaluated using subsurface drifters (Kjellsson and Döös, 2012). This feature, however, insignificantly impacts the basic results of this study (Paper G).

Due to inexact parameterisations of subgrid-scale processes, insufficient horizontal and vertical grid resolution, biases of atmospheric and hydrological forcing fields, too coarse topographic data, etc., virtually all the Baltic Sea models suffer from uncertainties. For instance, the RCO model produces a too shallow halocline (Meier, 2007) and artificial mixing during salt water inflows (Meier et al., 2003), too strong vertical stratification in the Gulf of Finland (Meier, 2007) and

numerical noise affecting the sea surface temperature (Löptien and Meier, 2011). The shortcomings of the RCO model are characteristic of all contemporary circulation models of the Baltic Sea that at times fail to reproduce even the simplest variables such as the sea level (Lagemaa et al., 2011).

The typical values of the internal Rossby radius in the Gulf of Finland are 2–4 km (Alenius et al., 2003). Therefore, models with a spatial resolution of 2 nautical miles are barely eddy-permitting for the Gulf of Finland (cf. Myrberg et al., 2010). Although an accurate representation of all mesoscale eddies cannot be expected, the model is evidently able to replicate at least the larger eddies and their contribution to current-driven transport, and allows some insight into the realistic dynamics of the sea and into certain statistical properties of Lagrangian transport. As the RCO model was designed to study past and future climate variability of the Baltic Sea on a centennial time scale, a horizontal resolution higher than 2 nautical miles was not feasible (Meier et al., 2003). For this reason the work presented in this thesis is focused on the evaluation of certain statistical properties of current-driven transport. Many of these properties have been shown to be almost invariant with respect to the particular choice of the model resolution (Andrejev et al., 2011) and associated problems with the accuracy of replication of the details of motions (Paper G).

Papers C and D rely on the output of the OAAS model developed by O. Andrejev and A. Sokolov (Andrejev and Sokolov, 1989, 1990; Sokolov et al., 1997; Andrejev et al., 2004a, 2004b; Andrejev et al., 2010). This model has been designed to replicate dynamics of sea areas with complicated geometry and strong stratification such as the Gulf of Finland. Its basic features are similar to those of the RCO model: it is a primitive-equation, free-surface, 3D baroclinic z -coordinate circulation model in Cartesian coordinates. Some of the model features (such as the equation of state) have been tuned for the Baltic Sea conditions (Millero and Kremling, 1976). As the winters during the period covered in simulations (1987–1991) were rather mild and the Gulf of Finland was mostly free of ice, a simple parameterisation was used for ice phenomena. For water temperatures below the freezing point, the wind stress was decreased by a factor of 10 in order to mimic the presence of ice. At 0 °C, the vertical heat flux was stopped as long as cooling conditions prevailed. The loss of heat during ice melting was approximated by reducing the upward heat flux in the early spring by a factor of four until the water temperature reached +1 °C.

The data sets used in Paper C and Paper D were generated during simulations of the currents in the Gulf of Finland to the east of 23°27' E with a spatial resolution of 1 nautical mile. The vertical resolution was 1 m in the entire water column except for the surface layer that had a thickness of 2 m. The model has been used in a variety of applications such as studies of upwelling in the entire Baltic Sea (Myrberg and Andrejev, 2003) and various dynamical and hydrophysical features of the Gulf of Finland (Andrejev et al., 2004a, 2004b; Gästgifvars et al., 2006; Myrberg et al., 2010).

The OAAS model was forced with the same meteorological data as the above-described implementation of the RCO model (Andrejev et al., 2010, 2011). River discharge was approximated using monthly mean values for 1970–1990 (Bergström and Carlsson, 1994). The salinity of river water was set to zero and its temperature equal to the ambient sea water temperature at the river mouth. The initial fields (water temperature and salinity) and the boundary information (the 3D structure of the salinity and temperature and sea level information) at the entrance to the gulf were interpolated from the output of the RCO model at 6-h resolution. To smooth the potential impact of the difference in the resolution between the models, the lateral diffusivity coefficient was increased in the OAAS model towards the boundary following a sine function in a sponge layer of a width of 16 nautical miles.

1.4. Lagrangian particle tracking

In fluid dynamics the flow field is usually specified either through the Lagrangian frame of reference, where the observer follows the motion of individual fluid parcels, or through the Eulerian frame of reference, where the flow is determined by the velocity at fixed points. Both of these approaches are useful when tracking the motion of substances immersed in the fluid. Although they can be expected to produce similar results, there are some important differences. For example, the Eulerian tracer approach (Höglund and Meier, 2012; Meier and Höglund, 2013) determines concentrations from an advection and diffusion equation, similar to the budget equations used for salinity and temperature. Hence, the Eulerian approach is not suitable for tracing pathways of single pollution parcels, which makes it difficult to connect the presence of a substance at a particular location with a specific upstream source.

The analysis in Papers A, B and E–G is based on the Lagrangian approach, namely, on statistical analysis of large sets of Lagrangian trajectories of test parcels. These trajectories are constructed on the basis of 3D velocity fields simulated by the RCO circulation model. Their analysis allows the identification and visualisation of several properties of currents that cannot be extracted directly from the current fields (Soomere and Quak, 2013).

The trajectories can be evaluated (or the Eulerian tracer equation can be integrated) either ‘on-line’ (simultaneously with the integration of the GCM) or ‘off-line’ (after the GCM has been run for some time and the velocity fields have been stored). The ‘on-line’ method can make use of velocity data at each internal integration time step of the GCM, hence the trajectories can be evaluated with a much higher temporal resolution than possible for ‘off-line’ calculations. However, the ‘off-line’ method is more efficient if there is a need to re-run experiments with different sets of parcels, e.g., when simulating the effect of different particle properties, or when the time, place and amount of parcels to be selected are not prescribed at the time of running the GCM. The Eulerian tracer equation generally needs to be integrated ‘on-line’ with the GCM (Höglund and Meier, 2012; Meier

and Höglund, 2013), while the Lagrangian trajectories can be both ‘on-line’ and ‘off-line’.

Both methods have been used in studies of pollution propagation in the Baltic Sea. The ‘on-line’ approach has been used for Eulerian tracers (Höglund and Meier, 2012) and in high-resolution simulations of Andrejev et al. (2010, 2011). The ‘off-line’ approach has been applied in Lu et al. (2012) and Lehmann et al. (2014). Murawski and Woge Nielsen (2013) employed a combined method of calculating oil spill propagation under joint impact of waves and surface currents.

The research in Papers A, B, E, F and G is based on the ‘off-line’ approach to calculations of Lagrangian trajectories. The current-driven paths of single passive water parcels (representing, e.g., persistent passive neutrally buoyant pollution particles, or similar agents of other adverse impacts on the sea surface or in the surface layer) are analysed with the use of a Lagrangian trajectory model, TRACMASS (Döös, 1995; de Vries and Döös, 2001). This model uses pre-computed Eulerian velocity fields at discrete grid points to evaluate an approximate path of water parcels (equivalently, of an adverse impact with neutral buoyancy). The Lagrangian trajectories of selected water parcels (passive particles or tracers) are calculated by solving the trajectory path through each grid cell. The procedure relies on an analytical solution of a differential equation that depends on the velocities on the walls of the grid box obtained using a linear interpolation of the velocity field in space (and also in time in the time-dependent version).

In the idealised case the velocities provided by a GCM can be interpreted as an exact representation of the dynamics. The resulting trajectories are then exact and invertible solutions to the relevant trajectory equations. After the integration of trajectory equations has been performed forward in time, it is possible to do a reverse tracking and to arrive at the starting position. This enables tracing origins of water or air masses to some extent (Döös et al., 2013).

The TRACMASS model was originally developed by Döös (1995) and Blanke and Raynaud (1997) for stationary velocity fields and generalised by de Vries and Döös (2001) for time-dependent fields. The code has been further developed and used in many studies of the global ocean (Döös and Coward, 1997; Drijfhout et al., 2003; Döös et al., 2008), of the Mediterranean Sea and the Baltic Sea (Döös et al., 2004; Jönsson et al., 2004; Engqvist et al., 2006; Soomere et al., 2011), as well as in the research of large-scale atmospheric circulation (Kjellsson and Döös, 2012). A detailed overview of the code is presented in Döös et al. (2013).

As I am specifically interested in surface transport patterns, the test parcels in Papers A, B, E, F and G are locked in the uppermost layer as in Andrejev et al. (2010) and only advected by horizontal velocity. In the RCO model velocities in this layer represent the currents at depths of 0–3 m. As discussed in the Introduction, the resulting trajectories are not representative for truly passive, neutrally buoyant parcels. They represent current-driven motion of objects or substances that are slightly lighter than the surrounding water (e.g., oil in otherwise calm conditions, or lost containers) or are locked in the uppermost layer for some

other reason. In essence, doing so, is a particular case of so-called binned random walk approach (Thygesen and Ådlandsvik, 2007).

The so-called non-spreading version of the TRACMASS code assumes that the GCM velocities fully represent the motions in the ocean (Döös et al., 2013). This assumption ignores the effects of subgrid-scale turbulence on the motion of fluid parcels. In such cases the initially close trajectories have an overly tendency to remain close over time, while in the real atmospheric and marine conditions the aggregated impact of small-scale features of the motion generally tends to spread closely packed particles (e.g., Ollitrault et al., 2005). It is well known that the spreading of trajectories in studies based on this version of TRACMASS has been usually much smaller than the spreading of real drifters (Jönsson et al., 2004; Engqvist et al., 2006; Döös and Engqvist, 2007; Döös et al., 2008; Kjellsson and Döös, 2012). The inclusion of the impact of small-scale features in the so-called spreading version of TRACMASS means that parcel tracking backwards in time generally does not lead back to the starting position of the parcel, and reverse tracking of water or air masses is generally not possible. The possible impact of subgrid turbulence on the results of calculations is also analysed in Paper G by means of the inclusion of a diffusion scheme in the TRACMASS model and repeating the calculations for 1982–2001.

2. Analysis of the structure of surface currents

For a casual observer the motion of surface water in the sea may appear random and chaotic, but careful observation over extended time intervals usually reveals a multitude of coherent structures. Such structures are particularly important for the efforts towards making shipping environmentally friendlier. It was noted already in the mid-1990s that in addition to ship types and cargoes, the geography of shipping routes was a major component of the risk and environmental impact associated with shipping (Lo and McCord, 1995; Judson, 1997; see also Soomere, 2013 for an overview). In international literature only few studies are available on the fairway choice based on environmental arguments (Eide et al., 2007; Schwehr and McGillivray, 2007). The most widely discussed issue concerns whales hit by ships in the North Atlantic and in the Mediterranean Sea (Ward-Geiger et al., 2005; Panigada et al., 2006). An important part of the solution was the identification of a systematic pattern of open sea areas often visited by whales. As a result it was decided to relocate the fairway entering Boston Harbour to the area of minimum probability of the presence of whales (Stokstad, 2009). This shift increased the sailing time by about 15 min.

These structures and patterns vary in size, time scale and persistency, ranging from the large-scale basinwide gyres that are only revealed by averaging over long time series of observations (Section 1.1) down to short-lived mesoscale and sub-mesoscale jets and vortices. For shorter time scales (a few days), the surface currents represent a combination of a complex field of eddies interspaced by meanders, fronts and filaments, as typical of short-lived mesoscale motions. Eddies are characterised by a roughly circular feature of swirling fluid motion and are among the most easily recognisable coherent structures in a surface flow field. They play an important part in transport of heat, mass, momentum, biological and chemical agents, etc., from areas of eddy formation to areas of their decomposition (Munk et al., 1997; Chelton et al., 2011). Satellite altimeter data sets and drifting buoys have revealed that the eddy kinetic energy often exceeds the long-term mean kinetic energy even in regions with high current velocities (Ishikawa et al., 1997). In some sea areas eddy structures occur regularly due to specific recurrent flow patterns, such as the case of Mediterranean Water eddy (so-called meddy) formation near the Strait of Gibraltar by outflow of the Mediterranean water into the Atlantic Ocean (Bower et al., 1995). Similar phenomena are often registered in the Baltic Sea, ranging from the intra-halocline eddies in the Gotland Deep (Zhurbas et al., 2012) to relatively small-scale synoptic eddies in the Gulf of Finland (Pavelson, 2005). When eddies form regularly, they have a profound influence on the structure of semi-persistent current patterns. For example, their presence may substantially modify the water exchange between the Gulf of Finland and the Northern Gotland Sea (Section 1.2).

Eddy detection from field measurements has been actively studied for the last 40 years (Sadarjoen and Post, 2000; Isern-Fontanet et al., 2003; Chaigneau et al., 2008; Nencioli et al., 2010; Souza et al., 2011). This research has greatly benefited

from technological advances in satellite technology and remote sensing imagery. While it is fairly easy to pick out strong eddy structures using satellite images, it is difficult to define precise boundaries that separate the eddy from the surrounding fluid motion and to track eddies over time due to their transient and highly volatile nature. It is even more difficult to construct reliable algorithms for automatic detection of eddies and to quantify the number and characteristic dimensions of eddies without human interference. However, with an increasing data stream from satellites and numerical models, it is highly desirable to further improve the methods for automatic eddy detection.

The state-of-the-art methods for eddy detection tend to proceed according to one of the two general principles. One class of methods is based on the detection of variations in some physical quantities, such as pressure or vorticity. Relatively strong gradients are required to be reasonably sure that the anomaly represents a persistent structure, so these methods tend to detect the strong, dominant vortex field. Another class of methods relies on the geometric properties of streamlines where the curvature of the streamline is indicative of vortex structures. Additional conditions are often required to avoid multiple detections of the same eddy.

This chapter describes several efforts towards improving automatic methods for the analysis of instantaneous flow fields. A method based on physical quantities, such as strain and vorticity fields, is discussed in Paper C. A hybrid detection method based on a combination of this physical method with a geometrical method that is based on the analysis of the curvature of single streamlines is implemented in Paper D.

2.1. Favourable patterns reducing environmental risks

A commonly accepted notion of risk R_a in natural sciences, engineering and industry (IRM, 2002) is expressed as the product of the probability P_a (of failure or accident) and the properly quantified severity C_a (cost or consequence) of this disaster:

$$R_a = P_a \times C_a. \quad (2.1)$$

The majority of the research in marine traffic risk has focused on the probability P_a (Fowler and Sørård, 2000; Soares and Teixeira, 2001; Goerlandt and Kujala, 2011, to name a few). Although the probability P_a of ship accidents may be made smaller by improving ship design, using better navigation maps and devices, etc., major offshore accidents continue to happen with some frequency. As enormous loads may occur during severe storms or accompany an ice attack (Kujala and Arughadhoss, 2012), it is economically unfeasible to design all the ships to fully resist such forces on all occasions. Moreover, contemporary ships or offshore structures are such complicated systems that even minor errors in their design (e.g., Collins et al., 1997), defects in their production, highly unlikely sequences of events in their operation (Anonymous, 2013) or human error or misbehaviour may

result in a significant failure. For the listed reasons, the use of the notion of risk in Eq. (2.1) is gradually increasing in the analysis of the potential impact of ship traffic (Montewka et al., 2011).

The methods used for the estimates of the damage and for the quantification of the risk R_a vary largely (Montewka et al., 2013). I only address the environmental damage to the nearshore and use the (piecewise) constant cost function C_a of the potential consequences. The analysis is mostly performed from the viewpoint of minimising environmental damage caused directly or indirectly by ship traffic. A specific feature of many accidents at sea is their large impact range (Soomere, 2013). Transportation of dangerous goods by rail or road is usually organised by avoiding sensitive (e.g., urban) areas and/or driving at specific time intervals (Kara and Verter, 2004). This approach is not directly applicable to the shipping and offshore industry. A major marine accident is often associated with a release of oil that may hit an area at hundreds of kilometres from the accident site. This feature severely complicates the process of minimising the impact of a potential disaster by preventively optimising the possible accident site. The problem is relatively simple for stationary objects like oil platforms, but in the case of fairways, the challenge is to provide a non-stationary (ideally, real-time) smart choice of a sailing line that minimises environmental risks.

A key requirement for the reduction of risk for ship traffic through decreasing the cost of consequences C_a is the existence of certain favourable patterns of the distribution of the relevant damage. In principle, any favourable pattern (cf. Stokstad, 2009), including patterns of currents or current-induced transport, may be used for this purpose. For example, jet currents can be used to reduce fuel consumption (Lo et al., 1991) or sea areas with lower waves can be used to decrease the risk of wave damage (Kite-Powell, 2011).

The most impressive patterns in the World Ocean are persistent currents such as the Gulf Stream, Kuroshio Current or Agulhas Current. Their potential for the reduction of coastal pollution is similar to the impact of wind and waves: the least harmful source is the one that is located maximally upstream from the vulnerable domain. Recent findings have opened a way for further progress in the practical use of current patterns: several semi-persistent patterns of currents, with a typical lifetime from weeks to a few months, have been recently identified for different areas of the Baltic Sea (Lehmann et al., 2002; Meier, 2007). The material presented in Chapter 1 reveals that the Gulf of Finland, where the currents were believed to be mostly chaotic and highly variable both seasonally and annually (Alenius et al., 1998; Soomere et al., 2008), also possesses persistent patterns at certain depths (Andrejev et al., 2004a).

A study of transport properties of numerically simulated surface currents in the Gulf of Finland using Lagrangian trajectories of test parcels similarly to the method described in Chapter 1 led to the identification of semi-persistent patterns (Soomere et al., 2011). The presence of strong meridional transport with a lifetime of a few weeks (Figure 3) in specific regions was particularly interesting. These

patterns, usually hidden or masked by the complexity of the instantaneous fields of currents, may essentially modify the transport of potential adverse effects.

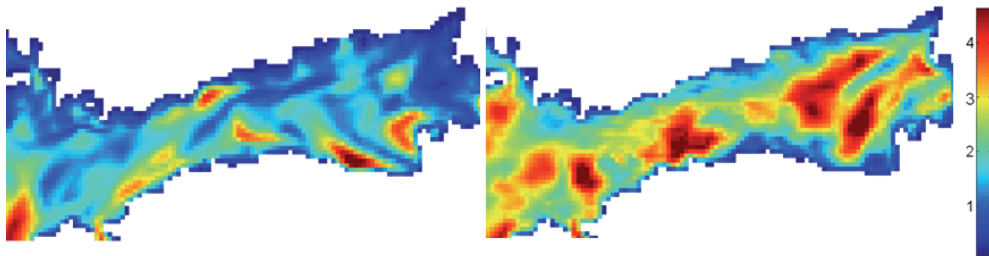


Figure 3. Average meridional transport (cm/s) for March to April in 1987 (left) and for September to October in 1988 (right) by Soomere et al. (2011).

2.2. Patterns in strain and vorticity fields

The material presented in Section 2.1 suggests that certain (normally concealed) patterns of current-induced transport constitute a frequent feature of the study area. This raises the question about simple methods for at least qualitatively recognising their presence based on widely used and easily computable parameters of the flow field. Paper C makes an attempt to determine certain concealed features of current fields and the associated transport using the Okubo–Weiss (OW) parameter. Its variations characterise the spatial patterns of strain and relative vorticity. As these quantities are likely to deviate from their background values in the regions of semi-persistent patterns, this parameter has a clear potential for the quantification of certain flow patterns and for the identification of certain semi-persistent structures without relying on the technique of Lagrangian trajectories. The purpose of Paper C is to determine to what extent the transport structures revealed in earlier results (e.g., Soomere et al., 2011) are reflected in the structure of fields of strain and relative vorticity.

The properties of surface currents are analysed in Paper C by considering how the velocity gradients at each model grid cell contribute to volume deformation (strain) and rotation (relative vorticity). The method is based on the work by Okubo (1970), who analysed the dispersion at the ocean surface by looking at the shape of the trajectories of pairs of parcels, and by Weiss (1991) on the enstrophy dynamics in 2D flows. In both approaches, the topology of particle trajectories and the basic features of the time evolution of vorticity gradients are defined by the sign of the OW parameter (Okubo, 1970)

$$W = s_n^2 + s_s^2 - \omega^2. \quad (2.2)$$

Here s_n and s_s are the normal and shear components of strain, respectively, and ω is the relative vorticity:

$$s_n = \frac{\partial u}{\partial x} - \frac{\partial v}{\partial y}, \quad s_s = \frac{\partial v}{\partial x} + \frac{\partial u}{\partial y}, \quad \omega = \frac{\partial v}{\partial x} - \frac{\partial u}{\partial y}. \quad (2.3)$$

The sign of the parameter W shows whether a flow region is strain-dominated ($W > 0$) or vorticity-dominated ($W < 0$). Large strain values occur at the boundary between water masses moving with different speeds, whereas high values of vorticity indicate substantial rotation and thus the presence of eddies.

The calculations of the OW parameter from the horizontal components of flow velocities (u, v) were performed for the Gulf of Finland based on simulations by O. Andrejev and A. Sokolov in the BONUS+ Baltic Way cooperation using the numerical model OAAS (Andrejev and Sokolov, 1989, 1990; Andrejev et al., 2010) with a horizontal resolution of about 1 nautical mile and a vertical resolution (thickness of layers) of 1 m. The model principles, setup and forcing are described in Section 1.3. The resolution of 1 nautical mile is sufficient to resolve most of the mesoscale effects in this water body where the baroclinic Rossby radius is mostly 2–4 km (Alenius et al., 2003).

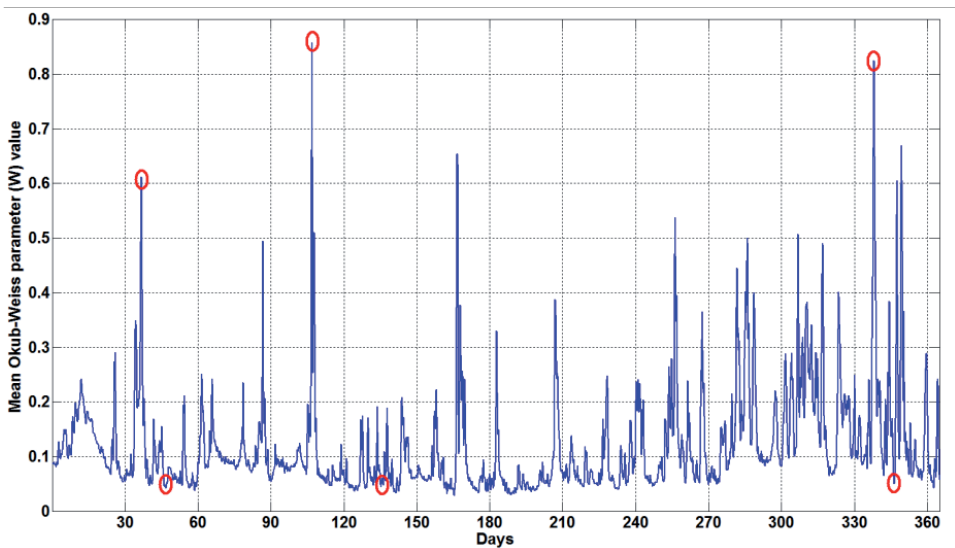


Figure 4. The Okubo–Weiss parameter averaged over the entire computational domain for each 3-h period. Results are presented for the year 1987. Red circles indicate time instants corresponding to panels shown in Figure 5.

The temporal course of the average OW parameter for the entire computational domain at 3-h time intervals (Figure 4) indicates that the currents are, on average, strain-dominated. Within short extreme events the typical values of this parameter (about 0.1) can increase by a factor of 10. Such events of large W occur more frequently at the end of the year, that is, during the typical windy autumn–winter season. Interestingly, the extreme values of W do not correspond to extreme wind speeds. Moreover, there is effectively no correlation between the OW parameter

and wind speed or direction (Paper C). This is surprising as the common opinion is that the dynamics of the Gulf of Finland is wind-dominated (Elken et al., 2003, 2014; Soomere and Myrberg, 2013) and once more indicates the complexity of the dynamics of this water body.

The maps of the OW parameter for single time instants (Figure 5) reveal extensive spatio-temporal variations in the structure of surface currents. Several maxima and minima of W are clearly linked to topographic features, coastal regions and/or islands in the eastern part of the Gulf of Finland. The runoff from the Neva River functions as a permanent source of strain in the eastern part of the gulf.

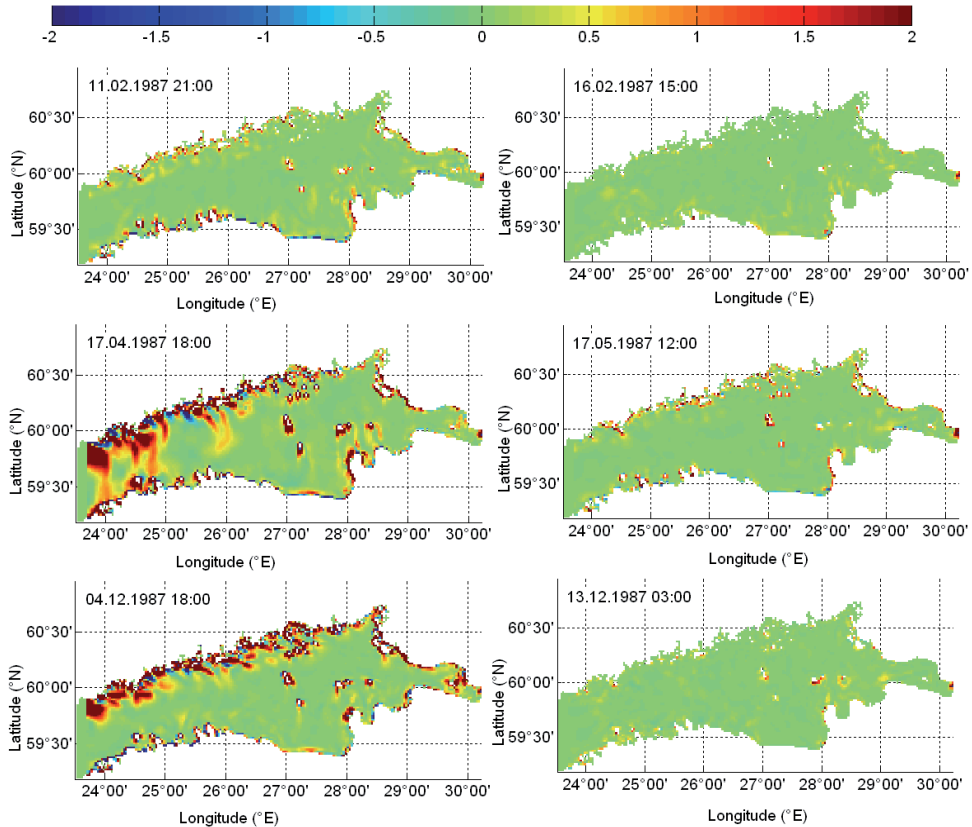


Figure 5. Spatial distribution of the Okubo–Weiss parameter in the Gulf of Finland during the windy (top and bottom pairs of panels) and calm (middle pair of panels) seasons. The panels on the left correspond to time instants with large peaks in average W (Figure 4), while the panels on the right correspond to time instants with relatively low average W . Red colour indicates strain-dominated and blue colour vorticity-dominated areas.

Whereas zones of high vorticity are, as expected, prominent near the coast, the areas hosting considerable strain are at times prominent also in the offshore domains of the Gulf of Finland. Such areas are most pronounced in the western

part of the gulf where they are mostly oriented in the north–south direction and indicate the possibility of rapid transport of water masses across the gulf similarly to the areas of rapid meridional transport (Figure 3). These areas evidently start to develop in the nearshore (similarly to strong upwellings) and may persist in the same region for several days. Unlike upwelling filaments (that usually contain colder water penetrating far offshore), such filaments of strain more likely represent offshore directed Ekman currents preceding the upwelling events. Alternatively, the pattern of areas with large strain between Tallinn and Helsinki may indicate the border between water masses moving at different velocity. Remarkably, such patterns persist for more than a week even in the calm season (Paper C).

Thus, patches of strong strain and relative vorticity regularly occur at two types of locations: (i) along the coast, probably due to topographic effects and coastal current fluctuations and (ii) in specific offshore areas near the mouth of the Neva River and in the north-western narrow part of the Gulf of Finland. Although evolving over time and at times extending into filaments that span from coast to coast, they stay permanently connected with the regions of their origin. This feature may indicate the presence of a semi-persistent (or often occurring) front between water masses with different properties, with a possible origin, for instance, from a strong upwelling or the presence of different gyres in the eastern and western parts of the Gulf of Finland. The net result is the region of highly volatile currents between Tallinn and Helsinki.

2.3. Methods for automatic detection of eddy structures

The OW parameter has been widely used to detect eddies in the ocean (Isern-Fontanet et al., 2004). Their cores and the locations of strong meanders of jet currents correspond to large negative values of W . Almost rectilinear shear flows may result in large positive values of W on a few occasions, for example, in the domains with strong shear such as the seaward border of the coastal currents, around separated jet flows through an otherwise relatively quiet sea area (e.g., penetration of upwelling filaments in the offshore direction) or contact areas of jets flowing in opposite directions. High positive values of W occur in contact areas of large-scale gyres and at relatively narrow entrances to basins such as the Gulf of Finland where the border area between the inflow along one coast and outflow at the other coast may develop large horizontal shear (Section 2.1, Myrberg and Soomere, 2013). Finally, high positive values of W are also characteristic of areas of intense divergence or convergence, independently of the sign of the phenomenon. Such areas are found in the World Ocean as the major convergence zones (Martinez et al., 2009). At smaller scales they may become evident as regions hosting strong local up- or downwelling.

A potential weakness of the OW method is that it relies on locally evaluated quantities. The method is thus less able to detect large-scale, weak vortices (Sadarjoen and Post, 2000). For the automatic detection of such eddies, the winding angle (WA), geometrical detection method is often more suitable.

According to the WA method, the vortex exists when instantaneous streamlines mapped onto a plane normal to the vortex core exhibit a roughly circular or spiral pattern (Robinson, 1991). The WA method characterises an eddy structure by a point that defines its centre and by a closed streamline corresponding to the eddy edge. The inner points bordered by this contour line belong to the eddy and determine its surface area.

Let us consider a 2D streamline beginning at point P_1 (Figure 6) and consisting of several segments with a length corresponding to the grid step. The winding angle of the streamline corresponds to the cumulative sum of the angles between all pairs of consecutive segments

$$WA = \sum_{j=2}^{N-1} \langle P_{j-1}, P_j, P_{j+1} \rangle = \sum_{j=2}^{N-1} \alpha_j, \quad (2.4)$$

where $\langle P_{j-1}, P_j, P_{j+1} \rangle = \alpha_j$ denotes the angle (with sign) between the segments $[P_{j-1}, P_j]$ and $[P_j, P_{j+1}]$. Positive values of α correspond to counterclockwise-rotating curves and negative values to clockwise-rotating curves. A streamline is associated with an eddy if $|WA| \geq 2\pi$.

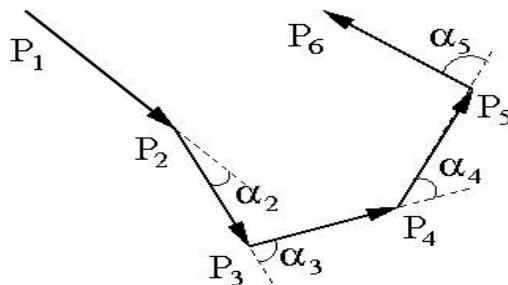


Figure 6. The winding angle (WA) method for a segmented streamline.

2.4. Coherent structures in the Gulf of Finland

Being slightly more successful in finding eddies than the OW method, the WA method reduces the total number of detected eddies (Chaigneau et al., 2008; Souza et al., 2011). However, the OW method is computationally efficient and easy to use, so it is attractive when a large number of velocity fields are analysed. In order to apply positive sides of both methods, I make an attempt to investigate velocity fields with a hybrid winding angle (HWA) method, where the OW method is first used to detect potential eddies and the WA method is used locally within these regions to test and improve the OW result. This approach substantially reduces the number of streamlines required for the WA analysis and makes the detection procedure more efficient.

The HWA method was applied to two domains, the patterns of currents in which were calculated using two different circulation models. The first domain was the Gulf of Finland. The 3D field of currents in this basin was the same as in Section 2.2.

The second domain (not shown here, see Paper D for details) was an archipelago coastal area Vatllestraumen south-west of Bergen, Norway. For this region the horizontal components of surface flow velocities (u, v) were obtained using the Bergen Ocean Model. This model was run on a rectangular regular grid with a step of 20 m in both directions (435×525 grid cells in the domain) and it used terrain-following vertical coordinates with 32 layers. The integration time step was 1.5 s. The simulations covered four days (16–20 January 2004). The first 24 h were used to spin up the model and simulation results were recorded from 17 January. The model used a non-hydrostatic formulation, and Smagorinsky and 2.5 Mellor–Yamada turbulence schemes for the horizontal and vertical momentum equations, respectively. The water level at the northern and southern boundaries of the domain was derived from astronomical tides with six components. The water level at the boundary of a narrow channel leading to an internal bay was set to a constant value (Paper D).

A total of 220 high-vorticity regions, potentially indicating the location of the cores of single mesoscale eddies, were identified in the Gulf of Finland by the OW method (Paper D). A streamline analysis was performed in the same domain, by choosing the points in the identified high-vorticity regions as starting points for the streamlines. The curvature of resulting streamlines was quite small (that is, the streamlines were almost straight). As a result, the HWA method was not able to detect any eddies within the areas that were highlighted as vorticity-dominated ones by the OW method in the Gulf of Finland.

Unlike the OAAS model and the Gulf of Finland, both the OW and HWA methods showed good results for the Vatllestraumen area. The OW method successfully identified regions of potential eddies and the HWA method highlighted single eddies in these regions. The number of potential eddy regions according to the OW method during a 12-hour-long simulation was in the range of 83–305. Using the HWA method, 16–132 single eddies were identified in these regions (Paper D). Although the subsequent eddy detection by the HWA method substantially reduced the number of eddies, there is a reasonable match between the HWA and the OW results and the number of individual patches for the Vatllestraumen case study (Paper D).

The output of the HWA method requires additional analysis since more than one streamline may identify the same eddy structure. To avoid duplication, the streamlines that identify the same eddy must be clustered together. Quite likely the OW parameter already provides sufficient clustering information, indicating that the streamlines which started within each region identify the same eddy structure, but this hypothesis needs further testing.

The presented comparison is intriguing because it is not clear why almost no distinctly identifiable eddies occur in the output of the eddy-resolving OAAS

model with a resolution of 1 nautical mile. A possible reason is that even this resolution is not sufficient for replication of long-living eddies in this area. Alternatively, the flow structure highlighted by the HWA method (Figure 7) suggests that the circular structure of eddies may be often distorted or masked by certain filaments formed in the surface layer.

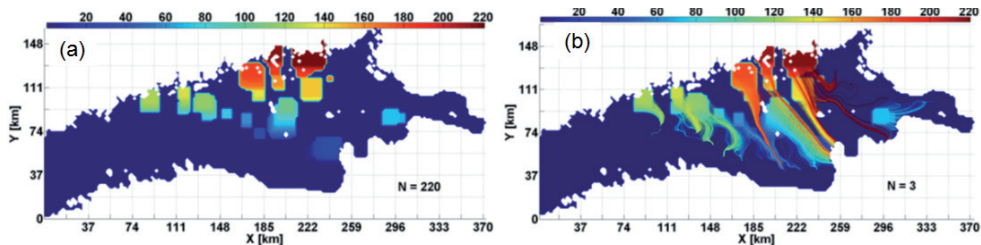


Figure 7. Detection of flow structures in the Gulf of Finland for 1 nautical mile surface velocity data on 17 December 1987 at 18:00. Panels show results for (a) the Okubo–Weiss and (b) the hybrid winding angle method.

This feature is not present in the simulations for Vättestraumen that contained a reasonable amount of eddies, although localised in specific regions, indicating that the model region is sufficiently resolved and the model parameters are adequate for the reproduction of small scale flow features.

The results confirm that the use of integrated measures of the internal structure of current fields such as the OW parameter may reveal certain otherwise hidden features of the motion of water masses. Although the OW parameter reflects, in essence, local properties of the surface-layer flow, its spatial distributions provide certain additional information about the transport of water masses that cannot be identified directly from the Eulerian or Lagrangian velocities. The analysis of the OW parameter alone only allows identification of patterns of transport similarly to Soomere et al. (2011). Its direction has to be specified from Eulerian velocities.

The presented results are consistent with the outcome of studies performed using Lagrangian trajectories (Soomere et al., 2011). Note that the two sets of results are not entirely independent. They both rely on the output velocity fields from 3D hydrodynamic models driven by the same wind data. The analysis here used the output from the 1 nautical mile OAAS model, whereas Soomere et al. (2011) used velocity data with a resolution of 2 nautical miles of the RCO model. They both highlight a pattern of pathways of surface waters perpendicular to the gulf between Tallinn and Helsinki and in the north-western Gulf of Finland. Another (less pronounced) pattern seems to exist in the eastern part of the gulf, near the mouth of the Neva River (where a similar pattern has been found in simulations of the flow compressibility, Kalda et al., 2014). More generally, the results suggest that the cross-gulf transport and hence the risk of coastal pollution in this area is very variable and apparently can be reduced by a smart choice of the fairway.

3. Modelling the equiprobability line

The existence of quasi-persistent patterns of currents in the Baltic Sea (Lehmann et al., 2002; Andrejev et al., 2004a, 2004b; Osiński and Piechura, 2010) and associated pathways of the current-driven transport (Soomere et al., 2011), discussed in the previous chapter, is a precondition for a sensible use of marine dynamics for the reduction of environmental risks stemming from shipping and offshore and coastal engineering activities (Soomere, 2013). A generic example of vulnerable areas is the nearshore that usually has the largest ecological value. For this reason I perform the following analysis focusing on the probability that adverse impacts passively driven by surface currents hit the coast or the nearshore area. Such occasions are called coastal (or neashore) hits.

A key question for elongated sea areas is how to minimise the joint probability of hitting either of the surrounding coastal sections. A first-order solution is the equiprobability line (introduced in Paper A), from which the probability of propagation of pollution to either of the coasts is equal. For some regions there may also appear an area of reduced risk, from which the propagation of pollution to any of the coasts is unlikely. The safest fairway would thus follow either the equiprobability line or the areas of reduced risk. This problem is addressed in Paper A in the context of the Gulf of Finland, using a large pool of Lagrangian trajectories of test parcels constructed based on the output of the RCO model.

The sensible use of this technology, however, requires not only adequate estimates of the persistency and variability of the quasi-persistent patterns and visualisation of their impact, but also of the confidence and uncertainty related to their practical use. These questions are addressed in Chapter 4.

The credibility of the results obviously depends on the choice of the governing parameters for the trajectory calculations such as the initial location of test parcels, the duration of single trajectory simulations, the number of trajectories involved for each calculation session, etc. For this reason, this chapter first presents a short description of the modelling environment, spatial and temporal scales necessary to be covered in such simulations in order to reach representative results in the context of the Gulf of Finland, requirements for the basic parameters of the calculations such as the width of the coastal zone and the duration of trajectory calculations, the range of time scales for which semi-persistent patterns may be important in this basin and the sensitivity of the results to the choice of the time lag between subsequent trajectory simulations based on Paper B.

3.1. Model parameters

An adequate representation of statistical features of Lagrangian transport using trajectories of single water (or pollution) parcels requires the use of a sufficient number of uncorrelated trajectories. The number of simultaneously calculated independent trajectories is implicitly limited by the number of grid cells that cover the study domain. Especially in non-spreading simulations (Section 1.4)

trajectories for parcels selected at different locations of a single cell and then reconstructed from modelled velocity data tend to be highly correlated during a long time. The reason is that the trajectory model has no information about what direction and how rapidly the real drifters would move under the impact of subgrid processes. A formal solution would be to mimic the spreading of trajectories in the real ocean, e.g., by inserting a random disturbance to each trajectory (e.g., Andrejev et al., 2010, 2011; Kjellsson and Döös, 2012). Doing so may adjust certain statistical features of ensembles of trajectories but evidently would not improve the match of simulated trajectories with pathways of real drifters. In other words, improving the estimated transport speed or dispersion is counterbalanced by a loss of transport direction and possibly other properties (Kjellsson and Döös, 2012; Kjellsson et al., 2013). The relevant questions are discussed in Paper G and Chapter 4.

The best way to increase the number of independent trajectories is to increase the spatial resolution of the ocean model. This is not always possible because of computational restrictions. The dependence of the properties of surface-current-driven transport of parcels from offshore areas to the nearshore on the resolution of the circulation model was analysed by Andrejev et al. (2011) using a resolution of 2, 1 and 0.5 nautical miles and otherwise identical setup and forcing. The spatial distributions of hits to the nearshore were found not to be particularly sensitive with respect to the resolution of the circulation model.

An important requirement for properly quantifying Lagrangian statistics is the length of the time interval covered by simulations and the homogeneity in time of the wind information. The cumulative values of the probability of coastal hit and the particle age (see Chapter 4) vary substantially within the first seasons of calculations. They reach an almost constant level after about 3–4 years in the Gulf of Finland (Andrejev et al., 2011). Therefore, it is necessary to cover, at least, 5 years in order to reach an acceptable estimate of the ‘climatological’ values of these measures in this basin.

A feasible way of raising the number of independent trajectories is to increase the time interval covered by the circulation modelling that provides the basis for the cumulative values indicated in the previous paragraph. However, the pattern of hits may change on longer time scales if there is a shift in the wind climate. Moreover, in several occasions long-term ‘climatologically valid’ distributions are almost meaningless. For example, for the south-western Baltic Sea two radically different regimes of the current-driven propagation of adverse impacts were identified: one for the typical inflow and another for outflow conditions (Lu et al., 2012). The fields of currents in this part of the Baltic Sea exhibit not only extensive seasonal variation but also a completely different structure during the inflow and outflow events (Lu et al., 2012). In such areas it is thus important to verify the results against a much longer history of currents over a few decades in specific regions. An attempt at this direction is made in Paper G for the Gulf of Finland.

Another sensible way of increasing the number of independent trajectories is therefore to repeat the calculations with a certain time lag. As the surface drift

speed in the Gulf of Finland is typically 10–20 cm/s (Kõuts et al., 2010; Soomere et al., 2011) and the currents are normally strongly circularly polarised (Lilover et al., 2011), a parcel usually moves only a few kilometres a day from its original location. Therefore, only these trajectories that start at least a couple of days after the previous one (in the case of the 2-mile RCO model) can be treated as independent ones. The use of this approach means that in order to minimise the uncertainty and to obtain reliable results, the simulations must be performed and optionally averaged over many small time intervals. The key time scales are the lag between subsequent simulations and the duration of the trajectories in time. In the context of statistics of simulated pollution transport, the basic requirement is that a significant number of pollution parcels reach the vulnerable area.

Formally, the overall procedure is as follows (Paper A). First, the initial locations of a certain number of water parcels (interpreted as carrying an adverse impact) are specified. The time interval of interest $[t_0, t_0 + t_D]$ with duration of t_D (usually ≥ 1 year) is divided into time windows of fixed length t_w . The paths (trajectories) of the parcels (interpreted as current-driven propagation of the adverse impact) are simulated over successive time intervals t_w , which may be overlapping. The lag between these windows is t_s (Figure 8). The resulting trajectories for each time window are saved for further analysis.

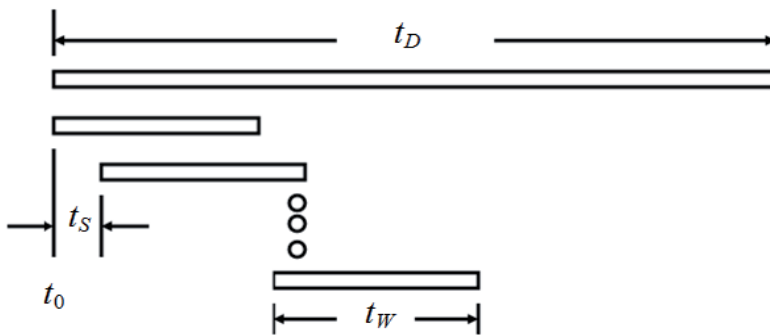


Figure 8. Splitting the simulation period into time windows.

The trajectories of water parcels depend on their initial locations, starting instant and the length of the time window. The choice of the time interval $[t_0, t_0 + t_D]$ may also substantially affect the results as demonstrated in Paper A on the example of monthly and seasonal variations in the properties of certain sets of trajectories. The choice of the time lag and the initial locations of the particles apparently have less impact on the results but may still affect the reliability of the conclusions.

3.2. Quantifying the nearshore and time scale for coastal hit

A central feature in calculations involving the immediate nearshore (e.g., of potential beaching of oil pollution) is how the vulnerable area is defined (e.g., Broström et al., 2011). This is less important when the vulnerable region extends to offshore where the presence of the coast does not directly modify the flow (Delpêche-Ellmann and Soomere, 2013a, 2013b). It becomes, however, decisive when the vulnerable area is the coast itself. The circulation models usually apply a no-flux condition at the bottom and land boundaries (Cushman-Roisin and Beckers, 2011; Meier and Höglund, 2013; Torsvik, 2013), hence the normal velocity component at these boundaries vanishes and must be strictly zero at all grid points adjacent to the model coastline.

This approximation often suppresses the numerically computed landward velocity (consequently, also the onshore motion of selected parcels) already at some distance from the model coastline. Therefore, the longshore drift may or may not be realistically represented in the model, but this sort of reduction of the landward advection of parcels is clearly a model artefact. The trajectories simulated by the non-spreading version of TRACMASS (which fully follows the precomputed velocity fields) are definitely influenced by this effect close to the coast and the probability of hitting a nearshore area may be underestimated. A viable option to account for this effect is to associate the vulnerable nearshore or coastal areas with grid cells located at a larger distance from the coastline.

The definition of the coastal zone is tightly related to the problem of an adequate choice of t_w (Paper A). As the potential side effects, connected with boundary effects in the nearshore, are evidently most pronounced for the parcels released relatively far offshore, the relevant simulations (Paper B) are performed for parcels initially placed in the middle of the Gulf of Finland. The trajectories were started from the centres of 93 cells along a straight line roughly representing the centreline of the gulf (Figure 9). The simulations were started at midnight each calendar day in 1987. This year as well as the five-year period 1987–1991 were quite typical in terms of wave intensity (Broman et al., 2006; Soomere et al., 2007) and thus also in terms of wind-driven energy supply to water masses. There were no exceptional storms in this year and the annual mean wind speed at Utö (Broman et al., 2006) and at Kalbådagrund (Figure 9) were just a few per cent lower than the five-year average for 1987–1991. Numerical experiments with the use of $t_w = 20$ days (Paper A) suggest that in many cases the trajectories first enter the nearshore area after about 10 days of propagation. The time window used for calculations of statistics of coastal hits should account for such situations.

Three versions of the nearshore area were specified as zones with widths of 1, 2 and 3 grid cells from the coast, called alert zones 1–3. I tracked whether the parcels entered any of these zones or were carried out of the Gulf of Finland. The border between the gulf and the Baltic Proper was set slightly to the west of Hiiumaa (Figure 9). A hit to each of the three alert zones (or its drift out of the gulf) was counted when a parcel for the first time entered the relevant zone (or left the gulf).

The presence of each parcel in each alert zone (or leaving the gulf) is accounted for only once. This method of counting implicitly means that the parcels that have drifted out of the gulf have never entered any of the alert zones (Paper B).

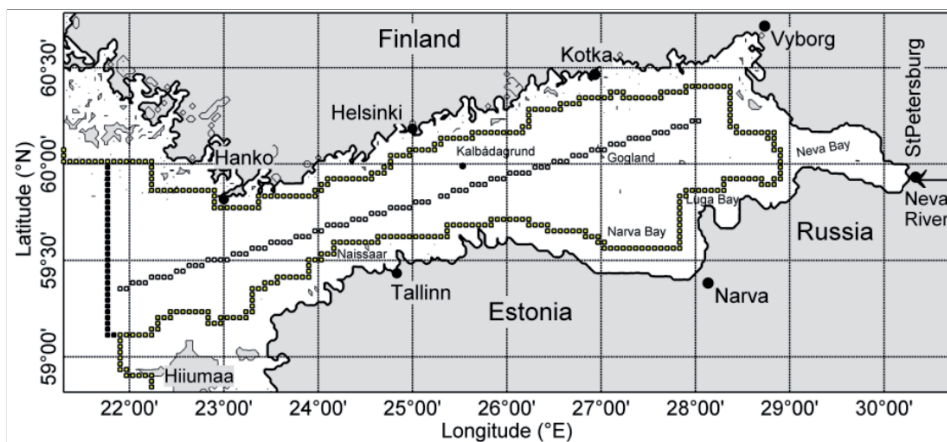


Figure 9. Starting points of trajectories (grey circles located approximately along the centreline of the Gulf of Finland) in simulations of coastal hits. Dark grid points indicate the nearshore area of alert zone 3. The entrance line to the gulf (bold line) is set along 59° N and 21°48' E.

The monthly average number of hits to the alert zones and the share of parcels that left the gulf considerably varied for different seasons (Figure 10). The average probability of entering alert zones 1 and 2 during spring and summer months was very low, about 2% and 4%, respectively, while during windy months it grew up to 20% and 30%, respectively. The annual average probability of entering these zones is about 5% and 11%, respectively.

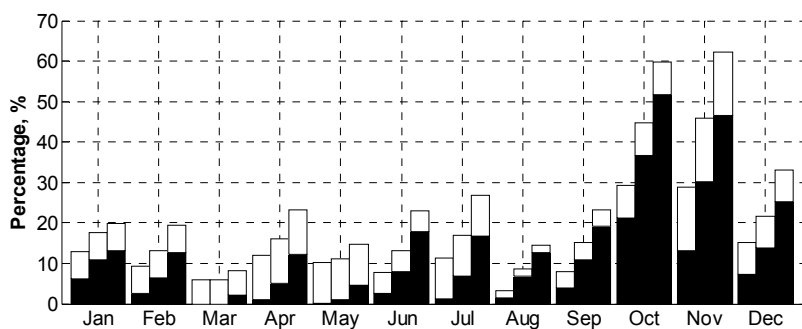


Figure 10. Monthly mean percentage of coastal hits (filled parts of bars) and the parcels leaving the gulf (white parts of bars) in 1987 for $t_W = 15$ days. The left, middle and right bars show the results for alert zones 1, 2 and 3, respectively.

The small probability of entering zones 1 and 2 suggests that the statistics of hits to the nearshore may have quite large uncertainty, especially during spring. A similar seasonal variability becomes evident for alert zone 3. The annual probability of entering this zone was 18% whereas during the windy months almost half of the selected parcels entered this zone. The probability for a parcel to either enter alert zone 3 or to leave the gulf was about 30% on annual average and exhibited extensive short-term variability (Figure 11).

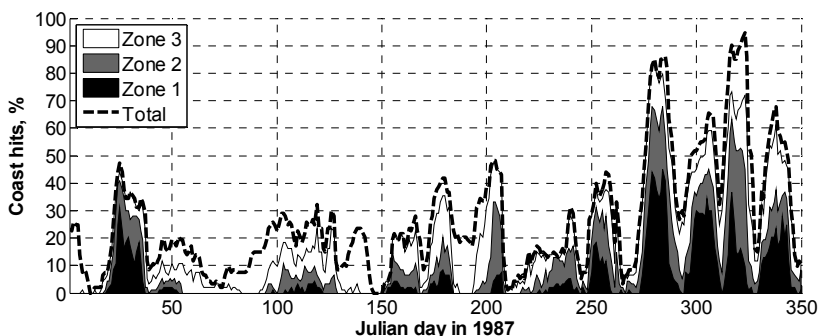


Figure 11. Percentage of hits to the nearshore for $t_w = 15$ days for different starting instants of trajectory calculations in 1987. The dashed line shows the total percentage of parcels that have either hit the coast or drifted out of the gulf.

Probabilities of coastal hits are close to 100% during the windiest periods. Such a great number of hits suggests that the values calculated with the use of alert zone 3 as a specification of the nearshore region, give a realistic representation of transport to the coast for the RCO velocity data. Note that the parcels in this experiment were selected at a maximally large distance from the coasts. For randomly distributed parcels the relevant probabilities are likely much higher.

The typical time over which the parcels reached the nearshore (defined alert zone 3) was evaluated in a similar manner. Test parcels were selected in the middle of the gulf (Figure 9). The simulations were started, as in the previous sections, at midnight each calendar day in 1987 but were performed for 3–13 days. The probability of coastal hits displayed a substantial seasonal variability for all choices of t_w , whereas it was quite large for some relatively calm months (Figure 12; further details are provided in Paper B). The total number of coastal hits grew rapidly within the first 10 days. The increase rate considerably decreased after that but did not stabilise within even two weeks. This feature is not unexpected and basically reflects the complexity of the dynamics of the Gulf of Finland.

During the calmest months (spring and summer), always more parcels were leaving the gulf than hitting the coast. In the windiest months parcels tended to hit the coast rather than leave the gulf. Typically 8–10 parcels left the Gulf of Finland within 15 days (Paper B) and thus their behaviour only insignificantly affected the results depicted in Figure 12. This number, however, suggests that the surface

water exchange between the Baltic Proper and the Gulf of Finland may be much more intense than the overall water exchange in the entire water column (Andrejev et al., 2004b).

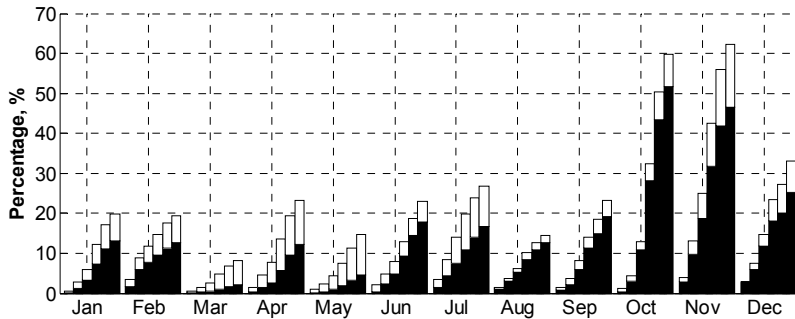


Figure 12. Monthly mean percentage of parcels hitting the coast (black) and leaving the gulf (white) for different lengths of the time window for alert zone 3 in 1987. For each month, columns from left to right show the percentage for $t_w = 3, 5, 7, 10, 13$ and 15 days.

3.3. Time scales for transport patterns

Semi-persistent current patterns have a high potential for the systematic transport of both water masses and adverse impacts such as nutrients, toxic substances or oil pollution between specific sea areas. Their smart use is a feasible way towards the reduction of anthropogenic impact on vulnerable areas by concentrating human activities in the regions, from which the transport of pollution to such areas is unlikely (Soomere and Quak, 2007).

The net transport is defined in Soomere et al. (2011) as the distance between the start and end positions of a trajectory, and calculated using a scheme described in Section 3.1 and an appropriate averaging procedure. The resulting areas of high net transport speed for a single time window largely coincide with areas of large instantaneous current speeds. Such areas are generally different for different time window lengths as the local jets and mesoscale eddies emerge, relocate and decay over time and may have different lifetimes.

An adequate choice of t_w is thus decisive for the identification of pathways of transport of water masses. In order to reasonably account for the potential impact of mesoscale eddies, the relevant time window should not be much shorter than the typical eddy turnover time. Although the values of the internal Rossby radii are relatively well known (Alenius et al., 2003), there exist very little data about the properties of single mesoscale eddies in the Gulf of Finland (Myrberg and Soomere, 2013). Numerical simulations and a few observations available (Soomere et al., 2008) suggest that the typical diameter of their cores is 10–20 km. The maximum current speed may reach 35 cm/s but normally remains between 10 and

20 cm/s. The typical turnover time is about 4–5 days. If one aims at averaging out their impact on the net transport, the relevant time window should cover several turns of typical eddies, that is, at least 15–20 days (Paper B).

A sensible upper limit for t_W in search for semi-persistent transport patterns is such that the net transport speed becomes close to the long-term average current speed (Soomere et al., 2011). For even longer t_W , such patterns will probably be averaged out of the spatial distributions of the net transport speed. The difference in question is estimated for 1987–1991 with the use of variable t_W and a constant time lag of $t_S = 1$ day between the windows. One parcel was selected in each of the 3131 grid cells in the Gulf of Finland. The range of time windows, suitable for identification of semi-persistent current patterns and at the same time capable of reasonably averaging out the potential impact of single mesoscale eddies on such patterns, is 5–15 days in the Gulf of Finland (Paper B).

The estimates of annual root mean square deviations of the net transport speed suggest that for calculations of trajectories and reduced risk areas relatively large values of the time lag may be used without losing the reliability of the results (Paper B). This conjecture comes into importance in optimisation of long-term calculations based on high-resolution simulations (Andrejev et al., 2010).

3.4. Counting hits to the opposite coasts

The problem of the optimisation of fairways in the open ocean in terms of minimising the probability of coastal pollution (quantified here as the probability of coastal hits driven by surface currents) or maximising the time until a coastal hit occurs can be reduced to the question of how far offshore should the fairway be shifted. The situation is radically different in smaller sea areas. One of the key issues in narrow bays and elongated sea areas is how to minimise the probability of pollutant parcels hitting the nearshore on either side of the fairway. The first step towards resolving this problem is to identify a line from which the probability of propagation of parcels to the opposite coasts is equal.

The concept of the equiprobability line is introduced in Paper A. In the relevant calculations the probability of pollutant parcels hitting either of the coasts is interpreted as the measure of the costs of consequences. The entire coastline is divided into two (or more) sections. The probability of propagation of selected parcels from each model grid point to each coastline section is evaluated simultaneously. The equiprobability line connects the points, from which the probability of propagation of parcels to different coastal sections is equal. This option mimics the situation in which the cost function in the risk definition (Section 2.1) is not constant and can be introduced in a straightforward manner for the sea areas like the Gulf of Finland, which are divided between two countries. In Paper A, the southern coast of the Gulf of Finland represents the coastline of Estonia, whereas the coasts of Russia and Finland are merged to represent the

northern coast. Another set of simulations assumed the separation point at the mouth of the Neva River (Paper E).

A measure of risk was calculated using two methods (a direct method and a smoothing method, afterwards referred to as Method I and Method II). Both are based on tracking trajectories using the RCO model output and the non-spreading TRACMASS code. They differ only in how the trajectories are grouped in the evaluation of the probability of parcels hitting a nearshore region. The difference in the resulting estimates of the location of the equiprobability line can be interpreted as a rough measure of the uncertainty of its location. The deviation of this line from the centreline of the gulf characterises the asymmetry of current-driven transport in the surface layer of this basin.

Method I is based on pointwise analysis of what happens with the 10-day-long trajectories (equivalently, time windows of equal length $t_w = 10$ days) for each of $N = 3131$ wet grid cells in the gulf. The trajectories are calculated with the time lag of $t_s = 10$ days for 1987–1991. Four parcels are selected in each grid cell (symmetrically with respect to its centre) at the beginning of each time window. The instantaneous position $[x_{ij}(t), y_{ij}(t)]$ and the minimum distance $\Delta_{ij}(t)$ of the trajectory from the coast (used to estimate whether the trajectory has entered the nearshore) were calculated for the entire time window and for each of the released tracers. Here $1 \leq i \leq N$ is the grid cell number and $1 \leq j \leq 4$ is the number of a parcel in the i th cell. For each cell, a counter reflecting a hit of either of the coastlines was initially set to 0 and switched to -1 , when at least three out of the four parcels reached the northern coastline and $+1$, when this happened to the southern coast within the time window. The map reflecting the relevant average quantity (reflecting the probability of parcels hitting the northern or southern nearshore) $\hat{p} : -1 \leq \hat{p} \leq 1$ for each cell (Figure 13) was calculated using all the counter values reflecting single time windows in 1987–1991.

In order to suppress the possible impact of underestimation of the spreading of initially closely located trajectories and to estimate the uncertainty of the location of the equiprobability line, the risk was recalculated using an implicit local smoothing process (Method II). The wet grid points were divided into clusters of 3×3 grid cells. Now it was tracked whether the majority of nine trajectories from each cluster (one from each cell) ended up at one of the coasts or stayed in the open sea area, depending on which the counter of coastal hits for the central cell was set to either 0 or ± 1 .

The relevant calculations in Paper A and Paper E differ in two aspects. Firstly, the length of the time window t_w is increased in Paper E from 10 to 20 days. Secondly, the separation point of the coast into the northern and southern parts is in Neva Bay in Paper E, whilst in Paper A it was set to the border between Estonia and Russia in Narva Bay at $28^\circ 2' \text{ E}$, $59^\circ 27.5' \text{ N}$.

The resulting distributions depend on a number of parameters used in the calculations. I performed several sensitivity experiments by varying the length of

the time window t_w and the time lag t_s between the time windows. The results were almost insensitive with respect to the variation in the time lag from one day up to ten days, provided the entire time interval of interest t_D was long enough compared to this lag. This feature is not unexpected because the averaging procedure over a pool of time windows suppresses the role of each single distribution. Also, the results showed almost no dependence on the length of the time window, provided it was long enough to cover about 50% of the first hits of the parcels to the nearshore (Paper A).

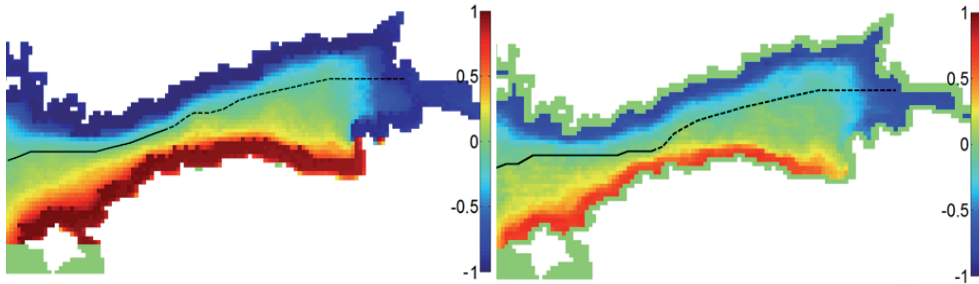


Figure 13. Probabilities of parcels to hit the nearshore of the northern or the southern coast for the years 1987–1991 calculated with the use of Method I (left panel) and Method II (right panel). The red colour indicates high probability of transport to the southern coast and the blue colour – to the northern coast. The green colour marks the location of the equiprobability line (black line) and the areas from which transport to either of the coasts is unlikely (Paper E).

The resulting maps of probabilities of parcels hitting the opposite coasts (Figure 13) are qualitatively similar for both discussed methods and reveal the presence of two basically different areas of the gulf. In the western part there is a narrow area in which the average values $\hat{p} \approx 0$. Parcels that start their drift from this area have no preference of hitting any of the coasts. This region evidently can be interpreted as the location of the equiprobability line.

In the central and eastern parts of the gulf there is a wide area in which $|\hat{p}| < 0.1$ (Paper E). As propagation of parcels from this area to either of the coasts is generally unlikely (Section 4.2), it obviously is an area of reduced risk, located approximately between the Tallinn–Helsinki line and the longitudes of Narva Bay. If such areas are relatively wide, it is natural that they host no well-defined equiprobability line. Instead, they entirely serve as almost safe regions in terms of coastal pollution by adverse hits released from ships and further carried by surface currents. The locations of these areas reveal substantial seasonal variability. To the north of Narva Bay there usually is a high probability of propagation to the southern coast. The equiprobability line is generally located to the north of the centreline of the gulf. A characteristic area occurs to the north of Hiiumaa, stretching almost to the Finnish archipelago from where the transport of adverse impacts to the Estonian nearshore is relatively likely.

The equiprobability line (equivalently, the formal optimum fairway) for Methods I and II is located at the zero-crossing points of the relevant values \hat{p} . These points are well defined in the narrow parts of the gulf that have a large north–south gradient of \hat{p} (see Figure 15 in Chapter 4). A reasonable estimate for the equiprobability line can be obtained from the zero-crossing of the values of \hat{p} smoothed for each longitude in the north–south direction over five subsequent grid cells, using a linear approximation between the smoothed values of \hat{p} at two grid points surrounding the zero-crossing (Paper E). This procedure led to a single clearly defined zero-crossing of \hat{p} for each longitude. The curves consisting of zero-crossing points were comparatively smooth, and no additional smoothing in the east–west direction was necessary. The equiprobability line is located in almost the same position for both methods. The two lines practically coincide between Hiiumaa and the Finnish mainland, differ by 1–2 grid points (3–6 km) in the western and eastern parts of the Gulf of Finland and reach 3–4 grid points (up to 14 km) in the widest part of the gulf to the north of Narva (Paper E).

3.5. Sensitivity studies

The sensitivity study performed in Paper B using the RCO model data for the Gulf of Finland, together with the material presented in Section 3.4, suggests that the basic outcome of the calculations is fairly insensitive with respect to specific model parameters.

An important question not directly addressed in this thesis is whether the coarse ocean model resolution used in the previous calculation may generate some artefacts. For the Gulf of Finland conditions the horizontal resolution of 2 nautical miles is quite coarse in terms of the internal Rossby radius (Section 1.2) and does not reproduce many local bathymetric features. Analysis in Soomere et al. (2011) and Andrejev et al. (2011), however, suggests that the basic parameters of the mean and mesoscale circulation (such as typical flow speeds and the energy balance between mean flow and synoptic eddies) are mostly adequately reproduced and can be used for estimates of the net transport. The temporal resolution of saved velocity data (6 h) evidently distorts to some extent the impact of inertial oscillations, but apparently is fair enough to properly account for single eddies.

Sensitivity of the results to the spatial resolution of the underlying ocean model was thoroughly studied by Andrejev et al. (2011). The problem was addressed based on coupled GCM–Lagrangian trajectory simulations of 10-day-long trajectories calculated for the period of 1 May 1987–31 December 1991 for the Gulf of Finland using the OAAS model (see Section 1.3 for details). Spatial maps for the probability of coastal hits (the probability of parcels selected in the open sea to reach the coast) and for the particle age (the time it takes for these parcels to reach the coast, see Section 4.1 for more details) were evaluated similarly to the distributions calculated in Paper A and Paper E, using three different horizontal resolutions of 2, 1 and 0.5 nautical miles but identical vertical resolution, initial,

boundary and forcing conditions, and trajectory calculation scheme (Andrejev et al., 2011).

This range of resolutions characterises a transition from a poor representation of mesoscale effects by an eddy-permitting model to the one expected to adequately resolve at least the statistical features of the field of mesoscale eddies in the Gulf of Finland (Andrejev et al., 2011). As the dynamics of water masses in the Gulf of Finland is extremely complicated, even the model with 0.5 nautical mile resolution does not perfectly resolve all the small-scale features of water motion (Andrejev et al., 2010).

The resulting maps of the distributions of the probabilities of coastal hits and particle age as well as their basic parameters (such as the average values and standard deviations) were fairly similar for different spatial resolutions. The fields for 1 and 0.5 nautical mile resolutions were particularly close, suggesting that the major features of such fields are fairly universal, provided the circulation model is able to replicate the largest mesoscale features.

There were, however, differences in the location of the optimum solutions for the fairways similar to the deviations described in Section 3.4. The differences between the optimised fairways at the 1 and 0.5 nautical mile resolutions were moderate, but the fairway for the 2 nautical mile model reflected a different pattern of underlying dynamics. A large part of the differences, however, were associated with the presence of numerous smaller islands in the higher-resolution models, which were ignored in the 2 nautical mile model. It was not possible to judge whether the differences were driven by the accuracy of simulations of hydrodynamics and/or whether the accuracy of the representation of the Finnish archipelago played a major role (Andrejev et al., 2011).

As the potential benefit from the use of the optimum fairway only very little depends on the spatial resolution of the ocean model (Andrejev et al., 2011), it is likely that the 2-mile model used in this study adequately replicates the overall appearance of the key distributions and that it gives a satisfactory depiction of the optimum solution for areas far from archipelagos and isolated islands (that are ignored in the ocean model).

4. Preventive methods for coastal protection

The concept of the equiprobability line, developed in Chapter 3, is only suitable for basins with relatively simple geometry. In terms of fairway design it is a local solution that does not usually provide the minimum risk for the entire water body (Soomere, 2013). This chapter starts from a discussion of possibilities of finding a relevant global optimum, either in terms of the probability of vulnerable areas being hit by the pollution released at different sites or in terms of the time it takes for the pollution released at a particular site to reach a vulnerable area (Andrejev et al., 2011; Soomere et al., 2011; Paper E). If a map of such probabilities (or the map of the particle age) has been constructed, the optimum fairway should roughly follow the minima for the probabilities or the maxima for the particle age. It is also straightforward to quantify the ‘cost’ of deviations from the optimum sailing line in these terms and to estimate the geometry of ‘corridors’ of relatively safe operation (Paper E).

In realistic sea areas the probability of different coastal areas being hit by adverse impacts released along the existing fairways and further transported by surface currents may be highly variable. Such variations and possible links between potential release sites of adverse impacts and particular coastal sections are quantified in Paper F for the major fairway in the Gulf of Finland. Paper G demonstrates that these links are almost insensitive with respect to the inclusion of subgrid-scale processes in the Langrangian trajectory model.

4.1. Probability and particle age

The idea to place the fairway along the equiprobability line (so that the average probability of the propagation of adverse impacts from this line to the opposite coasts is equal, Chapter 3) is only directly applicable to elongated basins with relatively simple geometry. An implicit condition for its implementation is that the underlying distribution of costs has a clearly defined ‘zero-crossing’ point for each cross-section of the basin. The use of this concept has obvious problems in multiple connected domains, equivalently, in sea areas hosting islands.

A global optimum for a potentially dangerous activity or for a fairway could be searched in terms of the probability of vulnerable areas being hit by the pollution released at different sites (Andrejev et al., 2011; Soomere et al., 2011; Paper E). An even richer measure in content is the time it takes for the pollution released at a particular site to reach a vulnerable area. This measure naturally characterises the cost of consequences: the longer time the (oil) pollution remains in the open sea, the larger fraction of it may be removed (or will be weathered) before it hits a vulnerable spot. The resulting time is conceptually similar to commonly used water age (Deleersnijder et al., 2001) and is called particle age (Andrejev et al., 2011; Paper E) or residence time of oil at sea (Murawski and Woge Nielsen, 2013).

If a map of such quantities has been constructed, the optimum location of a potentially dangerous activity is where the probability has a minimum or the

particle age has a maximum. The optimum fairway should roughly follow the minima for the probabilities or the maxima for the particle age. It is also possible to construct one measure from these two quantities and to develop the relevant fairway design (Murawski and Woge Nielsen, 2013).

The method based on probabilities of coastal hit (called Method III below) uses the calculation scheme described in Section 3.1 but assumes that the entire coastline is equally valuable (Andrejev et al., 2011; Paper E). Similarly to the analysis in Chapter 3, the nearshore is interpreted as a belt along the coast, three ocean model grid cells wide, and one parcel is selected in the centre of each sea grid cell (3131 cells altogether in the area shown in Figure 14). The counter for each selected parcel and simulation is initially set to 0 as in the calculations of the equiprobability line and is switched to 1 if the parcel reaches any section of the coast within the given time window. Alternatively, the age of each parcel is set as the time elapsed from the start of calculations until the parcel reaches the coast somewhere (Andrejev et al., 2011). I used two versions of the age method for parcels that left the gulf. In Method IVa the age counter is stopped when the parcel leaves the gulf for the first time and its possible reentering is ignored. If the parcel remains offshore until the end of the time window, this counter is set to t_w . Alternatively, this counter is set to t_w for all parcels leaving the gulf (Method IVb, Paper E). The average values of the counters for all parcels are determined, as above, based on averaging over a large number of subsequent time windows (Figure 14).

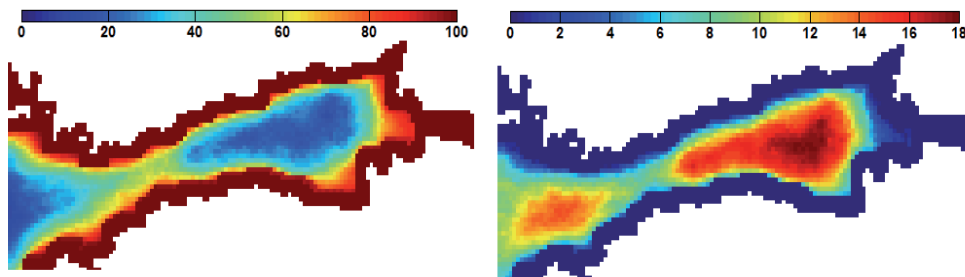


Figure 14. Probabilities of parcels hitting the coast (%), left panel) and particle age (days, right panel) for the years 1987–1991 calculated with the time window of 20 days (Paper E). Although a few islands with a size up to 10 km are located in the eastern Gulf of Finland, their nearshore is ignored in the calculations and only hits to the mainland coasts are accounted for.

As the RCO model grid covers the whole of the Baltic Sea, the dynamics of the entire sea is fully accounted for. However, as no parcels were selected outside the Gulf of Finland, the probability of hitting the coast by parcels selected in the open Baltic Sea is ignored. The field of particle age obviously depends on the treatment of parcels that leave the gulf in Methods IVa and IVb. For example, Method IVb evidently overestimates particle age for these regions of the gulf that encounter

intense water exchange with the Baltic Proper. Interestingly, Figure 15 suggests that Methods IVa and IVb may lead to quite different locations for the optimum fairway not only at the entrance to the Gulf of Finland but also in the entire gulf.

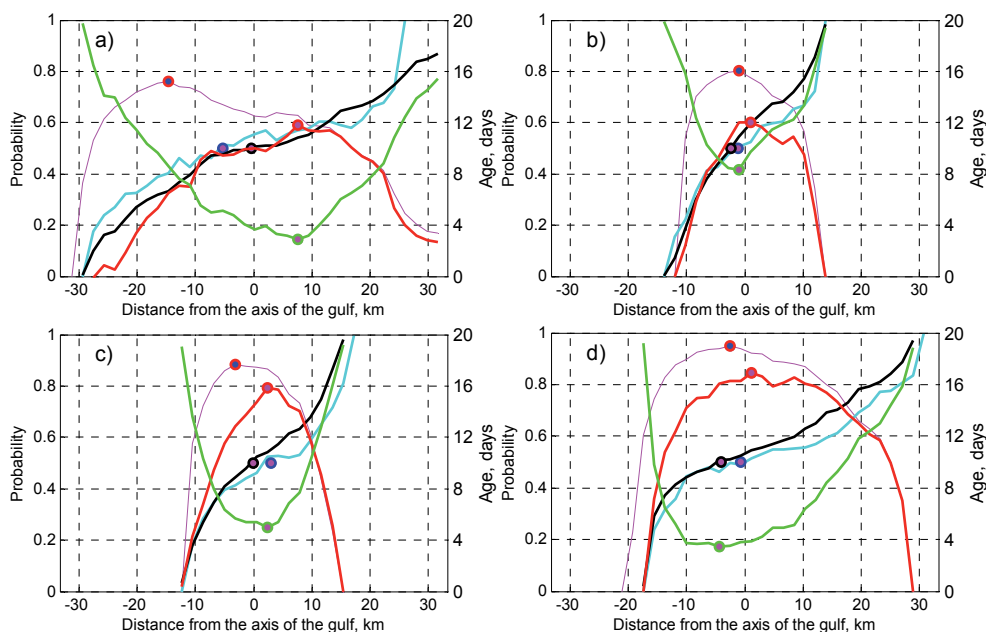


Figure 15. Examples of cross-sections of probabilities for coastal hits (green), particle age (Method IVa, red; Method IVb, magenta) and for the quantity characterising the probability of a hit to the opposite coasts (Method I, black; Method II, cyan; both shown as $(\hat{p} + 1)/2$, where $\hat{p} \approx 1$ and $\hat{p} \approx -1$ mean a high probability of a hit to the southern and the northern coasts, respectively): for the gulf entrance (a), western narrow part (b), middle of the gulf (c) and for the wider eastern part of the gulf (d). Circles indicate the location of the optimum fairway. The location of the cross-section is shown in Figure 16.

The values of all the quantities obviously depend to some extent on the length of the time window. It is likely that modifications to the probability and the quantity \hat{p} caused by an increase in t_w are minor and basically lead to a decrease in the uncertainty in their estimates (Paper B). The average age may substantially increase with the increase in t_w . For this reason, the largest values of particle age considerably exceed those calculated by Andrejev et al. (2011) using $t_w = 10$ days.

4.2. Optimum fairways and safe corridors

The final step of the procedure of risk optimisation consists in specifying the location of the optimum fairway based on the maps of any other convenient measure of the environmental or economic risk (Soomere and Quak, 2013). In this

thesis the quantity \hat{p} , probabilities of coastal hits and particle age are used for this purpose. For regions with complicated geometry and transport patterns, the shape of the relevant distributions and the process of calculation of the optimum fairway may be quite complicated (Andrejev et al., 2011; Murawski and Woge Nielsen, 2013). The described methods (in which the islands are ignored) lead to distributions of the above-mentioned quantities that generally have one local extremum (alternatively, one zero-crossing point of the quantity \hat{p}) for all cross-sections of the Gulf of Finland along latitudes (except possibly for the entrance and the easternmost part of the gulf) (Figure 14 and Figure 15). In other words, the resulting maps provide an elongated ‘trough’ of low values for probabilities or a similar ‘crest’ of particle age. This property makes it possible to use a simple algorithm for finding the optimum fairway that follows this trough or crest.

The latitude for the optimum fairway was found from the analysis of the cross-section of the relevant field along each longitude of the grid cells (Figure 15). The impact of small-scale noise in the underlying fields (especially in the eastern part where the north–south slope in these fields was small) was suppressed by means of smoothing the cross-section over five neighbouring grid points. The centre of the grid cell, corresponding to the minimum or maximum value of the smoothed cross-section, was associated with the location of the optimum fairway. Finally, smoothing these locations over five neighbouring values in the east–west direction led to reasonable locations for the optimum fairway in all cases (Paper E).

The optimum fairways are located somewhat asymmetrically, mostly to the north of the centreline of the gulf. Their average bias from the centreline of the gulf is 2–4 km. Only for Method IVb it is almost 8 km. This distribution is consistent with the slight prevalence of surface transport to the south (Soomere et al., 2011) and apparently reflects the anisotropy of the Ekman transport in the surface layer. As the predominant strong winds blow from the south-west or west, the Ekman transport is mainly to the south-east and the parcels selected in the northern part of the gulf stay offshore for a relatively long time.

The optimum fairways designed based on different criteria may considerably (up to 50 km at the entrance to the gulf) deviate from each other (Figure 15 and Figure 16). In general, they are all located in an immediate vicinity of the centreline of the gulf between latitudes 23°40' E and 26°20' E where they deviate from each other maximally by 10 km. This feature likely expresses the narrowness of this part of the Gulf of Finland, the smallest cross-section of which contains only 15 grid cells. As the nearshore already involves three cells at each coast, less than ten grid cells represent the offshore dynamics of trajectories and relatively steep gradients of the underlying fields in this section are natural. Much smaller north–south gradients of the underlying fields and larger deviations of the optimum fairways from each other occur in wider parts of this water body (Figure 15 and Figure 16). Several relatively extensive meanders in these lines are located at the gulf entrance and in the vicinity of the island of Gogland.

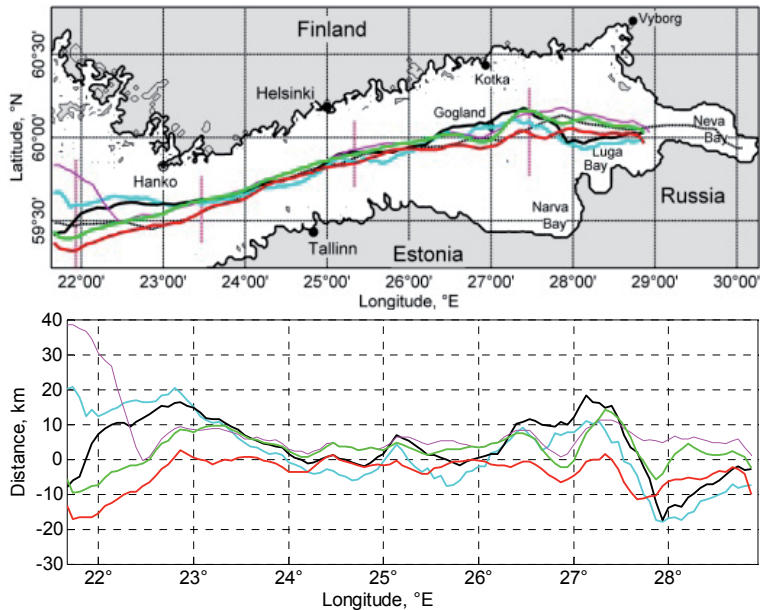


Figure 16. The location of the optimum fairways based on Methods I–IV calculated for the years 1987–1991 with the time window of 20 days. The centreline (the axis of the gulf, zero line in the lower panel) is determined based on sea points of the 2 nautical mile grid of the RCO model and thus does not necessarily exactly follow the geographical centreline of the gulf.

The systematic deviation of the optimum fairways to the north around 27°20' E and a smaller deviation to the south around 25°30' E may be associated with a slow anticyclonic gyre (Soomere et al., 2011). Their large deviation to the south around 28° E is evidently caused by the merging of the runoff of the Neva River with the general cyclonic circulation pattern in the Gulf of Finland (Andrejev et al., 2004a).

The differences between the optimum fairways obtained using different methods (Figure 16) to some extent manifest the uncertainty of this approach (Paper A; Paper E). The maximum deviations between these lines (including the equiprobability line based on Method I) are fairly small, normally below 4 km even in the relatively wide eastern part of the gulf (Figure 15 and Figure 16), and mostly below the resolution of the circulation model. The differences are greatest at the gulf entrance where some of the lines in question deviate up to 40 km from each other (Paper E).

Large systematic deviations of optimum fairways corresponding to Methods IVa and IVb indicate that parcels on the water surface in the northern part of the Gulf of Finland have a good chance of leaving the gulf. Somewhat surprisingly, the difference in the resulting optimum fairways is evident in the entire gulf. This feature may be associated with the overall cyclonic circulation pattern in this water body, which over longer time scales favours the transport of water masses towards the Baltic Proper along the northern coast of the gulf. This example also vividly

demonstrates how sensitive an optimum fairway may be with respect to small variations in the method.

The equiprobability lines estimated using Methods I and II are located relatively close to each other: their bias is only 1.6 km and the root mean square difference is 6.3 km (Paper E). This is expected because they are calculated using a similar concept and with only a slightly different set of trajectories. Note that the great differences between equiprobability lines derived in Papers A and E in the region to the north of Narva Bay are caused by the different choice of the separation point of the northern and southern coasts (where the resulting optimum fairways should head to). All equiprobability lines in Papers A and E show a characteristic deviation to the south in the vicinity of the Tallinn–Helsinki line.

The resulting optimum fairways have quite different meanings in terms of the potential gain. The equiprobability line only shares equally the potential damage between the opposite coasts. The gain from the use of the line estimated from the distribution of the probability of coastal hits can be roughly evaluated in terms of the decrease in the overall probability of such a hit. A convenient measure is the ratio of this probability calculated over the points of the optimum fairway, to the total average probability for the area in question. For the described modelling environment, the average probability for a coastal hit within 20 days is 0.62, whereas the similar average value along the optimum fairway is 0.347. Therefore, the gain may, theoretically, reach 44% in terms of probabilities. In reality, the gain will obviously be smaller because coastal areas with large values of this probability are normally not used for ship traffic (Andrejev et al., 2011).

Similarly, the gain (up to 42.5%) in terms of the average particle age (propagation time of the adverse impacts to vulnerable regions) can be roughly evaluated by means of comparison of the relevant total average over the entire sea area (8.7 days) with the similar average over the optimum fairway (12.4 days). As both values are calculated using 20-day-long time windows, they are considerably larger than the analogous values in Andrejev et al. (2011) where $t_w = 10$ days is used. The potential increase in the propagation time (equivalently, the time available for combating the adverse impact) is still considerable, about 3.7 days. Note that these estimates do not account for the potential lengthening of the fairway (Murawski and Woge Nielsen, 2013).

A convenient measure of the sensitivity of the resulting optimum fairway with respect to possible inaccuracies of calculations is the width of the ‘corridor’ in which the probability for a coastal hit (or the particle age) is allowed to vary to some extent compared to the theoretical extremum. This measure not only provides information about the flexibility of shipping in terms of keeping the environmental risks as low as possible but may highlight sea regions with different nature of current-induced transport. As an example, Paper E provides the relevant corridors of the average width of 15 km. This width corresponds to the increase in the probability of coastal hits by up to 0.029 and to a decrease in the particle age by up to 0.54 days compared to the exact extremum. Similar corridors of the same width of 15 km for the equiprobability lines are defined as the sea area between the lines

corresponding to certain variation in the balance between the probabilities of pollution transport to the opposite coasts. The procedure for the specification of the border lines of these corridors is identical to the one used for the evaluation of the optimum fairways described above (see Paper E for details).

The resulting corridors are quite wide at the entrance to the Gulf of Finland, very narrow in the Tallinn–Helsinki region, widen substantially in the vicinity of Gogland and become very narrow again in the area to the north of Luga Bay. Their minimum and maximum widths are 7.4/9.6 and 29.1/42 km, respectively, for Methods III and IVa. The relevant corridor, estimated using Method I and corresponding to the changes in the threshold value by $\pm 11.2\%$ of the maximum values (± 1), has a minimum width of only 2.1 km (that is, only 20–25% of that for the corridors corresponding to Methods III and IV) in the central part of the bay where the fields of \hat{p} have a steep north–south slope. This slope is moderate in the eastern and western parts of the gulf where the resulting corridor is up to 48.6 km wide (but narrows to 26.2 km near Gogland at the entrance to Neva Bay). The resulting corridor, evaluated using Method II, corresponds to a change in the threshold value $\pm 9.5\%$ of the maximum. It is considerably narrower (down to 1.2 km) in the vicinity of the Tallinn–Helsinki line but reaches a width of over 28 km near Gogland and 37.6 km at the entrance to the Gulf of Finland. Both the corridors largely follow the centreline in the narrowest part of the gulf, but deviate considerably to the north of it in the vicinity of Gogland. The optimum fairways and corridors almost coincide near Hanko but in the entrance area of the Gulf of Finland, the lines and corridors for Methods I and II deviate markedly.

4.3. Frequently hit coastal sections

As suggested in Paper B, the estimates of coastal hits, calculated with the use of alert zone 3 as specification of the nearshore region, give a realistic representation of transport to the coast for the RCO model velocity data. This definition of nearshore (width of about 11 km, 331 grid points, Figure 17) was also employed in studies of possible connections between the sources and sinks of pollution (Paper F). The starting points of the trajectories were chosen roughly, following the typical location of the sailing line of cargo ships from the Baltic Proper to Saint Petersburg. In order to mimic the natural spreading of shipping lines, parcels were selected in a belt covering three model grid cells in the north–south direction. In each simulation one parcel was selected at the centre of each of the 309 grid cells (Figure 17). The simulations cover the time interval 1987–1996 and were performed using the scheme presented in Figure 8 with $t_w = 20$ days and $t_s = 1$ day, similarly to simulations in Paper A, Paper B and Paper E. The total number of time windows used during each 5-year interval was 185 and resulted in 57 165 single trajectories.

Although the annual mean probability of coastal hits showed certain variability (from 25.9% in 1987 to 42% in 1995), the 5-year average values (32.9% for 1987–

1991 and 34.2% for 1992–1996) insignificantly differ from the average of 33.5% for the entire decade. The short-term variability of Lagrangian transport in the surface layer of the Gulf of Finland is so extensive that no adequate conclusion can be made based on one particular simulation (Papers A and B). This conjecture is also true on monthly scales (Paper F). Simulation results for single months (January 1987–1991) show extensive interannual variability of the monthly mean patterns of transport. For example, in January of 1988 a section of the northern (Finnish) nearshore, to the east of Helsinki, was the most affected one but in all other years the southern (Estonian) nearshore received the majority of hits. Results for different months of the year of 1990 demonstrate that the system has also a strong seasonal variability in both the percentage of hits and the particular area of hits.

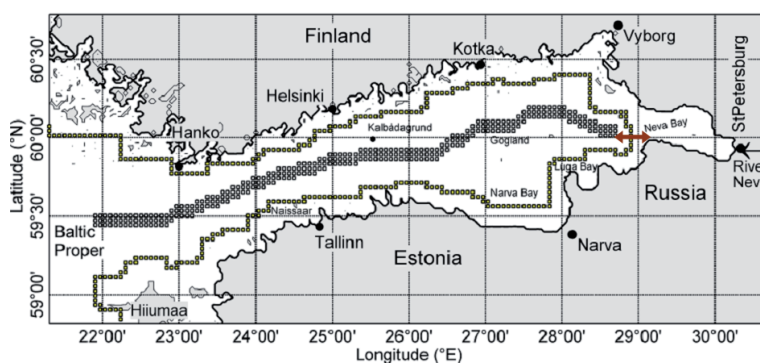


Figure 17. Initial location of selected parcels and the border of the nearshore in the Gulf of Finland. The double arrow indicates the separation point of the ‘southern’ and ‘northern’ parts of the nearshore in Figure 21.

Some features were still present in all months. The north-eastern nearshore of the gulf, from the entrance to the Neva Bay to Vyborg, had a large probability of being hit in January of all years. The most frequently hit areas during different months largely coincided with those that were hit in January. The typical number of hits per nearshore point was 1.5–2 for January of different years. The most frequently hit sections normally received 9–11 hits (Paper F), that is, about five times as many as the average. Also, the alongshore variation in the frequency of coastal hits was on the same level for different months.

More distinct patterns became evident on seasonal scales. The number of hits was highest, as expected based on Paper B, during the windy season and slightly less during windy to calm and calm to windy seasons (Paper F). During the calm season a few frequently hit areas occurred also between Tallinn and Narva and near Kotka. The northern nearshore of the Gulf of Finland was frequently hit only during the windy and the autumn (calm to windy) transitional seasons. The most frequent nearshore hits occurred between Hanko and Helsinki and in a short section to the south of Vyborg (which received many hits throughout the year, although

their number was somewhat smaller in July). The most affected section of the southern nearshore was in the vicinity of Tallinn (Paper F).

The averaged results for single years in 1987–1991 reveal a clear configuration (Figure 18). Hits to the nearshore are most frequent in the eastern part of the gulf, to the south of Vyborg. Simulations in Andrejev et al. (2004a) suggest that a powerful and persistent flow, possibly partially driven by the discharge from the Neva River, exists in the sub-surface layer (depths 2.5–7.5 m) from the entrance to the Neva Bay until the longitude of Vyborg. This intense flow may entrain the uppermost layer (Gästgifvars et al., 2006), redirect the surface-current-induced transport to the west and in this way implicitly protect that coast from being polluted by sources along the fairway (Paper F).

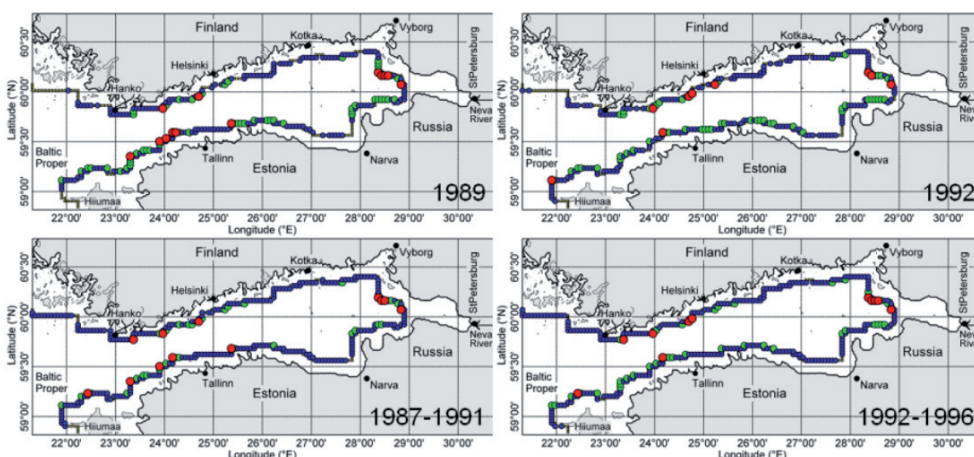


Figure 18. Annual average map of the most frequent hits to the nearshore in 1989 and 1992, and the 5-year average map of nearshore hits. Grey sections – areas with no hits, blue – sections that received <7 hits/yr (20% of the maximum, about twice as large as the average), green – 7–17.5 hits/yr (20–50% of the maximum), red – areas where the hit count is >17.5 (>50% of the maximum).

The model revealed frequent hits to the area between Hanko and Helsinki occurred in 1988 and 1990 (not shown in Figure 18) while only hits of medium frequency to this area occurred in other years. Another area frequently receiving a high number of hits was located near the southern coast of the gulf, to the west of Tallinn, around 24°00' E. The domain to the east of Helsinki until about 28°30' E is relatively safe with respect to the pollution stemming from the model fairway. It received a low number of coastal hits during most of the years. An extensive nearshore area between Tallinn and Narva (with a few short exceptions) also received a low number of hits in all years.

The most affected nearshore is a short section to the south of Vyborg. Hits to the southern coast of the gulf are relatively frequent in a short section to the north of Luga Bay, at selected points near the northernmost tip of Estonia and along almost the entire north-western coast of Estonia to the west of Tallinn. The

northern nearshore of the gulf has generally a lower probability of hits except for short sections between Helsinki and Hanko.

The extensive variability in the spatial pattern of frequently hit nearshore domains and in the number of hits on monthly and seasonal level is natural because of high variability in the patterns of currents of the Gulf of Finland (Alenius et al., 1998; Leppäranta and Myrberg, 2009). Still, it raises the question about uncertainties of the resulting estimates, especially in the spatial distribution of the most frequently hit areas. A partial answer is given in Paper F based on the analysis of this variability over longer time intervals.

The 5-year pointwise average values of nearshore hits exhibited a pattern very similar to the annual average distributions (Paper F). It reflected a medium frequency of hits in the area between Hanko and Helsinki and also in the area to the west of Tallinn, near the southern coast of the gulf, extending to Hiiumaa. Hits were most frequent in the north-western part of Estonia near 24°00' E and in the easternmost part of the gulf, to the south of Vyborg. The northern coast from Helsinki to 28°30' E and the southern coast, between Tallinn and Narva, were relatively safe according to the model in use.

The average number of coastal hits per year varies considerably, from 2.9 in 1987 to 4.7 in 1995 (standard deviation $\sigma = 0.597$, Paper F). This variability rapidly decreases with the increase in the averaging period. The 5-year averages of this quantity (3.68 in 1987–1991, 3.83 in 1992–1996) differ by less than 2% from the 10-year mean 3.76 in 1987–1996 (Paper F). The alongshore variability of this number remained substantial in the long-term average. A likely reason is that it is to some extent determined by geographical conditions and possibly by long-term features of surface transport. While 18 sections had no hits at all during the entire 10-year simulation, the most frequently hit domains received up to 50 hits a year. The standard deviation for alongshore variations in the number of hits was from 4.9 in 1987 to 6.5 in 1989 (Paper F). The values of σ calculated against the 10-year average count of pointwise hits were at the same level but varied very little, from 4.75 in 1989 to 4.89 in 1987. This stability of σ can be interpreted as an indicator of the presence of a long-living structure in the distribution of hits.

The frequently hit areas in Figure 18 are very similar for the periods of 1987–1991, 1992–1996 and for the entire 10-year interval of 1987–1996. The average hit counts for single points are practically the same for the two 5-year intervals (Paper F). On average, the count in 1987–1991 exceeds the one in 1992–1996 by 0.15 (which is about 4% of the relevant mean value). The standard deviation of the pointwise difference between the values for the two 5-year intervals is 1.51. Therefore, the pattern of areas that receive the largest number of current-driven hits from the fairway region is highly persistent.

Another possibility of estimating the uncertainty of the performed calculations is to consider only a part of the trajectories. The pattern of frequently hit areas, calculated using every second parcel, was exactly the same as the above pattern, obtained using the entire set of trajectories (Paper F).

4.4. Frequent sources of nearshore pollution

The circulation of the Gulf of Finland is represented by a rich family of usually concealed semi-persistent current-driven surface transport patterns (Soomere et al., 2011). Although these patterns are highly variable in space and time, they may have a systematic impact on current-driven transport from the fairway region to the coast. Their presence, together with the persistent pattern of coastal hits, suggests that certain single locations of the existing fairway may be predominant starting points of coastal pollution. Below I speak about dangerous parts of the fairway or, alternatively, about perilousness, having in mind this ability of these sites to serve as a starting point of current-driven hits to the nearshore (Paper F). The fairway points are characterised in terms of the frequency with which the parcels selected at each point reached the nearshore. Particular attention is paid to the points, parcels from where drift to the nearshore relatively more frequently (>30% of the maximum count on the annual scale) than on average.

Similarly to the distributions of the most frequently hit nearshore areas (Figure 18), the ability of different parts of the fairway to serve as a source of adverse impacts on the coast substantially varies over different months, seasons and years (Paper F). The probability for the selected parcels to reach the nearshore is the highest during the windy months. For example, according to the model, in January 1989 about 84% of the selected parcels reached the nearshore. Highly dangerous points to the west of Tallinn exist mostly during the windy season and a few other months (e.g., April, July and September).

The results averaged for single years reveal a lower but still considerable temporal variability in the perilousness of the fairway. The probability for the selected parcels to reach the nearshore varies considerably for different years. For example, in 1988–1989 this probability frequently exceeded 60% for a part of the fairway to the west of Tallinn but was much lower in the other years. Importantly, it reveals a persistent pattern along the fairway (Paper F). The relatively dangerous sections near the bayhead of the Gulf of Finland and to the south of Vyborg are evident in all years and seasons, and during most of the months. The section of the fairway between longitudes 25° E and 27°30' E provides the least danger.

The time the parcels selected at different points of the fairway take to reach the nearshore (particle age) shows a similar pattern. It also exhibits extensive short-term variability that is almost levelled off on the annual scale. The fairway section in the widest part of the gulf between Tallinn and Narva reveals the largest particle age. Its high values (>15 days on average) were registered in a section of the fairway from the entrance to the gulf almost until the mainland of Estonia in most of the years (Paper F). Generally, sections of the fairway that are the most remote from the coast provide a low level of danger of coastal pollution also in terms of particle age. A section, possibly with a higher level of danger (age 10–15 days) to the nearshore in the narrowest part of the gulf, between Tallinn and Hanko, extends almost to Hiiumaa in some years (Paper F). Another section of the fairway, posing a greater threat to the nearshore, is located in the easternmost part of the gulf, to the

south of Vyborg. A small part of this section is characterised by quite fast (<10 days in annual average) transport of the selected parcels to the coast.

The fairway can be divided into four parts. Relatively dangerous areas are located to the south of Vyborg in the eastern part of the gulf and slightly to the west of Tallinn. It takes, on average, 10–15 days (<10 days in a smaller section in the eastern part of the gulf) for the current-driven parcels to drift from these regions to the nearshore. The less dangerous parts are the sections from Narva to Tallinn and to the west of the mainland of Estonia, from where the drift time is 15–20 days (Paper F). In particular, any contaminant in the uppermost layer of the sea as well as oil spill in a short section of the fairway near the bayhead of the Gulf of Finland has a high chance to rapidly drift to the nearshore. This threat is enhanced by the predominance of south-western winds in this area.

An intriguing question is whether certain nearshore areas are systematically hit by adverse impacts released in specific parts of the fairway. As such connections are less important for areas that are infrequently hit, I only consider sections of the nearshore, for which the annual count of hits exceeded 60% of the maximum count for at least one of the ten years of 1987–1996. The maximum count for single years varied more or less synchronously with the average rate for the selected parcels to reach the nearshore, from 32 in 1994 to 49 in 1989. Such a relative criterion levels off the interannual variations in the total number of hits (Paper F). Most of these sections (total 43, Figure 19) had a largely varying number of hits in different years. As a rule, these hits stem from quite different fairway points. Therefore, the simulations did not reveal any persistent patterns of interconnections between potential sources of pollution and end stations of their drift. Such patterns may, though, exist for certain seasons and/or weather patterns.

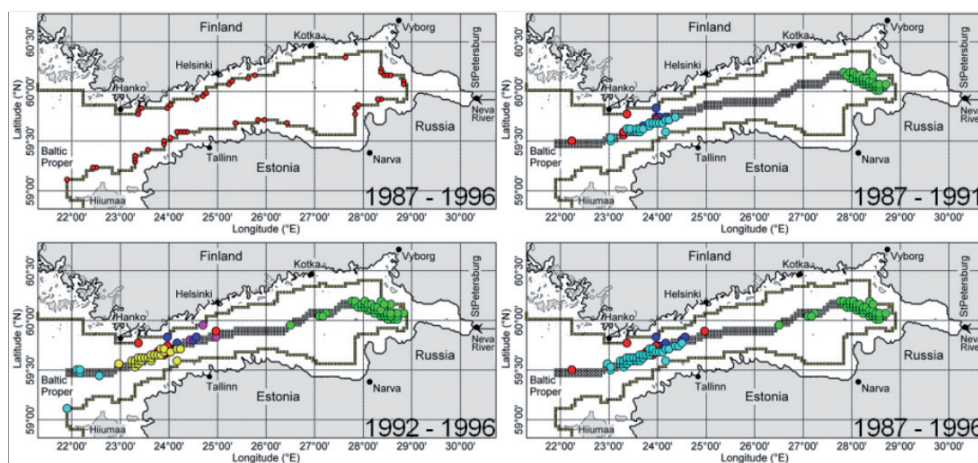


Figure 19. Upper left panel: most frequently hit nearshore areas (red: >60% of the annual maximum number of hits at least in three model years out of 1987–1991 or 1992–1996); other panels: interconnections between the above most frequently hit areas and the origin of the parcels. The link between the nearshore areas and the origin is shown by the same colour.

The nearshore areas highlighted in Figure 19 are naturally endangered by adverse impacts released along the major fairway and further transported by surface currents. Although these areas serve as probable end stations of the drift of various floating objects, the absence of a clear pattern of interconnections with certain sections of the fairway suggests that it is generally impossible to establish, at least using the model at our disposal, from where these objects originate.

The simulations still revealed that nine sections of the coastline frequently received a massive number of hits by parcels selected in relatively small parts of the fairway (Figure 19). These sections were identified by considering such nearshore domains that received at least 60% of the annual maximum number of hits in any three years out of five consecutive years (1987–1991 or 1992–1996). Five such sections were evident in both these 5-year intervals (Paper F).

4.5. Impact of horizontal eddy diffusivity on Lagrangian statistics

Given the very small internal Rossby radius in the Gulf of Finland (Section 1.2), the RCO model with a spatial resolution of 2 nautical miles only resolves a part of the mesoscale dynamics in this gulf. The dependence of the properties of surface-current-driven transport of passive parcels to the nearshore on the resolution of the circulation model of the Gulf of Finland was analysed by Andrejev et al. (2011) using an ocean model with a resolution of 2, 1 and 0.5 nautical miles and with otherwise identical setup and forcing data. Some features of current-driven transport (e.g., the exact location of the optimum fairway) were found to be quite sensitive with respect to the model resolution. However, some other properties of this transport (e.g., the basic features of the distributions of probabilities of nearshore hits and the time it takes for the parcels to reach the coast) became stable after about three years of integration (Section 3.5). As the pattern of nearshore hits by parcels selected along the fairway is largely governed by the aforementioned properties, it is likely that the spatial pattern of hits to the nearshore is not particularly sensitive with respect to the resolution of the circulation model either.

As discussed in Section 1.4, the non-spreading version of the TRACMASS model, used to quantify current-driven transport in Papers A, B and E–G does not replicate the natural level of the spreading of selected parcels. Namely, the simulated patches of parcels disperse much slower than real drifters (Jönsson et al., 2004; Engqvist et al., 2006; Döös and Engqvist, 2007; Döös et al., 2008; Kjellsson and Döös, 2012; Kjellsson et al., 2013). This feature is expected since the parcels are transported by velocity fields that do not contain information about subgrid-scale motions in a real marine environment. The described property may lead to unphysical clustering of trajectories of initially closely located passive parcels and, consequently, may play a role in the formation of a pattern of hits to the nearshore highly variable in space (Figure 18).

In order to test this possibility, Paper G focuses on the effect that the inclusion of subgrid-scale motions may have on the transport patterns estimated from purely advective Lagrangian trajectories. It is natural to assume that the inclusion of such

motions, for example, in terms of horizontal eddy-diffusivity, will considerably impact single Lagrangian trajectories. It is, however, unclear whether or how strongly the resulting statistical properties are affected.

The analysis is performed by including various representations of the effect of eddy-diffusivity (equivalently, various kinds of artificial spreading) on the parcel trajectories in the Gulf of Finland. Parcels were selected in four areas (called patches below) consisting of 5×5 grid cells. A cluster of four parcels (400 in total) was selected within each grid cell (Figure 20). The trajectories were simulated over four days, starting from 17 April 1987. This time slice covers a period with unusually strong variability in the surface current field and is thus favourable for the identification of the impact of numerical spreading.

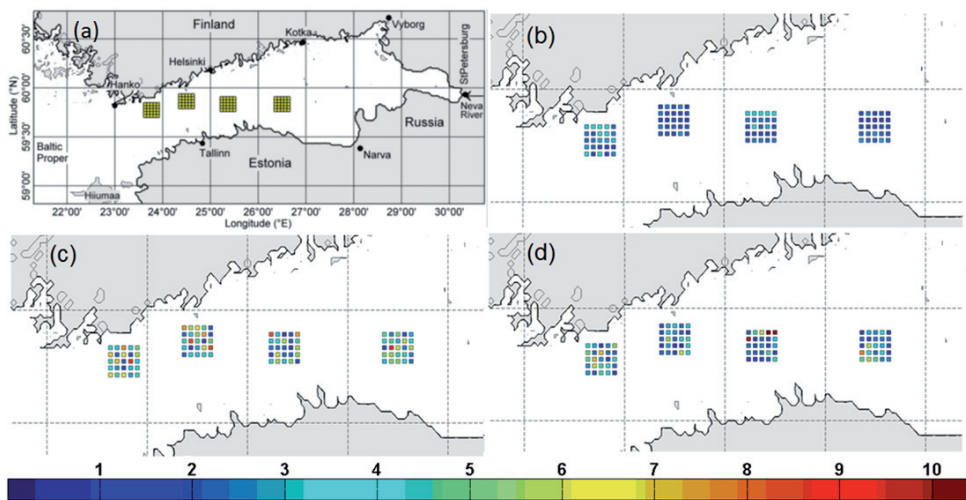


Figure 20. Four patches of selected parcels (a) and the maximum parcel separation for each four-parcel cluster seeded within a grid cell for the three different methods: (b) no eddy-diffusivity (pure advection); (c) eddy-diffusivity with a constant diffusion coefficient; (d) eddy-diffusivity with a time- and space-variable diffusion coefficient. The grid cell colour corresponds to a distance (km) as shown by the colour bar.

Particle diffusion is modelled in Paper G as a random walk process, where a random displacement is added to the trajectory position at each time step Δt in the simulation. The scheme was introduced in TRACMASS by Levine (2005). The results are based on three different datasets of trajectories: (i) non-diffusive simulation (pure advection), (ii) using a constant horizontal diffusion coefficient of $5 \text{ m}^2/\text{s}$ and (iii) using a variable horizontal diffusion coefficient calculated by the Smagorinsky model. In most of the model area the Smagorinsky diffusion coefficient is close to $5 \text{ m}^2/\text{s}$ (Paper G).

The maximum separation distance within each cluster of four parcels selected within single grid cells clearly depends on whether eddy-diffusivity was included in the model (Figure 20). The separation reached 1–4 km for simulations without diffusion and increased considerably, by a factor of two (to 1–10 km) when

diffusion was included. Differently from the non-spreading (purely advective) case, the separation between initially closely packed parcels is highly variable even between neighbouring grid cells when eddy-diffusivity is included. The largest variations occurred for the constant eddy-diffusivity case. The mean separation distance within each of the four patches is the largest in the westernmost patch in Figure 20, regardless of the particular model of spreading. This feature reflects the presence of locally strong surface currents. The variance in the separation distance is about 0.6–1.2 km without eddy-diffusivity and increases even more, to about 1.9–2.4 km with constant eddy-diffusivity (Paper G). The Smagorinsky model, which resulted in smaller separation distances than the constant eddy-diffusivity, may have equally large variability in regions with strong velocity field deformation, but comes closer to the non-diffusive results in less dynamic areas. The maximum particle separation distance varies considerably due to velocity field deformations, but the strong responses are confined to localised patches.

Lagrangian trajectories of parcels selected along the fairway (Figure 17) were calculated for the period 1982–2001 with six simulations per month, giving a total of 1440 runs. The following analysis is based on annually averaged percentages of coastal hits. Interannual variability of the monthly mean patterns of transport has been discussed in Paper F.

In spite of substantial changes to the statistics of the spreading of initially closely located parcels (see above), the differences in the total number of nearshore hits for 1982–2001 calculated with all three methods were less than 2%. The distribution of coastal hits along the northern and southern coasts of the Gulf of Finland averaged over 20 years (Section 4.3) almost did not change when eddy-diffusivity was included (Paper G).

Interestingly, the regions where the results of purely advective simulations depart from those obtained using the eddy-diffusivity model are not primarily at the extremes. In other words, the rate of hits to the regions that are extremely exposed to or completely sheltered from coastal hits remained unchanged and small variations only occurred in regions that received a moderate number of coastal hits. A possible interpretation of this result is that eddy-diffusivity contributes to pushing particles into less dominant parts of the coastal currents, but the counts of hits at the sections corresponding to peaks in Figure 21 are not reduced since the total number of coastal hits increases (Paper G).

The number of coastal hits during the 20-year period 1982–2001 ranged from a minimum of 21% (4700 trajectories) in 1985 to a maximum of 42% (9400 trajectories) in 1995. The mean value of coastal hits for the entire 20-year period was 31.9%. The five-year average values do not seem to indicate any long-term trend (Paper G). The effect of eddy-diffusivity is thus expressed by very slight increase in the number of coastal hits by about 1–2% in single years and reduction of the average time it takes for parcels to reach the coast, by less than 0.5 days (Paper G).

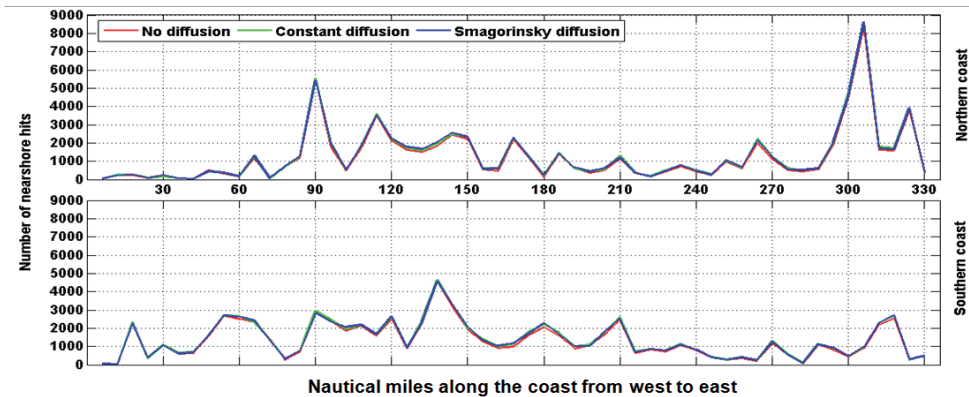


Figure 21. The most frequently hit nearshore areas averaged for the period 1982–2001 for the northern (upper panel) and southern (lower panel) coast of the Gulf of Finland (see Figure 17). The x -axis is the distance along the coast (in nautical miles), from the west of the gulf, near Hanko in the north and Hiiumaa in the south, to the eastern end of the gulf.

The inclusion of the impact of subgrid-scale processes, as expected, had considerable impact on the spreading of Lagrangian trajectories (and consequently on single trajectories) and on several properties of the statistics of transport. Clear modifications exist for the spreading rate and the increase in the average distance of the parcels from their origins. Interestingly, several other statistical properties of the transport were almost insensitive with respect to the presence or absence of subgrid-scale processes. Most importantly, the main features of the transport of the parcels to the nearshore areas and the time it took for the parcels to reach the nearshore remained essentially unchanged. Also, the spatial pattern of frequently hit coastal areas remained practically the same.

This stability suggests that the distributions of the probability of coastal hits and the time the parcel (or pollution) takes to reach the coast are generally insensitive with respect to the subgrid-scale processes and are basically defined by large-scale and mesoscale advection, the main features of which can be replicated using ocean models of moderate resolution. Moreover, this result suggests that the pattern of coastal areas that are frequently hit by adverse impacts (pollution, litter) from the offshore is also largely invariant with respect to the details of the Lagrangian transport models and the methods of parameterisation of subgrid-scale processes. An implicit consequence is that the estimates for the basinwide distribution of the probabilities of coastal hits by surface-driven pollution and the time it takes for the pollution to reach the coast (Andrejev et al., 2011; Paper E) apparently are also largely invariant with respect to the way of accounting for the impact of subgrid processes.

Conclusions

Summary of the results

The presence of organised systems or patterns of surface currents is an important precondition for the use of intrinsic features of currents for environmental management of potentially dangerous offshore activities. In this thesis the detection of such patterns was addressed by applying two techniques. The overall structure of surface velocity fields was analysed using the Okubo–Weiss parameter. Variations in this parameter characterise the spatial patterns of strain and relative vorticity, which are likely to deviate from their background values in the regions that host organised patterns of currents.

The surface flow in the Gulf of Finland (simulated using the OAAS model by O. Andrejev and A. Sokolov with a horizontal resolution of 1 nautical mile) is generally strain-dominated. Within short events the values of the Okubo–Weiss parameter can increase by a factor of 10. Such events tend to happen during the windy autumn–winter season but do not correspond to extreme wind speeds. Regions of high vorticity are prominent near the coast, while pronounced levels of strain at times occur in the offshore domains. In the western part of the gulf such levels are mostly oriented in the north–south direction and indicate the possibility of rapid transport of water masses across the gulf. The presence of eddies in high-vorticity areas was further investigated using a geometrical (streamline winding angle) method. This method showed good results for the Vátlestraumen area (Norway) that was modelled in very high resolution, but was not able to detect single eddies in vorticity-dominated areas of the Gulf of Finland.

The problem of minimising environmental risks of ship traffic was considered by optimising the sailing line so that parcels of pollution released along the fairway and further carried by surface currents would have a minimum chance of reaching the nearshore (to exert a coastal hit). The relevant technique is based on subsequent application of long-term numerical simulations of Eulerian velocity fields, calculation of Lagrangian trajectories, statistical analysis of their properties and specification of the optimum sailing line derived from this analysis. The study was performed for the Gulf of Finland using velocity fields from the Rossby Centre Ocean (RCO) model with a resolution of 2 nautical miles.

The described technique contains several parameters that have to be adjusted for each purpose, a particular sea area and circulation model. Reliable statistics of coastal hits can only be constructed when a significant number of parcels (carrying an adverse impact) reach the properly defined nearshore within a reasonable time window (trajectory length). The optimum width of the nearshore area when using the RCO model data and trajectories that are purely advected by simulated velocity fields is about three grid cells. The appropriate time windows in calculations of the propagation of pollution parcels to the coast are 10–20 days. The dependence of the results on the time lag is fairly small when the time lag between the windows is up to 10 days.

The concept of the equiprobability line as a first approximation of the optimum sailing line in elongated sea areas can be introduced in a straightforward manner for basins like the Gulf of Finland, which are divided between two countries. The probability that current-driven pollution parcels hit the coasts on either side of the basin is interpreted as the measure of the costs of consequences of accidents. The equiprobability line connects the points, from which the probability of propagation of the parcels to the two opposing coasts is equal. This line (calculated using large pools of Lagrangian trajectories reconstructed from the RCO velocity data and the TRACMASS code) mostly follows the centreline of the Gulf of Finland in its narrower part. In the wider part of the gulf it passes through an area of reduced risk, the propagation of pollution from which to either of the coasts is unlikely. Different methods used for the calculation of this line lead to small variations in its location.

The equiprobability line offers a local optimum for a fairway. A global optimum is searched in terms of the probability of the nearshore areas being hit by the pollution parcels released at different sites and of the time it takes for a hit to occur. The maps of these quantities are also constructed using the RCO data and the TRACMASS code. An approximation for the optimum fairway is constructed as a line that roughly follows the areas where the probability has a minimum or the time in question has a maximum. The resulting line only partially matches the geometrical centreline of the gulf and in some occasions meanders substantially.

The location of an optimum fairway is sensitive with respect to numerical noise and/or changes in the parameters in use, especially in areas where the overall risk level (e.g., probability of a coastal hit) is low. An attempt was made to characterise the applicability of the entire approach by comparison of the optimum fairways obtained using different quantifications of environmental risk. The extensive variation in the width of the 'corridors' corresponding to small deviations from the optimum solution signifies that the Gulf of Finland may contain areas with quite different internal dynamics and resulting current-driven surface transport. These areas can be separated based on the magnitude of cross-gulf gradients of the above-discussed quantities that characterise the 'ability' of a particular sea area to serve as a source of coastal pollution. While in the narrow central part of the Gulf of Finland these gradients are large and all versions of optimum fairways almost overlap, even large shifts in the fairway location in areas with small gradients would insignificantly affect environmental risks.

The probabilities of a hit to different sections of the nearshore and the potential of parcels released in different parts of the major fairway to reach the nearshore are both highly variable within short time intervals but exhibit a clearly repeating pattern over longer time intervals. Short sections to the south of Vyborg and to the north of Luga Bay, selected points near the northernmost tip of Estonia and the north-western coast of Estonia have a high chance for a coastal hit. The northern nearshore of the gulf has generally a lower probability of hits. The sections of the fairway, from which current-driven propagation of parcels to the coast is likely, are located in the eastern gulf area (to the south of Vyborg) and in the narrow part of

the gulf, slightly to the west of Tallinn. Still, the simulations did not reveal any long-term pattern of current-driven interconnections between specific parts of the fairway and single nearshore sections.

The sensitivity of the described patterns with respect to the impact of subgrid-scale processes was analysed by means of several versions of representation of this impact in the Lagrangian trajectory model. The inclusion of the impact of subgrid-scale processes considerably modified single Lagrangian trajectories, their spreading properties and several key properties of the statistics of transport (such as the spreading rate and the increase in the average distance of the parcels from their origins) compared to the purely advective transport. Several other statistical properties of the transport were almost insensitive with respect to the presence or absence of subgrid-scale processes. Most importantly, the statistics of the transport of the parcels to the coastal areas, the time it took until the parcels reached the nearshore and the spatial pattern of frequently hit coastal sections remains practically the same. This feature suggests that also the basinwide distributions of the probabilities of coastal hits by surface-driven pollution and the time it takes for the pollution to reach the coast may be invariant with respect to the way of accounting for the impact of subgrid processes.

Main conclusions proposed to defend

1. Patches of strain and relative vorticity were identified for the Gulf of Finland using the Okubo–Weiss parameter. These patches indicate the possible presence of semi-persistent (or frequent) motions along the coast, near the mouth of the Neva River and in the north-western part of the gulf.
2. A hybrid method for detection of mesoscale eddies, combining physical (Okubo–Weiss parameter) and geometrical (streamline winding angle) flow characteristics, showed good results for the Vatelestraumen area (Norway) but detected only a very small number of eddies in vorticity-dominated areas of the Gulf of Finland.
3. A model for the analysis of Lagrangian transport of persistent pollution parcels by surface currents was developed based on statistical analysis of Lagrangian trajectories of such parcels using the TRACMASS model and precomputed velocity fields.
4. Optimum values for the key parameters of this model (specification of the nearshore area, the length of the time window (trajectories), the time lag between time windows, the time interval to be covered, initial locations of selected parcels) were evaluated for several applications in the Gulf of Finland.
5. A method was developed for specifying the equiprobability line (from which the probability of current-driven propagation of pollution to the opposite coasts is equal) in the Gulf of Finland using velocity fields calculated by the Rossby Centre Ocean (RCO) model for 1982–2001.
6. Spatial distributions of probabilities of current-driven propagation of passively advected parcels to the nearshore and of the time it takes until the parcels reach

the nearshore were calculated for the Gulf of Finland based on 10-day and 20-day long trajectories.

7. Optimum fairways minimising the probability of coastal hits or maximising the time until a coastal hit occurs are mostly located to the north of the gulf axis (by 2–8 km on average). They meander substantially in some sections of the gulf. The typical root mean square deviation between the optimum fairways, specified from different criteria, is 6–16 km.
8. Nearshore areas to the south of Vyborg, to the north of Luga Bay, at the northernmost tip of Estonia and along the north-western coast of Estonia are most frequently hit by parcels selected along the major fairway. The northern nearshore of the gulf has a lower probability of such hits. The most probable sources of hits are in the eastern part of the gulf, to the south of Vyborg and in the narrow part of the gulf, slightly to the west of Tallinn.
9. The inclusion of artificial spreading of modelled Lagrangian trajectories substantially changes the appearance of single trajectories and spreading of initially closely located parcels but almost does not impact the pattern and frequency of hits to the nearshore.

Recommendations for further work

The particular implementation of the method proposed in the thesis only considers the role of surface currents in the process of specification of the optimum fairway or other potentially dangerous activities. For realistic applications, it would be desirable in the future to consider also wave- and wind-induced transport. A combined measure for assessing environmental risk derived from the probability of coastal hits and the time it takes for the pollution to reach the coast should be developed, similarly to the relevant attempt by Murawski and Woge Nielsen (2013). It is also desirable to apply the method to more realistic distributions of the value or vulnerability of different coastal and offshore regions similarly to Delpeche-Ellmann and Soomere (2013a, 2013b).

The spatial and temporal resolution of the ocean model and recorded current fields (2 nautical miles and 6 h, respectively) ignore a large part of mesoscale activity in the Gulf of Finland and distort the impact of inertial oscillations on the pollution drift. Although parallel studies (Andrejev et al., 2011) have demonstrated that the key features of the distributions of various measures of environmental risk are relatively stable with respect to the resolution of ocean model, an increase in the temporal resolution to 3 h and in the horizontal resolution to about 1 km (possibly down to 0.5 km) is highly desirable in future experiments (and feasible given the gradual improvement of computer facilities). Doing so is particularly important for properly resolving the presence of smaller islands in the eastern and northern parts of the gulf. Moreover, the Gulf of Finland covers only a small part of the environmentally sensitive Baltic Sea.

The technique of statistical analysis of Lagrangian trajectories evidently has a large potential for achieving progress in many other problems associated with the

advection of single parcels and items. It is obviously useful for tracking the pathways of (micro)plastic that is mostly advected by surface currents, and for establishing the areas of their high concentrations. The technique used for the evaluation of the most dangerous parts of the fairways can be directly used to find the potential sources of such a material and can in this way serve as a basis for the relevant decision-making process.

The results presented in the thesis are not conclusive for the Gulf of Finland with respect to the automatic detection of eddy structures. The near absence of long-living circular eddies in the instantaneous velocity fields even in areas with high vorticity does not imply that the semi-persistent current fields do not exist. A possible reason for the failure is that the resolution of the ocean model, albeit very high compared to the majority of contemporary models, was not sufficient for replication of long-living eddies in this gulf. Alternatively, the circular structure of eddies may be often distorted or masked by certain filaments formed in the surface layer of the Gulf of Finland. However, the occurrence of such structures at the same locations over time could be a strong indicator of the presence of a semi-persistent current field. This is a potential subject for further analysis, but will require either a higher-resolution model than available today, or analysis of data from other sources, such as satellite altimetry.

The properties of different quantities calculated in the thesis (probabilities of current-driven transport to opposite coasts, probabilities of coastal hits, residence time of released pollution or items at sea) have been only explored here from the viewpoint of specification of a simple model of an optimum fairway. The two-dimensional fields of these quantities have obviously a much larger potential for the use in different applications. A straightforward application is the quantification of the 'benefit' from a shift of certain parts of the fairway (Delpeche-Ellmann and Soomere, 2013a, 2013b).

While the analysis in the thesis mostly relies on the location of the maxima, minima or zero-crossings of these quantities, it is likely that several other properties of their two-dimensional distributions have a great value. For example, the magnitude of cross-gulf gradients of these quantities implicitly characterises not only the uncertainty of the solutions but also the potential consequences of the introduction of a non-optimum solution. While in the narrow central part of the Gulf of Finland these gradients are large and all versions of optimum fairways almost overlap, even large shifts in the fairway in areas with small gradients would insignificantly affect environmental risks. More generally, the magnitudes of the gradients in question indicate the similarities and differences in terms of transport by surface currents in different sea areas. These quantities, therefore, may be used in maritime spatial planning for identifying the sea regions with seemingly similar geometry but with radically different internal properties.

Bibliography

- Ådlandsvik B., Huse G. and Michalsen K. 2007. Introducing a method for extracting horizontal migration patterns from data storage tags. *Hydrobiologia*, 582(1), 187–197.
- Agardy T., Davis J., Sherwood K. and Vestergaard O. 2011. Taking steps toward marine and coastal ecosystem-based management – an introductory guide. *UNEP Regional Sea Report and Studies No. 189*.
- Alenius P. 1986. Kotkan merihiekka 1985 – virtaustutkimus. *Merentutkimuslaitos, Sisäinen raportti 5/1986*. [Kotka sea sand 1985 – current measurements. Finnish Institute of Marine Research, *Internal report 5/1986*], 28, 1–12 (in Finnish).
- Alenius P., Myrberg K. and Nekrasov A. 1998. Physical oceanography of the Gulf of Finland: a review. *Boreal Environ. Res.*, 3, 97–125.
- Alenius P., Nekrasov A. and Myrberg K. 2003. The baroclinic Rossby-radius in the Gulf of Finland. *Cont. Shelf. Res.*, 23, 563–573.
- Alhimenko A., Bolshev A., Yakovlev A., Klevanny K. and Liukkonen S. 1997. Modelling oil pollution under ice cover. In: Chung J.S., Frederking R.M.W., Saeki H. and Bekker A.T. (Eds.), *Proceedings of the Seventh (1997) International Offshore and Polar Engineering Conference*, pp. 594–601.
- Ambjörn C. 2000. Modelling of trajectory and fate of spills. In: Rodriguez G.R., Brebbia C.A., Perez and Martell E. (Eds.), *Environmental Coastal Regions III Environmental Studies Series*, 5, pp. 33–40.
- Ambjörn C. 2007. Seatrack Web, forecasts of oil spills, a new version. *Environ. Res. Eng. Manag. (Aplinkos tyrimai, inžinerija ir vadyba)*, 3(41), 60–66.
- Ambjörn C. 2008. Seatrack Web forecasts and backtracking of oil spills – an efficient tool to find illegal spills using AIS. In: *IEEE/OES US/EU-Baltic International Symposium, Tallinn, Estonia, May 27–29, 2008*. IEEE Press, New York, pp. 168–176.
- Andrejev O. and Sokolov A. 1989. Numerical modelling of the water dynamics and passive pollutant transport in the Neva inlet. *Meteorol. Hydrol.*, 12, 75–85 (in Russian).
- Andrejev O. and Sokolov A. 1990. 3D baroclinic hydrodynamic model and its applications to Skagerrak circulation modeling. In: *Proceedings of the 17th Conference of Baltic Oceanographers (Norrköping, Sweden)*, pp. 38–46.
- Andrejev O., Myrberg K., Alenius P. and Lundberg P.A. 2004a. Mean circulation and water exchange in the Gulf of Finland – a study based on three-dimensional modeling. *Boreal Environ. Res.*, 9, 1–16.
- Andrejev O., Myrberg K. and Lundberg P.A. 2004b. Age and renewal time of water masses in a semi-enclosed basin – Application to the Gulf of Finland. *Tellus A*, 56, 548–558.

- Andrejev O., Sokolov A., Soomere T., Värvi R. and Viikmäe B. 2010. The use of high-resolution bathymetry for circulation modelling in the Gulf of Finland. *Est. J. Eng.*, 16, 187–210.
- Andrejev O., Soomere T., Sokolov A. and Myrberg K. 2011. The role of spatial resolution of a three-dimensional hydrodynamic model for marine transport risk assessment. *Oceanologia*, 53, 309–334.
- Anonymous 2013. Viking Line's Amorella grounded off Åland Islands. *Maritime Bulletin*, Dec 14. (newspaper article).
- Aps R., Herkül K., Kotta J., Kotta I., Kopti R., Leiger R., Mander U. and Suursaar Ü. 2009. Bayesian inference for oil spill related Net Environmental Benefit Analysis. In: Brebbia C.A., Benassai B. and Rodriguez G.R. (Eds.), *Coastal Processes*, pp. 235–246.
- Ardhuin F., Marié L., Rascale N. and Forget P. 2009. Observation and estimation of Lagrangian, Stokes and Eulerian currents induced by wind and waves at the sea surface. *J. Phys. Oceanogr.*, 39, 2820–2838.
- BACC Author Team 2008. *Assessment of Climate Change for the Baltic Sea Basin*. Springer, Berlin, 473 pp.
- Bergström S. and Carlsson B. 1994. River runoff to the Baltic Sea: 1950–1990. *Ambio*, 23, 280–287.
- Blanke B. and Raynaud S. 1997. Kinematics of the Pacific Equatorial Undercurrent: an Eulerian and Lagrangian approach from GCM results. *J. Phys. Oceanogr.*, 27(6), 1038–1053.
- Blockley E.W., Martin M.J. and Hyder P. 2012. Validation of FOAM near-surface ocean current forecasts using Lagrangian drifting buoys. *Ocean Sci.*, 8, 551–565.
- Bolin B. and Rodhe H. 1973. A note on the concepts of age distribution and transit term in natural reservoirs. *Tellus*, 25, 58–62.
- Bower A.S., Armi L. and Ambar I. 1995. Direct evidence of meddy formation off the southwestern coast of Portugal. *Deep-Sea Res. I*, 42(9), 1621–1630.
- Breivik Ø., Allen A.A., Maisondieu C. and Roth J.C. 2011. Wind-induced drift of objects at sea: the leeway field method. *Appl. Ocean Res.*, 33(2), 100–109.
- Broman B., Hammarklint T., Rannat K., Soomere T. and Valdmann A. 2006. Trends and extremes of wave fields in the north-eastern part of the Baltic Proper. *Oceanologia*, 48, 165–184.
- Broström G., Carrasco A., Hole L.R., Dick S., Janssen F., Mattsson J. and Berger S. 2011. Usefulness of high resolution coastal models for operational oil spill forecast: the Full City accident. *Ocean Sci.*, 7, 805–820.
- Brunila O.-P. and Storgard J. 2013. Future development of oil transportation in the Gulf of Finland. In *Marine Navigation and Safety of Sea Transportation: Maritime Transport and Shipping*, 79–85.
- Burgherr P. 2007. In-depth analysis of accidental oil spills from tankers in the context of global spill trends from all sources. *J. Hazard. Mater.*, 140, 245–256.

- Calvert S., Deakins E. and Motte R. 1991. A dynamic system for fuel optimization trans-ocean. *J. Navig.*, 44, 233–265.
- Chaigneau A., Gizolme A. and Grados C. 2008. Mesoscale eddies off Peru in altimeter records: identification algorithms and eddy spatio-temporal patterns. *Progr. Oceanogr.*, 79, 106–119.
- Chang Y.L., Oey L., Xu F.H., Lu H.F. and Fujisaki A. 2011. 2010 oil spill: trajectory projections based on ensemble drifter analyses. *Ocean Dyn.*, 61, 829–839.
- Chelton D.B., Schlax M.G. and Samelson R.M. 2011. Global observations of nonlinear mesoscale eddies. *Progr. Oceanogr.*, 91, 167–216.
- Collins M.P., Vecchio F.J., Selby R.G. and Gupta P.R. 1997. The failure of an offshore platform. *ASI Concr. Int.*, 19, 28–35.
- Cushman-Roisin B.J. and Beckers J.-M. 2011. *Introduction to Geophysical Fluid Dynamics: Physical and Numerical Aspects*. Elsevier/Academic Press, Amsterdam/San Diego, 828 pp.
- Davis R.E. 1991. Lagrangian ocean studies. *Annu. Rev. Fluid Mech.*, 23, 43–64.
- Deissenberg C., Gurman V., Ryumina E. and Tsirlin A. 2001. An empirically tractable model of optimal oil spills prevention in Russian sea harbours. *Int. J. Environ. Pollut.*, 15(3), 301–309.
- Deleersnijder E., Campin J.-M. and Delhez E.J.M. 2001. The concept of age in marine modelling. I. Theory and preliminary model results. *J. Mar. Syst.*, 28, 229–267.
- Delpeche-Ellmann N.C. and Soomere T. 2013a. Investigating the marine protected areas most at risk of current-driven pollution in the Gulf of Finland, the Baltic Sea, using a Lagrangian transport model. *Mar. Poll. Bull.*, 67(1–2), 121–129.
- Delpeche-Ellmann N.C. and Soomere T. 2013b. Using Lagrangian models to assist in maritime management of coastal and marine protected areas. *J. Coast. Res.*, SI 65, 36–41.
- de Vries P. and Döös K. 2001. Calculating Lagrangian trajectories using time-dependent velocity fields. *J. Atmos. Oceanic Technol.*, 18, 1092–1101.
- Dick S., Kleine E. and Müller-Navarra S. 2001. *The Operational Circulation Model of BSH (BSH cmod). Model Description and Validation*. Berichte des Bundesamtes für Seeschifffahrt und Hydrographie 29/2001. Hamburg, Germany, 48 pp.
- Döös K. 1995. Inter-ocean exchange of water masses. *J. Geophys. Res.*, 100(C7), 13499–13514.
- Döös K. and Coward A.C. 1997. The Southern Ocean as the major upwelling zone of the North Atlantic Deep Water. *WOCE Newsletter*, 27, 3–17.
- Döös K. and Engqvist A. 2007. Assessment of water exchange between a discharge region and the open sea – a comparison of different methodological concepts. *Estuar. Coast. Shelf Sci.*, 74, 585–597.

- Döös K., Meier H.E.M. and Döscher R. 2004. The Baltic haline conveyor belt or the overturning circulation and mixing in the Baltic. *Ambio*, 33, 261–266.
- Döös K., Nycander J. and Coward A.C. 2008. Lagrangian decomposition of the Deacon Cell. *J. Geophys. Res.*, 113, C07028.
- Döös K., Rupolo V. and Brodeau L. 2011. Dispersion of surface drifters and model-simulated trajectories. *Ocean Model.*, 39, 301–310.
- Döös K., Kjellsson J. and Jönsson B. 2013. TRACMASS – A Lagrangian Trajectory Model. In: Soomere T. and Quak E. (Eds.), *Preventive Methods for Coastal Protection*. Springer, pp. 225–249.
- Drijfhout S.S., Katsman C.A., de Steur L., van der Vaart P.C.F., van Leeuwen P.J. and Veth C. 2003. Modeling the initial, fast sea-surface height decay of Agulhas ring “Astrid”. *Deep-Sea Res. II*, 50(1), 299–319.
- Eide M.S., Endresen Ø., Brett P.E., Ervik J.L. and Røang K. 2007. Intelligent ship traffic monitoring for oil spill prevention: risk based decision support building on AIS. *Mar. Poll. Bull.*, 54, 145–148.
- Elken J. and Matthäus W. 2008. Physical system description. In: The BACC Author Team, *Assessment of Climate Change for the Baltic Sea Basin*. Springer, Berlin, pp. 379–386.
- Elken J., Kask J., Kõuts T., Liiv U., Perens R. and Soomere T. 2001. Hydrodynamical and geological investigations of possible deep harbour sites in north-western Saaremaa Island: overview and conclusions. *Proc. Est. Acad. Sci. Eng.*, 7, 85–98.
- Elken J., Raudsepp U. and Lips U. 2003. On the estuarine transport reversal in deep layers of the Gulf of Finland. *J. Sea Res.*, 49, 267–274.
- Elken J., Mälkki P., Alenius P. and Stipa T. 2006. Large halocline variations in the northern Baltic Proper and associated meso- and basin-scale processes. *Oceanologia*, 48(S), 91–117.
- Elken J., Nõmm M. and Lagemaa P. 2011. Circulation patterns in the Gulf of Finland derived from the EOF analysis of model results. *Boreal Environ. Res.*, 16(Suppl A), 84–102.
- Elken J., Raudsepp U., Laanemets J., Passenko J., Maljutenko I., Pärn O. and Keevallik S. 2014. Increased frequency of wintertime stratification collapse events in the Gulf of Finland since the 1990s. *J. Mar. Syst.*, 129, 47–55.
- Elofsson K. 2010. The costs of meeting the environmental objectives for the Baltic Sea: a review of the literature. *Ambio*, 39(1), 49–58.
- Engqvist A., Döös K. and Andrejev O. 2006. Modelling water exchange and contaminant transport through a Baltic coastal region. *Ambio*, 35, 435–447.
- Feistel G., Nausch G. and Wasmund N. 2008. *State and Evolution of the Baltic Sea, 1952–2005*. Wiley, Hoboken, 703 pp.
- Fennel W., Seifert T. and Kayser B. 1991. Rossby radii and phase speeds in the Baltic Sea. *Cont. Shelf. Res.*, 11, 23–36.

- Fingas M.F. 2011. Buoys and devices for oil spill tracking. In: *Proceedings of the 34th AMOP Technical Seminar on Environmental Contamination and Response*. Environment Canada, Ottawa, pp. 213–228.
- Fowler T.G. and Sørgård E. 2000. Modeling ship transportation risk. *Risk Anal.*, 20, 225–245.
- Funkquist L. and Kleine E. 2007. *An introduction to HIROMB, an operational baroclinic model for the Baltic Sea*. Technical report, SMHI, Norrköping, Sweden, 48 pp.
- Gästgifvars M., Ambjörn C. and Funkquist L. 2002. Operational modelling of the trajectory and fate of spills in the Baltic Sea. In: *Proceedings of the 25th Arctic and Marine Oilspill Program (AMOP) Technical Seminar*. Environment Canada, Calgary, Canada, pp. 1115–1129.
- Gästgifvars M., Lauri H., Sarkanen A.-K., Myrberg K., Andrejev O. and Ambjörn C. 2006. Modelling surface drifting of buoys during a rapidly-moving weather front in the Gulf of Finland, Baltic Sea. *Estuar. Coast. Shelf Sci.*, 70, 567–576.
- Goerlandt F. and Kujala P. 2011. Traffic simulation based on ship collision probability modeling. *Reliab. Eng. Syst. Saf.*, 96, 91–107.
- Gottinger H.W. 2001. Econometric modelling, estimation and policy analysis of oil spill processes. *Int. J. Environ. Pollut.*, 15(3), 333–363.
- Griffa A., Piterbarg L.I. and Özgökmen T. 2004. Predictability of Lagrangian particle trajectories: effects of smoothing of the underlying Eulerian flow. *J. Mar. Res.*, 62, 1–35.
- Gucma L. 2008. Evaluation of oil spills in the Baltic Sea by means of simulation model and statistical data. In: Soares C.G., Kolev P.N. (Eds.), *Maritime Industry, Ocean Engineering and Coastal Resources. 12th International Congress of the International Maritime Association of the Mediterranean, Varna, Bulgaria, September 02–06, 2007*. Proceedings and Monographs in Engineering Water and Earth Sciences, Int. Maritime Assoc. Mediterranean, 1–2, pp. 1153–1159.
- Haapala J., Launiainen J., Keynäs K. and Pokki J. 1990. *Hankoniemen edustan virtaustutkimus*. Loppuraportti (in Finnish).
- Haidvogel D.B. and Beckmann A. 1999. *Numerical Ocean Circulation Modeling*. Imperial College Press, London, 344 pp.
- Hassler B. 2011. Accidental versus operational oil spills from shipping in the Baltic Sea: risk governance and management strategies. *Ambio*, 40, 170–178.
- HELCOM 2009. *Ensuring Safe Shipping in the Baltic*. Stankiewicz M. and Vlasov N. (Eds.), Helsinki Commission, Helsinki, 18 pp.
- Hibler W.D. 1979. A dynamic thermodynamic sea ice model. *J. Phys. Oceanogr.*, 9, 815–846.
- Höglund A. and Meier H.E.M. 2012. Environmentally safe areas and routes in the Baltic proper using Eulerian tracers. *Mar. Poll. Bull.*, 64(7), 1375–1385.

- Höglund A., Meier H.E.M., Broman B. and Kriezi E. 2009. *Validation and Correction of Regionalised ERA-40 Wind Fields over the Baltic Sea Using the Rossby Centre Atmosphere Model RCA3.0*. Rapport Oceanografi No 97, Swedish Meteorological and Hydrological Institute, Norrköping, Sweden, 29 pp.
- IMO 2007. *Particularly Sensitive Sea Areas*. International Maritime Organisation, London, 150 pp.
- IRM 2002. *Risk Management Standard*. The Institute of Risk Management, London, 14 pp.
- Isern-Fontanet J., Garcia-Ladona E. and Font J. 2003. Identification of marine eddies from altimetric maps. *J. Atmos. Oceanic Technol.*, 20, 772–778.
- Isern-Fontanet J., Font J., Garcia-Ladona E., Emelianov M., Millot C. and Taupier-Letage I. 2004. Spatial structure of anticyclonic eddies in the Algerian basin (Mediterranean Sea) analyzed using the Okubo–Weiss parameter. *Deep-Sea Res. II*, 51, 3009–3028.
- Ishikawa Y., Toshiyuki A. and Akitomo K. 1997. Global surface circulation and its kinetic energy distribution derived from drifting buoys. *J. Oceanogr.*, 53, 489–516.
- Jędrasik J., Cieślakiewicz W., Kowalewski M., Bradtke K. and Jankowski A. 2008. 44 Years Hindcast of the sea level and circulation in the Baltic Sea. *Coast. Eng.*, 55(11), 849–860.
- Jönsson B., Lundberg P. and Döös K. 2004. Baltic sub-basin turnover times examined using the Rossby Centre Ocean model. *Ambio*, 23, 257–260.
- Jönsson B., Döös K., Nycander J. and Lundberg P. 2008. Standing waves in the Gulf of Finland and their relationship to the basin-wide Baltic seiches. *J. Geophys. Res. Oceans*, 113, C03004.
- Judson B. 1997. A tanker navigation safety system. *J. Navig.*, 50, 97–108.
- Kachel M.J. 2008. *Particularly Sensitive Sea Areas*. Hamburg Studies on Maritime Affairs, 13, Springer, Berlin, 376 pp.
- Kalda J., Soomere T. and Giudici A. 2014. On the compressibility of the surface currents in the Gulf of Finland, the Baltic Sea. *J. Mar. Syst.*, 129, 56–65.
- Kara B.Y. and Verter V. 2004. Designing a road network for hazardous materials transportation. *Transp. Sci.*, 38, 188–196.
- Keevallik S. and Soomere T. 2010. Towards quantifying variations in wind parameters across the Gulf of Finland. *Est. J. Earth Sci.*, 59, 288–297.
- Keramitsoglou I., Cartalis C. and Kassomenos P. 2003. Decision support system for managing oil spill events. *Environ. Manage.*, 32, 290–298.
- Kite-Powell H. 2011. The value of ocean surface wind information for maritime commerce. *Mar. Technol. Soc. J.*, 45, 75–84.
- Kjellsson J. and Döös K. 2012. Surface drifters and model trajectories in the Baltic Sea. *Boreal Environ. Res.*, 17(6), 447–459.

- Kjellsson J., Döös K. and Soomere T. 2013. Evaluation and tuning of model trajectories and spreading rates in the Baltic Sea using surface drifter observations. In: Soomere T. and Quak E. (Eds.), *Preventive Methods for Coastal Protection*. Springer, pp. 251–282.
- Kleine E. 1994. *Das operationelle modell des BSH für Nordsee und Ostsee, konzeption und übersicht*. Bundesamt für Seeschifffahrt und Hydrographie, 126 pp. (in German).
- Kononen K., Kuparinen J., Mäkelä K., Laanemets J., Pavelson J. and Nömmann S. 1996. Initiation of cyanobacterial blooms in a frontal region at the entrance to the Gulf of Finland, Baltic Sea. *Limnol. Oceanogr.*, 41, 98–112.
- Ko T.T. and Chang Y.-C. 2010. Integrated marine pollution management: a new model of marine pollution prevention and control in Kaohsiung, Taiwan. *Ocean Coast. Manag.*, 53, 624–635.
- Kostianoy A.G., Litovchenko K.T., Lebedev S.A., Stanichny S.V. and Pichuzhkina O.E. 2005. Operational satellite monitoring of oil spill pollution in the southeastern Baltic Sea. In: *Oceans 2005 Europe International Conference, Brest, France, June 20–23, 2005*. IEEE, pp. 182–183.
- Kostianoy A.G., Ambjörn C. and Soloviev D.M. 2008. Seatrack Web: a numerical tool to protect the Baltic Sea marine protected areas. In: *IEEE/OES US/EU-Baltic International Symposium, Tallinn, Estonia, May 27–29, 2008*. IEEE Press, New York, pp. 7–12.
- Kõuts T., Verjovkina S., Lagemaa P. and Raudsepp U. 2010. Use of lightweight on-line GPS drifters for surface current and ice drift observations. In: *2010 IEEE/OES US/EU Baltic International Symposium, Riga, Latvia, August 25–27, 2010*. IEEE Press, New York, 11 pp.
- Kujala P. and Arughadhoss S. 2012. Statistical analysis of ice crushing pressures on a ship's hull during hull-ice interaction. *Cold Reg. Sci. Technol.*, 70, 1–11.
- Kurkina O., Pelinovsky E., Talipova T. and Soomere T. 2011. Mapping the internal wave field in the Baltic Sea in the context of sediment transport in shallow water. *J. Coast. Res.*, SI 64, 2042–2047.
- Laakkonen A., Mälkki P. and Niemi Å. 1981. Studies of the sinking, degradation and sedimentation of organic matter off Hanko Peninsula, entrance of the Gulf of Finland, in 1979. *MERI*, 9, 3–42.
- Laas P., Simm J., Lips I. and Metsis M. 2014. Spatial variability of winter bacterioplankton community composition in the Gulf of Finland (the Baltic Sea). *J. Mar. Syst.*, 129, 127–134.
- Lagemaa P., Elken J. and Kõuts T. 2011. Operational sea level forecasting in Estonia. *Est. J. Eng.*, 17, 301–331.
- Lass H.U. and Matthäus W. 1996. On temporal wind variations forcing salt water inflows into the Baltic Sea. *Tellus A*, 48, 663–671.
- Lavrova O., Bocharova T. and Kostianoy A. 2006. Satellite radar imagery of the coastal zone: slicks and oil spills. In: Marcal A. (Ed.), *Global Developments in*

- Environmental Earth Observation from Space, 25th Symposium of the European Association of Remote Sensing Laboratories (EARSeL), University of Porto, Oporto, Portugal, June 06–11, 2005*, pp. 763–771.
- Lefebvre-Chalain H. 2007. Fifteen years of particularly sensitive sea areas: a concept in development. *Ocean Coast. Law. J.*, 13, 47–69.
- Lehmann A. 1995. A three-dimensional baroclinic eddy-resolving model of the Baltic Sea. *Tellus A*, 47, 1013–1031.
- Lehmann A. and Hinrichsen H.-H. 2000. On the thermohaline variability of the Baltic Sea. *J. Mar. Syst.*, 25, 333–357.
- Lehmann A., Krauss W. and Hinrichsen H.-H. 2002. Effects of remote and local atmospheric forcing on circulation and upwelling in the Baltic Sea. *Tellus A*, 54, 299–316.
- Lehmann A., Getzlaff K. and Harlass J. 2011. Detailed assessment of climate variability in the Baltic Sea area for the period 1958 to 2009. *Clim. Res.*, 46, 185–196.
- Lehmann A., Myrberg K. and Höflich K. 2012. A statistical approach to coastal upwelling in the Baltic Sea based on the analysis of satellite data for 1990–2009. *Oceanologia*, 54, 369–393.
- Lehmann A., Hinrichsen H.-H. and Getzlaff K. 2014. Identifying potentially high risk areas for environmental pollution in the Baltic Sea. *Boreal Environ. Res.*, 19 (in press).
- Leppäranta M. and Peltola J. 1986. *Satunnaiskulkumallin soveltyvuudesta Itämerelle* [On the applicability of a random walk model to the Baltic Sea]. Finnish Institute of Marine Research, Internal Report 4, Helsinki, 31 pp. (in Finnish).
- Leppäranta M. and Myrberg K. 2009. *Physical Oceanography of the Baltic Sea*. Springer Praxis, Berlin, 378 pp.
- Levine R.C. 2005. *Changes in Shelf Waters due to Air-Sea Fluxes and Their Influence on the Arctic Ocean Circulation as Simulated in the OCCAM Global Ocean Model*. PhD thesis, University of Southampton, Faculty of Engineering Science and Mathematics, School of Ocean and Earth Science, 225 pp.
- Liblik T. and Lips U. 2012. Variability of synoptic-scale quasi-stationary thermohaline stratification patterns in the Gulf of Finland in summer 2009. *Ocean Sci.*, 8(4), 603–614.
- Lips I., Rünk N., Kikas V., Meerits A. and Lips U. 2014. High-resolution dynamics of the spring bloom in the Gulf of Finland of the Baltic Sea. *J. Mar. Syst.*, 129, 135–149.
- Lilover M.-J. 2012. Tidal currents as estimated from ADCP measurements in “practically non-tidal” Baltic Sea. In: *IEEE/OES Baltic 2012 International Symposium, May 8–11, 2012, Klaipeda, Lithuania, Proceedings*. IEEE, 4 pp.

- Lilover M.-J. and Stips A.K. 2011. An alternative parameterization of eddy diffusivity in the Gulf of Finland based on the kinetic energy of high frequency internal wave band. *Boreal Environ. Res.*, 16, 103–116.
- Lilover M.-J., Pavelson J. and Kõuts T. 2011. Wind forced currents over shallow Naissaar Bank in the Gulf of Finland. *Boreal Environ. Res.*, 16(Suppl. A), 164–174.
- Lo H.K., McCord M.R. and Wall C.K. 1991. Value of ocean current information for strategic routing. *Eur. J. Oper. Res.*, 55, 124–135.
- Lo H.K. and McCord M.R. 1995. Routing through dynamic ocean currents—general heuristics and empirical results in the Gulf-stream region. *Transp. Res. Part B Methodol.*, 29, 109–124.
- Lončar G., Leder N. and Paladin M. 2012. Numerical modelling of an oil spill in the northern Adriatic. *Oceanologia*, 54(2), 143–173.
- Löptien U. and Meier H.E.M. 2011. The influence of increasing water turbidity on the sea surface temperature in the Baltic Sea: a model sensitivity study. *J. Mar. Syst.*, 88, 323–331.
- Lu X., Soomere T., Stanev E.V. and Murawski J. 2012. Identification of the environmentally safe fairway in the South-Western Baltic Sea and Kattegat. *Ocean Dyn.*, 62, 815–829.
- Madec G. 2008. *NEMO Ocean Engine*. Note du Pole de modélisation, Institut Pierre-Simon Laplace (IPSL), France, No 27, 217 pp.
- Martinez E., Maamaatuaiahutapu K. and Taillandier V. 2009. Floating marine debris surface drift: convergence and accumulation toward the South Pacific subtropical gyre. *Mar. Poll. Bull.*, 58, 1347–1355.
- Meier H.E.M. 1999. *First Results of Multi-Year Simulations Using a 3D Baltic Sea Model*. SMHI Reports Oceanography, No 27, Norrköping, Sweden, 48 pp.
- Meier H.E.M. 2005. Modeling the age of Baltic Sea water masses: quantification and steady-state sensitivity experiments. *J. Geophys. Res.*, 110, C02006.
- Meier H.E.M. 2006. Baltic Sea climate in late 21st century: a dynamical downscaling approach using two global models and two emission scenarios. *Clim. Dyn.*, 27, 39–68.
- Meier H.E.M. 2007. Modeling the pathways and ages of inflowing salt- and freshwater in the Baltic Sea. *Estuar. Coast. Shelf Sci.*, 74, 610–627.
- Meier H.E.M. and Höglund A. 2012. Environmentally safe areas and routes in the Baltic Proper using Eulerian tracers. *Mar. Poll. Bull.*, 64, 1375–1385.
- Meier H.E.M. and Höglund A. 2013. Studying the Baltic Sea circulation with Eulerian tracers. In: Soomere T. and Quak E. (Eds.), *Preventive Methods for Coastal Protection*. Springer, pp. 101–130.
- Meier H.E.M., Döscher R. and Faxén T. 2003. A multiprocessor coupled ice-ocean model for the Baltic Sea: application to salt inflow. *J. Geophys. Res.*, 108(C8), 32–73.

- Melsom A., Counillon F., LaCasce J.H. and Bertino L. 2012. Forecasting search areas using ensemble ocean circulation modeling. *Ocean Dyn.*, 62, 1245–1257.
- Mietus M. (co-ordinator) 1998. *The Climate of the Baltic Sea Basin, Marine Meteorology and Related Oceanographic Activities*. Report No. 41, World Meteorological Organisation, Geneva, 64 pp.
- Millero F.J. and Kremling K. 1976. The densities of Baltic Sea waters. *Deep Sea Res.*, 23(12), 1129–1138.
- Montewka J., Krata P., Goerlandt F., Mazaheri A. and Kujala P. 2011. Marine traffic risk modelling – an innovative approach and a case study. *Proc. Inst. Mech. Eng. Part O J. Risk. Reliab.*, 225, 307–322.
- Montewka J., Weckström M. and Kujala P. 2013. A probabilistic model estimating oil spill clean-up costs – A case study for the Gulf of Finland. *Mar. Poll. Bull.*, 76, 61–71.
- Munk W., Armi L., Fischer K. and Zachariasen F. 1997. Spirals on the sea. *Proc. Roy. Soc. London*, 456, 1217–1280.
- Murawski J. and Woge Nielsen J. 2013. Applications of an oil drift and fate model for fairway design. In: Soomere T. and Quak E. (Eds.), *Preventive Methods for Coastal Protection*. Springer, pp. 376–415.
- Myrberg K. and Andrejev O. 2003. Main upwelling regions in the Baltic Sea — a statistical analysis based on three-dimensional modelling. *Boreal Environ. Res.*, 8, 97–112.
- Myrberg K. and Andrejev O. 2006. Modelling of the circulation, water exchange and water age properties of the Gulf of Bothnia. *Oceanologia*, 48(S), 55–74.
- Myrberg K. and Soomere T. 2013. The Gulf of Finland, its hydrography and circulation dynamics. In: Soomere T. and Quak E. (Eds.), *Preventive Methods for Coastal Protection*. Springer, 181–222.
- Myrberg K., Ryabchenko V., Isaev A., Vankevich R., Andrejev O., Bendtsen J., Erichsen A., Funkquist L., Inkala A., Neelov I., Rasmus K., Rodriguez M.M., Raudsepp U., Passenko J., Söderkvist J., Sokolov A., Kuosa H., Anderson T.R., Lehmann A. and Skogen M.D. 2010. Validation of three-dimensional hydrodynamic models in the Gulf of Finland based on a statistical analysis of a six-model ensemble. *Boreal Environ. Res.*, 15, 453–479.
- Nekrasov A.V. and Lebedeva I.K. 2002. Estimation of baroclinic Rossby radii in Luga-Koporye region. *BFU Res. Bull.*, 4–5, 89–93.
- Nencioli F., Dong C., Dicky T., Washburn L. and McWilliams J. C. 2010. A vector geometry-based eddy detection algorithm and its application to a high-resolution numerical model product and high-frequency radar surface velocities in the southern California Bight. *J. Atmos. Oceanic Technol.*, 27, 564–579.
- Okubo A. 1970. Horizontal dispersion of floatable particles in the vicinity of velocity singularities such as convergences. *Deep-Sea Res.*, 17, 445–454.
- Ollitrault M., Gabillet C. and Colin de Verdiere A. 2005. Open ocean regimes of relative dispersion. *J. Fluid. Mech.*, 533, 381–407.

- Omstedt A., Elken J., Lehmann A. and Piechura J. 2004. Knowledge of the Baltic Sea physics gained during the BALTEX and related programmes. *Progr. Oceanogr.*, 63, 1–28.
- Osiński R., Rak D., Walczowski W. and Piechura J. 2010. Baroclinic Rossby radius of deformation in the southern Baltic Sea. *Oceanologia*, 52, 417–429.
- Panigada S., Pesante G., Zanardelli M., Capoulade F., Gannier A. and Weinrich M.T. 2006. Mediterranean fin whales at risk from fatal ship strikes. *Mar. Poll. Bull.*, 52, 1287–1298.
- Pavelson J. 2005. *Mesoscale Physical Processes and Related Impact on the Summer Nutrient Fields and Phytoplankton Blooms in the Western Gulf of Finland*. PhD Thesis, Tallinn University of Technology, Estonia, 216 pp.
- Pavelson J., Laanemets J., Kononen K. and Nõmmann S. 1997. Quasi-permanent density front at the entrance to the Gulf of Finland: response to wind forcing. *Cont. Shelf Res.*, 17, 253–265.
- Periáñez R. 2004. A particle-tracking model for simulating pollutant dispersion in the Strait of Gibraltar. *Mar. Poll. Bull.*, 49, 613–623.
- Raudsepp U. 1998. Current dynamics of estuarine circulation in the lateral boundary layer. *Estuar. Coast. Shelf Sci.*, 47, 715–730.
- Robinson S.K. 1991. Coherent motions in the turbulent boundary layer. *Annu. Rev. Fluid Mech.*, 23, 601–639.
- Rusli M.H.B. 2012. Protecting vital sea lines of communication: a study of the proposed designation of the Straits of Malacca and Singapore as a particularly sensitive sea area. *Ocean Coast. Manage.*, 57, 79–94.
- Sadarjoen I.A. and Post F.H. 2000. Detection, quantification, and tracking of vortices using streamline geometry. *Computers & Graphics*, 24, 333–341.
- Samuelsson P., Jones C.G., Willén U., Ullerstig A., Gollvik S., Hansson U., Jansson C., Kjellström E., Nikulin G. and Wyser K. 2011. The Rossby centre regional climate model RCA3: model description and performance. *Tellus A*, 63, 4–23.
- Schwehr K.D. and McGillivray P.A. 2007. Marine ship Automatic Identification System (AIS) for enhanced coastal security capabilities: an oil spill tracking application. In: *Proceedings of the 2007 OCEANS Conference, Vancouver, Canada, September 29–October 04, 2007*. IEEE Press, New York, pp. 1131–1139.
- SMHI and FIMR 1982. *Climatological ice atlas for the Baltic Sea, Kattegat, Skagerrak and Lake Vänern (1963-1979)*. Norrköping, Sweden, 220 pp.
- Soares C.G. and Teixeira A.P. 2001. Risk assessment in maritime transportation. *Reliab. Eng. Syst. Saf.*, 74, 299–309.
- Sokolov A., Andrejev O., Wulff F. and Rodriguez M.M. 1997. *The data assimilation system for data analysis in the Baltic Sea*. System Ecology Contributions, 3, Stockholm University, Sweden, 66 pp.

- Soomere T. 1995. Generation of zonal flow and meridional anisotropy in two-layer weak geostrophic turbulence. *Phys. Rev. Lett.*, 75, 2440–2443.
- Soomere T. 2003. Anisotropy of wind and wave regimes in the Baltic proper. *J. Sea Res.*, 49(4), 305–316.
- Soomere T. 2013. Towards mitigation of environmental risks. In: Soomere T. and Quak E. (Eds.), *Preventive Methods for Coastal Protection*. Springer, 1–27.
- Soomere T. and Keevallik S. 2003. Directional and extreme wind properties in the Gulf of Finland. *Proc. Est. Acad. Sci. Eng.*, 9, 73–90.
- Soomere T. and Quak E. 2007. On the potential of reducing coastal pollution by a proper choice of the fairway. *J. Coast. Res.*, SI 50, 678–682.
- Soomere T. and Quak E. 2013. *Preventive Methods for Coastal Protection: Towards the Use of Ocean Dynamics for Pollution Control*. Springer, 442 pp.
- Soomere T., Myrberg K., Leppäranta M. and Nekrasov A. 2008. The progress in knowledge of physical oceanography of the Gulf of Finland: a review for 1997–2007. *Oceanologia*, 50, 287–362.
- Soomere T., Delpeche N., Viikmäe B., Quak E., Meier H.E.M. and Döös K. 2011. Patterns of current-induced transport in the surface layer of the Gulf of Finland. *Boreal Environ. Res.*, 16(Suppl A), 49–63.
- Souza J.M.A.C., de Boyer Montégut C. and Le Traon P. Y. 2011. Comparison between three implementations of automatic identification algorithms for the quantification and characterization of mesoscale eddies in the South Atlantic Ocean. *Ocean Sci.*, 7, 317–334.
- Stipa T. 2004. Baroclinic adjustment in the Finnish coastal current. *Tellus A*, 56, 79–87.
- Stokstad E. 2009. US poised to adopt national ocean policy. *Science*, 326, 1618.
- Suursaar Ü. 2010. Waves, currents and sea level variations along the Letipea–Sillamäe coastal section of the southern Gulf of Finland. *Oceanologia*, 52, 391–416.
- Talpsepp L. 1986. On the jet current in the Gulf of Finland. In: *Proceedings of the 15th Conference of the Baltic Oceanographers, Copenhagen, Denmark*, pp. 613–626.
- Talpsepp L., Nõges T., Raid T. and Kõuts T. 1994. Hydrophysical and hydrobiological processes in the Gulf of Finland in summer 1987: characterization and relationship. *Cont. Shelf Res.*, 14, 749–763.
- Thygesen U.H. and Ådlandsvik B. 2007. Simulating vertical turbulent dispersal with finite volumes and binned random walks. *Mar. Ecol. Progr. Ser.*, 347, 145–153.
- Torsvik T. 2013. Introduction to computational fluid dynamics and ocean modelling. In: Soomere T. and Quak E. (Eds.), *Preventive Methods for Coastal Protection*. Springer, 65–100.
- Tufte L., Trieschmann O., Hunsäenger T. and Barjenbruch U. 2004. Spatial analysis and visualization of oil spill monitoring results of the North Sea and

- Baltic Sea. In: Ehlers M., Posa F., Kaufmann H.J., Michel U. and DeCarolis G. (Eds.), *Proceedings of the Conference on Remote Sensing for Environmental Monitoring, GIS Applications and Geology IV, Maspalomas, Spain, September 14–16, 2004*. Proceedings of the Society of Photo-Optical Instrumentation Engineers (SPIE), 5574, pp. 90–99.
- Uiboupin R., Raudsepp U. and Sipelgas L. 2008. Detection of oil spills on SAR images, identification of polluters and forecast of the slicks trajectory. In: *IEEE/OES US/EU-Baltic International Symposium, Tallinn, Estonia, May 27–29, 2008*. IEEE, pp. 270–274.
- Uppala S.M., Kållberg P.W., Simmons A.J., Andrae U., da Costa B.V., Fiorino M., Gibson J.K., Haseler J., Hernandez A., Kelly G.A., Li X., Onogi K., Saarinen S., Sokka N., Allan R.P., Andersson E., Arpe K., Balmaseda M.A., Beljaars A.C.M., van de Berg L., Bidlot J., Bormann N., Cairnes S., Chevallier F., Dethof A., Dragosavac M., Fisher M., Fuentes M., Hagemann S., Hólm E., Hoskins B.J., Isaksen I., Janssen P.A.E.M., Jenne R., McNally A.P., Mahfouf J.-F., Morcrette J.-J., Rayner N.A., Saunders R.W., Simon P., Sterl A., Trenberth K.E., Untch A., Vasiljevic D., Viterbo P. and Woollen J. 2005. The ERA-40 re-analysis. *Q. J. R. Meteorol. Soc.*, 131, 2961–3012.
- Vandenbulcke L., Beckers J.-M., Lenartz F., Barth A., Poulain P.-M., Aidonidis M., Meyrat J., Arduin F., Tonani M., Fratianni C., Torrisi L., Pallela D., Chiggiato J., Tudor M., Book J.W., Martin P., Peggion G. and Rixen M. 2009. Super-ensemble techniques: application to surface drift prediction. *Prog. Oceanogr.*, 52, 149–167.
- Verjovkina S., Raudsepp U., Kõuts T. and Vahter K. 2010. Validation of searack web using surface drifters in the Gulf of Finland and Baltic Proper. In: *2010 IEEE/OES US/EU Baltic International Symposium, Riga, Latvia, August 25–27, 2010*. IEEE Press, New York, 7 pp.
- Viikmäe B., Soomere T., Parnell K.E. and Delpeche N. 2011. Spatial planning of shipping and offshore activities in the Baltic Sea using Lagrangian trajectories. *J. Coast. Res.*, SI 64, 956–960.
- Wang K., Lepparanta M., Gästgifvars M. and Vainio J. 2007. A comparison of drift between sea ice and oil spills in the Baltic Sea: the runner 4 case. In: Yue Q.J. and Ji S.Y. (Eds.), *19th International Conference on Port and Ocean Engineering under Arctic Conditions (POAC 2007), Dalian Univ. Technology, Dalian, Peoples Republic of China, June 27–30, 2007. Recent Development of Offshore Engineering in Cold Regions*, pp. 847–854.
- Ward-Geiger L.I., Silber G.K., Baumstark R.D. and Pulfer T.L. 2005. Characterization of ship traffic in right whale critical habitat. *Coast. Manage.*, 33, 263–278.
- Weiss J. 1991. The dynamics of enstrophy transfer in two-dimensional hydrodynamics. *Physica D*, 48, 273–294.
- Zhubas V.M., Laanemets J., Kuzmina N.P., Muraviev S.S. and Elken J. 2008a. Direct estimates of the lateral eddy diffusivity in the Gulf of Finland of the

- Baltic Sea (based on the results of numerical experiments with an eddy resolving model). *Oceanology*, 48, 175–181.
- Zhurbas V., Laanemets J. and Vahtera E. 2008b. Modeling of the mesoscale structure of coupled upwelling/downwelling events and the related input of nutrients to the upper mixed layer in the Gulf of Finland, Baltic Sea. *J. Geophys. Res.*, 113, C05004.
- Zhurbas V.M., Elken J., Paka V.T., Piechura J., Väli G., Chubarenko I.P., Golenko N. and Shchuka S. 2012. Structure of unsteady overflow in the Słupsk Furrow of the Baltic Sea. *J. Geophys. Res.*, 117(4), C04027.

Acknowledgements

This thesis is based on my work done during the last four years in the Institute of Cybernetics at Tallinn University of Technology. I thank my supervisors, Prof. Tarmo Soomere and Dr. Tomas Torsvik for much patience and guidance.

I am especially grateful to my grandfather Rahuleid, who was a geologist, for encouraging and inspiring me to pursue doctoral studies and science. Unfortunately, he is unable to read the final version of this thesis.

I would like to thank my colleagues from the Laboratory of Wave Engineering, particularly Nicole Delpeche-Ellmann for fruitful discussions on various topics.

Last but not least, I thank my family for supporting me in the choices I have made. My sincerest gratitude goes to my son Norman and my fiancée Mari. This thesis would not have been possible without their support and patience.

* * *

The research presented in this thesis was originally motivated by the BONUS project BalticWay which attempted to propose ways to reduce pollution risks in the Baltic Sea by smart placing of human activities. The studies were also supported by the targeted financing of the Estonian Ministry of Education and Research (Grant No. SF0140007s11), by the European Union (European Regional Development Fund) through the Mobilitas project MTT63 and the Centre of Excellence for Non-linear Studies CENS, and to a lesser extent by the project TERIKVANT in the framework of the Environmental Technology R&D Programme KESTA.

Abstract

This thesis deals with several ways of detection of coherent and semi-persistent patterns in the surface layer of seas and oceans and explores the possibilities for their use for environmental management of potentially dangerous offshore activities. First, a short overview of the study area (Gulf of Finland in the Baltic Sea), the Rossby Centre Ocean model (RCO) and OAAS (by O. Andrejev and A. Sokolov) circulation model, used for replication of the surface velocities, and the TRACMASS code, used for evaluation of Lagrangian trajectories of selected passively advected parcels, is presented.

A discussion of the potential of coherent and semi-persistent currents for mitigation of hazards associated with offshore pollution is followed by an insight into possibilities of automatic detection of such patterns in strain and vorticity fields using the Okubo–Weiss parameter and subsequent application of the geometrical (streamline winding angle) criterion. The resulting hybrid method works well for the high-resolution Eulerian velocity fields in the Vatløstraumen area (Norway) but detects only a small number of eddies in the Gulf of Finland.

The main body of the thesis addresses the possibilities of using statistical analysis of Lagrangian trajectories of persistent parcels of pollution, passively advected by surface currents, to calculate the spatial distributions of probabilities and times for such parcels to reach the coastal area (to exert a coastal hit), and of the subsequent use of these distributions for environmental management of ship traffic and specification of environmentally optimised fairways. The analysis is mostly based on trajectories evaluated by the non-spreading version of the TRACMASS code from velocity fields calculated by the RCO circulation model for 1982–2001. The sensitivity studies, designed for estimating the key parameters in the model, revealed that the optimum width of the nearshore area in this set-up is about three ocean model grid cells, the appropriate length of trajectories is 10–20 days and the total time interval to be covered is at least a few years.

A method is developed for establishing the location of the equiprobability line, from where the probability of current-driven propagation of pollution to the opposite coasts is equal. Spatial distributions of probabilities and of the time it takes for pollution parcels to reach the nearshore are calculated based on 10–20-day-long trajectories. The optimum fairways minimising the probability and maximising the time for coastal hits are mostly located to the north of the centreline of the gulf. The root mean square deviation between the optimum fairways specified from different criteria is 6–16 km. The most frequently hit nearshore areas are short fragments between Hanko and Helsinki and to the south-east of Vyborg, and longer segments from Tallinn to Hiiumaa. A short section of the fairway to the south of Vyborg and a segment to the west of Tallinn are the most probable starting points of parcels. The inclusion of the artificial spreading of the modelled Lagrangian trajectories substantially changes the appearance of single trajectories and the spreading of initially closely located parcels but almost does not impact the pattern and frequency of hits to the nearshore.

Resümee

Doktoritöös käsitletakse erinevaid meetodeid koherentsete ja poolpüsivate hoovuste muustrite tuvastamiseks merede ja ookeanide pinnakihis ning uuritakse võimalusi nende rakendamiseks avamerel toimivate potentsiaalselt ohtlike tegevuste keskkonnajuhtimises. Esitatakse lühiülevaade uurimispiirkonnast (Soome laht Läänemeres), tsirkulatsioonimudelitest RCO ja OAAS (millega on arvatud pinnahoovuste kiiruste andmestikud) ning TRACMASS tarkvarast, millega leitakse lisandite edasikandumise Lagrange'i trajektoorid. Kirjanduse alusel käsitletakse võimalusi rakendada koherentsete ja poolpüsivate hoovuste potentsiaali avamerelt pärit reostuse mõju leevendamiseks. Vaadeldakse kiirusvälja keeriselisuse jm. muustrite automaatse tuvastamise meetodeid, kasutades järjestikku Okubo-Weiss'i parameetrit ja voolujoonte pöördenuurkade summal baseeruvat geomeetrilist kriteeriumit. Taoline hübriidmeetod toimib edukalt kõrge lahutusvõimega Euleri kiirusväljade puhul Vathestraumeni (Norra) piirkonnas, kuid tuvastab ainult üksikuid keeriseid Soome lahes.

Töö põhiosas uuritakse võimalusi kasutada pinnahoovuste poolt edasi kantavate püsivate reostusosakeste trajektooride statistilist analüüsi laevaliikluse keskkonnajuhtimiseks ning keskkonna jaoks optimaalsete laevateede konstrueerimiseks. Rakenduste aluseks on selliste osakeste randa jõudmise tõenäosuse ja aja ruumilised jaotused. Analüüs põhineb peamiselt RCO tsirkulatsioonimudeli väljundi (kiiruste andmestik aastate 1982–2001 jaoks) põhjal TRACMASS tarkvara hajumist ignoreeriva versiooni abil arvatud trajektooridel. On leitud, et sellise mudeli rakendamisel peab rannavööndi optimaalne laius olema kolm tsirkulatsioonimudeli võrgupunkti, trajektooride pikkus 10–20 päeva ning simulatsiooni kogupikkus vähemalt mõned aastad.

On esitatud võrdtõenäosusjoone kontseptsioon ja meetod selle leidmiseks. Joon kirjeldab punkte, millesse sattunud lisandid triivivad vastastikku paiknevatele rannikuosadele võrdse tõenäosusega. Kõnesolev joon on arvatud mitmete erinevate Soome lahe põhja- ja lõunaranniku eralduspunktide jaoks.

Teine komplekt optimaalseid laevateid kulgeb piki reostusosakeste randa triivimise tõenäosuse ja aja ruumiliste jaotuste ekstreemumeid. Need jaotused on arvatud 10–20 päeva pikkuste trajektooride alusel. Erinevate meetoditega arvatud optimaalsed laevateed paiknevad lähestikku Soome lahe kitsamas osas, kuid erinevad mõnevõrra lahe laiemates osades. Optimaalsete laevateede ruutkeskmine erinevus on 6–16 km.

Kõige sagedamini tabab laevateelt pärinev reostus lühikesi rannaosi Hanko ja Helsingi vahel, Viiburist lõunas, Soome lahe kirderannikul ning Tallinna ja Hiiumaa vahelisel alal. Kõige suurem tõenäosus randa jõudmiseks on osakestel, mis on sattunud merre lühikesel laevatee lõigul Viiburist lõunas ja pikemal lõigul Tallinnast läänes. Tehisliku hajumise lisamine mudelisse mõjutab oluliselt üksikuid trajektoore ja algselt lähestikku paiknevate osakeste hargnemist, kuid ei oma peaaegu mingit mõju rannikutabamuste sagedusele ja muustrile.

Appendix A: Curriculum Vitae

1. Personal data

Name	Bert Viikmäe
Date and place of birth	25.01.1982, Valga, Estonia
Address	Akadeemia tee 21, 12618 Tallinn
Phone	(+372) 620 4167
e-mail	bert@ioc.ee

2. Education

Educational institution	Graduation year	Education (field of study / degree)
Tallinn University of Technology	2005	Informatics / MSc
Estonian Information Technology College	2003	Information Systems Development / Applied higher education

3. Language competence/skills

Language	Level
Estonian	native language
English	fluent
Russian	average
Finnish	average

4. Special courses and further training

Period	Educational or other organisation
2009	<i>TRACMASS – A Lagrangian Trajectory code</i> , Tallinn University of Technology, Estonia
2011	BalticWay summer school <i>Preventive methods for coastal protection</i> , Lithuania

5. Professional employment

Period	Organisation	Position
Sept. 2010 – to date	Institute of Cybernetics, Tallinn University of Technology	Research Scientist
July 2009 – Sept. 2010		Engineer- programmer
May 2009 – July 2009	Softronic Baltic AS	Software Developer
Oct. 2007 – Mar. 2009	TietoEnator Eesti AS	Software Developer
Nov. 2003 – Oct. 2007	Proekspert AS	Software Engineer
Apr. 2003 – Nov. 2003	Eesti Ekspressi Kirjastuse AS	Software Developer

6. Research activity

6.1. Publications

Articles indexed by the Web of Science database (1.1):

Viikmäe B., Soomere T., Parnell K.E. and Delpeche N. 2011. Spatial planning of shipping and offshore activities in the Baltic Sea using Lagrangian trajectories. *Journal of Coastal Research*, Special Issue 64, 956–960.

Soomere T., **Viikmäe B.**, Delpeche N. and Myrberg K. 2010. Towards identification of areas of reduced risk in the Gulf of Finland, the Baltic Sea. *Proceedings of the Estonian Academy of Sciences*, 59(2), 156–165.

Soomere T., Delpeche N., **Viikmäe B.**, Quak E., Meier H.E.M. and Döös K. 2011. Patterns of current-induced transport in the surface layer of the Gulf of Finland. *Boreal Environment Research*, 16(Suppl. A), 49–63.

Soomere T., Berezovski M., Quak E. and **Viikmäe B.** 2011. Modelling environmentally friendly fairways using Lagrangian trajectories: a case study for the Gulf of Finland, the Baltic Sea. *Ocean Dynamics*, 61(10), 1669–1680.

Viikmäe B. and Soomere T. 2014. Spatial pattern of current-driven hits to the nearshore from a major marine highway in the Gulf of Finland. *Journal of Marine Systems*, 129, 106–117.

Viikmäe B., Torsvik T. and Soomere T. 2013. Impact of horizontal eddy-diffusivity on Lagrangian statistics for coastal pollution from a major marine fairway. *Ocean Dynamics*, 63(5), 589–597.

Viikmäe B. and Torsvik T. 2013. Quantification and characterization of mesoscale eddies with different automatic identification algorithms. *Journal of Coastal Research*, Special Issue 65, 2077–2082.

Peer-reviewed articles in other international journals (1.2) and collections (3.1):

Viikmäe B., Soomere T., Viidebaum M. and Berezovski A. 2010. Temporal scales for transport patterns in the Gulf of Finland. *Estonian Journal of Engineering*, 16(3), 211–227.

Andrejev O., Sokolov A., Soomere T., Värvi R. and **Viikmäe B.** 2010. The use of high resolution bathymetry for circulation modelling in the Gulf of Finland. *Estonian Journal of Engineering*, 16(3), 187–210.

Berezovski M., Berezovski A., Soomere T. and **Viikmäe B.** 2010. On wave propagation in laminates with two substructures. *Estonian Journal of Engineering*, 16(3), 228–242.

Viikmäe B., Torsvik T. and Soomere T. 2012. Analysis of the structure of currents in the Gulf of Finland using the Okubo–Weiss parameter. In: *Proceedings of the IEEE/OES Baltic 2012 International Symposium ‘Ocean: Past, Present and Future. Climate Change Research, Ocean Observation & Advanced Technologies*

for Regional Sustainability', May 8–11, Klaipėda, Lithuania. IEEE Conference Publications, 7 pp.

Articles published in other conference proceedings (3.4):

Delpeche N., Soomere T. and **Viikmäe B.** 2010. Towards a quantification of areas of high and low risk of pollution in the Gulf of Finland, with the application to ecologically sensitive areas. In: Reckermann M. and Isemer H.-J. (Eds.), *6th Study Conference on BALTEX, 14–18 June 2010, Międzyzdroje, Island of Wolin, Poland: Conference Proceedings, Geesthacht, Germany*. International BALTEX Secretariat Publication, 46, 138–139.

Andrejev O., Sokolov A., Soomere T., Myrberg K. and **Viikmäe B.** 2010. Using multi-year circulation simulations to identify areas of reduced risk for marine transport. Application to the Gulf of Finland. In: Reckermann M. and Isemer H.-J. (Eds.), *6th Study Conference on BALTEX: 14–18 June 2010, Międzyzdroje, Island of Wolin, Poland: Conference Proceedings, Geesthacht, Germany*. International BALTEX Secretariat Publication, 46, 135–136.

Viikmäe B., Soomere T., Delpeche N., Meier H.E.M. and Döös K. 2010. Utilizing Lagrangian trajectories for reducing environmental risks. In: Reckermann M. and Isemer H.-J. (Eds.), *6th Study Conference on BALTEX: 14–18 June 2010, Międzyzdroje, Island of Wolin, Poland: Conference Proceedings, Geesthacht, Germany*. International BALTEX Secretariat Publication, 46, 159–160.

Võhandu L., Alumäe T., **Viikmäe B.** and Sirts K. 2005. Estonian speech-driven PC-interface for disabled persons. In: Langemets M. and Penjam P. (Eds.), *The Second Baltic Conference on Human Language Technologies: Proceedings, April 4–5, 2005, Tallinn, Estonia*. Tallinn: Institute of Cybernetics (Tallinn University of Technology); Institute of the Estonian Language, 359–364.

Abstracts of conference presentations (5.2):

Viikmäe B. and Torsvik T. 2013. Analysis and comparison of automatic eddy detection methods. In: *BSSC 9th Baltic Sea Science Congress: New Horizons for Baltic Sea Science, 26–30 August, 2013, Klaipėda, Lithuania, Abstract Book: Klaipėda*. Coastal Research and Planning Institute of Klaipėda University (KU CORPI), 265.

Torsvik T., Soomere T., Kalda J. and **Viikmäe B.** 2013. Improving the forecast of coastal pollution using surface drifter trajectories. In: *BSSC 9th Baltic Sea Science Congress: New Horizons for Baltic Sea Science, 26–30 August, 2013, Klaipėda, Lithuania, Abstract Book: Klaipėda*. Coastal Research and Planning Institute of Klaipėda University (KU CORPI), 118.

Viikmäe B., Torsvik T. and Soomere T. 2013. In search for hidden transport patterns governing the coastal pollution. In: Russell P.E. and Masselink G. (Eds.), *ICS2013 International Coastal Symposium: Book of Abstracts, Plymouth University, 8–12 April 2013*. CERF, 280.

Viikmäe B., Torsvik T. and Soomere T. 2012. Analysis of the structure of currents in the Gulf of Finland using the Okubo–Weiss parameter. In: *6th European Postgraduate Fluid Dynamics Conference: Conference Programme [10–12 July 2012, London, UK]*, 60.

Viikmäe B. and Soomere T. 2012. Spatial pattern of hits to the nearshore from a major marine highway in the Gulf of Finland. In: *Joint Numerical Modelling Group 16th Biennial Conference: Book of Abstracts [21–23 May 2012, Brest, France]*, 25.

Viikmäe B., Torsvik T. and Soomere T. 2012. Analysis of the structure of currents in the Gulf of Finland using the Okubo-Weiss parameter. In: *IEEE/OES Baltic International Symposium: Presentation Abstracts [08–11 May 2012, Klaipeda, Lithuania]*, 48.

Viikmäe B. and Soomere T. 2012. Patterns of hits to the nearshore from a major fairway in the Gulf of Finland. *Geophysical Research Abstracts*, 14, EGU2012-5974.

Viikmäe B., Soomere T. and Delpeche-Ellmann N. 2011. Optimizing fairways to reduce environmental risks in the Baltic Sea. In: *8th Baltic Sea Science Congress: Book of Abstracts [22–26 Aug 2011, St. Petersburg, Russian Federation]*, 88.

Viikmäe B., Soomere T. and Delpeche-Ellmann N. 2011. Optimizing fairways for environmental management in the Baltic Sea. In: *3rd International Workshop on Modeling the Ocean: Book of Abstracts [06–09 June 2011, Qingdao, China]*, 66.

Viikmäe B., Soomere T. and Delpeche N. 2011. Technology for finding optimum fairways for environmental management in the Baltic Sea. In: *International Conference ‘Particles in Turbulence 2011’ on Fundamentals, Experiments, Numeric and Applications: Book of Abstracts [16–18 March 2011, Potsdam, Germany]*, 78.

Viikmäe B., Soomere T. and Delpeche N. 2011. Using Lagrangian trajectories to find areas of reduced risk of coastal pollution in the Gulf of Finland. In: *5th International Student Conference on ‘Biodiversity and Functioning of Aquatic Ecosystems in the Baltic Sea Region’: Conference Proceedings [06–08 October 2010, Palanga, Lithuania]*, 106.

Viidebaum M., **Viikmäe B.** and Delpeche N. 2010. Sensitivity study of the Lagrangian trajectory model TRACMASS. In: *5th International Student Conference on ‘Biodiversity and Functioning of Aquatic Ecosystems in the Baltic Sea Region’: Conference Proceedings [06–08 October 2010, Palanga, Lithuania]*, 104–105.

Viikmäe B., Soomere T. and Delpeche-Ellmann N. 2010. Potential of using Lagrangian trajectories for environmental management in the Gulf of Finland. In: *The 10th International Marine Geological Conference: Abstract Volume [24–28 August 2010, St. Petersburg, Russian Federation]*, 148.

Viikmäe B., Soomere T. and Delpeche N. 2010. The use of Lagrangian trajectories for minimization of the risk of coastal pollution. In: *Joint Numerical Modelling*

Group 15th Biennial Conference: Programme and Book of Abstracts [10–12 May 2010, Delft, Netherlands], 7.

Soomere T., Delpeche N. and **Viikmäe B.** 2010. The use of current-induced transport for coastal protection in the Gulf of Finland, the Baltic Sea. *Geophysical Research Abstracts*, EGU2010-6056.

Viikmäe B., Isotamm R. and Delpeche N. 2010. An empirical method to determine patterns of the risk of coastal pollution in the Gulf of Finland. In: *Joint Baltic Sea Research Programme BONUS. Annual Conference: Programme and Abstracts [19–21 January 2010, Vilnius, Lithuania]*, 6.

Soomere T., Delpeche N. and **Viikmäe B.** 2010. Semi-persistent patterns of transport in surface layers of the Gulf of Finland. In: *Joint Baltic Sea Research Programme BONUS. Annual Conference: Programme and Abstracts [19–21 January 2010, Vilnius, Lithuania]*, 32.

Delpeche N., Isotamm R., **Viikmäe B.** and Soomere T. 2009. Application of a trajectory model to select areas of high risk of pollution. In: *Coping with Uncertainty: A Multidisciplinary Research Conference on Risk Governance in the Baltic Sea Region, Stockholm, 15–17 November 2009: Book of Abstracts*. Södertörn University, 29.

Isotamm R., **Viikmäe B.** and Delpeche N. 2009. An empirical method to determine a low-risk fairway in the Gulf of Finland. In: *Coping with Uncertainty: A Multidisciplinary Research Conference on Risk Governance in the Baltic Sea Region, Stockholm, 15–17 November 2009: Book of Abstracts*. Södertörn University, 31.

Appendix B: Elulookirjeldus

1. Isikuandmed

Ees- ja perekonnanimi Bert Viikmäe
Sünniaeg ja -koht 25.01.1982, Valga
Aadress Akadeemia tee 21, 12618 Tallinn
Telefon (+372) 620 4167
e-mail bert@ioc.ee

2. Hariduskäik

Õppeasutus	Lõpetamise aeg	Haridus (eriala / kraad)
Tallinna Tehnikaülikool	2005	Informaatika / tehnikateaduse magister
Eesti Infotehnoloogia Kolledž	2003	Infosüsteemide arendus / rakenduslik kõrgharidus

3. Keelteoskus

Keel	Tase
inglise	kõrgtase
eesti	emakeel
vene	kesktase
soome	kesktase

4. Täiendõpe

Õppimise aeg	Täiendõppe läbivijja nimetus
2009	<i>TRACMASS – A Lagrangian Trajectory code</i> , Tallinna Tehnikaülikool, Eesti
2011	BalticWay suvekool <i>Preventiivsed meetodid keskkonna kaitseks</i> , Klaipeda, Leedu

5. Teenistuskäik

Töötamise aeg	Tööandja nimetus	Ametikoht
Sept. 2010 – tänaseni	Tallinna Tehnikaülikool,	Teadur
Juuli 2009 – sept. 2010	Küberneetika Instituut	Insener-programmeerija
Mai 2009 – juuli 2009	Softronic Baltic AS	Tarkvara arendaja
Okt. 2007 – märts 2009	TietoEnator Eesti AS	Tarkvara arendaja
Nov. 2003 – okt. 2007	Proekspert AS	Tarkvarainsener
Aprill 2003 – nov. 2003	Eesti Ekspressi Kirjastuse AS	Tarkvara arendaja

6. Teadustegevus

Avaldatud teadusartiklite ja konverentsiteeside ning peetud konverentsietekannete loetelu on toodud ingliskeelse CV juures.

Paper A

Soomere T., **Viikmäe B.**, Delpeche N. and Myrberg K. 2010. Towards identification of areas of reduced risk in the Gulf of Finland. *Proceedings of the Estonian Academy of Sciences*, 59(2), 156–165.



Towards identification of areas of reduced risk in the Gulf of Finland, the Baltic Sea

Tarmo Soomere^{a*}, Bert Viikmäe^a, Nicole Delpêche^a, and Kai Myrberg^b

^a Institute of Cybernetics at Tallinn University of Technology, Akadeemia tee 21, 12618 Tallinn, Estonia

^b Finnish Environment Institute, P.O. Box 140, FI-00251, Helsinki, Finland

Received 15 January 2010, revised 4 March 2010, accepted 8 March 2010

Abstract. A Lagrangian trajectory model, TRACMASS with the use of velocity fields calculated by the Rossby Centre (Swedish Hydrological and Meteorological Institute) circulation model, is employed to analyse trajectories of current-driven surface transport in the Gulf of Finland, the Baltic Sea, for the period of 1987–1991. Statistical analysis of trajectories is performed to calculate a map of probabilities for adverse impacts released in different sea areas to hit the coast. There is a clearly defined curve (equiprobability line) in the western part of the gulf from which the chances of the propagation of adverse impacts to either of the coasts are equal. The current-driven propagation of tracers from a wide area (of reduced risk) to the coast in the central and eastern parts of the gulf is unlikely within about three weeks. A safe fairway in terms of coastal protection goes over the equiprobability line and the area of reduced risk.

Key words: pollution transport, risk analysis, currents, hydrodynamic modelling, Gulf of Finland, Baltic Sea.

INTRODUCTION

The existence of quasi-persistent patterns of currents in various parts of the Baltic Sea (Lehmann et al., 2002; Andrejev et al., 2004a, 2004b; Osinski and Piechura, 2009) leads to the interplay of the high variability and extreme complexity of the surface currents with the presence of rapid pathways of the current-driven transport (Soomere et al., 2010). This combination opens a principally new way towards a technology that uses the marine dynamics for the reduction of environmental risks stemming from shipping and offshore and coastal engineering activities. The key benefit is an increase in the time during which an adverse impact (for example, an oil spill) reaches a vulnerable area after an accident has happened (Soomere and Quak, 2007). The use of this technology, however, requires adequate estimates of the persistency and variability of the patterns, and of the confidence and uncertainty related to their practical use.

The drift of adverse impacts, oil spills, lost containers, ships without propulsion, etc. is jointly governed

by wind stress, waves, and currents. The properties of transport by wind and waves are understood quite well (ASCE, 1996; Sobey and Barker, 1997; Reed et al., 1999; Castanedo et al., 2006). As the instantaneous field of currents is created under the joint influence of a large pool of local and remote forcing factors, the prediction of the current-induced contribution to the drift is still a challenge. Theoretically, transport of water particles and drift of tracers can be described to some extent with the use of deterministic circulation models. There is, however, not yet a model capable of sensibly forecasting the drift or a deterministic method to combine different models to reproduce the floating object drift (Vandenbulcke et al., 2009). The results are highly sensitive with respect to the particular model and small variations of the initial and forcing conditions (Griffa et al., 2004). The problem is even more complicated in strongly stratified sea areas such as the Gulf of Finland where the drift is frequently steered by multi-layered dynamics (Gästgifvars et al., 2006).

A feasible way to reduce the uncertainties of the current-induced drift patterns consists in the implicit or explicit use of statistical approaches. An attempt in this

* Corresponding author, soomere@cs.ioc.ee

direction is made by means of numerical identification of patterns of net transport and the ratio of the net and bulk transport in the Gulf of Finland, the Baltic Sea (Soomere et al., 2010).

The focus of this paper is a statistical technique for the optimization of the potential risk stemming from anthropogenic activities in elongated sea areas. The classical definition of risk expresses it as the product of the probability of an accident and the cost of its consequences. The cost of the consequences of an accident in the marine environment substantially depends not only on the nature or magnitude of the adverse impact but also on the place hit. Moreover, the consequences could frequently be reduced by gaining some time to combat the adverse impact.

We aim at decreasing the risk by means of maximizing the time over which the current-driven propagation of the consequences of an accident will affect high-cost areas. As the nearshore frequently has the largest ecological value (Kokkonen et al., 2010), in this study we consider the coastal zone as a generic example of a high-cost area. The proposed approach is evidently independent of the particular definition of the coastal area and, equivalently, of the particular form of the cost function.

A direct application of the approach is a problem of the optimization of marine transport routes in order to minimize the probability of a coastal pollution and/or to maximize the time over which adverse impacts reach the coasts. For open ocean coasts this can be done by shifting the fairway offshore or by relocating it in a certain manner to minimize the adverse impacts to the environment (Stokstad, 2009).

A key question for narrow bays and elongated sea areas is how to minimize the joint probability of hitting either of the coasts. The first-order solution for narrow basins is the equiprobability line, from which the probability of propagation of pollution to either of the coasts is equal. If the transport patterns were completely isotropic and homogeneous, this line would coincide with the axis of the basin. For wider sea areas there may also appear quite a wide area of reduced risk, from which the propagation of pollution to any of the coasts is unlikely. The safest fairway would thus follow a combination of the equiprobability line and the area(s) of reduced risk.

A systematic solution to the formulated problem presumes inverse tracking of the propagation of adverse impacts. It is well known that neither a straightforward solution to this problem nor a universal solution method exists. We shall address it by means of statistical analysis of a large pool of numerically simulated trajectories of drifters in the surface layer. The key idea, therefore, is not to produce another operational model to represent the drift after an accident has actually happened but rather to identify beforehand the regions where it is statistically safer to travel.

The analysis is performed for the Gulf of Finland (Fig. 1), an elongated, stratified sub-basin of the Baltic Sea with a length of about 400 km, width between 48 and 125 km, and a mean depth of 37 m only. This region, declared a particularly sensitive sea area by the International Maritime Organisation (Soomere et al., 2008), hosts extremely heavy and rapidly increasing ship traffic.

The calculations are based on the results of long-term, high-resolution simulations of the circulation in the entire Baltic Sea. A Lagrangian trajectory model is applied to extract useful information from these simulations. The goal is to evaluate favourable features of the current-driven transport that have time scales of the order of a week and that can be extracted neither directly from the velocity data nor from the long-term average circulation patterns.

MODELLING THE ENVIRONMENT

The tool for the analysis of current-driven transport of adverse impacts is a Lagrangian trajectory model, TRACMASS (Döös, 1995; Vries and Döös, 2001). It uses pre-computed three-dimensional Eulerian current velocity fields to evaluate an approximate path of water particles (equivalently, neutral tracer of an adverse impact) based on an analytical solution of a differential equation for motion that depends on the velocities on the grid box walls. This off-line method of calculation makes it possible to reckon a large pool of trajectories for different starting instants and positions once the velocity fields are available. The method was originally developed for stationary velocity fields (Döös, 1995; Blanke and Raynaud, 1997), then expanded to time-dependent fields (Vries and Döös, 2001) by implementation of a linear interpolation of the velocity field both in time and in space, and has become a standard tool for studies of complex motions of water particles in the marine environment (Jönsson et al., 2004; Döös and Engqvist, 2007).

In this study we use the surface-layer velocity fields calculated for 1987–1991 for the entire Baltic Sea using the Rossby Centre Ocean circulation model (RCO) with a temporal resolution of 6 hours. This time period was chosen in order to make the results comparable with circulation simulations (Andrejev et al., 2004a, 2004b) and studies of average transport patterns in the same basin (Soomere et al., 2010). The RCO is a primitive equation circulation model coupled with an ice model (Meier et al., 2003). It covers the entire Baltic Sea with the horizontal resolution of 2×2 nautical miles and uses 41 vertical levels in z -coordinates. The thickness of the uppermost layer is 3 m.

The model is forced by wind data on the 10 m level, air temperature and specific humidity on the 2 m level,

precipitation, cloudiness, and sea level pressure fields, and it also accounts for river inflow and water exchange through the Danish Straits. This data set is calculated from the ERA-40 re-analysis using a regional atmosphere model with a horizontal resolution of 25 km (Höglund et al., 2009). As the atmospheric model tends to underestimate extreme wind speeds, the wind is adjusted using simulated gustiness. Further details of the model set-up and validation experiments are discussed in (Meier, 2001, 2007; Meier et al., 2003).

Trajectories of water particles (equivalently, current-driven propagation of an adverse impact) are simulated for a few weeks for certain distributions of the initial positions. The resulting trajectories are saved for further analysis and the simulations for the same initial positions of particles are restarted from another time instant. The process is repeated over the chosen time period.

High risk to a nearshore section is assumed when pollution reaches a distance of less than three grid points (about 11 km) from the coast (cf. Lessin et al., 2009). As a first approximation, the percentage of tracers that approach the nearshore zone of this width within a certain time interval is used as an estimate of the risk. Alternatively, the average time it takes the tracer to reach such points is a measure of risk associated with the starting point. In this study we use a simplified approach and rely only on the fact of reaching the nearshore.

In order to avoid problems connected with potentially insufficient accuracy of the representation of vertical velocities in the RCO model, the trajectories are locked in the uppermost layer. This is done by means of switching off the three-dimensional tracing in the TRACMASS model. The resulting trajectories are, thus, not truly Lagrangian: they are not passively advected by the velocity fields and rather represent motion of tracers that are slightly lighter than the surrounding water (such as oil in otherwise calm conditions) or are confined to the upper layer by other constraints. This set-up of trajectory modelling is best suited for representing, for example, the drift patterns of lost containers.

TIME SCALES AND PATTERNS OF TRANSPORT

First a series of experiments was performed to estimate the typical time over which the particles reached the nearshore. The trajectories were started from centres of 96 cells located along the straight line in Fig. 1, roughly representing the axis of the Gulf of Finland (that is, at points remotest from the coasts). The simulations were started at midnight each calendar day in 1987 and run for 10 days. As discussed below, this is roughly the time during which the largest amount of tracers released along the axis of the Gulf of Finland reaches the nearshore.

The number of particles that entered the nearshore (called below hits of the nearshore) during these days showed very high variability (Fig. 2). The count (equivalently, the percentage of particles) varied from zero up to about 60. In general, the smallest number of hits occurred in the calm season (April–July) and the highest, not surprisingly, in the windy autumn and winter season. There was, however, also a certain time section of the calm period when the number of hits was close to 50.

On average, about 30% of the particles released along the axis of the gulf hit the nearshore of either of the coasts within 10 days. This estimate is in accordance with numerical results of Prof. S. Ovsienko (pers. comm.) and apparently reflects the lower bound of the probability for a hit of a coastal zone by an adverse impact released in a random location of the gulf. Other factors influencing the drift such as wind, waves, and spreading (of oil spills) apparently increase this probability as they generally magnify the excursions of the released substances and/or enlarge the sea area hosting the adverse impact.

The typical time for a hit in both calm and windy seasons also largely varied. For example, Fig. 3 illustrates that in May 1987 a few hits occurred already during the first day of propagation while in July the first hit took place only on the ninth day. The further behaviour of the particles was also substantially different. In May the maximum number of particles located in the nearshore was 19 and almost no hit was observed starting from day 8. The number of such particles was between 30 and 43 during almost a week (days 12–17) in July (Fig. 3). In total, no more than 19% of the particles simultaneously resided in the nearshore in May whereas this percentage reached 43 in July.

The typical time of the first hit to the coast was 3 days in 1987. A substantial number of hits, though, occurred already on the first day, which also was the median value of the number of days in question. This low number apparently is due to the smallness of the basin and the closeness of some of the release points to the coastal zone. The typical time when the largest number of particles was found in the nearshore was 11 days from the start of the simulations in 1987. This value is close to the median value (12 days).

The overall character of the current field is well known for the Gulf of Finland. The vertically averaged mean circulation of this basin is cyclonic with an average velocity of a few centimetres per second (Alenius et al., 1998; Lehmann et al., 2002). This overall scheme is superposed by numerous meso-scale baroclinic eddies and many local features (Andrejev et al., 2004a, 2004b; Soomere et al., 2008). The transport in the uppermost layer is largely governed by the Ekman drift, especially in relatively windy seasons when the

dynamics of the uppermost layer is apparently to some extent decoupled from the underlying layers.

These motion configurations are, however, only valid on average. The above estimates suggest that the transport of adverse impacts to the coasts not necessarily follows the long-term average flows. Instead, it is governed by much faster processes and has the time scale of a few days up to a few weeks. One of the reasons for the extreme complexity of current patterns in this basin is that the internal Rossby-radius of deformation (which governs the size of meso-scale features) is only 2–4 km in the Gulf of Finland. This feature indicates the necessity of the use of high-resolution models (≤ 1.5 km) for this water body (Alenius et al., 2003).

A great role of local, short-term drivers is reflected in the extremely large variability of the probability of hitting the southern and northern coasts of the Gulf of Finland (Fig. 4) for different time periods. In the simulation started on 1 October 1987 almost all hits to the nearshore occurred along the northern coast whereas 59% of the particles reached the nearshore. The overwhelming majority of particles launched on 1 December, however, came to the southern coast (52% of the particles reached the nearshore in this case).

THE EQUIPROBABILITY LINE

The presented examples show that there exists no a priori safe location in the Gulf of Finland in terms of a low probability of the propagation of adverse impacts to the coastal area. A first step towards solving the problem of minimizing the probability of hitting any section of the coast is to identify a line (or area) from which the probability of the propagation to the opposite coasts is equal. In simulations below, the southern coast represents the coastline of Estonia whereas the coasts of Russia and Finland are merged to represent the northern coast.

Below we use two methods (a direct method and a smoothing one) for numerical estimation of the location of the equiprobability line and areas of reduced risk. Both are based on tracking trajectories with the use of the TRACMASS code and differ only in how the trajectories are grouped in the evaluation of the probability the particles released in a particular sea area enter a nearshore region. The difference in the positions between the two estimates of the location of the line can be interpreted as a rough measure of the uncertainty of its location. The deviation of this line from the axis of the gulf characterizes the asymmetry of the surface-layer current-driven transport in this basin.

The simulation process is depicted in Fig. 5. In order to obtain reliable statistics of the transport patterns, the simulations cover a relatively long time interval t_D , which typically involves at least one season but frequently one or more years. It is divided into time

windows of equal length $t_W \ll t_D$. The duration t_W is chosen based on the above estimates of the typical time scales of phenomena under research and typically is from a few days up to a few weeks. The windows are separated from each other by the time lag $t_S \ll t_W$, the duration of which varies from 6 hours (which is the time step of available velocity fields) to 10 days.

A pool of trajectory simulations is started at a certain time instant t_0 when a cluster of particles is released into the Gulf of Finland. In the above examples one particle was released into the centre of each grid cell of a set of 96 cells along a straight line more or less coinciding with the axis of the gulf (Fig. 1). For the simulations below, one or more particles were released into each of 3131 sea points of the gulf.

The trajectories are first simulated over a time window $[t_0, t_0 + t_W]$. The results are saved for further analysis. The same cluster of tracers is then released at time instant $t_0 + t_S$. The trajectories are again calculated over a window with a duration of t_W . The process is repeated $(t_D - t_W)/t_S$ times. Finally, the outcome of simulations is averaged over all time windows. For example, for a yearly simulation with the time window of $t_W = 20$ days and with a lag $t_S = 10$ days, the averaging is performed over 35 ensembles of trajectories, the last examples of which start on 12 December and end at the midnight of 31 December.

Within each time window, the instantaneous position $[x_{ij}(t), y_{ij}(t)]$ and the distance $\Delta_{ij}(t)$ of the trajectory from the coast were calculated for the entire time window and for each of the released tracers. Here i is the grid cell number, $1 \leq i \leq N$, N is the total number of cells into which the tracer is released, j is the number of a tracer particle in the i -th cell, $1 \leq j \leq N_i$, and N_i is the total number of particles released into the i -th cell. The instantaneous location of the tracer is used to estimate whether the trajectory has entered the nearshore.

The direct method for the estimation of the location of the equiprobability line and safe areas in the Gulf of Finland is based on point-wise analysis of what happens with the trajectories for each of $N = 3131$ grid cells in the gulf with the time lag of 10 days. Four particles ($N_i = 4$, $1 \leq i \leq N$) are released in each grid cell (symmetrically with respect to the cell centre) at the beginning of each time window. A count is made if over 50% (that is three or all four) of the trajectories travelled to the same coast within the time window. If yes, the cell is assumed the value of $c = \pm 1$ depending on the count of the hits to the nearshore of the southern or the northern coast. If no more than two tracers reached a particular coast within the time window (incl. the situation when two tracers reached the southern and the other two the northern coast), the cell is assumed the value of $c = 0$. Finally, a map reflecting the probability of hitting the nearshore of either of the coasts is obtained

as an average of the described distributions over all the windows of the time interval in question. From the construction of this map it follows that the range of the resulting values \bar{c} for a cell is from -1 to 1 and an estimate of the probability for tracer drift to the southern or the northern nearshore can be obtained by means of cell-wise mappings $p_N = (1 + \bar{c})/2$ or $p_S = (1 - \bar{c})/2$, respectively.

The resulting distributions depend on a number of parameters used in the calculations. Quite substantial seasonal and less pronounced interannual variability of these maps and the resulting location of the equiprobability line are discussed below. We performed several sensitivity experiments by means of varying the length of the time window t_W and the time lag t_S between the time windows. The results were almost insensitive with respect to the variation of the time lag from one day up to ten days provided the entire time interval of interest t_D was long enough compared to this lag. This feature is not unexpected because the averaging procedure over a pool of time windows suppresses the role of each single distribution. Also, the results showed almost no dependence on the length of the time window provided it was long enough to cover about 50% of the first hits of the tracers to the nearshore. Notice that the optimum values of the listed parameters are strongly site-specific and should be re-evaluated for each sea area and problem under investigation.

The use of the discussed time window means that only hits within the first 20 days of the dynamics are accounted for in the resulting maps. Strictly speaking, the results, therefore, are based only on a fraction of all the tracers and serve as an approximation of the desired spatial probability distribution. As the majority of particles have already hit one of the coasts within this length of time window, the resulting map reflects the behaviour of this majority. Also, it is natural to assume that the further hits have the same probability distribution of hitting the different coasts and thus the corrections potentially resulting from waiting until all the tracers hit a coast would be fairly minor.

The resulting map (Fig. 6) reveals the presence of two basically different areas of the gulf. In the western part there is a narrow sea area in which the average values for the cells are close to zero. Tracers released to either side of this area have a high probability of drifting to the relevant coast. This area evidently can be interpreted as the estimate of the location of the equiprobability line. In the central and eastern parts of the gulf, however, there is a wide area in which $|\bar{c}| \leq 0.1$. Consequently, propagation of tracers from this area to either of the coasts is generally unlikely. Such areas apparently host no well-defined equiprobability line. Instead, they entirely serve as almost safe regions (areas of reduced risk) in terms of coastal pollution.

Both the locations of these areas, potentially impacting either of the coasts, and the location of the equiprobability line reveal substantial seasonal variability (which will be discussed in detail elsewhere). Consequently, a similar variability exists for both high risk and reduced risk areas in this basin. The variability is the largest for the entrance area of the Gulf of Finland, which apparently is strongly affected by the dynamics of the open Baltic Sea.

Similar maps for annual probabilities of hitting different coasts also reveal certain interannual variability (Fig. 7). There are, however, features that persist over many years and also become evident in analogous maps for different seasons. There is a persistent area of reduced risk in the central and eastern parts of the gulf approximately between the Tallinn–Helsinki line and the latitudes of Narva Bay. To the north of Narva Bay there usually is a high probability of the propagation of an adverse impact to the southern coast. The equiprobability line is usually located to the north of the axis of the gulf except for a small part of this water body. There is a characteristic area to the north of Hiiumaa stretching almost to the Finnish archipelago from where the transport of adverse impacts to the Estonian nearshore has a relatively high probability.

The described method of cell-wise analysis of the transport generally leads to a considerable level of noise that does not always result in a clear separation of sea areas with the prevailing direction of the transport to a particular coast, especially in the central and eastern parts of the gulf. A part of the noise apparently is connected with a small number of tracers (four) for each cell.

In order to suppress the noise and to estimate the uncertainty of the location of the line and areas in question, we use another method that involves an implicit local smoothing process. The sea area is divided into clusters of 3×3 grid cells. By tracing nine trajectories in each cluster (one from each cell) it is established whether the majority of the trajectories end up at one of the coasts or stay in the open sea area. The basic idea is the same as above, only the values of $N_i = 9$, $1 \leq i \leq N$, and the initial positions of the tracer with respect to the cluster centres are different. The equiprobability line and the low-risk areas are based on probabilities calculated for the centres of the clusters. The resulting maps of probabilities of hitting the opposite coasts (Fig. 8) are qualitatively similar to those in Fig. 6. The equiprobability line is located in almost the same position as for the above method. The locations for the line based on these two estimates practically coincide between Hiiumaa and the Finnish mainland, differ by 1–2 grid points (3–6 km) in the western and eastern parts of the Gulf of Finland, and reach 3–4 grid points (up to 14 km) in a small section between Tallinn and Helsinki.

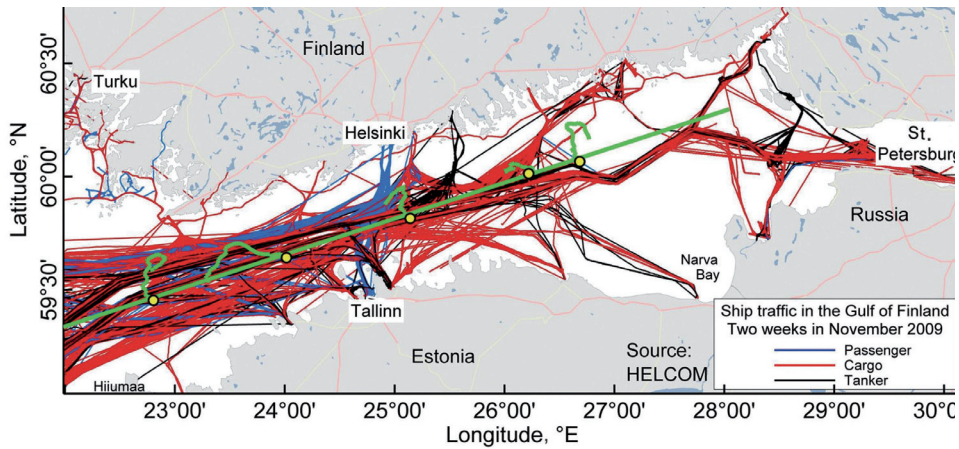


Fig. 1. Scheme of the current major fairways in the Gulf of Finland. The green straight line shows the initial location of tracers used for the construction of Figs 2–4 and the green curves show examples of trajectories, starting from points indicated by yellow circles.

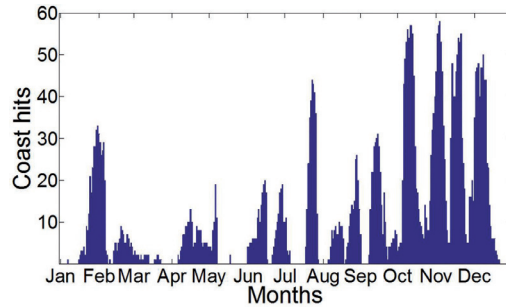


Fig. 2. Percentage of particles entering the nearshore during 10 days for the year 1987. The horizontal axis shows the starting time of calculations.

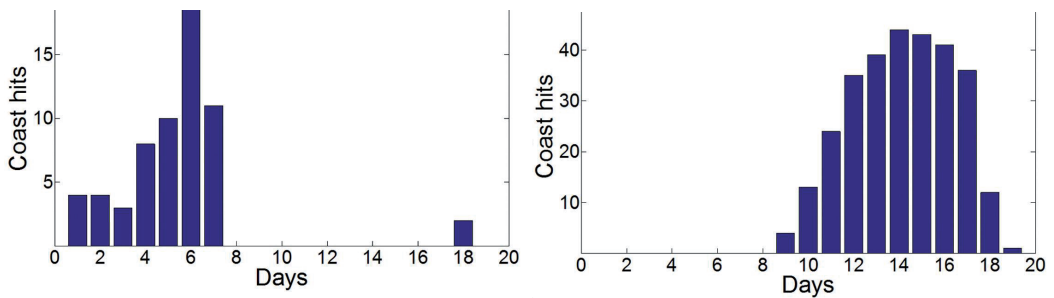


Fig. 3. Percentage of particles located in the nearshore on different days after their release on 1–20 May 1987 (left panel) and on 10–30 July 1987 (right panel). The horizontal axis shows the consecutive number of a day for the particular run.

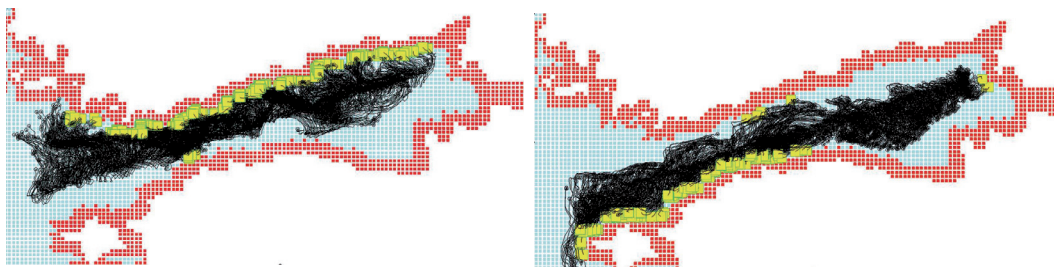


Fig. 4. Trajectories (black lines) and location of the hits (green squares) to the nearshore (red area) within 20 days for particles released on 1 October (left panel) and on 1 December 1987 (right panel).

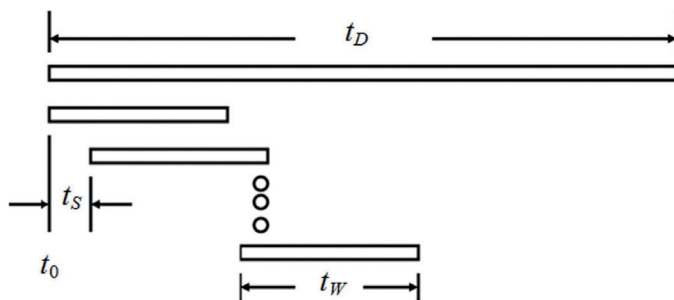


Fig. 5. Schematic diagram illustrating the overall simulation routine.

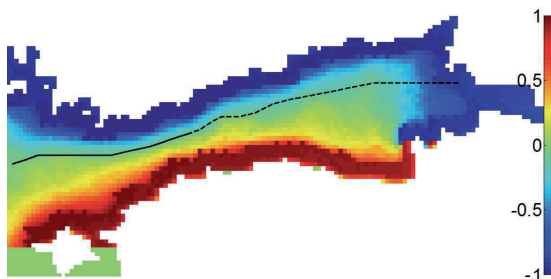


Fig. 6. Probabilities of hitting the nearshore of the northern or the southern coast for the years 1987–1991 calculated with the use of the direct method. The red colour indicates a high probability of transport to the southern (Estonian) coast and the blue colour, to the northern coast. The green colour marks the estimated location of the equiprobability line (black line) and the areas from which transport to either of the coasts is unlikely.

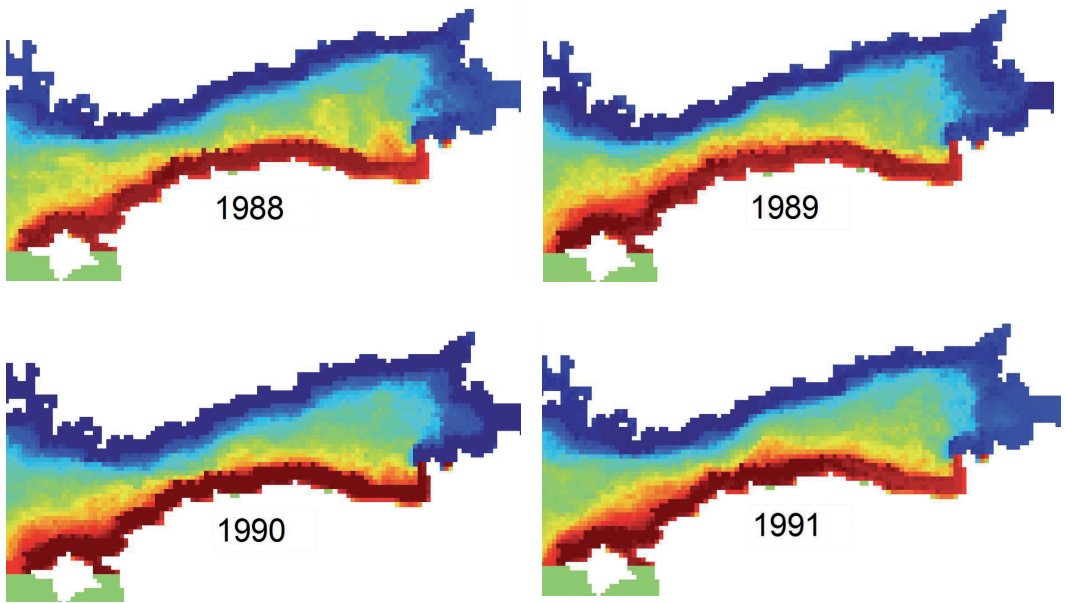


Fig. 7. Probabilities of hitting the nearshore of the northern or the southern coast for the years 1988–1991 calculated with the use of the direct method. Notations and scales are the same as for Fig. 6.

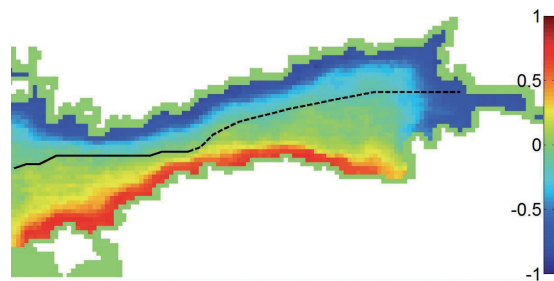


Fig. 8. Probabilities of hitting the nearshore of the northern or the southern coast for the years 1987–1991 calculated with the use of the smoothing method. Notations are the same as for Fig. 6. Notice that this method is only meaningful for the clusters whose centres are located at a distance of >11 km from the coast.

DISCUSSION AND CONCLUSIONS

The primary purpose of this research was to find a first guess to the solution to a variation of the inverse problem of the identification of the areas in which an accident would least likely affect the coasts of the Gulf of Finland. The results revealed several unexpected features of the distribution of the probabilities of the transport to the different coasts. A well-defined equiprobability line is substantially shifted northwards from the axis of the gulf in its western part. The fairly small difference (usually below 6–7 km, at a few locations around 10 km) between its locations obtained by the two methods – an estimate of the uncertainty related with this type of solution – supports the reliability of the analysis.

Therefore, the probability that adverse impacts released to the entrance area and the western part of the gulf hit the southern coast is considerably larger than that they hit the northern coast. This property apparently matches the joint effect of the prevailing direction of strong and persistent winds (they are from the southwest) and the geometry of this basin. The resulting Ekman transport is predominantly to the east but also has a considerable component to the south (Soomere et al., 2010). This conjecture is consistent with the asymmetric distribution of the frequency of upwellings in the Gulf of Finland (which mostly occur along the northern coast of this water body (Myrberg and Andrejev, 2003)) and the accompanying prevailing transport of surface waters to the south.

In conclusion, application of a trajectory model and pre-computed velocity fields combined with relevant statistical analysis serves as a feasible method to determine areas of high and low risk in terms of coastal pollution in different basins of the Baltic Sea with their specific hydrographic characteristics, like in the elongated Gulf of Finland. This technology has a clear potential to reduce the consequences of an accident (equivalently, to impact the decision-making process concerning spatial planning of dangerous activities) in the statistical sense. Straightforward extensions of the proposed approach eventually are useful for preventively placing dangerous activities in regions in which an accident would have a minimum threat to vulnerable areas.

ACKNOWLEDGEMENTS

This study is a part of the BONUS+ project BalticWay, which attempts to identify the regions that are associated with increased risk to other sea areas and to propose ways to reduce pollution risks in the Baltic Sea by placing activities in other areas that may be less affected. The research was partially supported by the

Marie Curie RTN SEAMOCs (MRTN-CT-2005-019374), the Marie Curie Reintegration Grant ESTSpline (PERG02-GA-2007-224819), targeted financing by the Estonian Ministry of Education and Research (grant SF0140077s08), and the Estonian Science Foundation (grant No. 7413). The contribution of Anders Anbo towards application of the TRACMASS model in the Institute of Cybernetics is gratefully acknowledged. We are grateful to Anders Höglund (SMHI), who extracted and prepared the RCO model data, to Raul Isotamm, who coded several algorithms used for the calculation of the transport patterns and the equiprobability line, and to the HELCOM team who prepared Figure 1.

REFERENCES

- Alenius, P., Myrberg, K., and Nekrasov, A. 1998. Physical oceanography of the Gulf of Finland: a review. *Boreal Env. Res.*, **3**, 97–125.
- Alenius, P., Nekrasov, A., and Myrberg, K. 2003. The baroclinic Rossby-radius in the Gulf of Finland. *Cont. Shelf Res.*, **23**, 563–573.
- Andrejev, O., Myrberg, K., Alenius, P., and Lundberg, P. A. 2004a. Mean circulation and water exchange in the Gulf of Finland – a study based on three-dimensional modelling. *Boreal Env. Res.*, **9**, 1–16.
- Andrejev, O., Myrberg, K., and Lundberg, P. A. 2004b. Age and renewal time of water masses in a semi-enclosed basin – application to the Gulf of Finland. *Tellus*, **56A**, 548–558.
- [ASCE] American Society of Civil Engineers. 1996. State-of-the-art review of modeling transport and fate of oil spills. ASCE Committee on Modeling Oil Spills, Water Resources Engineering Division. *J. Hydraul. Eng.*, **122**(11), 594–609.
- Blanke, B. and Raynaud, S. 1997. Kinematics of the Pacific Equatorial Undercurrent: an Eulerian and Lagrangian approach from GCM results. *J. Phys. Oceanogr.*, **27**(6), 1038–1053.
- Castanedo, S., Medina, R., Losada, I. J., Vidal, C., Mendez, F. J., Osorio, A., Juanes, J. A. and Puente, A. 2006. The Prestige oil spill in Cantabria (Bay of Biscay). Part I: Operational forecasting system for quick response, risk assessment, and protection of natural resources. *J. Coastal Res.*, **22**(6), 1474–1489.
- Döös, K. 1995. Inter-ocean exchange of water masses. *J. Geophys. Res.*, **100**(C7), 13499–13514.
- Döös, K. and Engqvist, A. 2007. Assessment of water exchange between a discharge region and the open sea – a comparison of different methodological concepts. *Estuar. Coast. Shelf Sci.*, **74**, 585–597.
- Gästgifvars, M., Lauri, H., Sarkanen, A.-K., Myrberg, K., Andrejev, O., and Ambjörn, C. 2006. Modelling surface drifting of buoys during a rapidly-moving weather front in the Gulf of Finland, Baltic Sea. *Estuar. Coast. Shelf Sci.*, **70**, 567–576.
- Griffä, A., Piterbarg, L. I., and Ozgokmen, T. 2004. Predictability of Lagrangian particle trajectories: effects of smoothing of the underlying Eulerian flow. *J. Mar. Res.*, **62**, 1–35.

- Höglund, A., Meier, H. E. M., Broman, B., and Kriezi, E. 2009. *Validation and Correction of Regionalised ERA-40 Wind Fields over the Baltic Sea Using the Rossby Centre Atmosphere Model RCA3.0*. Rapport Oceanografi No. 97, Swedish Meteorological and Hydrological Institute, Norrköping, Sweden.
- Jönsson, B., Lundberg, P., and Döös, K. 2004. Baltic sub-basin turnover times examined using the Rossby Centre Ocean Model. *Ambio*, **23**(4–5), 257–260.
- Kokkonen, T., Ihaksi, T., Jolma, A., and Kuikka, S. 2010. Dynamic mapping of nature values to support prioritization of coastal oil combating. *Environ. Modell. Softw.*, **25**(2), 248–257.
- Lehmann, A., Krauss, W., and Hinrichsen, H.-H. 2002. Effects of remote and local atmospheric forcing on circulation and upwelling in the Baltic Sea. *Tellus*, **54A**, 299–316.
- Lessin, G., Ossipova, V., Lips, I., and Raudsepp, U. 2009. Identification of the coastal zone of the central and eastern Gulf of Finland by numerical modeling, measurements, and remote sensing of chlorophyll *a*. *Hydrobiologia*, **692**, 187–198.
- Meier, H. E. M. 2001. On the parameterization of mixing in three-dimensional Baltic Sea models. *J. Geophys. Res.*, **106**, 30997–31016.
- Meier, H. E. M. 2007. Modeling the pathways and ages of inflowing salt- and freshwater in the Baltic Sea. *Estuar. Coast. Shelf Sci.*, **74**, 717–734.
- Meier, H. E. M., Döscher, R., and Faxén, T. 2003. A multi-processor coupled ice-ocean model for the Baltic Sea: application to salt inflow. *J. Geophys. Res.*, **108**(C8), 3273.
- Myrberg, K. and Andrejev, O. 2003. Main upwelling regions in the Baltic Sea – a statistical analysis based on three-dimensional modelling. *Boreal Env. Res.*, **8**, 97–112.
- Osinski, R. and Piechura, J. 2009. Latest findings about circulation of upper layer in the Baltic Proper. In *BSSC 2009 Abstract Book, August 17–21, 2009*. Tallinn, 103.
- Reed, M., Johansen, O., Brandvik, P. J., Daling, P., Lewis, A., Fiocco, R., Mackay, D., and Prentki, R. 1999. Oil spill modeling towards the close of the 20th century: overview of the state of the art. *Spill Sci. Techn. Bull.*, **5**(1), 3–16.
- Sobey, R. J. and Barker, C. H. 1997. Wave-driven transport of surface oil. *J. Coastal Res.*, **13**(2), 490–496.
- Soomere, T. and Quak, E. 2007. On the potential of reducing coastal pollution by a proper choice of the fairway. *J. Coast. Res.*, Special Issue **50**, 678–682.
- Soomere, T., Myrberg, K., Leppäranta, M., and Nekrasov, A. 2008. The progress in knowledge of physical oceanography of the Gulf of Finland: a review for 1997–2007. *Oceanologia*, **50**, 287–362.
- Soomere, T., Delpeche, N., Viikmäe, B., Quak, E., Meier, H. E. M., and Döös, K. 2010. Patterns of current-induced transport in the surface layer of the Gulf of Finland. *Boreal Env. Res.*, **15**, in press.
- Stokstad, E. 2009. U.S. poised to adopt national ocean policy. *Science*, **326**, 1618.
- Vandenbulcke, L., Beckers, J.-M., Lenartz, F., Barth, A., Poulain, P.-M., Aidonidis, M., Meyrat, J., Arduin, F., Tonani, M., Fratianni, C., Torrisi, L., Pallela, D., Chiggiato, J., Tudor, M., Book, J. W., Martin, P., Peggion, G., and Rixen, M. 2009. Super-ensemble techniques: application to surface drift prediction. *Progr. Oceanogr.*, **82**(3), 149–167.
- Vries, P. de and Döös, K. 2001. Calculating Lagrangian trajectories using time-dependent velocity fields. *J. Atmos. Ocean. Techn.*, **18**(6), 1092–1101.

Laevaliiklusega seonduvate keskkonnariskide optimeerimise võimalustest Soome lahes

Tarmo Soomere, Bert Viikmäe, Nicole Delpeche ja Kai Myrberg

On analüüsitud hoovuste tekitatud lisandite transporti Soome lahe pinnakihis aastatel 1987–1991. Rootsi Meteoroloogia ja Hüdroloogia Instituudi arvatud hoovuste kiiruste andmestikust on tarkvara TRACMASS abil leitud lisandite edasikandumise trajektooreid. Nende statistilise analüüsi kaudu on hinnatud erinevatele merealadele sattunud lisandite randa triivimise tõenäosust. On näidatud, et Soome lahe lääneosas eksisteerib nn võrdtõenäosusjoon, millest põhja poole sattunud lisandid triivivad suurema tõenäosusega lahe põhjaranda, ja vastupidi. Soome lahe idaosa avamerel on piirkonnad, kuhu sattunud lisandite kandumine randa on vähetõenäoline. Ohutuim laevatee kulgeb piki kirjeldatud joont ja läbi selliste piirkondade.

Paper B

Viikmäe B., Soomere T., Viidebaum M. and Berezovski M. 2010. Temporal scales for transport patterns in the Gulf of Finland. *Estonian Journal of Engineering*, 16(3), 211–227.

Temporal scales for transport patterns in the Gulf of Finland

Bert Viikmäe^a, Tarmo Soomere^{a,b}, Mikk Viidebaum^a and
Mihhail Berezovski^a

^a Institute of Cybernetics at Tallinn University of Technology, Akadeemia tee 21, 12618 Tallinn, Estonia; bert@ioc.ee

^b Visiting scientist to the Australian National Network in Marine Sciences, James Cook University, Townsville, Australia

Received 17 July 2010, in revised form 06 August 2010

Abstract. The basic time scales for current-induced net transport of surface water and associated time scales of reaching the nearshore in the Gulf of Finland, the Baltic Sea, are analysed based on Lagrangian trajectories of water particles reconstructed from three-dimensional velocity fields by the Rossby Centre circulation model for 1987–1991. The number of particles reaching the nearshore exhibits substantial temporal variability whereas the rate of leaving the gulf is almost steady. It is recommended to use an about 3 grid cells wide nearshore area as a substitute to the coastal zone and about 10–15 day long trajectories for calculations of the probability of reaching the nearshore. An appropriate time window for estimates of the properties of net transport patterns is 4–10 days.

Key words: hydrodynamic modelling, currents, Lagrangian transport, Gulf of Finland, Baltic Sea.

1. INTRODUCTION

International ship transport has dramatically increased in the Baltic Sea basin over the last two decades and at present accounts for up to 15% of the world's cargo transportation. The largest threat to the environment is oil transportation that has increased more than by a factor of two in 2000–2006 [¹]. One of the major marine highways in the European waters enters the Baltic Sea through the Danish Straits, crosses the Baltic Proper and stretches through the Gulf of Finland (Fig. 1) to Saint Petersburg, the major population and industrial centre in this area, and to a number of new harbours in its vicinity. Sustainable management of this traffic flow is a major challenge in the Baltic Sea, which is designated as a Particularly Sensitive Sea Area by the International Maritime Organization [^{2,3}].

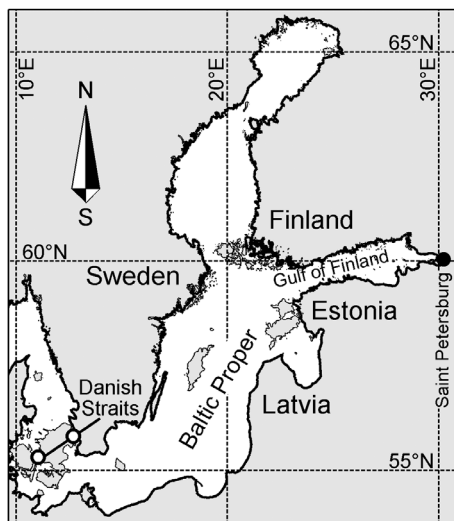


Fig. 1. Location scheme of the Baltic Sea and the Gulf of Finland.

Frequent stormy winds, short period of daylight and cold weather in autumn and winter make the shipping quite tricky in the entire Baltic Sea. The presence of heavy ice almost every winter drastically complicates the navigation in the Gulf of Finland, the easternmost prolongation of the Baltic Sea with a length of about 400 km, maximum width of 125 km and a mean depth of 37 m [4]. As the width of this gulf is at some places below 50 km and in many places water is too shallow, there are several narrow passages where the concentration of traffic is exceptionally high. In addition, the fairway from the Baltic Proper to the eastern region of the gulf crosses intense fast ferry traffic between Helsinki and Tallinn where more than 50 gulf crossings take place daily during the high season [5]. These features increase the risk of a potential release of various adverse impacts (oil or chemical pollution, lost containers or other large buoyant items, etc., and associated impacts or hazards to both the environment and to other vessels) owing either to an accident, technical problems or human mistakes or misbehaviour.

The drift of agents of adverse impacts released into the surface layer (oil spills, lost containers, etc.) is influenced by wind stress, waves, and currents. The properties of transport by wind and waves are relatively well known [6,7]. Much less is known about the transport driven by the field of currents [8]. Currents are created under influence of several local and remote forcing factors, which makes their prediction quite challenging. It is even more complicated in strongly stratified sea areas such as the Gulf of Finland where the drift frequently is steered by multi-layered dynamics [9].

Surface currents in the Gulf of Finland are highly variable both seasonally and annually [4,10]. Recent analyses have demonstrated the existence of semi-persistent patterns of currents in this gulf and in some other parts of the Baltic Sea [11–13]. Such patterns with a lifetime of a few weeks apparently provide relatively fast current-driven transport in certain sea areas. This combination serves as a challenge for a technology that attempts to use the marine dynamics for reducing the risk of coastal pollution [14]. The goal of such technologies is to minimize the risk of pollution (and to identify areas, which are statistically safer to travel to) in terms of minimizing the probability of reaching the valuable areas. An equivalently equal gain is a systematic increase of time during which an adverse impact (for example, an oil spill) reaches a vulnerable area after an accident has happened.

A generic example of vulnerable areas is the nearshore that usually has the largest ecological value. While the probability of coastal pollution for open ocean coasts can be reduced by shifting ship routes farther offshore, the problem for narrow bays, like the Gulf of Finland, is how to minimize the probability of hitting any of the coasts. The first order solution is the equiprobability line, the probability of propagation of pollution from which to either of the coasts is equal [13]. There may also exist areas of reduced risk, propagation of pollution from which to either of the coasts is unlikely. The safe fairway would either follow the equiprobability line or use an area of reduced risk.

The problem of identification of areas of reduced risk is addressed in [13,15] by means of statistical analysis of a large pool of Lagrangian trajectories of test particles, constructed based on the results of a 3D circulation model. Such an analysis also allows the identification and visualization of several properties of currents that cannot be extracted directly from the current fields. The results, however, depend to a certain extent on the choice of the underlying velocity fields as well as the governing parameters for the trajectory calculations such as the initial location of test particles released into the sea, the duration of single trajectory simulations, the number of trajectories involved for each calculation session, etc.

The purpose of this study is to evaluate certain spatial and temporal scales necessary to be covered in such simulations in order to reach representative results in the context of the Gulf of Finland. After a short description of the modelling environment we focus on requirements for the basic parameters of the calculations such as the width of the coastal zone and the duration of trajectory calculations. Finally, the range of time scales for which semi-persistent patterns may be important in this basin is estimated and the sensitivity of the results on the choice of the time lag between subsequent trajectory simulations is discussed.

2. MODELLING ENVIRONMENT AND METHODS

In this study, the 3D velocity fields, simulated for 1987–1991, provided by the Swedish Meteorological and Hydrological Institute, were used for calculations of trajectories of potential adverse impacts. This time period was chosen in order to

make the results comparable with circulation simulations [11,16] and studies into probability distributions for coastal hits in the Gulf of Finland [13]. The velocity fields were calculated by the Rossby Centre Ocean circulation model (RCO). This is a primitive circulation model coupled with an ice model [17] that covers the entire Baltic Sea with a spatial resolution of 2×2 nautical miles (NM) and has 41 vertical layers in z -coordinate. We only use the horizontal velocities in the uppermost, surface-layer with a thickness of 3 m. A time step splitting scheme is used in the RCO, with 150 s for the baroclinic and 15 s for the barotropic time step in underlying runs. In order to keep the data set of currents within a reasonable limit, the model output is saved with a temporal resolution of 6 h.

The model is forced by wind data on the 10 m level, air temperature and specific humidity on the 2 m level, precipitation, cloudiness, and sea level pressure fields. It also accounts for river inflow and water exchange through the Danish Straits. The forcing data is calculated from the ERA-40 re-analysis using a regional atmosphere model with a horizontal resolution of 25 km and a scheme of adjusting the wind properties using simulated gustiness [18]. Details of the model set-up and validation experiments are discussed in [17,19,20]. Given the very small internal Rossby radius in the Gulf of Finland (typically 2–4 km [21]), the model apparently resolves a certain part of the meso-scale dynamics in this gulf in terms of statistics of meso-scale eddies but an exact representation of the location and properties of single eddies cannot be expected. The model also captures inertial waves in the gulf but owing to a coarse resolution of the saved output data (about half of the period of internal waves), the role of these oscillations in the drift of particles is apparently only partially accounted for.

The current-driven transport of adverse impacts is analysed with the use of a Lagrangian trajectory model, TRACMASS [22,23]. It uses pre-computed 3D Eulerian current velocity fields to evaluate an approximate path of water particles (equivalently, of an adverse impact with neutral buoyancy). The model relies on an analytical solution of a differential equation for motion that depends on the velocities on the grid box walls using linear interpolation of the velocity field both in time and in space.

As we are specifically interested in surface transport patterns, the test particles are locked in the uppermost layer as in [13,15]. The resulting trajectories are, thus, not truly Lagrangian: they are not passively advected by the velocity fields and basically represent motion of objects that are slightly lighter than the surrounding water (such as oil in otherwise calm conditions) or objects which are confined to the upper layer by other constraints (for example, lost containers).

The overall procedure is as follows [13]. First, the initial locations of a certain number of water particles (interpreted as carrying an adverse impact) are specified. The time period of interest $[t_0, t_0 + t_D]$ with duration of t_D (usually ≥ 1 year) is divided into time windows of fixed length t_W . The motion paths (trajectories) of the cluster of water particles (interpreted as current-driven propagation of the adverse impact) are first simulated over the interval $[t_0, t_0 + t_W]$. The resulting trajectories are saved for further analysis. The simulations for the

same initial positions of particles are restarted at another time instant $t_0 + t_S$. The trajectories are again calculated over a time window with a duration of t_W (that usually to a large extent overlaps with the previous window). The process is repeated $(t_D - t_W)/t_S$ times (Fig. 2). Finally, the outcome of simulations is averaged over all time windows. For example, for a yearly simulation with the time window of $t_W = 20$ days and with a lag $t_S = 10$ days, the averaging is performed over 35 ensembles of trajectories, the last examples of which start on 12 December and end at the midnight of 31 December.

It is intuitively clear that the key time scale of the described method is the length of the time window. In the context of simulation of pollution transport the basic requirement is that t_W has to be long enough to allow for a significant number of particles to reach the vulnerable area(s). The choice of the time period $[t_0, t_0 + t_D]$ may also substantially affect the results as demonstrated in [13] on the example of monthly and seasonal variations of the properties of certain sets of trajectories. The choice of the time lag and the initial locations of the particles apparently have less significant impact on the results but may still affect the reliability of the conclusions.

Another central feature is how the vulnerable area is defined. This is less important when the vulnerable region extends to offshore where the presence of the coast does not directly modify the flow. It becomes, however, decisive when the vulnerable area is the coast itself. The circulation models usually assume that the velocity component normal to the sea bottom vanishes. For shallow-water coastal areas this often means that the simulated flow is largely longshore. Consequently, the propagation of the particles' trajectories simulated by TRACMASS (which does not account for any sub-grid scale effects and fully follows the precomputed velocity fields) close to the coast is very unlikely and the probability of hitting a nearshore area may be underestimated. In this case it might be necessary to associate the vulnerable areas with grid cells located at a larger distance from the coastline.

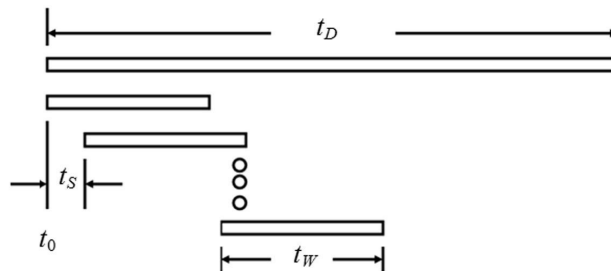


Fig. 2. Definition sketch of splitting the simulation period into time windows.

3. DEFINITION OF THE NEARSHORE

The procedure of the definition of the coastal zone is tightly related to the problem of the adequate choice of t_W . As the potential side effects, connected with boundary effects in the nearshore, apparently are most pronounced for the particles released relatively far offshore, the relevant simulations are performed for particles initially placed in the middle of the Gulf of Finland. The trajectories were started from centres of 93 cells along a straight line roughly representing the axis of the gulf (that is, at points remotest from the coasts, Fig. 3). The simulations were started at midnight each calendar day in 1987. This year as well as the 5-year period 1987–1991 were quite typical in terms of wave intensity [24,25] and thus also in terms of energy supply to water masses. There were no exceptional storms in this year and the annual mean wind speed at the Island of Utö [24] and at Kalbådgrund were just a few percent lower than the 5-year average for 1987–1991.

Numerical experiments with the use of $t_W = 20$ days [13] suggest that in many cases the trajectories first enter the nearshore area after about 10 days of propagation. Such events are below called hits to the nearshore or coastal hits. The time window used for calculations of statistics of coastal hits should account for such situations. On the other hand, t_W should not be much longer than the typical time during which the largest number of hits occurs. Also, the typical spreading of initially closely located particles over the time window should remain well below the width of the narrowest part of the gulf. If the latter condition is violated, the uncertainty in the positioning of the particle caused by sub-grid-scale turbulence would be about the same size as the extension of the open sea area and the related statistics of coastal hits would be meaningless.

Recent numerical simulations [15] and ongoing drifter experiments (K. Döös, pers. comm., 2010) suggest that the typical spreading rate is about 2 mm/s (and apparently somewhat larger in strong wind conditions) both in the Gulf of Finland and in the Baltic Proper. Therefore, within about three weeks of windy

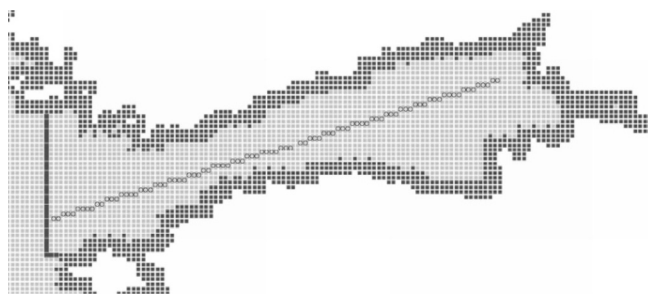


Fig. 3. Starting points of trajectories (grey circles located approximately along the axis of the Gulf of Finland) in simulations of coastal hits. Dark grid points indicate the nearshore area of alert zone 3. The entrance line to the gulf (bold line) is set along 59°N and 21°48'E.

months the sub-grid turbulence may separate the particles, in average, by 15 km. This suggests that for time windows longer than about 20 days the final position of the particle would be basically random. Based on these arguments, t_w was set to 15 days in simulations described in this section.

The nearshore area was simulated by means of three zones with a typical width of 1, 2 and 3 grid cells from the coast, called alert zone 1–3 below. The width of each zone was kept both in the direction of the coordinate axes as well as in the NW–SE and NE–SW direction. Simultaneously with tracking the transport of particles to the nearshore we also checked whether the particles were carried out of the Gulf of Finland. The border between the gulf and the Baltic Proper was set slightly to the west of Hiiumaa (Fig. 3). A hit to each of the three alert zones occurs when a particle first time enters the relevant zone. The presence of each particle in an alert zone (or its drift out of the gulf) is accounted for only once and its subsequent presence or re-entering the alert zone (or the gulf) is ignored. This method of counting implicitly means that particles that have drifted out of the gulf have never entered any of the alert zones.

The monthly average number of hits of particles to the alert zones and the share of particles leaving the gulf considerably vary for different seasons (Fig. 4). The average probability of entering alert zones 1 and 2 during spring and summer months is very low, about 2% and 4%, respectively, while during windy months it grows up to 20% and 30%, respectively. The annual average probability of entering these zones is about 5% and 11%, respectively. The small probabilities of entering zones 1 and 2 suggest that the statistics of hits to the nearshore, based on trajectories reaching these zones, may have quite large uncertainty, especially during spring.

A similar seasonal variability becomes evident for the alert zone 3. The annual probability of entering this zone is 18% whereas during the windy months almost a half of the released particles entered this zone. The annual average of the joint probability for a particle to either enter alert zone 3 or to leave the gulf is about 30%. This probability exhibits extensive short-term variability (Fig. 5).

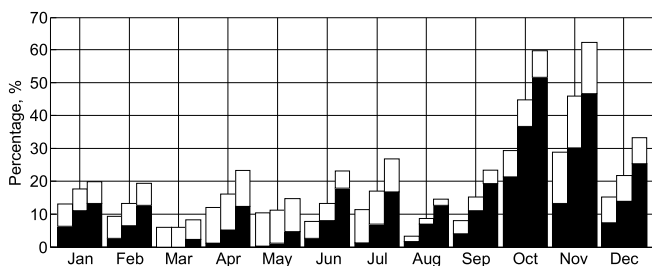


Fig. 4. Monthly mean percentage for coastal hits (filled parts of bars) and the particles leaving the gulf (white parts of bars) in 1987 for $t_w = 15$ days. The left, middle and right bars show the results for alert zones 1, 2 and 3, respectively.

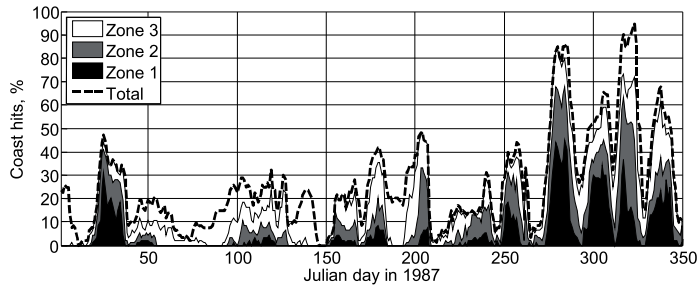


Fig. 5. Percentage of hits to the nearshore for $t_w = 15$ days for different starting instants of trajectory calculations in 1987. The uppermost dashed line shows the total percentage of particles that have either hit the coast or drifted out of the gulf.

Its values are quite close to 100% during the windiest periods. This considerable amount of hits suggests that statistics, calculated with the use of alert zone 3 as a model, nearshore is representative for the velocity data in use. Notice that the particles in this experiment are released at a maximally large distance from the coasts. For randomly distributed particles the relevant probabilities obviously will be much higher.

4. TIME SCALES OF HITTING THE COAST AND LEAVING THE GULF

A series of experiments was performed to estimate the typical time over which the particles reached the nearshore. Test particles were released at the largest possible distance from the coast for a given longitude and alert zone 3 was chosen to represent the nearshore. Doing so apparently results in an estimate for the upper bound of the relevant time scale. The simulations were started, as in the previous sections, at midnight each calendar day in 1987 but run for 3–13 days. Figure 6 first indicates that the probability of coastal hits has a substantial seasonal variability for all choices of t_w . Interestingly, this probability may be quite large for some relatively calm months.

Given the relatively large initial distance between particles and the coast, it is not unexpected that the chances for a particle to hit the coast increase rapidly when t_w increases from 3 to 10 days. The rate of increase is evidently essentially non-linear and considerably decreases when the time window is lengthened from 10 to 13 days. An exception is the flow in January and July when the frequency of coastal hits for other time window lengths is small. As discussed above, for the windiest months about a half of particles either hit the coast or leave the gulf by the 15th day (Fig. 4).

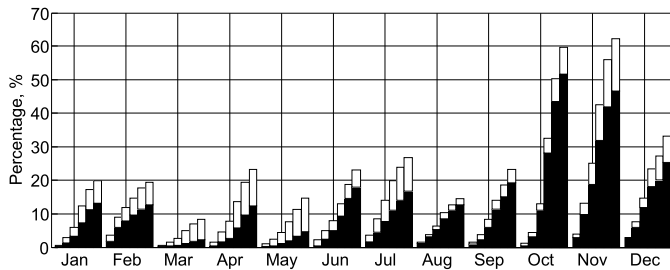


Fig. 6. Monthly mean percentage of coastal hits (black) and leaving the gulf (white) for different lengths of the time window for alert zone 3 in 1987. For each month, columns from left to right show the percentage for $t_W = 3, 5, 7, 10, 13$ and 15 days.

Therefore, we can conclude that the total number of coastal hits grows rapidly within the first 10 days after a release of the potential adverse impact. The increase rate considerably decreases after that but does not stabilize within even two weeks. This feature is not unexpected and basically reflects the complexity of the dynamics of the Gulf of Finland.

The results obtained with the use of alert zones 1 and 2 (equivalently, with different widths of the coastal zone) are qualitatively similar to the presented ones. They are, however, not directly comparable and building a quantitative measure for their comparison is meaningless as these situations reflect completely different problem setups.

The number of particles, drifting out of the gulf, increases more or less linearly. Comparison of Figs. 5 and 7 demonstrates that there is no evident correlation between the probabilities for nearshore hits and for leaving the gulf. Interestingly, the number of particles that have drifted out of the gulf insignificantly depends on the particular choice of the alert zone and exhibits much smaller seasonal variability.

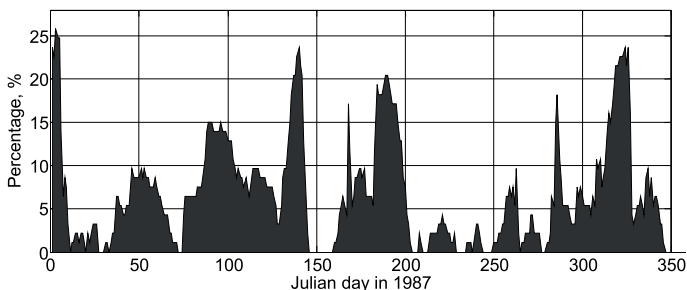


Fig. 7. The percentage of particles that have left the gulf within 15 days for alert zone 3 and different starting instants of trajectory calculations in 1987.

For the calmest months, there are always more particles leaving the gulf than hitting the coast whereas during the windiest months particles tend to hit the coast rather than leave the gulf (Fig. 6). This feature suggests that the ‘open sea’ and ‘nearshore’ dynamics in the Gulf of Finland are relatively well separated even when the nearshore is defined as an 11 km wide area and covers over 40% of the width of the gulf in its narrowest part. The particles tend to more frequently leave the gulf during spring and summer and less frequently during the windy months. This is somewhat counter-intuitive because surface currents should be more intense during windy months.

The mismatch between the rates of hitting the coast and leaving the coast may stem from the different balance between the impact of the Ekman drift and the mean circulation and internal meso-scale dynamics on the surface drift in different seasons. According to the traditional idealized view, the mean circulation of the Gulf of Finland (that is large enough to experience the effects of the Earth’s rotation) is cyclonic and intrinsically baroclinic (due to the pronounced horizontal buoyancy gradients) with an average velocity of a few cm/s [^{4,10}]. Both the mean and instantaneous circulation patterns contain numerous meso-scale eddies (analogues to oceanic synoptic rings) with a typical size clearly exceeding the internal Rossby radius [¹⁶]. The RCO model, although it is probably not able to reproduce details of meso-scale dynamics, is still apparently capable to mirror the basic features of the meso-scale eddies. Owing to the small internal Rossby radius (2–4 km [²¹]), the presence of a number of meso-scale eddies with typical diameters in the order of 10–20 km is expected in the Gulf of Finland. Simulations in [^{11,16}] suggest that also long-living meso-scale eddies apparently gradually drift to the west and in this way contribute to the motion of entrained surface particles towards the Baltic Proper.

The surface dynamics is largely determined by the Ekman drift and relatively weakly correlated with the dynamics of underlying water masses during windy months. In calm seasons and under ice cover, however, the underlying dynamics evidently will play a much larger role in the surface dynamics. Such a situation has been described in [⁹] for decreasing wind conditions when the surface drift apparently was strongly affected by subsurface dynamics.

Another key component of the dynamics here is the sea-surface slope that results from the voluminous fresh water supply to the eastern part of the gulf and that enhances the outflow of water to the Baltic Proper. The more or less steady rate of particles leaving the gulf suggests that the outflow is generally regular. It only diminishes for short time intervals during windy months when wind-stress and resulting Ekman drift apparently dominate at the sea-surface, override the anisotropic transport to the west and cause relatively large excursions of the surface particles in all directions, optionally until the nearshore.

The number of particles that leave the Gulf of Finland within 15 days is typically 8–10 (about 10% of the released ones, Fig. 7) and thus their behaviour only insignificantly affects the results depicted in Fig. 6. This number, however, suggests that the surface water exchange between the Baltic Proper and the Gulf

of Finland may be much more intense than the overall water exchange in the entire water column [16]. If about 10% of surface water leaves the gulf within two weeks, it might take only about half a year for the total removal of the surface water from the gulf. In reality, however, much of the water is apparently transported back and forth at the entrance to the gulf [16] and the net exchange forms a relatively small fraction from the total exchange.

5. TIME SCALES OF NET TRANSPORT PATTERNS

The persistence of currents in the uppermost layer of the Gulf of Finland, defined in terms of the conservation of the flow direction over five years [11,16] was found to be very small. This result does not contradict with the existence of semi-persistent transport pathways in which, for example, the flow direction varies over a certain shorter time scale as it is customary for coastal currents of an alternating direction. Such patterns, with a typical lifetime from the first weeks up to a few months have been recently identified for different areas of the Baltic Sea [12,16,20,26]. Their existence has a high potential for the rapid and systematic transport of different neutrally buoyant adverse impacts such as nutrients, toxic substances, or oil pollution between specific sea areas in the form of relatively stable jet-like flows over a few days.

The location and magnitude of such patterns of transport can be, to a first approximation, identified by means of numerical simulation of the net transport of water masses over relatively short time intervals. The net transport is defined here as the distance between the start and end positions of a trajectory. The resulting areas of high net transport for a single time window largely coincide with areas of large instantaneous current speeds. Such areas will generally be different for different time windows as the local jets and meso-scale eddies emerge, relocate and decay over time. An average over a large number of (optionally partially overlapping) time windows (Fig. 2) may highlight regions where water transport is systematically more intense than the average, for example, areas where jets alter their direction over time scales that are considerably longer than the time windows used for their highlighting. The properties of the resulting patterns for the Gulf of Finland will be described elsewhere [27] and here we only address their potential temporal scales and the parameters of the method for their identification.

A particular choice of the length of the time window is decisive not only for the representativeness and reliability of the statistics in the above calculations of coastal hits but also for the identification of pathways of rapid transport of water masses. A too short time window will simply lead to a somewhat smoothed pattern of the instantaneous current field while the use of a too long window would result in a variation of the mean circulation pattern.

The above material suggests that in calm conditions and under ice cover the surface transport is strongly affected by the underlying mean circulation and

meso-scale dynamics. In order to properly account for the potential impact of meso-scale eddies, the relevant time window should be about the typical eddy turnover time or longer. Although the values for the internal Rossby radii are relatively well known [21], there exist very few data about the properties of single meso-scale eddies in the Gulf of Finland Numerical Simulations and a few available observations [4] suggest that the typical diameter of their cores is 10–20 km and the maximum current speed may reach values up to 35 cm/s but should normally remain between 10–20 cm/s. The typical turnover time is thus about 4–5 days. Therefore, if one aims at averaging out their impact, the relevant time window should cover several turns of typical eddies, that is, be at least 15–20 days.

A convenient quantity allowing to roughly estimate the overall ability of the calculations of the net transport to highlight rapid pathways is the difference in the speed of average net transport from the long-term average current speed for a particular t_w . This difference apparently is the largest for short time windows when the net transport speed is close to the instantaneous current speed. A sensible upper limit for t_w is such that the net transport speed becomes close to the long-term average current speed. For even longer time windows the semi-persistent flow patterns probably will be averaged out of the spatial distributions of the net transport speed.

The difference in question is estimated with the use of a sequence of simulations of trajectories for 1987–1991 with the use of variable t_w and a constant time lag of $t_s = 1$ day between the windows. One particle was released into each of 3131 grid cells in the Gulf of Finland. Figure 8 presents the average values over all five years and approximately 1900 time windows. The average speed of net transport is, as expected, the largest for relatively short time windows. It decreases rapidly, from about 4.4 cm/s to 3.4 cm/s when t_w increases from 4 to 10 days. For even longer time windows the decrease is less steep. The speed in question decreases below 3 cm/s for $t_w \geq 15$ days and is close to the long-term average speed in this basin (about 2.5 cm/s). Therefore, the range of time

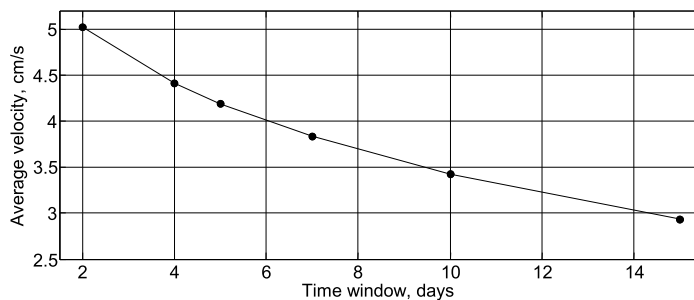


Fig. 8. Dependence of the average speed of net transport on the length of time window for 1987–1991.

windows suitable for identification of semi-persistent current patterns and in the same time capable of averaging out the potential impact of single meso-scale eddies to such patterns is between 5 and 15 days in the Gulf of Finland. Note that this estimate does not guarantee the existence of any particular patterns and only indicates the suitable range for t_w .

A complementary view to the described estimate can be obtained by means of an analysis of the relative changes in the average net transport speed when the length of the time window is increased. This is illustrated on the example of a pointwise comparison of net transport speeds against a reference set consisting of the values of net transport speed at all 3131 sea grid points averaged over all calculations of single trajectories from each point with $t_w = 2$ days and a time lag of 1 day for the years 1987–1991. Figure 9 depicts the average root-mean-square difference (RMSD) between the reference set and a similar set of speeds calculated with longer time windows. The average RMSD between the results, calculated with $t_w = 2$ and $t_w = 4$ days, is about 15% (the percentage calculated is based on the average speed of the reference set with $t_w = 2$) and increases to about 60% for $t_w \geq 20$ days. This result once more indicates that a suitable length for time windows for searching potential semi-persistent flow patterns in the Gulf of Finland should not exceed 2–3 weeks.

Finally, we shortly consider the potential sensitivity of the results of the analysis of pools of trajectories with respect to variations in the time lag t_s between the start instants of subsequent runs. Its choice essentially affects the amount of calculations. As an indicator, we compared pointwise the averaged net transport speeds, calculated for single years between 1987–1991 with the use of time lags of 1, 5 and 10 days. The impact of the particular time lag on the results is generally small even when quite large values of the lag are used (Fig. 10).

The annual RMSD of the values of the net transport speed is below 2% when the time lag is increased from 1 day to 5 days. This value increases to 2.7%–3.8% when the time lag is 10 days. The relevant absolute values of the RMSD in speed are 0.09–0.12 cm/s. These estimates suggest that for calculations of trajectories and reduced risk areas it is acceptable to use relatively large values of the

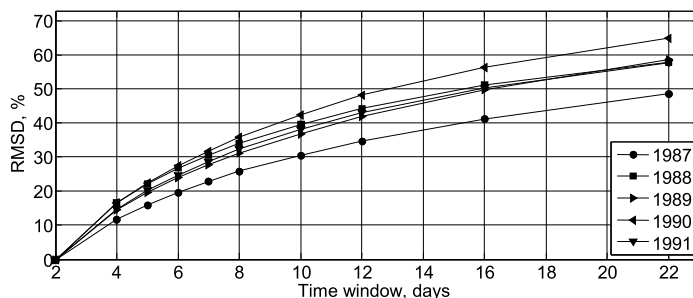


Fig. 9. Dependence of RMSD on the duration of time window for different years.

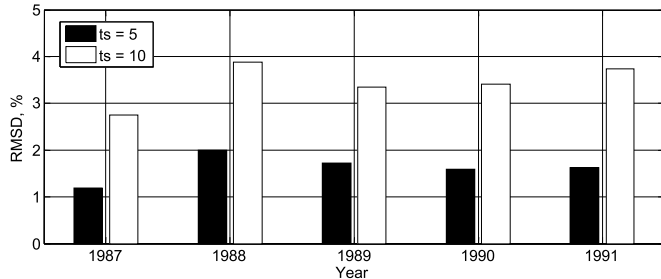


Fig. 10. RMSD of the net transport speed for t_s equal to 5 and 10 days from the speed for $t_s = 1$ day.

time lag without losing reliability of the results. This conjecture comes into importance in optimization of long-term calculations based on high-resolution simulations [15].

6. DISCUSSION AND CONCLUSIONS

In general, it is not unexpected that the number of particles, hitting the coast and/or leaving the Gulf of Finland, exhibits substantial temporal variability and high sensitivity with respect to several parameters used in the calculation and analysis of Lagrangian trajectories of water (or pollution) particles. The major lesson is that the applications of this method for the identification of (pollution) transport patterns and areas of reduced risks, based on the analysis of large pools of trajectories of particles, need a careful choice of the governing parameters for each particular sea area and circulation model in use.

First of all, a reliable statistics of coastal hits can only be constructed when a sensible amount of particles (carrying the adverse impact) reaches the properly defined nearshore within a reasonable time. For the particular circulation model in question (Rossby Centre Ocean Model with a spatial resolution of 2 NM in the entire Baltic Sea) it is appropriate to use an about 3 grid cells (6 NM, about 11 km, called alert zone 3 above and in [13]) wide nearshore area as the proper representation of the coastal zone. A sensible length of time windows in calculations of coastal hits is, at least, 10–15 days. In average, at least one third of particles released in the gulf enter this zone within approximately two weeks. The proportion of particles drifting out of the gulf is much smaller, about 10%, more or less uniformly round the year. This rate is quite large in the context of water exchange with the Baltic Proper and suggests that the exchange of surface water might be much more intense than that of deeper water.

The character of variations in the statistics of coastal hits suggests, not unexpectedly, that the key parameter in the above estimates is the horizontal

resolution of the circulation model. The minimum width for a proper representation of the nearshore in this context is about three grid cells. For the Gulf of Finland conditions the 2 NM resolution is quite coarse and does not reproduce many local bathymetric features. The basic parameters of the mean and meso-scale circulation (such as typical flow speeds and the energy balance between mean flow and synoptic eddies), however, apparently are adequately reproduced and can be used for estimates of the net transport. The temporal resolution of saved velocity data (6 h) evidently distorts to some extent the impact of inertial oscillations, but apparently is fair enough to properly account for single eddies. An increase in the temporal resolution to 3 h in the Baltic Proper and in the horizontal resolution to about 1 km in the Gulf of Finland is desirable in future experiments.

The necessary length of trajectory calculations is to a large extent governed by the width of the sea area in question or, equivalently, by the distance from the release of an adverse impact to the vulnerable area. The potential spreading of initially closely located water particles owing to sub-grid turbulence is not accounted for here. Its impact apparently is small in terms of statistics of isotropic flow patterns but may considerably affect the probability of coastal hits in elongated basins such as the Gulf of Finland.

The appropriate time windows for adequate estimates of semi-persistent transport patterns evidently should be somewhat shorter, about 4–10 days. The smallest reasonable values match the typical turnover time of meso-scale eddies in the gulf. The use of time windows longer than about two weeks apparently will smooth out such patterns because the average speed of net transport, calculated for the larger values, is close to the overall average velocity in the gulf. The dependence of the results on the time lag between the windows, estimated in terms of the RMSD of pointwise averaged net transport speed for the entire gulf, is fairly small up to time lag of 10 days.

The strong seasonality in hitting rates to the coast suggests that several properties of the transport may have time scales on the order of a few weeks. This time scale considerably exceeds the so-called synoptic time scale (the typical turnover time of the meso-scale eddies, about a week in the gulf) but is substantially shorter than the length of typical seasonal variations (2–4 months). Such a separation of the synoptic and seasonal time scales encourages the search for phenomena that persist over an intermediate time scale between the synoptic and seasonal time scales in the Gulf of Finland. This is hardly possible in the open ocean where the synoptic time scale is about 1 month and the lifetime of a large part of meso-scale features overlaps with the seasonal variations. This range is therefore the most promising for detection of yet unknown features (such as semi-persistent patterns with a lifetime about 0.5–1 month) in the dynamics of the Gulf of Finland.

ACKNOWLEDGEMENTS

This study is a part of the BONUS+ project BalticWay, which attempts to propose ways to reduce pollution risks in the Baltic Sea by smart placing of human activities. The research was partially supported by the Marie Curie Reintegration Grant ESTSpline (PERG02-GA-2007-224819), targeted financing by the Estonian Ministry of Education and Research (grant SF0140077s08), and the Estonian Science Foundation (grant No. 7413). The authors sincerely thank Kristofer Döös and Andreas Lehmann for their valuable comments and hints.

REFERENCES

1. HELCOM. *Ensuring Safe Shipping in the Baltic* (Stankiewicz, M. and Vlasov, N., eds.). Helsinki Commission, Helsinki, 2009.
2. Kachel, M. J. *Particularly Sensitive Sea Areas*. Hamburg Studies on Maritime Affairs, vol. 13. Springer, 2008.
3. *Particularly Sensitive Sea Areas*. International Maritime Organisation, 2007, London.
4. Soomere, T., Myrberg, K., Leppäranta, M. and Nekrasov, A. The progress in knowledge of physical oceanography of the Gulf of Finland: a review for 1997–2007. *Oceanologia*, 2008, **50**, 287–362.
5. Parnell, K. E., Delpeche, N., Didenkulova, I., Dolphin, T., Erm, A., Kask, A., Kelpšaitė, L., Kurennoy, D., Quak, E., Räämet, A. et al. Far-field vessel wakes in Tallinn Bay. *Estonian J. Eng.*, 2008, **14**, 273–302.
6. [ASCE] American Society of Civil Engineers. State-of-the-art review of modeling transport and fate of oil spills. ASCE Committee on Modeling Oil Spills, Water Resources Engineering Division. *J. Hydraul. Eng.*, 1996, **122**, 594–609.
7. Reed, M., Johansen, O., Brandvik, P. J., Daling, P., Lewis, A., Fiocco, R., Mackay, D. and Prentki, R. Oil spill modeling towards the close of the 20th century: overview of the state of the art. *Spill Sci. Technol. Bull.*, 1999, **5**, 3–16.
8. Vandenbulcke, L., Beckers, J.-M., Lenartz, F., Barth, A., Poulain, P.-M., Aidonidis, M., Meyrat, J., Arduin, F., Tonani, M., Fratianni, C., Torrisi, L. et al. Super-ensemble techniques: application to surface drift prediction. *Progr. Oceanogr.*, 2009, **82**, 149–167.
9. Gästgifvars, M., Lauri, H., Sarkanen, A.-K., Myrberg, K., Andrejev, O. and Ambjörn, C. Modelling surface drifting of buoys during a rapidly-moving weather front in the Gulf of Finland, Baltic Sea. *Estuar. Coast. Shelf Sci.*, 2006, **70**, 567–576.
10. Alenius, P., Myrberg, K. and Nekrasov, A. Physical oceanography of the Gulf of Finland: a review. *Boreal Env. Res.*, 1998, **3**, 97–125.
11. Andrejev, O., Myrberg, K., Alenius, P. and Lundberg, P. A. Mean circulation and water exchange in the Gulf of Finland – a study based on three-dimensional modelling. *Boreal Env. Res.*, 2004, **9**, 1–16.
12. Osinski, R. and Piechura, J. Latest findings about circulation of upper layer in the Baltic Proper. In *BSSC 2009 Abstract Book, August 17–21, 2009*. Tallinn, 103.
13. Soomere, T., Viikmäe, B., Delpeche, N. and Myrberg, K. Towards identification of areas of reduced risk in the Gulf of Finland. *Proc. Estonian Acad. Sci.*, 2010, **59**, 156–165.
14. Soomere, T. and Quak, E. On the potential of reducing coastal pollution by a proper choice of the fairway. *J. Coast. Res.*, 2007, SI **50**, 678–682.
15. Andrejev, O., Sokolov, A., Soomere, T., Värvi, R. and Viikmäe, B. The use of high-resolution bathymetry for circulation modelling in the Gulf of Finland. *Estonian J. Eng.*, 2010, **16**, 187–210.
16. Andrejev, O., Myrberg, K. and Lundberg, P. A. Age and renewal time of water masses in a semi-enclosed basin – application to the Gulf of Finland. *Tellus B*, 2004, **56A**, 548–558.

17. Meier, H. E. M., Döscher, R. and Faxén, T. A multiprocessor coupled ice-ocean model for the Baltic Sea: application to salt inflow. *J. Geophys. Res.*, 2003, **108**(C8), Art. No. 3273.
18. Höglund, A., Meier, H. E. M., Broman, B. and Kriezi, E. *Validation and Correction of Regionalised ERA-40 Wind Fields over the Baltic Sea Using the Rossby Centre Atmosphere Model RCA3.0*. Rapport Oceanografi No. 97, Swedish Meteorological and Hydrological Institute, Norrköping, Sweden, 2009.
19. Meier, H. E. M. On the parameterization of mixing in three-dimensional Baltic Sea models. *J. Geophys. Res.*, 2001, **106**, C30997–C31016.
20. Meier, H. E. M. Modeling the pathways and ages of inflowing salt- and freshwater in the Baltic Sea. *Estuar. Coast. Shelf Sci.*, 2007, **74**, 717–734.
21. Alenius, P., Nekrasov, A. and Myrberg, K. The baroclinic Rossby-radius in the Gulf of Finland. *Cont. Shelf Res.*, 2003, **23**, 563–573.
22. Döös, K. Inter-ocean exchange of water masses. *J. Geophys. Res.*, 1995, **100**, C13499–C13514.
23. de Vries, P. and Döös, K. Calculating Lagrangian trajectories using time-dependent velocity fields. *J. Atmos. Oceanic Technol.*, 2001, **18**, 1092–1101.
24. Broman, B., Hammarklint, T., Rannat, K., Soomere, T. and Valdmann, A. Trends and extremes of wave fields in the north-eastern part of the Baltic Proper. *Oceanologia*, 2006, **48**, 165–184.
25. Soomere, T. and Zaitseva, I. Estimates of wave climate in the northern Baltic Proper derived from visual wave observations at Vilsandi. *Proc. Estonian Acad. Sci. Eng.*, 2007, **13**, 48–64.
26. Lehmann, A., Krauss, W. and Hinrichsen, H.-H. Effects of remote and local atmospheric forcing on circulation and upwelling in the Baltic Sea. *Tellus*, 2002, **54A**, 299–316.
27. Soomere, T., Delpeche, N., Viikmäe, B., Quak, E., Meier, H. E. M. and Döös, K. Patterns of current-induced transport in the surface layer of the Gulf of Finland. *Boreal Env. Res.*, 2011, **16**. Forthcoming.

Soome lahe pinnakihi hoovustraspordi ajamastaapidest

Bert Viikmäe, Tarmo Soomere, Mikk Viidebaum ja Mihhail Berezovski

On analüüsitud ajamastaape, mis iseloomustavad veemasside kandumist ranna lähistele ja vee netotranspordi omadusi Soome lahe pinnakihis. Rossby Centre (Rootsi Meteoroloogia ja Hüdroloogia Instituut) tsirkulatsioonimudeli abil aastate 1987–1991 jaoks arvatatud hoovuste kiiruste andmestiku alusel rekonstrueeritud veosakeste trajektoore analüüsi kaudu on näidatud, et tõenäosus vee kandumiseks lahe keskelt ranna lähistele varieerub oluliselt aasta lõikes, kuid pinnakihi vee triiv lahest välja on suhteliselt ühtlane. On näidatud, et sobivaks rannapiirkonna mudeliks on tsirkulatsioonimudeli kolme horisontaalsammu laiune vöönd. Usaldatava statistika leidmiseks on tarvis kasutada vähemalt 10–15 päeva pikkusi trajektoore rekonstruktsioone. Seevastu hoovuste netotranspordi omaduste leidmiseks on soovitatav kasutada 4–10 päeva pikkusi rekonstruktsioone.

Paper C

Viikmäe B., Torsvik T. and Soomere T. 2012. Analysis of the structure of currents in the Gulf of Finland using the Okubo-Weiss parameter. In: *IEEE/OES Baltic 2012 International Symposium*, May 8–11, 2012, Klaipeda, Lithuania, Proceedings. IEEE, 7 pp.

Analysis of the Structure of Currents in the Gulf of Finland using the Okubo-Weiss parameter

B. Viikmäe, T. Torsvik and T. Soomere
Institute of Cybernetics at Tallinn University of Technology
Akadeemia tee 21
12618, Tallinn, Estonia

Abstract—We analyze transport properties of surface water flow in the Gulf of Finland, the Baltic Sea, using spatial distributions of the Okubo-Weiss parameter, which reveals the spatial pattern of strain and relative vorticity at a specific time. The calculations are based on surface velocities calculated using the OAAS model with a spatial resolution of 1 nautical mile for 1987 in the framework of BONUS+ BalticWay cooperation. The currents are, on average, strain-dominated, with typical OW parameter values about 0.1. During short instances the OW parameter can abruptly increase by a factor 10. These events are not correlated with wind speed but occur slightly more frequently during the windy autumn season. Substantial areas of strong strain and relative vorticity regularly occur along the coast (due to topographic effects and coastal current fluctuations) and at two offshore areas; (i) in the eastern part near the mouth of the Neva river and (ii) in the north-western part of the gulf. The patterns of strong strain in the western part of the gulf originate from the northern nearshore but at times span down to the southern coast.

I. INTRODUCTION

The properties of currents in the Gulf of Finland have been in the focus of basic research and various applications during several generations of scientists since the time of Rolf Witting [1,2]. The bottlenecks in the relevant knowledge and the importance of understanding realistic patterns of current-driven transport has been reinforced during the latter decades in connections with the need for sustainable management of the gradually increasing ship traffic flow in the Baltic Sea. This issue is particularly important in the Gulf of Finland (Fig. 1), the easternmost prolongation of the Baltic Sea with a length of about 400 km, maximum width of 125 km and a mean depth of 37 m [2,3]. An exceptionally high concentration of traffic occurs around longitude 25°E where

the major fairway from the Baltic Proper to the eastern region of the gulf crosses intense fast ferry traffic between Helsinki and Tallinn where more than 50 gulf crossings take place daily during the high season [4]. This feature substantially increases the risk of a potential release of various adverse impacts (oil or chemical pollution, lost containers or other large buoyant items, etc., and associated impacts or hazards to both the environment and to other vessels) owing either to an accident, technical problems or human mistakes.

The analysis of current-driven transport of such adverse impacts subject to extremely volatile flow dynamics in this region [2,5,6] is a major challenge and a central component in risk assessment related to coastal and ocean pollution. The drift of agents of adverse impacts released into the marine surface layer (oil spills, lost containers, etc.) is influenced by wind stress, waves, and currents. The properties of transport by wind and waves are relatively well known [7,8]. Much less is known about the transport driven by the field of currents [9]. Currents are created under influence of several local and remote forcing factors, which makes their prediction quite challenging. It is even more complicated in strongly stratified sea areas such as the Gulf of Finland where the drift frequently is steered by multi-layered dynamics [5].

Surface currents in the Gulf of Finland are highly variable both seasonally and annually [2,3,6]. Recent analyses have demonstrated the existence of semi-persistent patterns of currents in this gulf [6,10,11]. A particularly interesting result of this analysis is the presence of strong meridional transport (Fig. 2) in specific regions in the Gulf of Finland [11]. Current patterns with a lifetime of a few weeks can potentially enhance the current-driven transport in certain sea

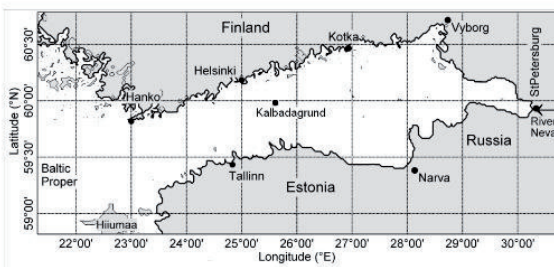


Figure 1. Map of the Gulf of Finland

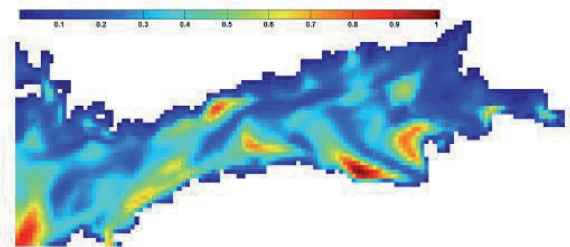


Figure 2. Average meridional transport, "windy-to-calm" season (March-April) 1987 [11].

areas. This is a challenge for the development of technology where the naturally occurring marine dynamics is exploited to reduce the risk of coastal pollution [12] and to maximize the time required for an adverse impact to reach vulnerable areas.

The problem of highlighting hidden patterns in the current-induced transport has been addressed in Refs. [10,13], where the transport properties of simulated velocity data has been analyzed by statistical methods applied to realizations of Lagrangian trajectories of test particles. Such an analysis allows the identification of time dependent current properties and semi-persistent patterns that cannot easily be extracted directly from the Eulerian velocity fields. The results, however, depend intimately on the underlying velocity fields as well as the governing parameters for the trajectory calculations such as the initial location of test particles, the duration of single trajectory simulations, the number of trajectories involved for each calculation session, etc.

In this study we employ another way to highlight such concealed features of current fields and transport created by semi-persistent patterns. The analysis relies on the Okubo-Weiss parameter for the simulated velocity data, which reveals the spatial pattern of strain and relative vorticity at a specific time. We demonstrate that, using this parameter for the quantification of flow patterns, it is possible to identify certain semi-persistent spatial structures of currents without relying on Lagrangian trajectories. The key purpose of this study is to determine to what extent the transport structures revealed in earlier results using Lagrangian particle trajectories are reflected in the spatial structure of widely used and easily computable parameters of the flow such as strain or relative vorticity.

II. METHOD

We choose to analyze the properties of surface currents by considering how the velocity gradients at each computed grid cell contribute to volume deformation (strain) and rotation (relative vorticity). The method is based on work by Okubo [14], who analyzed the dispersion at the ocean surface by looking at the shape of the trajectories of particle pairs, and Weiss [15], who analyzed the enstrophy dynamics in two-dimensional (2D) flows. In both approaches, the topology of particle trajectories and the basic features of the behavior of the time evolution of vorticity gradients are defined by the sign of the Okubo-Weiss (OW) parameter [15]

$$W = s_n^2 + s_s^2 - \omega^2. \quad (1)$$

Here s_n and s_s are the normal and shear components of strain, respectively, and ω is the relative vorticity:

$$s_n = \frac{\partial u}{\partial x} - \frac{\partial v}{\partial y}, \quad s_s = \frac{\partial v}{\partial x} + \frac{\partial u}{\partial y}, \quad \omega = \frac{\partial v}{\partial x} - \frac{\partial u}{\partial y}. \quad (2)$$

The sign of the OW parameter W allows us to determine whether a flow region is strain-dominated ($W > 0$) or vorticity-dominated ($W < 0$).

Different components of the OW parameter represent different actions of the flow field to the volumes of water. Consider a 2D quadratic material element of fluid at the water surface (Fig. 3) as representing the volume of water within a single grid cell at a given time. Strain is a measure of deformation, and for a 2D element this always involves a combination of compression and stretching along different principle axes due to the normal and tangential stress components acting on the element boundary. Large strain values occur at the boundary between water masses moving with different speeds. The contribution of vorticity is to rotate the element without any changes in its shape.

The OW parameter has been widely used to detect eddies in the ocean [16]. The core domains of eddy-like motions and the locations of strong meanders of jet currents correspond to large negative values of W . Almost rectilinear shear flows may result in large positive values of W in two occasions. They naturally characterize the domains with strong shear such as the seaward border of the coastal currents, around separated jet flows through an otherwise relatively quiet sea area (e.g. penetration of upwelling filaments in the offshore direction) or contact areas of jets flowing in opposite directions. The latter situation is characteristic for contact areas of large-scale gyres. It also happens at relatively narrow entrances to basins such as the Gulf of Finland where the border area between the inflow along one coast and outflow at the other coast may develop large horizontal shear [2,3]. Finally, large positive values of W are also characteristic to areas of intense divergence or convergence, independent on the sign of the phenomenon. Such areas occur in the World Ocean as the major convergence zones [17]. At smaller scale they may become evident as regions hosting strong local upwelling or downwelling.

We use in the calculations of the OW parameter the horizontal components of flow velocities (u, v) from circulation simulations performed by O. Andrejev and

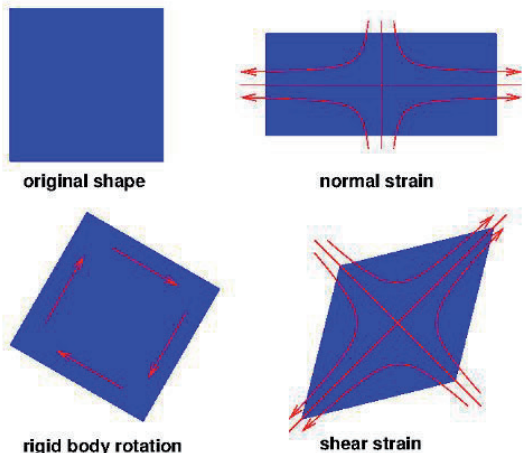


Figure 3. Sketch of element deformation and rotation.

A. Sokolov for the Gulf of Finland in the Baltic Sea using the numerical model OAAS [18,19]. This model has been specifically designed for the use in basins with complicated bathymetry and hydrography. A detailed overview of its principles and equations, methods for their solving, overall setup, boundary conditions and forcing data can be found in [13,18,19]. The velocity data are from a model run with a horizontal resolution of about 1 nautical miles (nm) and a vertical resolution (thickness of layers) of 1 m performed in the BONUS+ Baltic Way cooperation framework. The resolution of 1 nm is sufficient to resolve most of the meso-scale effects in this water body where the baroclinic Rossby radius is mostly 2–4 km [20]. The performance of the model in various resolutions has been analysed and tested in a number of earlier studies [6,21,22].

The initial conditions (such as water temperature and salinity) and the relevant information at the open boundary at the entrance to the Gulf of Finland at the longitude of 23°27' E (salinity and temperature fields and sea level) are extracted from simulations performed with the Rossby Centre Ocean model [23,24]. Both models are forced with the meteorological data from a regionalization of the ERA-40 re-analysis with a horizontal resolution of 25 km [25].

A simulation period of 1987–1991 was chosen in order to compare with earlier results [6,10,26]. The components of the OW parameter were calculated using a 2nd order central difference scheme for each available velocity data set, produced by the OAAS model at 3 hour time intervals. Due to the small velocity gradients and relatively large grid spacing it was necessary to apply a scaling factor in order to

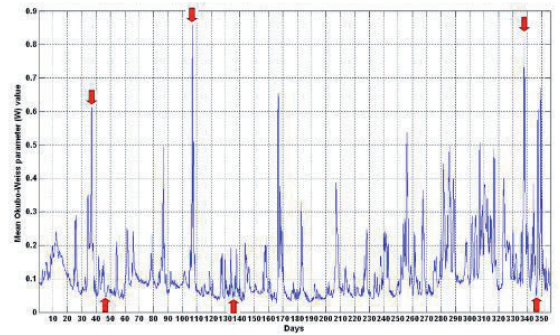


Figure 4. Okubo-Weiss parameter averaged over the entire computational domain for each 3 hour period. Results are presented for the year 1987. Red arrows indicate time instants corresponding to panels shown in Fig. 7.

ensure that calculations were performed with sufficient significant digits, and a factor of 1.0×10^{13} was selected for this purpose. Because we are primarily interested in the relative strength of the strain and relative vorticity, the magnitude of the OW parameter is not very important, and the scaling factor is a matter of convenience. A zone of data points near the open boundary at the western side of the Gulf of Finland was excluded in the calculations of the OW parameter, due to the artificial nature of velocity representation at boundaries in numerical models.

III. RESULTS

Figure 4 shows the average OW parameter for the entire computational domain at 3 hour time intervals. The currents

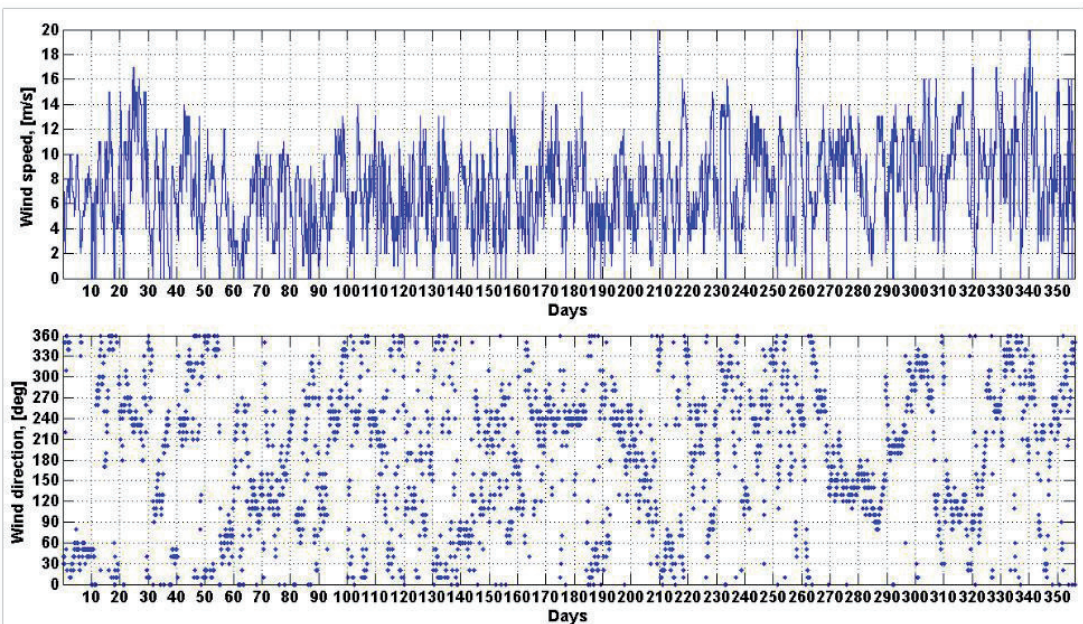


Figure 5. Wind speed and direction measured at Kalbådgrund in 1987.

are on average strain-dominated, with short instances of extreme events that can abruptly increase the typical OW parameter value (about 0.1) by a factor 10. Extreme “events” of large W occur more frequently at the end of the year, which corresponds to the typical windy autumn season.

Figure 5 shows the wind speed and direction at Kalbådgrund during 1987. The tendency for increased wind speed in the autumn months is visible in the data set. A comparison of Figs. 4 and 5 indicates that the extreme values of the OW parameter do not correspond to extreme wind speed. Moreover, scatter plots in Fig. 6 show that there is effectively no correlation between the OW parameter and wind speed or direction. The Pearson correlation coefficient for the OW parameter and wind speed is $r = 0.1108$, hence these variables are nearly completely uncorrelated. This is surprising as the common opinion is that the dynamics of the Gulf of Finland is wind-dominated [1,3,6].

A possible explanation is that the extreme values in the current field may lag behind the peak wind speed values in time or correspond to specific events driven by rapidly moving wind patterns. The scatter plot of the OW parameter and wind direction show a cluster of peaks at 260° – 280° , but also extreme values at 30° and 50° . These values correspond to wind directions almost along the Gulf of Finland.

The 2D maps of computed OW parameter at different time instances (Fig. 7) reveal its extensive spatial variations. The Several maxima and minima of the OW parameter are clearly linked to topographic features, the coastal regions and the islands in the eastern part of the Gulf of Finland. The runoff from Neva river is seen as a constant source of strain in the eastern part of the domain.

The large values of W (both positive and negative) near the coast can be explained by the retardation of the coastal current. Coastal topography creates zones of large relative vorticity interspersed by zones of equally strong strain. The resolution of the OAAS model used in this paper (1 nm) is not

sufficient to resolve the details of the coastal current [15] so the spatial distribution of vorticity and strain zones is probably imprecise. A certain flow retardation always occurs near the coast. Therefore, although the location of the simulated individual vorticity and strain zones may be slightly differ from actual ones, the presence of large values of the OW parameter at the coast, and especially along the coast of Finland, seems reasonable.

Whereas zones of high vorticity are prominent near the coast, zones of large strain are at times prominent also in the offshore domains of the Gulf of Finland. Such areas in the western part of the gulf are mostly oriented in the north-south direction and apparently are related to contact areas of local circulation cells. Still, they indicate the possibility of rapid transport of water masses across the gulf [11].

The most prominent areas of large values of W become evident in the western part of the Gulf of Finland. The north-western domain of the gulf between Hanko, Helsinki and Tallinn seem to be particularly inclined to large strain. Such areas evidently start to develop in the nearshore and may persist in the same region for several days. Interestingly, in all occasions when they reached the centerline of the gulf in 1987, they developed long filaments stretching almost across the gulf similar to filaments of extremely strong upwellings. Differently from upwelling filaments (that usually contain colder water penetrating far offshore), such filaments of strain may also represent off-shore directed Ekman currents preceding the upwelling events.

Alternatively, the pattern of areas with large strain between Tallinn and Helsinki may indicate the border between water masses moving at different velocity; for example, the border region of anticyclonic gyre identified in [11]. It is, however, remarkable that such patterns persist for more than a week even in the calm season and its filament-like structure of large strain was clearly evident even when results were averaged over about one week.

IV. CONCLUSIONS AND DISCUSSION

Results of the analysis show that patches of strong strain and relative vorticity regularly occur at specific locations belonging to two categories: (i) along the coast, due to topographic effects and coastal current fluctuations, and (ii) at specific offshore areas, namely in the eastern part near the mouth of the Neva river and in the north-western part of the basin where the Gulf of Finland narrows between the cities of Tallinn, Helsinki and Hanko. These patches are visible for several days and sometimes weeks. Although they evolve over time, they stay connected with the regions of their origin.

The strong strain patterns in the western part of the Gulf of Finland extend as filaments in the meridional direction, and at times span from coast to coast. This feature may indicate the presence of a semi-persistent front between water masses with different properties. The origin of such a front may be, for instance, a strong upwelling or the presence of different gyres in the eastern and western part of the Gulf of Finland. The

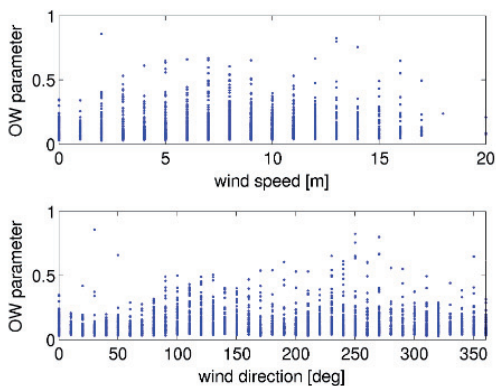


Figure 6. Correlation between the computed OW parameter and measured wind speed (top panel) and wind direction (bottom panel) at Kalbådgrund in 1987.

net result of their contact is the creation of a region of highly volatile currents in the region between Tallinn and Helsinki that are highlighted in the spatial distributions of the Okubo-Weiss parameter.

The presented results are to a large extent consistent with the outcome of earlier studies performed using Lagrangian trajectories [11], and suggest that this earlier result (Fig. 2) was not a numerical artifact. The usual presence of higher strain values mostly in the nearshore areas (except for the “filament” region between Tallinn and Helsinki) owing to coastal currents under higher wind speeds implicitly verifies the reliability of the calculations of optimum fairway [12,26] in which the nearshore area up to 6 nm from the coast was ignored. We also underline that the results presented here and in [11] are not entirely independent, since they both rely on the same type of output velocity field from a hydrodynamic model driven by the same type of wind data. Our analysis of the Okubo-Weiss parameter has used output from a

hydrodynamic model with a special resolution of 1 nm, whereas the earlier trajectory analysis [11] was based on the velocity data with a resolution of 2 nm.

The results confirm that the use of integrated measures of the internal structure of current fields such as the Okubo-Weiss parameter may reveal certain otherwise hidden features of the motion of water masses. Although the Okubo-Weiss parameter reflects, in essence, local properties of the surface-layer flow, its spatial distributions may be used for better understanding of the optional properties of the transport of water masses that cannot be identified directly from the Eulerian or Lagrangian velocities. The analysis of the Okubo-Weiss parameter alone only allows identification of patterns or pathways of anomalously rapid transport similarly to numerical experiments in [11], whereas the direction of the transport has to be specified from Eulerian velocities of the flow field.

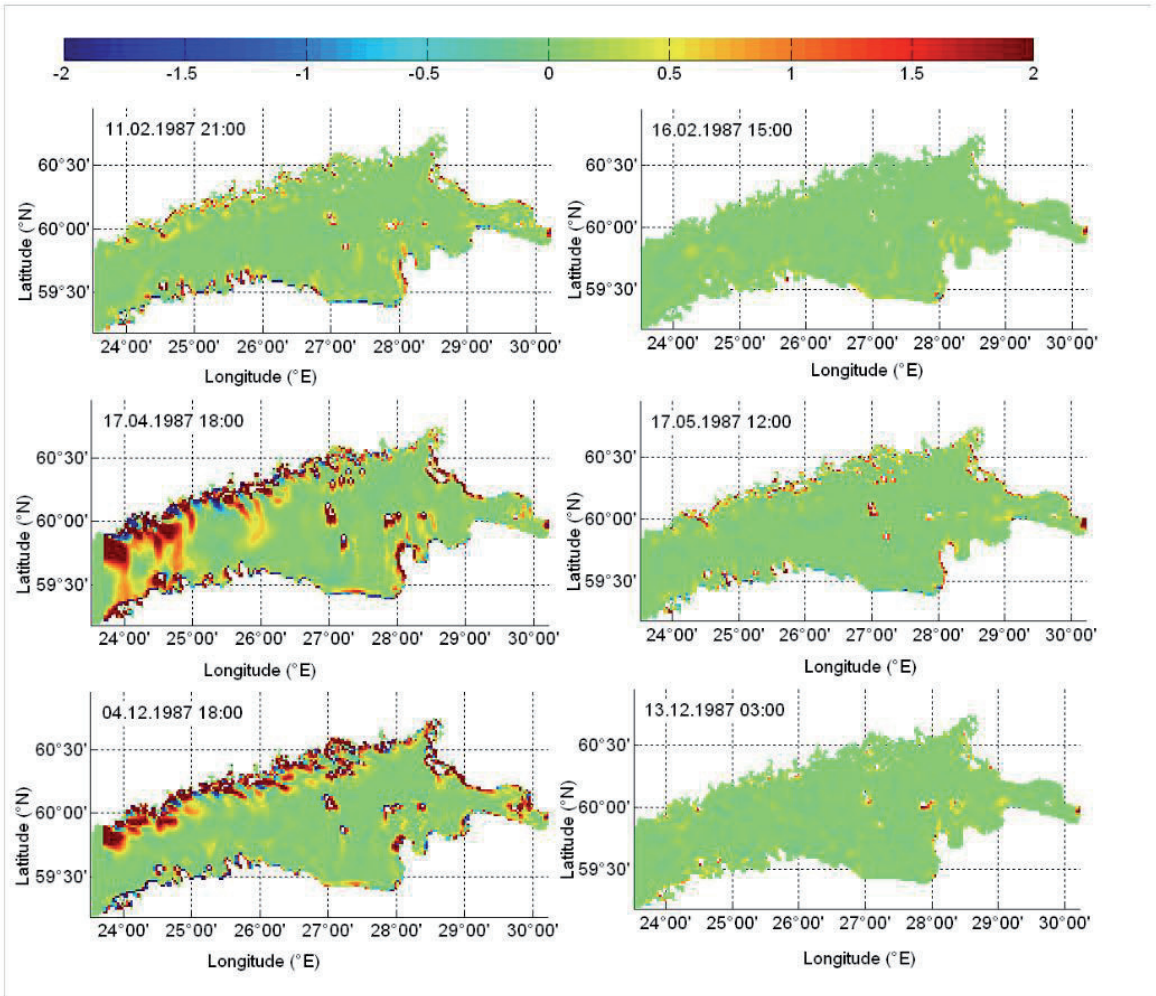


Figure 7. Spatial distribution of the Okubo-Weiss parameter in the Gulf of Finland during the windy (top and bottom pairs of panels) and calm season (middle pair of panels). The panels on the left correspond to time instants with large peaks in the average W (Fig. 4), while the three panels on the right correspond to time instants with relatively lower average W . Red color indicates strain-dominated regions and blue indicates vorticity-dominated areas.

Consistently with the calculation of net transport of currents in the Gulf of Finland [11], the performed analysis highlights a similar pattern of pathways of fast transport of surface waters perpendicular to the gulf between Tallinn and Helsinki and in the north-western domain of the Gulf of Finland. Another (less pronounced) pattern seems to exist in the eastern part of the gulf, near the mouth of Neva river. A similar pattern has been found in the same area in previous simulations of the flow compressibility of the sea surface [27]. The results of this study confirm the previous findings that there is a reduced area of risk of coastal pollution in the eastern part and there are several optimal fairways in this part, but because of this upwelling filament between Tallinn and Helsinki, the risk of coastal pollution in this area is very high

and due to this part of the gulf being very narrow, there are not many choices for the optimum fairway.

ACKNOWLEDGMENT

This work was supported by the European Union through the Mobilias grant MTT63 and through support to the Estonian Centre of Excellence for Non-linear Studies (CENS) from the European Regional Development Fund, by the targeted financing by the Estonian Ministry of Education and Research (grant SF0140007s11), and Estonian Science Foundation (grant No 9125). The authors thank the Finnish Meteorological Institute for providing the Kalbådagrund wind data and Oleg Andrejev and Aleksander Sokolov for

providing the velocity data from the OAAS model in the framework of the BONUS+ BalticWay cooperation.

REFERENCES

- [1] [M. Leppäranta and K. Myrberg, *Physical Oceanography of the Baltic Sea*. Berlin, Heidelberg: Springer, 2009.
- [2] P. Alenius, K. Myrberg, and A. Nekrasov, "Physical oceanography of the Gulf of Finland: a review," *Boreal Environ. Res.*, vol. 3, pp 97-125, 1998.
- [3] T. Soomere, K. Myrberg, M. Leppäranta, and A. Nekrasov, "The progress in knowledge of physical oceanography of the Gulf of Finland: a review for 1997-2007," *Oceanologia*, 50, pp 287-362, 2008.
- [4] K.E. Parnell, N. Delpeche, I. Didenkulova, T. Dolphin, A. Erm, A. Kask, L. Kelpšaitė, D. Kurennoy, E. Quak, A. Räämet, et al. "Far-field vessel wakes in Tallinn Bay," *Estonian J. Eng.*, 14, pp 273-302, 2008.
- [5] M. Gästgifvars, H. Lauri, A.-K. Sarkanen, K. Myrberg, O. Andrejev, and C. Ambjörn, "Modelling surface drifting of buoys during a rapidly-moving weather front in the Gulf of Finland, Baltic Sea," *Estuar. Coast. Shelf Sci.*, 70, pp 567-576, 2009.
- [6] O. Andrejev, K. Myrberg, P. Alenius, and P.A. Lundberg, "Mean circulation and water exchange in the Gulf of Finland – a study based on three-dimensional modeling," *Boreal Environ. Res.*, 9, pp 1-16, 2004.
- [7] ASCE Committee on Modeling Oil Spills, Water Resources Engineering Division, American Society of Civil Engineers, "State-of-the-art review of modeling transport and fate of oil spills," *J. Hydraul. Eng.*, 122, pp 594-609, 1996.
- [8] M. Reed, O. Johansen, P.J. Brandvik, P. Daling, A. Lewis, R. Fiocco, D. Mackay, and R. Prentki, "Oil spill modeling towards the close of the 20th century: overview of the state of the art," *Spill Sci. Technol. Bull.*, 5, pp 3-16, 1999.
- [9] L. Vandenbulcke, J.-M. Beckers, F. Lenartz, A. Barth, P.-M. Poulain, M. Aidonidis, J. Meyrat, F. Ardhuin, M. Tonani, C. Fratianni, L. Torrisi, et al., "Super-ensemble techniques: application to surface drift prediction," *Progr. Oceanogr.*, vol. 82, pp 149-167, 2009.
- [10] T. Soomere, B. Viikmäe, N. Delpeche, and K. Myrberg, "Towards identification of areas of reduced risk in the Gulf of Finland," *Proc. Estonian Acad. Sci.*, vol. 59, pp. 156-165, 2010.
- [11] T. Soomere, N. Delpeche, B. Viikmäe, E. Quak, H.E.M.Meier, and K. Döös, "Patterns of current-induced transport in the surface layer of the Gulf of Finland," *Boreal Environ. Res.*, vol. 16, Suppl. A, pp. 49-63, 2011.
- [12] T. Soomere, O. Andrejev, A. Sokolov, and K. Myrberg, "The use of Lagrangian trajectories for identification the environmentally safe fairway," *Marine Pollut. Bull.*, vol. 62, pp. 1410-1420, 2011.
- [13] O. Andrejev, A. Sokolov, T. Soomere, R. Värvi, and B. Viikmäe "The use of high-resolution bathymetry for circulation modelling in the Gulf of Finland," *Estonian J. Eng.*, vol. 16, pp 187-210, 2010.
- [14] A. Okubo, "Horizontal dispersion of floatable particles in the vicinity of velocity singularities such as convergences," *Deep-Sea Res.*, vol. 17, pp. 445-454, 1970.
- [15] J. Weiss, "The dynamics of enstrophy transfer in two-dimensional hydrodynamics," *Physica D*, vol. 48, pp. 273-294, 1991.
- [16] J. Isem-Fontanet, J. Font, E. Garcia-Ladona, M. Emelianov, C. Millot, and I. Taupier-Letage, "Spatial structure of anticyclonic eddies in the Algerian basin (Mediterranean Sea) analyzed using the Okubo-Weiss parameter," *Deep-Sea Res. II*, vol. 51, pp. 3009-3028, 2004.
- [17] E. Martineza, K. Maamaatuaiahutapua, V. Taillandierb, "Floating marine debris surface drift: Convergence and accumulation toward the South Pacific subtropical gyre," *Marine Pollut. Bull.*, vol. 58, pp 1347-1355, 2009.
- [18] O. Andrejev and A. Sokolov, "Numerical modelling of the water dynamics and passive pollutant transport in the Neva inlet," *Meteorol. Hydrol.*, vol. 12, pp 75-85 (in Russian), 1989.
- [19] O. Andrejev and A. Sokolov, "3D baroclinic hydrodynamic model and its applications to Skagerrak circulation modeling," in *Proceedings of the 17th Conference of Baltic Oceanographers* (Norrköping, Sweden), pp. 38-46, 1990.
- [20] P. Alenius, A. Nekrasov, and K. Myrberg, "The baroclinic Rossby-radius in the Gulf of Finland," *Cont. Shelf Res.*, vol. 23, pp. 563-573, 2003.
- [21] O. Andrejev, K. Myrberg, and P.A. Lundberg, "Age and renewal time of water masses in a semi-enclosed basin – Application to the Gulf of Finland," *Tellus A*, 56, pp. 548-558, 2004.
- [22] K. Myrberg, V. Ryabchenko, A. Isaev, R. Vankevich, O. Andrejev, J. Bendtsen, A. Erichsen, L. Funkquist, A. Inkala, I. Neelov, K. Rasmus, M. Rodriguez Medina, U. Raudsepp, J. Passenko, J. Söderkvist, A. Sokolov, H. Kuosa, T.R. Anderson, A. Lehmann, and M.D. Skogen, "Validation of three-dimensional hydrodynamic models of the Gulf of Finland," *Boreal Environ. Res.*, vol. 15, pp 453-479, 2008.
- [23] H.E.M. Meier, "Modeling the pathways and ages of inflowing salt- and freshwater in the Baltic Sea," *Estuar. Coastal Shelf Sci.*, vol. 74, pp 717-734, 2007.
- [24] H.E.M. Meier, R. Döscher, and T. Faxén, "A multiprocessor coupled ice-ocean model for the Baltic Sea: Application to salt inflow," *J. Geophys. Res.*, vol. C108, 3273, 2003.
- [25] P. Samuelsson, C.G. Jones, U. Willén, A. Ullerstig, S. Gollvik, U. Hansson, C. Jansson, E. Kjellström, G. Nikulin, and K. Wyser "The Rossby Centre Regional Climate Model RCA3: Model description and performance," *Tellus A*, vol. 63, pp 4-23, 2011.
- [26] [30] T. Soomere, M. Berezovski, E. Quak, B. Viikmäe, "Modeling environmentally friendly fairways using Lagrangian trajectories: a case study for the Gulf of Finland, the Baltic Sea," *Ocean Dynamics*, vol. 61, pp. 1669-1680, 2011.
- [27] J. Kalda, T. Soomere, and A. Giudici, "On the compressibility of the surface currents in the Gulf of Finland, the Baltic Sea," *J. Marine Syst.*, 2012 (submitted).

Paper D

Viikmäe B. and Torsvik T. 2013. Quantification and characterization of mesoscale eddies with different automatic identification algorithms. *Journal of Coastal Research*, Special Issue 65, 2077–2082.

Quantification and characterization of mesoscale eddies with different automatic identification algorithms

Bert Viikmäe† and Tomas Torsvik†

† Institute of Cybernetics, Tallinn
University of Technology
Akadeemia tee 21, 12618 Tallinn, Estonia
bert@ioc.ee; tomas.torsvik@ioc.ee



www.cerf-jcr.org



www.JCRonline.org

ABSTRACT

Viikmäe, B., Torsvik, T., 2013. Quantification and characterization of mesoscale eddies with different automatic identification algorithms *In: Conley, D.C., Masselink, G., Russell, P.E. and O'Hare, T.J. (eds.), Proceedings 12th International Coastal Symposium* (Plymouth, England), *Journal of Coastal Research*, Special Issue No. 65, pp. 2077-2082, ISSN 0749-0208.

Automatic methods for detection of mesoscale eddies are usually based on either physical (e.g. Okubo-Weiss parameter) or geometrical (e.g. streamline winding-angle) flow characteristics. In this paper, a hybrid method combining the strengths of the two different approaches is applied to the Eulerian velocity fields for two case studies: (i) the Gulf of Finland (the Baltic Sea) and (ii) the Raunefjord and Vattestraumen area south-west of Bergen, Norway. Velocity fields are investigated with a hybrid winding-angle method (HWA), where the Okubo-Weiss parameter is first used to detect potential eddies, and the winding-angle method is used locally within these regions to test the Okubo-Weiss result. In the Gulf of Finland, the HWA method results in a substantially reduced number of detected eddies compared with the Okubo-Weiss result, indicating that the Okubo-Weiss parameter severely overestimates the number of eddies. In Vattestraumen, there was a better correspondence between results obtained by the HWA and the Okubo-Weiss methods. The HWA method requires careful analysis since more than one streamline may identify the same eddy structure.

ADDITIONAL INDEX WORDS: *Winding-angle method, Okubo-Weiss parameter, Eulerian velocity field, current-driven transport, vortex detection.*

INTRODUCTION

Turbulent surface current motion is characterized by a complex field of eddies or vortices interspaced by meanders, fronts and filaments. Eddies are generally more energetic than the surrounding currents, and play an important part in transport of heat, mass and momentum, as well as biological and chemical agents, from areas of formation to areas of decomposition (Munk *et al.*, 1970; Chelton *et al.*, 2011). Eddy detection using field measurements has been applied during last 40 years (Isern-Fontanet *et al.*, 2003); and has greatly benefited from technological advances in satellite construction and remote sensing imagery. Lagrangian methods for ocean studies (Davis, 1991) constitute another important branch for measurements of surface current dynamics.

Numerical models are widely used in studying geophysical phenomena, hindcasting or forecasting; obtaining approximate surface current conditions. Due to the vital role of mesoscale variability for transport problems by surface currents, it is important that the simulated current field contains dominant features similar to real current field in the ocean. The models should therefore have sufficient resolution to be eddy-permitting, and preferably eddy resolving, for the main features in the mesoscale range. Having an eddy-permitting or eddy-resolving model is a necessary, but not sufficient, condition to obtain mesoscale turbulent features. Turbulent features may develop within the model domain even when the model forcing is smooth,

but often a smooth forcing field will produce unrealistically smooth surface current fields.

Eddies are generally recognized as roughly circular features of swirling fluid motion. It is fairly easy to pick out these features using satellite images, but it is difficult to define precise boundaries that separate the eddy from surrounding fluid motion, and to track eddies over time due to their transient and highly volatile nature. As a result, it is not straight forward to detect eddies by automatic methods and to quantify their number and characteristic dimensions. However, with increasing data becoming available from satellites and numerical models, it is highly desirable to improve the methods for automatic eddy detection, and several methods have been proposed in recent publications (Sadarjoen and Post, 2000; Chaigneau *et al.*, 2008; Nencioli *et al.*, 2010; Souza *et al.*, 2011).

Eddy detection by Lagrangian methods require that the eddies are stable, in this case a drifter moving at a roughly circular track can be used. Such detection is more difficult if the eddy structure meanders and the swirling motion is slow. That is why substantial number of drifters are often required to obtain a reasonable characterization of the eddy field.

When analyzing instantaneous flow fields from satellite images, two methods of eddy detection are available. Detection methods based on physical quantities depend on local variations in some quantity, such as pressure or vorticity. Relatively strong gradients are required to be reasonably sure that the anomaly represents a persistent structure, so these methods tend to detect the strong, dominant vortex field. Another method depends on the geometric properties of streamlines, in which case the curvature of the

DOI: 10.2112/SI65-351.1 received 07 December 2012; accepted 06 March 2013.

© Coastal Education & Research Foundation 2013

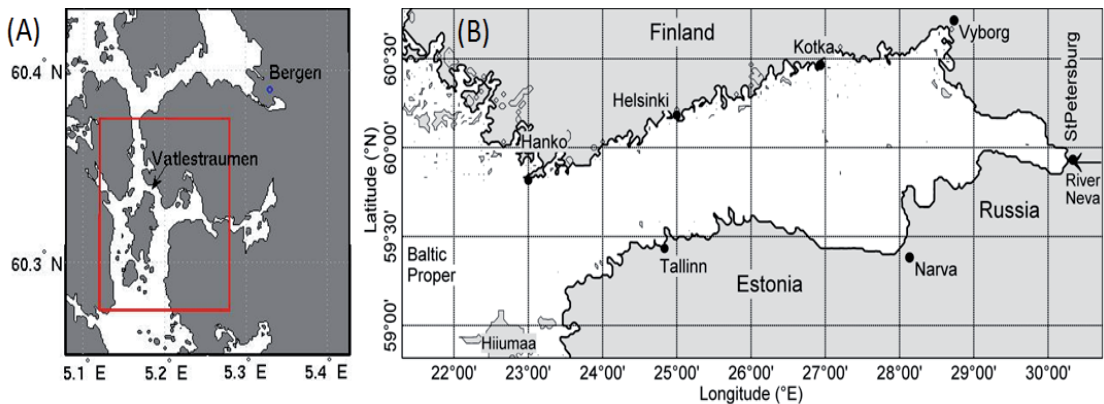


Figure 1. Schematic of two different modelling domains: Vattestraumen, an archipelago coastal area south-west of Bergen, Norway (Panel A) and the Gulf of Finland, the easternmost prolongation of the Baltic Sea (Panel B).

streamline is indicative of vortex structures. An eddy structure is detected if a streamline undergoes a rotation of $\pm 2\pi$ and the end point after rotation is close to the starting point. In the present paper, both the physical and geometrical detection methods are used to examine the existence of eddies in simulated velocity fields.

MODELLING ENVIRONMENT

Two domains and two different models were used in this study. The first domain is the Gulf of Finland, the easternmost prolongation of the Baltic Sea (Fig.1B). In this case the horizontal components of surface flow velocities (u, v) were used from circulation simulations performed for the Gulf of Finland (the Baltic Sea) using the numerical model OAAS (Andrejev *et al.*, 1989; Andrejev *et al.*, 1990). This model has been specifically designed for the use in basins with complicated bathymetry and hydrography. A detailed overview of its principles and equations, methods for their solving, overall setup, boundary conditions and forcing data can be found in (Andrejev *et al.*, 1989; 1990; 2010). The velocity data are from a model run with a horizontal resolution of ~ 1 nautical miles (nm) and a vertical resolution (thickness of layers) of 1 m performed in the BONUS+ Baltic Way cooperation framework (Soomere *et al.*, 2011). The resolution of 1 nm is sufficient to resolve most of the mesoscale effects in this water body where the baroclinic Rossby radius is mostly 2–4 km (Alenius *et al.*, 2003). The performance of the model in various resolutions has been analysed and tested in a number of earlier studies (Andrejev *et al.*, 2004a; b; Myrberg *et al.*, 2008).

The second domain in the present study is an archipelago coastal area south-west of Bergen, Norway (Fig.1A). For this region the horizontal components of surface flow velocities (u, v) were obtained using Bergen Ocean Model (BOM) with equidistant $20 \times 20 \text{ m}^2$ horizontal grid resolution (435 \times 525 grid cells) and terrain-following vertical coordinates with 32 layers. The time step of the model was 1.5 s, and the total simulation time was 4 days, from 2004-01-16 to 2004-01-20. The first 24 hours were used to spin up the model, and model results were recorded from 2004-01-17. A non-hydrostatic model formulation was used for the simulations, and Smagorinsky and 2.5 Mellor-Yamada turbulence schemes were used for the horizontal and vertical momentum equations, respectively. Astronomical tides with 6

tidal components ($M_2, S_2, N_2, K_2, K_1, O_1$) were used to determine the water level at the northern and southern boundaries, with the slight shift in amplitude and phase between the boundaries forcing the tidal current (Hendershott *et al.*, 1970). The water level at the eastern boundary, a narrow channel leading to a bay, was set to 4 cm above mean sea level. Flow relaxation schemes were used for all open boundaries.

METHODS

Physical detection method: Okubo-Weiss parameter

A physical detection method depends on gradients of some physical quantity, such as pressure or vorticity. A popular method which is often applied to detect 2D flow structures is based on the Okubo-Weiss (OW) parameter (Okubo, 1970; Weiss, 1991), defined as

$$W = s_n^2 + s_s^2 - \omega^2, \quad (1)$$

where s_n and s_s are the normal and shear components of strain, respectively, and ω is the relative vorticity of the flow, defined in terms of velocity gradients as

$$s_n = \frac{\partial u}{\partial x} - \frac{\partial v}{\partial y}, \quad s_s = \frac{\partial v}{\partial x} + \frac{\partial u}{\partial y}, \quad \omega = \frac{\partial v}{\partial x} - \frac{\partial u}{\partial y}, \quad (2)$$

where x and y refer to grid size, u and v are the horizontal and vertical velocity components.

A flow region is strain-dominated if $W > 0$, and vorticity-dominated if $W < 0$. In most cases OW values close to zero do not indicate any specific structure, so it is common practice to define a threshold value W_0 so that the flow region is strain-dominated for $W > W_0$ and vorticity-dominated for $W < -W_0$, and neither for $|W| < W_0$. A potential weakness of the OW method is that it relies on locally evaluated quantities that make the method less likely to detect large scale, weak vortices (Sadarjoen and Post, 2000).

Geometrical detection method: Winding-angle

According to winding-angle (WA) method, the vortex exists when instantaneous streamlines mapped onto a plane normal to the vortex core exhibit a roughly circular or spiral pattern

(Robinson, 1991). The WA method is based on geometrical criteria unlike physical OW method.

The curvature of the streamline function can be used for the detection of mesoscale eddies and this is achieved using the winding-angle (WA) detection algorithm (Sadarjoen *et al.*, 1998; Sadarjoen, 1999; Sadarjoen and Post, 2000). The WA method characterizes an eddy structure by a point that defines its center and by a closed streamline contour corresponding to the eddy edge. The inner points bordered by this contour line belong to the eddy and determine its surface area. Let us consider a 2D streamline beginning at point P_1 (Fig. 2) and consists of several segments, which length corresponds to the step size (~ 20 m). The winding-angle of the streamline corresponds to the cumulated sum of the angles between all pairs of consecutive segments

$$WA = \sum_{i=2}^{N-1} \langle P_{j-1}, P_j, P_{j+1} \rangle = \sum_{j=2}^{N-1} \alpha_j \quad (3)$$

where $\langle P_{j-1}, P_j, P_{j+1} \rangle = \alpha_j$ denotes the signed angle between the segments $[P_{j-1}, P_j]$ and $[P_j, P_{j+1}]$. Positive values of α correspond to counterclockwise-rotating curves and negative

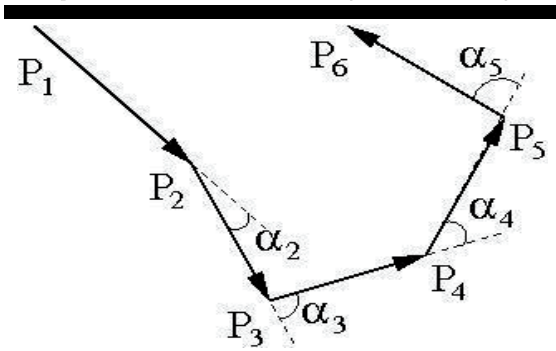


Figure 2. Winding-angle (WA) method for a segmented streamline.

values correspond to clockwise-rotating curves. A streamline is associated with an eddy if its $|WA| \geq 2\pi$. Being slightly more successful in finding eddies than the OW method, the WA method

reduces the excess number of detected eddies (Chaigneau *et al.*, 2008; Souza *et al.*, 2011). However, the OW method is computationally efficient and easy to use, so it is attractive when a large number of velocity fields are analyzed. In this paper we therefore investigate velocity fields with a hybrid winding-angle method (HWA), where the OW method is first used to detect potential eddies, and the WA method is used locally within these regions to test the OW result. This substantially reduces the number of streamlines required for the WA analysis, making the detection procedure more efficient.

RESULTS

Case study 1: Gulf of Finland

The case study was based on simulated currents in the eastern prolongation of the Baltic Proper. The size of the domain is 370 km from west to east and the width is 70-130 km. Tidal currents in this domain are insignificant. The number of vorticity regions identified in the Gulf of Finland domain by the OW method was 220 (Fig. 3A). A streamline analysis was performed in the same domain, by choosing the points of the vorticity regions identified by the OW method as starting points for the streamlines (Fig. 3B). Although the streamlines indicated that there was some curvature, it occurred only over several tens of kilometres (mean eddy radius is 2-4 km) and due to the small curvature of the streamlines (lines were almost straight), the HWA method was not able to detect any eddies within the areas indicated as vorticity-dominated by the OW method.

Case study 2: Vatløstraumen

The case was based on simulated tidal currents in an archipelago coastal area south-west of Bergen, Norway. The computational domain is 10.5 km in the north-south direction, with open boundaries on each side, and 8.7 km in the east-west direction, with a narrow channel with a strong tidal current at the eastern boundary connecting to a large bay area. The model area contains a narrow strait, Vatløstraumen, with tidal currents up to about 1 m/s, and lies along the main commercial sailing route south from Bergen harbor. The calculations for this domain were performed during a 12 hour period, to take into account the tidal currents. Both methods worked in this domain, the first, OW method, was used successfully to find regions of potential eddies and the WA method, used as a hybrid method, detected if these identified regions contain real eddies. The number of potential eddy regions identified with the OW method during the 12h simulation was 83-305 and the number of real eddies in these, identified by the HWA method, was 16-132 (Table 1, Fig. 4-5).

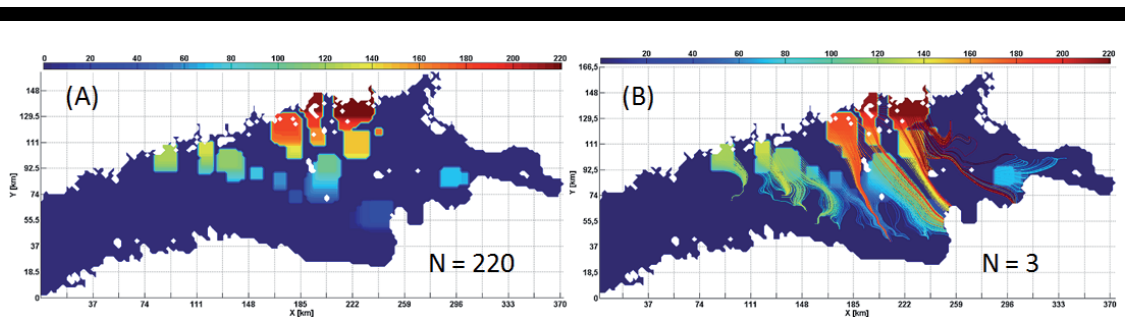


Figure 3. Detection of flow structures in the Gulf of Finland for 1 nm surface velocity data on 1987-12-17 18:00. Panels show results for (A) OW method, and (B) HWA method.

Table 1. Number of identified eddies with the OW and the HWA methods in Vatstestraumen domain.

Hour	OW method	HWA method
1	267	62
2	135	71
3	94	46
4	83	16
5	227	132
6	236	126
7	275	130
8	157	71
9	145	34
10	157	31
11	258	63
12	305	61

result is to some extent sensitive to the threshold value W_0 , which was set to $\sim 10\%$ of the minimum OW value. For the Vatstestraumen case this threshold value was maintained as a constant value throughout the 12h simulation period, which is likely to have influenced the large variability of detected eddies with the OW method (Table 1).

The subsequent eddy detection by the HWA method substantially reduced the number of detected eddies. For the Gulf of Finland case study, several of the patches identified by the OW method did not contain circular streamline features. Hence the OW result severely overestimated the number of eddies for this case. For the Vatstestraumen case study, the OW eddy count is also much higher than the HWA result, but still there is a better correspondence between the HWA and the OW results and the

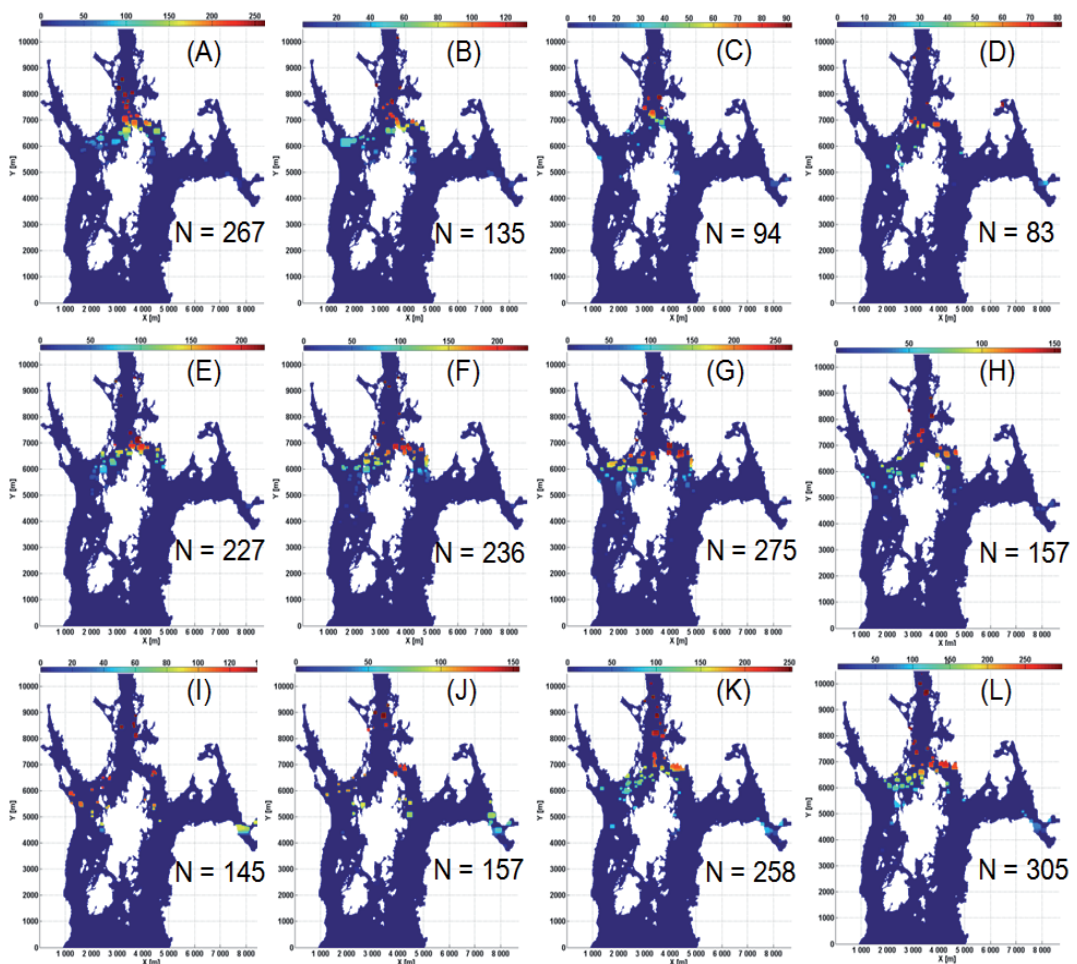


Figure 4. Results for OW method. Panels (A) - (L) indicate hours 1-12 and N depicts the number of eddies identified.

CONCLUDING REMARKS

Two test cases have been examined in order to investigate the performance of automated detection algorithms for eddy detection. The OW method indicated a large number of eddies. The OW

number of individual patches (Figures 3-5).

The HWA method requires additional analysis since more than one streamline may identify the same eddy structure. In order to avoid that the HWA method counts these as two individual eddies, the streamlines that identify the same eddy structure must be

clustered together. In the preceding analysis it was assumed that the OW parameter provided sufficient clustering information, i.e. that streamlines started within each region identified by the OW parameter would identify the same eddy structure. This hypothesis has not been substantially tested, and may be a weakness of the method presented here.

The detection of eddy features can be used as an indicator for the dynamic variability of the current field. For the Gulf of Finland, although the OAAS model is in principle eddy-permitting at the resolution of 1 nm, this is not reflected in the current field. Possible reasons could be that the forcing fields used in the model are very homogeneous, or that the parameters used for the turbulence schemes are too large, so that small scale features are

ACKNOWLEDGEMENT

This work was supported by the European Union through the Mobilitas grant MTT63 and through support to the Estonian Centre of Excellence for Non-linear Studies (CENS) from the European Regional Development Fund, by the targeted financing by the Estonian Ministry of Education and Research (grant SF0140007s11), and Estonian Science Foundation (grant No 9125). The authors thank the Finnish Meteorological Institute for providing the Kalbådgrund wind data and Oleg Andrejev and Aleksander Sokolov for providing the velocity data from the OAAS model in the framework of the BONUS+ BalticWay cooperation.

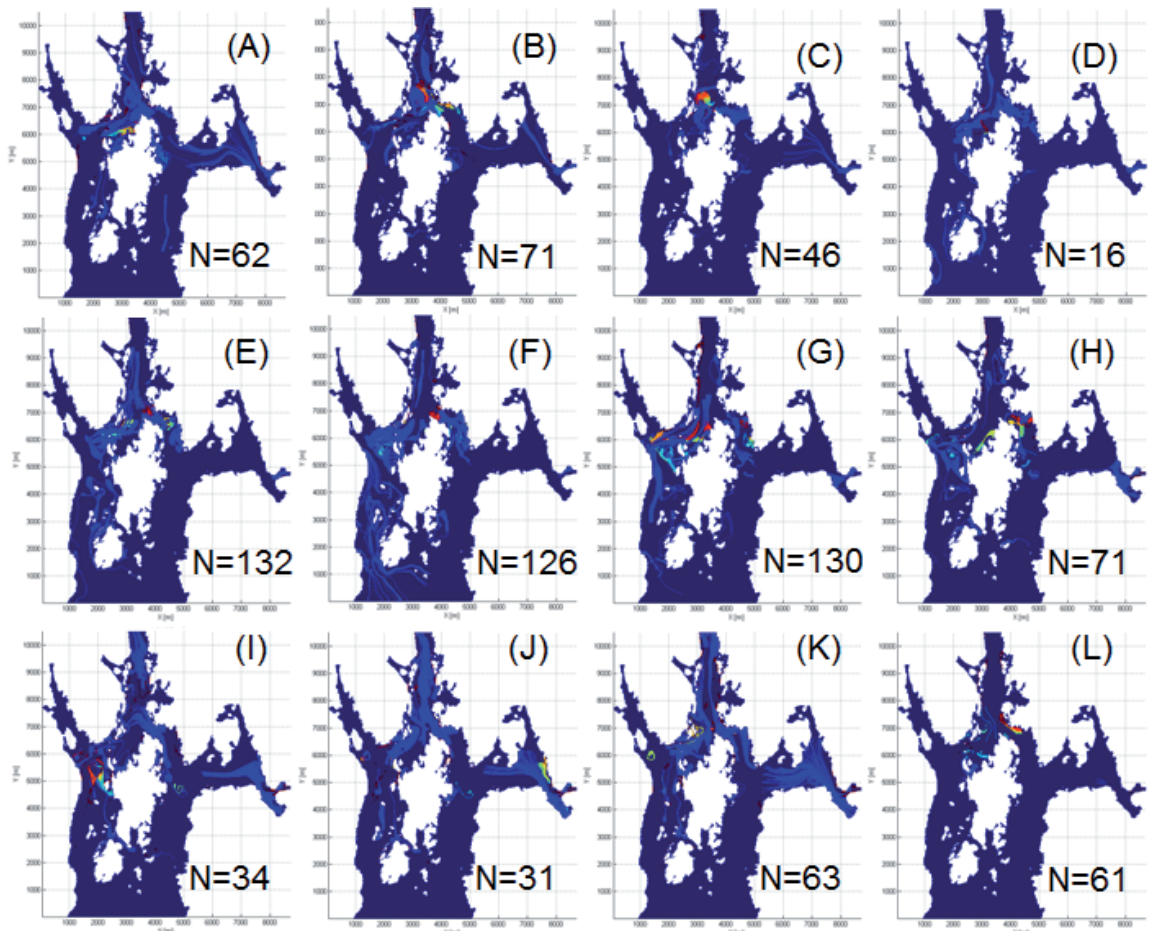


Figure 5. Results for HWA method. Panels (A) - (L) indicate hours 1-12 and N depicts the number of eddies identified.

smoothed out. The Vatlstraumen simulations contained a reasonable amount of eddies, although localized in specific regions, indicating that the model region is sufficiently resolved and the model parameters are adequate for reproduction of small scale flow features.

LITERATURE CITED

- Alenius, P., Nekrasov, A. and Myrberg, K., 2003. The baroclinic Rossby-radius in the Gulf of Finland. *Continental Shelf Research*, 23, 563-573.
 Andrejev, O. and Sokolov, A., 1989. Numerical modelling of the water dynamics and passive pollutant transport in the Neva inlet. *Meteorological Hydrology*, 12, 75-85 (in Russian).

- Andrejev, O. and Sokolov, A., 1990. 3D baroclinic hydrodynamic model and its applications to Skagerrak circulation modeling. *Proceedings of the 17th Conference of Baltic Oceanographers* (Norrköping, Sweden), pp. 38-46.
- Andrejev, O., Myrberg, K., Alenius, P. and Lundberg, P. A., 2004a. Mean circulation and water exchange in the Gulf of Finland – a study based on three-dimensional modeling. *Boreal Environmental Research*, 9, 1-16.
- Andrejev, O., Myrberg, K. and Lundberg, P. A., 2004b. Age and renewal time of water masses in a semi-enclosed basin – Application to the Gulf of Finland. *Tellus A*, 56, 548-558.
- Andrejev, A., Sokolov, A., Soomere, T., Värvi, R. and Viikmäe, B., 2010. The use of high-resolution bathymetry for circulation modelling in the Gulf of Finland. *Estonian Journal of Engineering*, 16, 187-210.
- Chaigneau, A., Gizolme, A. and Grados, C., 2008. Mesoscale eddies off Peru in altimeter records: Identification algorithms and eddy spatio-temporal patterns. *Progress in Oceanography*, 79, 106-119.
- Chelton, D. B., Schlax, M. G. and Samelson, R. M., 2011. Global observations of nonlinear mesoscale eddies. *Progress in Oceanography*, 91, 167-216.
- Davis, R. E., 1991. Lagrangian Ocean Studies. *Annual Review of Fluid Mechanics*, 23, 43-64.
- Hendershott, M., and Munk, W., 1970. Tides. *Annual Review of Fluid Mechanics*, 2, 205-224.
- Isern-Fontanet, J., Garcia-Ladona, E. and Font, J., 2003. Identification of Marine Eddies from Altimetric Maps. *Journal of Atmospheric and Oceanic Technology*, 20, 772-778.
- Munk, W., Armi, L., Fischer, K. and Zachariassen, F., 1997. Spirals on the sea. *Proceedings of Royal Society London*, 456, 1217-1280.
- Myrberg, K., Ryabchenko, V., Isaev, A., Vankevich, R., Andrejev, O., Bendtsen, J., Erichsen, A., Funkquist, L., Inkala, A., Neelov, I., Rasmus, K., Rodriguez Medina, M., Raudsepp, U., Passenko, J., Söderkvist, J., Sokolov, A., Kuosa, H., Anderson, T. R., Lehmann, A. and Skogen, M. D., 2008. Validation of three-dimensional hydrodynamic models of the Gulf of Finland. *Boreal Environmental Research*, 15, 453-479.
- Nencioli, F., Dong, C., Dicky, T., Washburn, L. and McWilliams, J. C., 2010. A vector geometry-based eddy detection algorithm and its application to a high-resolution numerical model product and high-frequency radar surface velocities in the southern California Bight. *Journal of Atmospheric and Oceanic Technology*, 27, 564-579.
- Okubo, A., 1970. Horizontal dispersion of floatable particles in the vicinity of velocity singularities such as convergences. *Deep-Sea Res.*, 17, 445-454.
- Robinson, S. K., 1991. Coherent motions in the turbulent boundary layer. *Annual Review of Fluid Mechanics*, 23, 601.
- Sadarjoen, I. A., Post, F. H., Ma, B., Banks, D. C., Pagendarm, H.- G., 1998. Selective Visualization of Vortices in Hydrodynamic Flows. *Proceedings of IEEE Visualization* (Triangle Research Park, North Carolina, USA), pp. 419-422.
- Sadarjoen, I. A. and Post, F. H., 1999. Geometric Methods for Vortex Extraction. *Proceedings of Joint EG/IEEE TCYG Symposium* (Vienna, Austria), pp. 53-62.
- Sadarjoen, I. A. and Post, F. H., 2000. Detection, quantification, and tracking of vortices using streamline geometry. *Computers & Graphics*, 24, 333-341.
- Soomere, T., Delpeche, N., Viikmäe, B., Quak, E., Meier, H. E. M., Döös, K., 2011. Patterns of current-induced transport in the surface layer of the Gulf of Finland. *Boreal Environmental Research*, 16(Suppl. A), 49-63.
- Souza, J. M. A. C., de Boyer Montégut, C. and Le Traon, P. Y., 2011. Comparison between three implementations of automatic identification algorithms for the quantification and characterization of mesoscale eddies in the South Atlantic Ocean. *Ocean Science*, 7, 317-334.
- Weiss, J., 1991. The dynamics of enstrophy transfer in two-dimensional hydrodynamics. *Physica D*, 48, 273-294.

Paper E

Soomere T., Berezovski M., Quak E. and **Viikmäe B.** 2011. Modelling environmentally friendly fairways using Lagrangian trajectories: a case study for the Gulf of Finland, the Baltic Sea. *Ocean Dynamics*, 61(10), 1669–1680.

Modelling environmentally friendly fairways using Lagrangian trajectories: a case study for the Gulf of Finland, the Baltic Sea

Tarmo Soomere · Mihhail Berezovski · Ewald Quak · Bert Viikmäe

Received: 1 October 2010 / Accepted: 10 May 2011 / Published online: 31 May 2011
© Springer-Verlag 2011

Abstract We address possibilities of minimising environmental risks using statistical features of current-driven propagation of adverse impacts to the coast. The recently introduced method for finding the optimum locations of potentially dangerous activities (Soomere et al. in Proc Estonian Acad Sci 59:156–165, 2010) is expanded towards accounting for the spatial distributions of probabilities and times for reaching the coast for passively advecting particles released in different sea areas. These distributions are calculated using large sets of Lagrangian trajectories found from Eulerian velocity fields provided by the Rossby Centre Ocean Model with a horizontal resolution of 2 nautical miles for 1987–1991. The test area is the Gulf of Finland in the northeastern Baltic Sea. The potential gain using the optimum fairways from the Baltic Proper to the eastern part of the gulf is an up to 44% decrease in the probability of coastal pollution and a similar increase in the average time for reaching the coast. The optimum fairways are mostly located to the north of the gulf axis (by 2–8 km on average) and meander substantially in some sections. The robustness of this approach is quantified as the typical root mean square deviation (6–16 km) between the optimum fairways specified from different criteria. Drastic

variations in the width of the ‘corridors’ for almost optimal fairways (2–30 km for the average width of 15 km) signifies that the sensitivity of the results with respect to small changes in the environmental criteria largely varies in different parts of the gulf.

Keywords Risk modelling · Lagrangian transport · Statistics of currents · Baltic Sea · Pollution transport · Ship routing

1 Introduction

Most of the modelling efforts addressing the transport of adverse impacts (e.g. oil spill) focus on the solution of the direct problem of propagation of substances in the marine environment (e.g. to assist the countermeasures after an actual oil spill in a specific location). There are very few examples of models targeted at the preventive reduction of environmental risks, aiming at an optimisation of the location of potentially dangerous activities (e.g. ship traffic) so that the consequences of the resulting unfortunate event would be minimal once it indeed occurred.

A precondition for the use of such a way of thinking is the heterogeneity of the relevant physical or ecological fields. A recent solution of this kind is the relocation of the fairway entering the harbour in Boston (Massachusetts, USA) in order to minimise the probability of collisions of ship traffic with globally endangered right whales (Stokstad 2009). This preventive action is based on the existence of an area which is only infrequently visited by whales and thus offers a clear decrease in the probability for an unfortunate collision.

In the case of a release of, for example, oil pollution from ships, the situation is far more complicated, with three

Responsible Editor: Herman Gerritsen

Based on the presentation “*The Use of Lagrangian Trajectories for Minimization of the Risk of Coastal Pollution*” to the 15th Biennial Workshop of Joint Numerical Sea Modelling Group (JONSMOD).

This article is part of the Topical Collection on *Joint Numerical Sea Modelling Group Workshop 2010*

T. Soomere (✉) · M. Berezovski · E. Quak · B. Viikmäe
Institute of Cybernetics at Tallinn University of Technology,
Akadeemia tee 21,
12618 Tallinn, Estonia
e-mail: soomere@cs.ioc.ee

factors jointly governing the drift: currents, wind and waves. In the absence of currents, the probability of a vulnerable area (such as a spawning or nursing area) being affected obviously is roughly inversely proportional to the downwind/downwave distance of this area from the pollution release site. The area associated with the lowest risk is thus as far ‘upwind/upwave’ from the vulnerable location as possible. Therefore, we concentrate in our work on the remaining factor, i.e. we investigate the contribution of current-induced transport to the propagation of adverse impacts.

The instantaneous field of currents has a highly complicated structure even if the wind is practically stationary. Often, the resulting transport is even in antiphase with wave- and wind-induced transport (e.g. Andrejev et al. 2004a; Gästgifvars et al. 2006). The forecast of current-induced transport of drifters (and, consequently, an oil spill) is therefore much less reliable (Vandenbulcke et al. 2009). Although some trajectories of water particles frequently are extremely complicated (Fig. 1), still they are almost never completely random. Even if the underlying mesoscale dynamics has a timescale of only a few days, there exist current patterns that persist for weeks (Andrejev et al. 2004a, b; Soomere et al. 2011). These patterns make the probability of transport of various substances from different sea areas to specific vulnerable regions highly variable. The

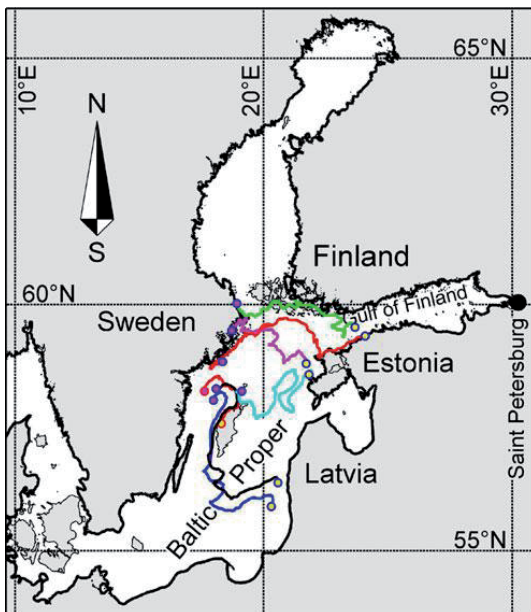


Fig. 1 Location scheme of the Baltic Sea and the Gulf of Finland. Magenta circles show the starting points and yellow circles the end points of 60 days of propagation of water particles calculated using the RCO model data and TRACMASS code

key idea for a substantial decrease in remote environmental risks (e.g. ship-caused pollution that can affect areas far from the accident site) exploited here is a smart use of such current patterns to minimise the consequences of potential accidents (e.g. by routing ship traffic through specific areas and avoiding others: Soomere and Quak 2007; Soomere et al. 2010).

In this article, we are using the Gulf of Finland, an elongated basin in the Baltic Sea (Fig. 1), for a case study, motivated by two aspects. On one hand, the concentration of ship traffic (including tankers of various kinds) is exceptionally high in this water body (HELCOM 2009). Therefore, there exists a high probability that various adverse impacts may be released along the shipping route, whereas consequences of major oil pollution could be devastating for this particularly sensitive sea area (Kachel 2008). On the other hand, there exist reliable and thoroughly validated ocean models for this region (Myrberg et al. 2010) that is known to host numerous semi-persistent patterns of both surface and subsurface currents (Andrejev et al. 2004a, b; Soomere et al. 2010).

The approach taken obviously depends on the definition of the vulnerable areas and/or the ‘cost’ of reaching them. The simplest example, to some extent mimicking the importance of coastal areas in the marine ecosystem, consists in setting the complete nearshore as the vulnerable area (Soomere and Quak 2007). We also restrict our attention to the problem of minimising the probability of coastal pollution by oil released from ship traffic.

The problem of the identification of favourable regions (called areas of reduced risk), from which the propagation of adverse impacts to vulnerable areas is unlikely, presumes the inverse tracking of pollution propagation. A straightforward solution for this question is not possible and no universal solution method exists. A feasible way towards approximate solutions consists in the statistical analysis of a large pool of particular solutions to the relevant direct problem of current-driven transport.

There are several ways to present the results of such analysis in terms of 2D distributions (‘maps’) characterising various aspects of the potential of vulnerable regions being hit by adverse impacts released into particular sea points. For elongated sea areas (such as the Gulf of Finland), it is rational to search for the line (called the *equiprobability line*) such that for each point on this line, it is equally probable that the spill reaches one coastline or the opposite one (Soomere et al. 2010). It is heuristically clear that the location of the equiprobability line is largely determined by local features of current-driven transport. Therefore, this line generally does not provide a global optimum for environmental risks and there is an obvious need to introduce more elaborated options that allow minimising the probability for hit of any coastal section. An approx-

imate solution for the location of the environmentally *optimum fairway* corresponding to the global optimum in terms of probabilities of coastal hit is to route the ships along the ‘troughs’ of the 2D map of these probabilities (Andrejev et al. 2011). Alternatively, it is possible to use the ‘crests’ of similar maps for the average time elapsed from the release of an impact into a particular point until it reaches a vulnerable spot (Andrejev et al. 2011). In our further presentation, this time is called (*particle age*). A few examples of such maps are presented in Section 3.

To a first approximation, the usefulness of the entire approach can be characterised in terms of the deviation of the optimum fairway from the location of the centreline of the basin (or, alternatively, from the typically used sailing lines). Even if such a deviation is small (either in terms of bias or root mean square deviation), the patterns of gradients of the underlying maps may provide useful information about how sensitive is the particular environment with respect to variations in the fairway.

The approach in use is based on a subsequent application of several techniques, each of which contains a number of parameters that may potentially affect the resulting 2D maps and the optimum fairways. This issue is evident already in the early analysis (Soomere et al. 2010) where the equiprobability lines calculated using slightly different sets of trajectories showed clear differences. Andrejev et al. (2011) demonstrate that there is a strong dependence of the optimum fairways on the resolution of the ocean model. Also, the strong seasonal variation of transport patterns (calculated by Soomere et al. 2011 using a method similar to the one employed in the current paper) suggests that seasonally optimum fairways may be drastically different for windy and calm seasons. There seem to exist, however, a limit for such variability. Andrejev et al. (2011) show that the basic properties of the fields of probability and particle age reach values close to their asymptotic values within about 3 years for a selection of ocean model resolutions, starting from the one used in this paper (2 nautical miles) down to 0.5 miles. This property suggests that the locations for optimum fairways defined over different time intervals with a duration of longer than 5 years insignificantly differ.

In this paper, we address two key questions related to the potential variability of the optimum fairways, namely concerning the *robustness* of this approach and the *stability* of the optimal fairway calculated using four different methods under otherwise equivalent conditions. By ‘robustness’, we refer to the issue that the computed maps inevitably contain some noise and that the resulting lines are normally not straight and may substantially differ when based on different criteria used in building the maps. Therefore, following such lines exactly is not always a good solution, and ships sailing in areas with heavy traffic frequently need some freedom for manoeu-

ring, anyway. This leads to the issue of the ‘stability’ of the optimum in the sense that it is important to estimate how sensitive the environmental risks are in relation to small variations in the ships’ routes.

Concerning the first question, we make an attempt to quantify the uncertainties of the discussed method for the estimation of the optimal fairway. In order to do this, we use the same basic set of cost function, underlying hydrodynamic model, forcing conditions and particle tracking scheme, but consider four different ways for the specification of the relevant curve. They differ from each other in the definition of the gain and, to a lesser extent, by the pool of test particles used in the simulations. The resulting variations implicitly characterise the intrinsic uncertainties (and thus robustness) of the entire approach.

The other question investigated is the sensitivity of the resulting fairway location with respect to small variations away from the theoretical optimum. This issue is studied by means of calculating a ‘corridor’ surrounding the optimum fairway under the condition that the probability for an unfortunate event (or the particle age) differs to some extent from the relevant minimum. The resulting width of the corridor together with the values for gradients for the underlying fields characterise the degree of freedom for captains and, equivalently, for the decision making.

2 Modelling environment

The procedure of specification of the optimum fairway depicted in (Soomere et al. 2010) and used below contains the following steps. The initial component is a 3D ocean model that produces Eulerian velocity fields. Its output is used to compute Lagrangian trajectories of a large number of water (and pollution) particles released at different locations and at different time instants. The trajectories are then analysed with respect to a given cost function and/or problem setup. The optimum locations for fairways are found as local or global minima of the resulting cost function. Alternatively, a compromise could be sought, for example, a sailing line that provides equidistribution of costs or risks.

Each of these steps has been extensively documented in the international literature. An early attempt to use the entire procedure using a reasonable amount of computation resources and offering a simple example of an approximate solution to the relevant inverse problem—the equiprobability line—is described in Soomere et al. (2010). The new development here is the comparative analysis of the resulting optimum locations for the fairway based on different criteria (minimum probability, maximum particle age, equidistribution of probability) and establishing several

interesting properties of the relevant 2D distributions and locations for almost optimum fairways.

In this paper, we use 3D current velocity fields calculated using the Rossby Centre (Swedish Meteorological and Hydrological Institute) ocean circulation model (RCO) for the entire Baltic Sea. This primitive equation circulation model uses 41 vertical levels in the z -coordinate and has a horizontal resolution of 2×2 nautical miles (nm), which is generally sufficient to resolve most of the mesoscale dynamics in the open part of the Baltic Sea. As the typical values of the Rossby radius in the Gulf of Finland are 2–4 km (Alenius et al. 2003), this implementation of the RCO model is barely eddy-permitting in the Gulf of Finland (cf. Albretsen and Røed 2010). The model is forced with 10-m wind (adjusted using simulated gustiness), 2-m air temperature, 2-m specific humidity, precipitation, total cloudiness and sea level pressure fields from a regionalization of the ERA-40 reanalysis over Europe using a regional atmosphere model with a horizontal resolution of 25 km during 1961–2007 (Samuelsson et al. 2011). For further details of the model setup and an extensive validation of the model output, we refer the reader to Meier (2001, 2007) and Meier et al. (2003).

In order to simplify the physical interpretation and the analysis below, we only use the horizontal velocities in the uppermost layer with a thickness of 3 m. The entire setup is therefore suitable for tracking particles that are locked in the surface layer, for example, lost containers or other items that are slightly lighter than water. In order to demonstrate the basic features of the proposed approach, we also ignore the changes that occur to the oil pollution in the course of time in marine environment and associate its path with the one valid for passively transported particles. Although the model time step is 150 s for the baroclinic and 15 s for the barotropic time step, the output is stored once in 6 h to keep the size of output information at a reasonable level. An overview of the implementation of its output for the use in our approach is described in (Soomere et al. 2010).

The second key step is the calculation of Lagrangian trajectories of water particles. We employ a scheme in which the modelling efforts of ocean hydrodynamics are separated from the trajectory calculation as in Soomere et al. (2010). The TRACMASS model (Blanke and Raynard 1997; Döös 1995; de Vries and Döös 2001) is used to calculate the trajectories from the precomputed RCO velocity fields based on a linear interpolation of these fields in space and time at each point of a particular grid cell. The basic requirements (such as the number of particles used, the length of time window, the definition of the neashore, etc.) for the implementation of the TRACMASS code have been established by Viikmäe et al. (2010) for a selection of applications.

The resulting trajectories evidently depend to some extent on the temporal resolution of both the circulation data and the trajectory calculation scheme. In extreme cases, the resulting differences may lead to a really large divergence of initially close trajectories. The spreading of the trajectories calculated using TRACMASS is usually much smaller than the spreading of real drifters owing to the effect of subgrid turbulence (Jönsson et al. 2004; Engqvist et al. 2006; Döös and Engqvist 2007; Döös et al. 2008), and initially close trajectories have an overly tendency to stay close. On one hand, this feature suggests that the potential impact of the particular time step of saving the circulation data or that of the temporal resolution in trajectory reconstruction is minor on the statistics of a large number of trajectories. On the other hand, there is a clear physical reason for the relatively small spreading of calculated trajectories, namely, the version of TRACMASS used in the current work ignores local spreading owing to various subgrid-scale effects such as diffusive processes, small-scale turbulence or local vertical motions of water particles. An attempt to estimate the magnitude of the natural spreading in the test area has been undertaken by Andrejev et al. (2010). They introduced a very strong level of subgrid-scale motions (up to 50% of the simulated velocities) and also accounted for the mostly rotational character of the motions in the Gulf of Finland. The resulting average spreading rate for the period from December 1990 to November 1991 was about 176 m/day (about 2 mm/s). Consequently, it takes, on average, more than 20 days for two initially closely located particles to drift into different grid cells for the 2-nm horizontal resolution of the RCO model. This suggests that for the given length of calculations (10 days in Soomere et al. 2010 and 20 days in the current study), the ignoring of subgrid-scale processes may modify a part of trajectories, but the majority of the simulated trajectories apparently will remain at a distance of less than one grid step from their position according to more realistic calculations. Therefore, it is apparently reasonable to assume that for the particular horizontal resolution of the ocean model and length of trajectories, the ignoring of subgrid spreading does not significantly affect the resulting 2D fields. Doing so is, however, a major simplification that might not be entirely justified in applications because of the overall sensitivity of the optimum location on several details of the entire approach, such as the resolution of the underlying ocean model (Andrejev et al. 2011).

The amount of trajectories to be analysed depends on the particular problem to solve. Usually, only the behaviour of the particles over a few days of propagation is important as the particles lose the connection with their initial location. In order to specify the properties of each release location, it therefore makes sense to calculate trajectories over suitable

time interval and repeat the release of particles after some time. This philosophy is used in several studies (Soomere et al. 2010, 2011; Viikmäe et al. 2010; Andrejev et al. 2011). The entire time period of interest is divided into time windows of duration, t_w . A desired number of particles is selected in the sea at the beginning of the study period. Their motion is calculated over the time window t_w and saved for further analysis. The calculation is then repeated with the same configuration of the tracers, but with a certain time lag. The subsequent trajectories are thus not entirely independent, but this feature is apparently only of minor importance.

In all calculations below, we assume that a coastal hit occurs when the particle in question comes to the distance of three grid steps (about 11 km) from the mainland coast (Viikmäe et al. 2010). In order to make our results directly comparable with those obtained in earlier studies (Andrejev et al. 2004a, b; Soomere et al. 2010, 2011), we perform trajectory simulations for 1987–1991 with the use of time windows of equal length shifted with respect to each other by 1 day. Differently from the earlier studies, we use 20-day-long time windows.

3 Analysis of trajectories

The third essential step consists of the analysis of the resulting pool of trajectories. The particular methods used in this part substantially depend on the nature of the underlying problem to be tackled. For example, in Soomere et al. (2011), the focus was on finding semi-persistent patterns in the Gulf of Finland, whilst Soomere et al. (2010) studied the geometric location of the equiprobability line, which—as already discussed in Section 1—can be interpreted as an optimum fairway based on the criterion that the probability of pollution released on the fairway hitting the coastline must be equal for both the northern and the southern coasts of the Gulf of Finland.

Soomere et al. (2010) addressed this problem using two methods that only differed from each other by the number and location of the particles used to characterise the properties of sea points as release locations of an adverse impact. Method I (called *the direct method*): In this simpler version, four particles were released in each grid cell. For each cell, a counter related to the probability of pollution hitting either of the coastlines was set to ± 1 , when at least three out of the four particles reached one and the same coastline (-1 for the northern and $+1$ for the southern coast) within the time window; otherwise, the counter was set to 0. The relevant average quantity \hat{p} : $-1 \leq \hat{p} \leq 1$ for each cell (Fig. 2) was calculated over a large number of the counter values reflecting simulations covering 5 years, 1987–1991, which were divided into partially overlapping

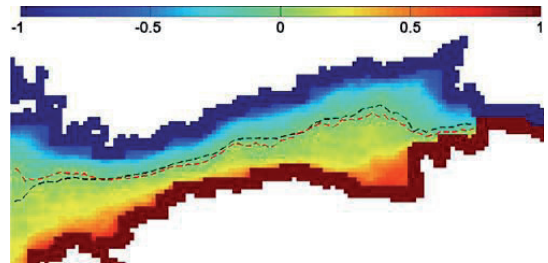


Fig. 2 Distribution characterising the probability of hitting the northern and southern coasts using the smoothing method II and $t_w=20$ days. Black and red lines indicate the equiprobability lines for methods I and II, respectively

time windows of equal length $t_w=20$ days and shifted in time by 1 day. Method II (called *the smoothing method*): In this version, it was counted whether or not five or more particles released into the centres of the cell of interest and into the cluster of the eight cells surrounding it reached one and the same coast.

In our calculations with methods I and II, we mostly use the same parameters as Soomere et al. (2010), with one exception: The separation point of the coast into the northern and southern parts is now in Neva Bay (whilst in Soomere et al. 2010 it was set to the border between Estonia and Russia in Narva Bay at $28^{\circ}2' E$, $59^{\circ}27.5' N$).

Method III (*the probability method*; Andrejev et al. 2011) employs a different approach in which there is no separation of the coastline into two parts. The counter for each particle and simulation is given a value of 1 or 0, simply reflecting whether or not this particle reaches any section of the coast within the given time window. As for the above methods, for each cell, the average values of the counter for all particles in this cell and for a large number of simulations over subsequent 20-day time windows is determined (Fig. 3). Method IV (*the particle age method*; Andrejev et al. 2011) calculates, alternatively, the ‘age’ of each inserted particle, defined as the time elapsed from the instant of the release until the particle reaches the coast somewhere. As above, the average value over a large number of simulations is taken, this time over the particle age (Fig. 4).

In our calculations with the use of methods III and IV (Figs. 3 and 4), one particle is released into the centre of each sea grid cell (3,131 cells altogether in the area shown in Figs. 3, 4 and 5). As the RCO model grid covers the entire Baltic Sea, the dynamics of the entire sea is fully accounted for; however, as no particles were released into the area outside of the Gulf of Finland, the probability of hitting the coast by adverse impacts released in the open Baltic Sea is ignored. Doing so insignificantly affects the

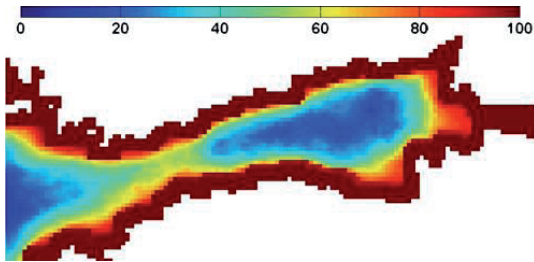


Fig. 3 Probabilities (%) of hitting the coast for the years 1987–1991 calculated with the time window of 20 days

resulting field of probabilities as most particles propagating out of the Gulf of Finland do not hit a coast anyway. The field of particle age, however, obviously depends on the particular way of the treatment of particles that leave the gulf. We use two assumptions in order to highlight this issue. Firstly, the age counter is stopped when the particle leaves the gulf for the first time and its possible reentering is ignored (method IVa). This assumption leads to an obvious underestimation of particle age at the entrance of the gulf because a part of particles apparently will drift a long time in the open sea of the Baltic Proper. Alternatively, particles leaving the gulf are associated with the longest possible age (method IVb). This assumption apparently overestimates particle age for these regions of the gulf that encounter intense water exchange with the Baltic Proper. Interestingly, Fig. 5 suggests that these choices may lead to quite different locations for the optimum fairway not only at the entrance to the Gulf of Finland but also in the entire gulf.

The values of all the quantities obviously depend on some extent on the length of the time window. Whilst modifications caused by an increase in t_w to the probability and the quantity \hat{p} apparently are minor and basically lead to a decrease in the uncertainty in their estimates, the average age may substantially increase with the increase in t_w . For this reason, the largest values of particle age

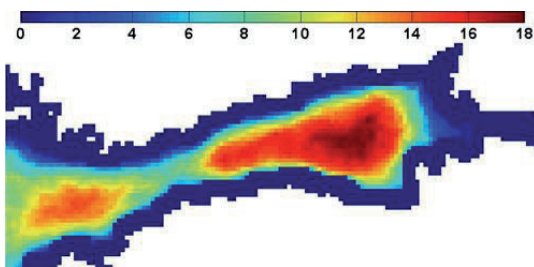


Fig. 4 Particle age (days) for the years 1987–1991 calculated with the time window of 20 days

considerably exceed those calculated in Andrejev et al. (2011) using $t_w=10$ days. Note that although there exist a few islands with a size up to 10 km in the eastern Gulf of Finland, their nearshore is ignored in the calculations below and only hits to the mainland coasts are accounted for. The used set of trajectories led to sensible values of all the 2D fields in question in the area between latitudes $21^{\circ}41'$ E and $28^{\circ}57'$ E covered by 110 grid cells.

4 Optimum fairway

The final step of the whole procedure—regardless of which of the four methods is used—consists in specifying the location of the optimum fairway for avoiding to hit the coastline based on the previously determined maps of the quantity \hat{p} , probabilities or particle age. Note again that any other convenient measure of the environmental or economic risk can be used in this setup.

For a sea area of simple, elongated shape possessing homogenous and isotropic current fields, the resulting maps, ideally, provide an elongated ‘trough’ of low values for probabilities or, equivalently, a similar ‘crest’ of particle age. The optimum fairway then goes along this trough or crest. For regions with complicated geometry, strongly anisotropic or heterogeneous transport patterns, the shape of the relevant distributions may be quite complicated (for example, there may be several minima in the field) and finding the optimum fairway may need some other conditions (Andrejev et al. 2011).

Figures 2, 3 and 4 suggest that the described method (including ignoring the islands) leads to distributions that generally have one local extremum of the probability and age (and also one zero-crossing point of the quantity \hat{p}) for all cross-sections of the Gulf of Finland along latitudes except for the entrance and for the easternmost part of the gulf. This property makes it possible to use a simple algorithm for finding the optimum fairway designed as follows. The underlying data for Figs. 2, 3 and 4 were first corrected manually in order to adjust a few clearly erroneous values for several bays deeply cut into the mainland. In the model resolution, the currents in these areas were very small and almost no particle propagation occurred. The relevant values were set to the extreme values of the quantities in question. This correction has no impact on the behaviour of the relevant fields in the vicinity of the optimum fairways.

The latitude for the optimum fairway was then found from the analysis of the cross-section of the relevant field along each longitude of the grid cells (Fig. 5). The impact of small-scale noise in the underlying fields in some parts of the bay (especially in the eastern part where the north–south slope in these fields was small) was suppressed by

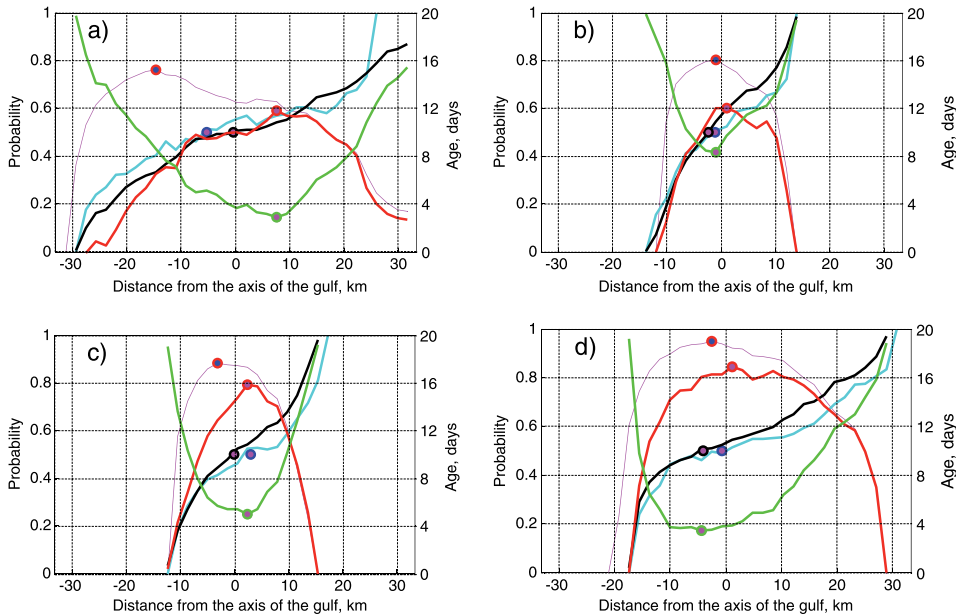


Fig. 5 Examples of cross-sections of probabilities for coastal hits (*green*), particle age (method IVa, *red*; method IVb, *magenta*) and for the quantity characterising the probability of hitting the northern and southern coasts (method I, *black*; method II, *cyan*; both shown as $(\hat{p} + 1)/2$, where $\hat{p} \approx 1$ and $\hat{p} \approx -1$ mean a high probability of

hitting the southern and the northern coasts, respectively): for the gulf entrance (**a**), western narrow part (**b**), middle of the gulf (**c**) and for the wider eastern part of the gulf (**d**). *Circles* indicate the location of the optimum fairway. The location of cross-sections is shown in Fig. 6

means of smoothing the cross-section over five neighbouring grid points.

The optimum fairway (the equiprobability line) for methods I and II is located at the zero-crossing points of the relevant values \hat{p} characterising the probability of hitting the northern and southern coasts. These points are well defined in the relatively narrow parts of the gulf where the north–south gradient of the quantity \hat{p} is comparatively large (Fig. 5). The above-described smoothing of the cross-section also leads to a single clearly defined zero-crossing of \hat{p} for each longitude for both methods I and II. An estimate for the location of each zero-crossing was found using a linear approximation between the smoothed values of \hat{p} at two grid points surrounding the zero-crossing. The curves consisting of zero-crossing points were comparatively smooth, and no additional smoothing in the east–west direction was necessary.

For the fields of probabilities and particle age, the centre of the grid cell corresponding to the minimum or maximum value of the relevant smoothed cross-section was associated with the location of the optimum fairway at this longitude. Doing so led to reasonable locations for the fairway in all cases. As the obtained curves were confined to discrete values of the centres of grid cells and sometimes contained abrupt shifts by two to three cells to the south or north, the

curves were finally smoothed over five neighbouring values in the east–west direction.

The optimum fairways are located somewhat asymmetrically, most of them to the north of the centreline of the gulf (except the one corresponding to method IVa that is located by almost 4 km to the south; Table 1). Note that the centreline, also called gulf axis in what follows, is determined based on sea points of the 2-nm grid of the

Table 1 Bias (the mean deviation of two lines, below the diagonal, kilometres) and root mean square deviation (above the diagonal, kilometres) of the optimum fairways and the centreline of the Gulf of Finland from each other

	Centreline	Method I	Method II	Probability	Age (IVa)	Age (IVb)
Centreline	X	8.76	10.1	5.45	5.96	11.1
Method I	3.84	X	6.27	7.11	11.0	11.75
Method II	2.22	-1.62	X	10.8	12.9	10.8
Probability	2.82	-1.02	0.6	X	7.24	11.9
Age (IVa)	-3.90	-6.74	-6.12	-7.72	X	16.3
Age (IVb)	7.76	3.92	5.54	4.94	11.66	X

Positive values of the bias mean that the line indicated in the leftmost column is located, on average, to the north of the line indicated in the uppermost row

RCO model and thus does not necessarily exactly follow the geographical centreline of the gulf. Their overall bias from the gulf axis is mostly 2–4 km, and only for method IVb is it almost 8 km. This distribution is consistent with the slight prevalence of surface transport to the south in this water body (Soomere et al. 2011) and apparently reflects the anisotropic nature of the Ekman transport in surface layer: As the predominant strong winds blow from the southwest, the Ekman transport to the south prevails in the open part of this water body and the particles released to the northern part of the gulf stay offshore for a long time. A certain contribution to this asymmetry may also stem from the presence of a relatively strong subsurface flow in the northern part of the gulf (Andrejev et al. 2004a, b).

Figures 5, 6 and 7 demonstrate that the different criteria for the optimum fairway may lead to considerable differences (up to 50 km at the entrance to the gulf) of the relevant locations of optimums. In general, all the lines are located in an immediate vicinity of the centreline of the gulf between latitudes 23°40' E and 26°20' E where they deviate from each other maximally by 10 km. Such a concentration of the optimum fairways apparently results from the narrowness of this part of the Gulf of Finland: Its narrowest cross-section contains only 15 grid cells (from which three nearshore cells at each coast are associated with coastal hits), and thus less than ten grid cells represent the offshore dynamics of trajectories. The properties of the underlying fields in this section (including relatively steep gradients in the north–south direction) evidently are mostly governed by the geometry of the sea area.

Much larger deviations of the optimum fairways from the axis of the Gulf of Finland occur in wider parts of this water body where the north–south gradients of the underlying fields are considerably smaller (Figs. 6 and 7). Several relatively extensive meanders in these lines are located at the gulf entrance and in the vicinity of the Island of Gogland (Suursaari). The resolution in use is too low in order to decide whether the meanders near Gogland are caused by the presence of islands or result from the general structure of the current-driven transport in this area. The

systematic deviation of the optimum fairways to the north around 27°20' E and a smaller deviation to the south around 25°30' E may be associated with a slow anticyclonic gyre that exists in this part of the gulf for the years in question (Soomere et al. 2011). The large deviation to the south around 28° E evidently reflects the predominant transport to the north in this area caused jointly by the voluminous runoff of the River Neva and general cyclonic circulation pattern in the Gulf of Finland (Andrejev et al. 2004a).

The spreading of the estimates of the location of the optimum fairway obtained using different methods (Fig. 7 and Table 1) to some extent characterises the intrinsic uncertainty (and therefore also robustness) of this approach. The optimum fairways based on the probabilities for coastal hit (method III) and one version of the particle age method (method IVb) largely follow each other except in the gulf entrance area. The line corresponding to method IVb is mostly located substantially to the north of the centreline of the Gulf of Finland and approaches this line in very limited sections (Figs. 6 and 7 and Table 1). The maximum deviations between these lines are fairly small, normally below 4 km even in the relatively wide eastern part of the gulf. In the central and western parts, these lines (as well as the equiprobability line based on method I) follow each other very closely, and the deviations are below the resolution of the circulation model. A reasonably large root mean square difference between these lines (11.9 km, Table 1) is owing to their behaviour at the gulf entrance where they deviate up to 40 km from each other.

The large systematic deviation of optimum fairways corresponding to different setups of the particle age method (methods IVa and IVb) indicates that surface particles in the northern part of the Gulf of Finland have a large chance to leave the gulf within 20 days. Somewhat surprisingly, the impact of different setups of the time counter is clearly present in the entire gulf. This feature may be associated with the overall cyclonic circulation in this water body that favours the transport of water masses towards the Baltic Proper along the northern coast of the gulf. This example also vividly demonstrates how sensitive the resulting

Fig. 6 Location of the optimum fairways based on methods I–IV. Colour code is the same as for Fig. 5. Dotted black line indicates the geometrical centreline of the gulf for the 2-nm grid and vertical lines—the cross-sections in Fig. 5. Note that the location of smoothed optimum fairways (methods III and IV) may slightly deviate from those indicated in Fig. 5

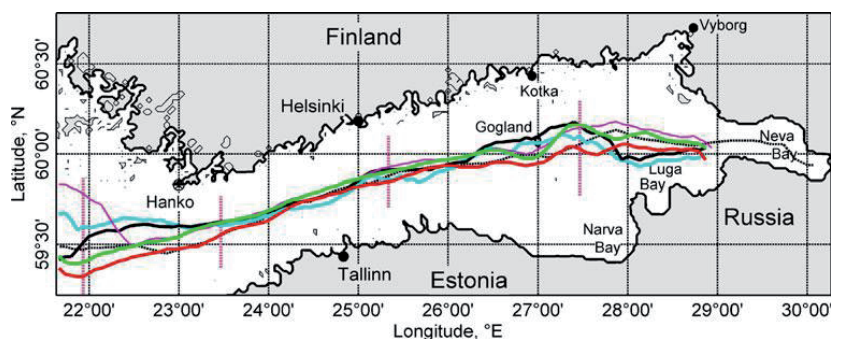
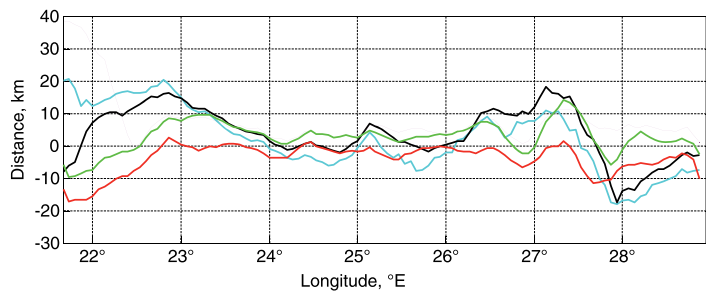


Fig. 7 Deviation of the optimum fairways based on methods I–IV from the gulf axis. Colour code is the same as for Fig. 5. The positive direction is to the north



optimum fairway may be with respect to seemingly small variations in the method.

The equiprobability lines estimated using the direct and the smoothing methods (I and II) are located relatively close to each other: Their bias is only 1.6 km and the root mean square difference is 6.3 km (Table 1 and Fig. 7). This is not unexpected because they are calculated using a similar concept and with only a slightly different set of trajectories. Note that these lines differ considerably from similar lines described in Soomere et al. (2010) in the region to the north of Narva Bay. The reason is that the separation point of the northern and southern coasts was set to the border between Estonia and Russia in (Soomere et al. 2010). Consequently, a part of the geographic southern coast of the gulf (from Narva Bay to the interior of Neva Bay) was associated with the northern coast. This choice affects the fields of \hat{p} in the entire eastern part of the gulf because the resulting optimum fairways should basically head to the separation point. Note also that all equiprobability lines (both here and in Soomere et al. 2010) contain a characteristic deviation to the south in the vicinity of the Tallinn–Helsinki line. This feature apparently is connected with the specific structure of the numerically reproduced long-term surface dynamics in this region (Soomere et al. 2011).

5 Sensitivity of the location of the optimum fairway

The resulting optimum fairways have quite different meanings in terms of the potential gain stemming from their use. For example, the use of the equiprobability line only divides equally the potential loss between the opposite coasts. The gain from the use of the line estimated from the distribution of the probability of coastal hits can be roughly evaluated in terms of the decrease in the overall probability of such a hit. A convenient measure is the ratio of this probability calculated over the points of the optimum fairway over the total average probability for the area in question. For the described modelling environment, the average probability for a coastal hit within 20 days is 0.62,

whereas the similar average value along the optimum fairway is 0.347. Therefore, the gain may, theoretically, reach 44% in terms of probabilities. In reality, the gain obviously will be smaller because coastal areas with large values of this probability are normally not used for ship traffic (Andrejev et al. 2011).

Similarly, the gain in terms of the average particle age (propagation time of the adverse impacts to vulnerable regions) can be roughly evaluated by means of comparison of the relevant total average over all the sea area (8.7 days) with the similar average over the optimum fairway (12.4 days) and is up to 42.5%. As both these values are calculated using 20-day-long time windows, they are considerably larger than the analogous values in Andrejev et al. (2011) where $t_w=10$ days is used. The potential increase in the propagation time (equivalently, the time available for combating the adverse impact) is still remarkable, about 3.7 days.

A convenient measure of the sensitivity of the resulting optimum fairway with respect to small variations in the actual sailing line is the width of the ‘corridor’ in which the probability for a coastal hit (or the particle age) is allowed to vary to some extent compared with the theoretical maximum. The width of such corridors also provides information about the flexibility of shipping and the degree of freedom for captains who try to keep the environmental risks close to the theoretical minimum. The variations in the width of such corridors may highlight sea regions with different nature of internal dynamics in terms of current-induced transport.

As an example, Figs. 8 and 9 provide the relevant corridors of the average width of 15 km (8.1 nautical miles). This width corresponds to the increase in the probability of coastal hits by up to 0.0293 and to a decrease in the particle age by up to 0.54136 days compared with the exact extremum. The procedure for the determination and smoothing of the relevant border lines to the south and north of the optimum fairways is identical to the one used for the determination of zero-crossings in the cross-sections of the field \hat{p} characterising the probability of hitting the northern and southern coasts. First, the two crossing points

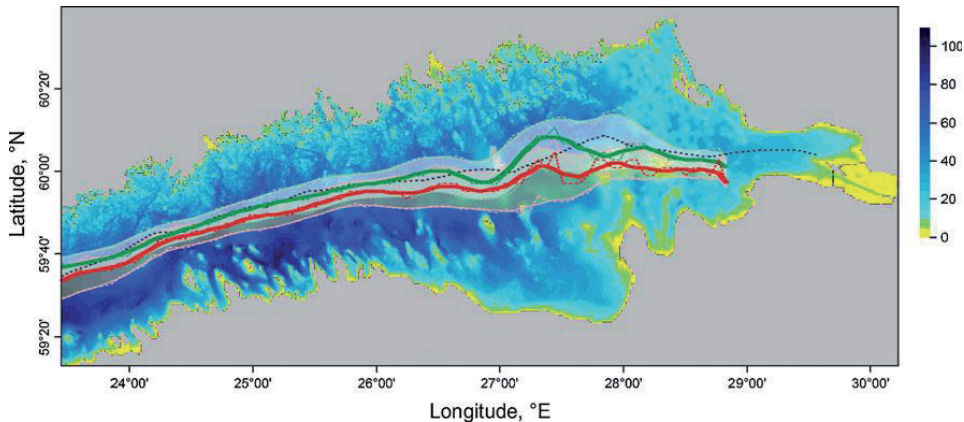


Fig. 8 Optimum fairway based on probabilities for coastal hit (green) and particle age (red, method IVa) and the relevant ‘corridors’ with the average width of 15 km. The dotted line shows the geometrical

centreline of the gulf. The background colour scale shows water depth (metres) in the resolution of 0.25–0.5 nm (Andrejev et al. 2010)

of the probability value $p = p_{\min} + 0.0293$ (p_{\min} is the minimum probability for the particular longitude) are found separately for each latitude and then the relevant curve is smoothed over five neighbouring points. An analogous scheme is used for particle age.

The width of the resulting corridors varies significantly in the east–west direction. They are quite wide at the entrance to the Gulf of Finland (not shown in Fig. 8), very narrow in the Tallinn–Helsinki region, widen substantially in the eastern wide part of the gulf in the vicinity of Gogland and become very narrow again in the area to the north of Luga Bay before entering Neva Bay. The width of the corridors varies remarkably: The minimum and maximum widths are 7.35/9.6 and 29.1/42 km, respectively, for methods III and IVa.

Similar corridors of the same width of 15 km for the equiprobability lines are defined as the sea area between the

lines corresponding to a certain variation in the balance between the probabilities of pollution transport to the opposite coasts. Their width varies even more drastically (Fig. 9). The relevant fields of \hat{p} have a very steep north–south slopes near the zero-crossing in the central part of the bay. For example, the relevant corridor estimated using the direct method (method I) and corresponding to the changes of the threshold value by $\pm 11.189\%$ from the maximum values (± 1) has a minimum width of only 2.1 km (that is, only 20–25% of that for the corridors corresponding to methods III and IV). The situation is substantially different in the eastern and western parts of the gulf where the north–south slope in the underlying field is moderate. The resulting corridor is up to 48.6 km wide, whereas the equiprobability line is located quite asymmetrically, near the northern border. The corridor is also quite wide, up to 26.2 km in the area near Gogland, and narrows considerably at the entrance to Neva Bay.

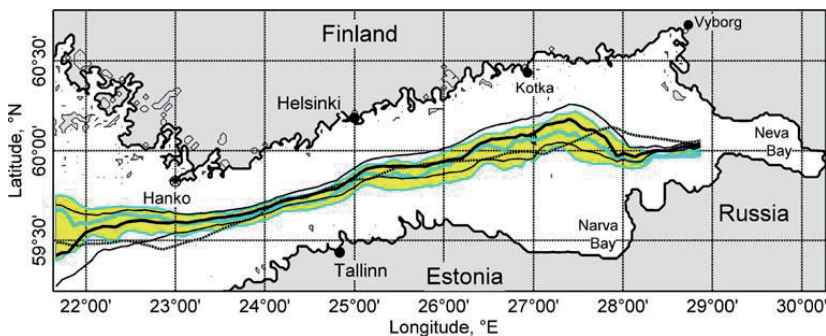


Fig. 9 Sea area in which the quantity characterising the probability of hitting the northern and southern coasts, found using the direct method I, varies from -0.11189 to $+0.11189$ (thin cyan lines surrounding the yellow area) and in which the similar quantity found using the

smoothing method II varies from -0.09542 to $+0.09542$ (thin black lines). Solid cyan and black lines indicate the relevant equiprobability lines and the dotted line the centreline of the gulf

As expected, a similar appearance of the resulting corridor becomes evident in the case of the smoothing method (method II, Fig. 9). The relevant corridor corresponds to an almost equal the change to the threshold value ($\pm 9.542\%$ from the maximum), but is considerably narrower (down to 1.19 km) in the vicinity of the Tallinn–Helsinki line. As above, the corridor reaches a width of over 28 km near Gogland and 37.6 at the entrance to the Gulf of Finland. Both the corridors estimated using methods I and II largely follow the centreline in the narrowest part of the gulf, but deviate considerably to the north of it in the vicinity of Gogland. Both the optimum fairways and corridors almost coincide near Hanko where they are located up to 10 km to the north from the centreline. In the entrance area of the Gulf of Finland, the lines and corridors for methods I and II deviate substantially.

6 Discussion and conclusions

The proposed approach of minimising environmental risks by means of approximately solving the relevant inverse problem basically binds three standard applications—long-term numerical simulations of Eulerian velocity fields, calculation of Lagrangian trajectories and statistical analysis of certain probabilities—into one entity. The connections between the single applications are such that the user may easily replace each component with a more elaborated one without the loss of generality.

The discussed exercise is performed in the conditions of the Gulf of Finland with the use of barely eddy-permitting model in quite a moderate resolution. On one hand, it highlights the potential of such multistep modelling system (based on a combination of 3D simulations of Eulerian ocean dynamics followed by extensive statistical analysis of large pools of Lagrangian particle trajectories) for preventive planning of maritime activities. On the other hand, it reveals several instructive features of its outcome and also the importance of the feasible choice of the target function.

The resulting optimum locations of the fairway (or, more generally, loci for any activities connected with potential coastal pollution), not surprisingly, substantially depend on the specific target. The solutions that rely on the condition of minimising the risk (or, equivalently, maximising the response time) mirror the anisotropic nature of surface currents (and especially specific features of current-induced transport of water to the Baltic Proper) in the study area (Andrejev et al. 2004a, b; Soomere et al. 2011). The basic suggestion—to shift the fairway away from the geometrical centreline of the gulf—follows the early suggestions targeted to minimise coastal pollution for the entire gulf based on qualitative arguments (Soomere and Quak 2007).

A much more important outcome of the study is that a largely meandering fairway may lead to a much more substantial decrease in environmental risks than a uniform shift.

The results also indicate that solutions targeted to the equidistribution of the costs (or responsibilities) between the neighbours on different coasts (methods I and II; Soomere et al. 2010) may correspond to clearly increased levels in the environmental risk compared with the overall minimum. Moreover, these solutions apparently are quite sensitive with respect to the particular division of the coast into sections.

The spreading of the optimum fairways in different sea areas characterises the applicability and robustness of the entire approach to some extent. An interesting, albeit not unexpected, feature is that all the lines in question almost coincide in the narrowest part of the gulf where the relevant distributions have a well-defined, narrow extremum (or zero-crossing) in the north–south direction. In such conditions, the approach will evidently result in a robust outcome that is only weakly sensitive with respect to the particular methods or parameters in use. In the wider parts of the gulf, the variations in the location of optimum fairways are much more substantial. Consequently, the particular location for an optimum fairway is relatively sensitive with respect to any kind of (numerical) noise and/or to changes in the parameters in use.

Another interesting feature is the extensive variation in the width of the corridors corresponding to small deviations from the optimum solution. This property (that is only weakly correlated with the width of the Gulf of Finland and that is the most pronounced for the equiprobability line) signifies that this water body may contain areas with quite different internal dynamics and current-driven transport properties. These areas can be separated based on the magnitude of cross-gulf gradients of the fields characterising the ‘ability’ of a particular sea area to serve as a source of coastal pollution. On one hand, the narrowest part of the gulf serves as an example of areas where a limited distance between the opposite coasts leads to a well-defined optimum (or zero-crossing) for the location of fairways. This situation apparently is typical for elongated sea areas. On the other hand, some other areas of the Gulf of Finland display quite small cross-sectional gradients of the underlying fields of probabilities and particle age. It may happen that even a large shift in the fairway location within such areas would insignificantly affect environmental risks. The proposed approach, therefore, may be used as a tool for identifying regions with such different internal properties for the use in maritime spatial planning.

Finally, we would like to emphasize that the particular implementation of the proposed approach is based on several simplifications, the validity of some of which are

not obvious. First of all, the approach only considers the impact of the field of surface currents on the location of the optimum fairway, whilst realistic applications have to account for the impact of wave- and wind-induced transport. Another major simplification that might not be entirely justified in both idealised models and practical applications is the neglecting of the potential impact of subgrid-scale processes that may considerably alter the statistics of trajectories especially for longer time intervals. The experience with the proposed approach has demonstrated the overall sensitivity of the optimum location of fairways on several details of the entire approach such as the resolution of the underlying ocean model (Andrejev et al. 2011). The sensitivity of the results on different choices of the constituents (in particular on the missing or ignored aspects of ocean dynamics such as subgrid turbulence) definitely merits more detailed attention and will be addressed in subsequent studies.

Acknowledgement This study was supported by the funding from the European Community's Seventh Framework Programme (FP/2007–2013) under grant agreement no. 217246 made with the joint Baltic Sea research and development programme BONUS. The BalticWay project attempts to identify the regions in the Baltic Sea that are associated with increased risk compared to other sea areas and to propose ways to reduce the risk of them being polluted by placing activities in other areas that may provide less risk. The research was also partially supported by the Marie Curie Reintegration Grant ESTSpline (PERG02-GA-2007-224819), the targeted financing by the Estonian Ministry of Education and Science (grants SF0140077s08 and SF0140007s14) and the Estonian Science Foundation (grant no. 7413). The contribution of Anders Anbo towards the application of the TRACMASS model in the Institute of Cybernetics and the help from Kristofer Döös during its use are gratefully acknowledged. We are also grateful to Anders Höglund (SMHI) who extracted and prepared the RCO model data.

References

- Albretsen J, Røed LP (2010) Decadal simulations of mesoscale structures in the northern North Sea/Skagerrak using two ocean models. *Ocean Dyn* 60:933–955
- Alenius P, Nekrasov A, Myrberg K (2003) The baroclinic Rossby-radius in the Gulf of Finland. *Cont Shelf Res* 23:563–573
- Andrejev O, Myrberg K, Alenius P, Lundberg PA (2004a) Mean circulation and water exchange in the Gulf of Finland—a study based on three-dimensional modelling. *Boreal Environ Res* 9:1–16
- Andrejev O, Myrberg K, Lundberg PA (2004b) Age and renewal time of water masses in a semi-enclosed basin—application to the Gulf of Finland. *Tellus* 56A:548–558
- Andrejev O, Sokolov A, Soomere T, Värvi R, Viikmäe B (2010) The use of high-resolution bathymetry for circulation modelling in the Gulf of Finland. *Estonian J Eng* 16:187–210
- Andrejev O, Soomere T, Sokolov A, Myrberg K (2011) The role of spatial resolution of a three-dimensional hydrodynamic model for marine transport risk assessment. *Oceanologia* 53:335–371
- Blanke B, Raynard S (1997) Kinematics of the Pacific Equatorial Undercurrent: an Eulerian and Lagrangian approach from GCM results. *J Phys Oceanogr* 27:1038–1053
- De Vries P, Döös K (2001) Calculating Lagrangian trajectories using time-dependent velocity fields. *J Atmos Oceanic Technol* 18:1092–1101
- Döös K (1995) Inter-ocean exchange of water masses. *J Geophys Res* 100:C13499–C13514
- Döös K, Engqvist A (2007) Assessment of water exchange between a discharge region and the open sea—a comparison of different methodological concepts. *Estuar Coast Shelf Sci* 74:585–597
- Döös K, Nycander J, Coward AC (2008) Lagrangian decomposition of the Deacon Cell. *J Geophys Res* 113:C07028
- Engqvist A, Döös K, Andrejev O (2006) Modeling water exchange and contaminant transport through a Baltic coastal region. *Ambio* 35:435–447
- Gästgifvars M, Lauri H, Sarkanen A-K, Myrberg K, Andrejev O, Ambjörn C (2006) Modelling surface drifting of buoys during a rapidly-moving weather front in the Gulf of Finland, Baltic Sea. *Estuar Coast Shelf Sci* 70:567–576
- Jönsson B, Lundberg P, Döös K (2004) Baltic sub-basin turnover times examined using the Rossby Centre Ocean Model. *Ambio* 23:257–260
- HELCOM (2009) Ensuring safe shipping in the Baltic (Stankiewicz M, Vlasov, N, eds.). Helsinki Commission, Helsinki, p 18
- Kachel MJ (2008) Particularly sensitive sea areas. *Hamburg Studies on Maritime Affairs*, 13, Springer, p 376
- Meier HEM (2001) On the parameterization of mixing in three-dimensional Baltic Sea models. *J Geophys Res* 106:C30997–C31016
- Meier HEM (2007) Modeling the pathways and ages of inflowing salt- and freshwater in the Baltic Sea. *Estuar Coast Shelf Sci* 74:610–627
- Meier HEM, Döscher R, Faxén T (2003) A multiprocessor coupled ice-ocean model for the Baltic Sea: application to salt inflow. *J Geophys Res* 108:C3273
- Myrberg K, Ryabchenko V, Isaev A, Vankevich R, Andrejev O, Bendtsen J, Erichsen A, Funkquist L, Inkala A, Neelov I, Rasmus K, Rodriguez Medina M, Raudsepp U, Passenko J, Söderkvist J, Sokolov A, Kuosa H, Anderson TR, Lehmann A, Skogen MD (2010) Validation of three-dimensional hydrodynamic models in the Gulf of Finland based on a statistical analysis of a six-model ensemble. *Boreal Environ Res* 15:453–479
- Samuelsson P, Jones CG, Willén U, Ullerstig A, Gollvik S, Hansson U, Jansson C, Kjellström E, Nikulin G, Wyser K (2011) The Rossby Centre Regional Climate Model RCA3: model description and performance. *Tellus* 63A(1):4–23. doi:10.1111/j.1600-0870.2010.00478.x
- Soomere T, Quak E (2007) On the potential of reducing coastal pollution by a proper choice of the fairway. *J Coast Res Special Issue* 50:678–682
- Soomere T, Viikmäe B, Delpeche N, Myrberg K (2010) Towards identification of areas of reduced risk in the Gulf of Finland, the Baltic Sea. *Proc Est Acad Sci* 59:156–165
- Soomere T, Delpeche N, Viikmäe B, Quak E, Meier HEM, Döös K (2011) Patterns of current-induced transport in the surface layer of the Gulf of Finland. *Boreal Environ Res* 16(Suppl A):49–63
- Stokstad E (2009) U.S. poised to adopt national ocean policy. *Science* 326:1618
- Vandenbulcke L, Beckers J-M, Lenartz F, Barth A, Poulain P-M, Aidonidis M, Meyrat J, Arduin F, Tonani M, Fratianni C, Torrisi L, Pallela D, Chiggato J, Tudor M, Book JW, Martin P, Peggion G, Rixen M (2009) Super-ensemble techniques: application to surface drift prediction. *Prog Oceanogr* 82:149–167
- Viikmäe B, Soomere T, Viidebaum M, Berezovski A (2010) Temporal scales for transport patterns in the Gulf of Finland. *Estonian J Eng* 16:211–227

Paper F

Viikmäe B. and Soomere T. 2014. Spatial pattern of current-driven hits to the nearshore from a major marine highway in the Gulf of Finland. *Journal of Marine Systems*, 129, 106–117.



Spatial pattern of current-driven hits to the nearshore from a major marine fairway in the Gulf of Finland

Bert Viikmäe ^{a,*}, Tarmo Soomere ^{a,b}

^a Institute of Cybernetics at Tallinn University of Technology, Akadeemia tee 21, 12618 Tallinn, Estonia

^b Estonian Academy of Sciences, Kohtu 6, 10130 Tallinn, Estonia

ARTICLE INFO

Article history:

Received 23 January 2012

Received in revised form 22 May 2013

Accepted 18 June 2013

Available online 7 July 2013

Keywords:

Pollution maps

Surface currents

Lagrangian transport

Gulf of Finland

Baltic Sea

ABSTRACT

The spatial pattern of hits to the nearshore by tracers originating in a major fairway in the Gulf of Finland and transported by surface currents is analysed based on Lagrangian trajectories of water parcels reconstructed using the TRACMASS model from three-dimensional velocity fields by the Rossby Centre circulation model RCO for 1987–1996. The probabilities for a hit to different parts of the nearshore and the ability of different sections of the fairway to serve as starting points of tracers (equivalently, certain type of nearshore pollution) have extensive seasonal variability. The potential of the fairway to impact the nearshore in this manner is roughly inversely proportional to its distance from the nearest coast. A short section of the fairway to the south of Vyborg and a segment to the west of Tallinn are the most probable starting points of tracers. The most frequently hit nearshore areas are short fragments between Hanko and Helsinki, the north-eastern coast of the gulf to the south of Vyborg, and longer segments from Tallinn to Hiiumaa on the southern coast of the gulf.

© 2013 Elsevier B.V. All rights reserved.

1. Introduction

The Baltic Sea hosts one of the heaviest ship traffics in the world. Although relatively small in size, still up to 15% of the world's ship cargo is transported along its numerous fairways. The number and the size of ships have grown in recent years. The largest threat to the environment is oil transportation, which increased by more than a factor of two in 2000–2008 and a 40% increase is expected by the year 2015 (HELCOM, 2009). One of the major marine highways in the European waters enters the Baltic Sea through the Danish Straits, crosses the Baltic Proper and stretches through the Gulf of Finland (Fig. 1) to Saint Petersburg, the largest population and industrial centre in this area, and to a number of new harbours in its vicinity.

Sustainable management of this traffic flow is a major challenge in the Baltic Sea, which is designated as a Particularly Sensitive Sea Area (PSSA) by the International Maritime Organisation. When an area is approved as a PSSA, specific measures can be used to control the maritime activities in it (IMO, 2007; Kachel, 2008). The problems of detection, modelling and forecasting of the fate of oil spills in the Baltic Sea have been addressed in numerous publications since the mid-1990s (Ambjörn, 2000; Johannessen et al., 2006; Kostianoy et al., 2005; Lavrova et al., 2006; Tufte et al., 2004; Uiboupin et al., 2008); also the relevant econometric issues (Aps et al., 2009; Elofsson, 2010; Gottinger, 2001), statistical models of collision and grounding probability (Gucma, 2008), optimum allocation of the

available monitoring resources (Deissenberg et al., 2001) and propagation of pollution under ice cover (Alhimenko et al., 1997; Wang et al., 2007) have been treated. The official HELCOM oil spill forecast system Seatrack Web, launched at the turn of the millennium (Ambjörn, 2000; Gästgifvars et al., 2002) and regularly updated (Ambjörn, 2007), has become an important constituent of operational oceanography in the region (Ambjörn, 2008; Kostianoy et al., 2005, 2008; Lavrova et al., 2006; Uiboupin et al., 2008).

Apart from oil pollution, a variety of adverse impacts, (chemical) substances and objects, carrying a certain danger, can be potentially released from ships. They may be carried to substantial distances by the complex interaction of different metocean drivers (currents, waves, direct impact of wind) and may be modified by a number of physical and chemical processes (e.g. weathering of the oil pollution, dispersion of chemicals, and change in the radioactivity level of nuclear wastes). The number of drivers is quite large and even the very best models of the propagation and fate of adverse impacts of different kinds still suffer from some limitations that result in imperfect predictions (e.g., Ambjörn, 2007) and can be quite demanding computationally.

The direct impact of wind and waves on the propagation of pollution and different objects in the upper layer of the sea is relatively well understood (Ardhuin et al., 2009; Breivik et al., 2011) and relevant parameterisations were implemented into operational models decades ago. The situation with current-driven transport is much less satisfactory. Although there exist attempts to replicate the three-dimensional (3D) propagation of oil spills (Chang et al., 2011), the tracking of pathways of even single drifters (or pollution parcels) and the regions of their

* Corresponding author. Tel.: +372 5062155.
E-mail address: bert@ioc.ee (B. Viikmäe).

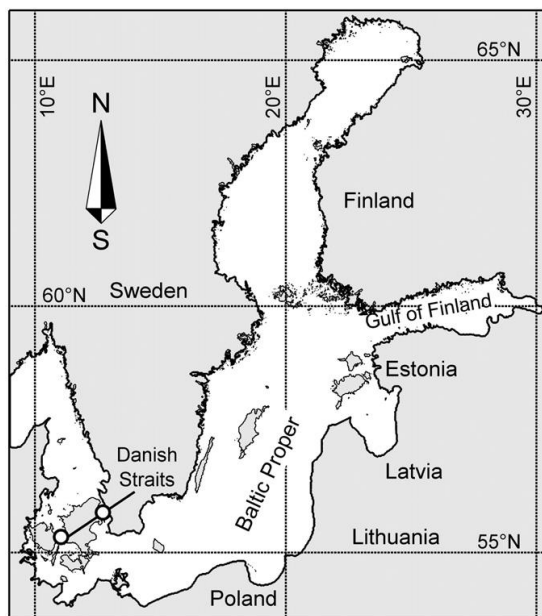


Fig. 1. Scheme of the Baltic Sea and the Gulf of Finland.

impact is extremely complicated also for small sea domains, the very best ocean models and their ensembles (Fingas, 2011; Vandembulcke et al., 2009). The situation is by no means better in the Baltic Sea (Kjellsson and Döös, 2013; Verjovkina et al., 2010).

In this light, a better understanding of the properties of current-driven transport provides the largest unused potential towards more exact representation of the propagation of various adverse substances and dangerous, dubious or precious objects in the surface layer. This perception calls for us to seemingly take a step back, to intentionally ignore the direct impact of wind and waves on objects on top of water and substances in the uppermost layer of the sea, and to focus on the impact the surface currents may have on their pathways.

The resulting framework is directly applicable for persistent substances that are dissolved in strongly stratified environments under calm conditions when the contaminants (e.g. dissolved radioactive substances) largely remain in the uppermost layer and are mostly carried by surface currents (e.g., Periañez, 2004). This setup is only conditionally valid for oil pollution or the drift of floating objects extending over the sea surface or exposed to the wave action in most of the open ocean as it does not consider other meteocean drivers, chemical processes, buoyancy effects, etc. Thus, it is not always justified from the viewpoint of practical applications. For example, the predominant driving force for oil advection at offshore locations of the Gulf of Finland (the test area in this paper) varies: it is the direct wind impact during stormy seasons and the system of currents during calm seasons (Murawski and Nielsen, 2013). There is no consensus about the exact magnitude of wind-driven drift of oil spills, estimates for which vary from 0.8% to 5.8% of the wind speed (Pahlke, 1985). A frequently used value estimated in offshore conditions is 3% (Reed and Aamo, 1994). This value may be overestimated for semi-enclosed regions like the Gulf of Finland where the wind-driven surface current speed is only about 1.4% of the wind speed (Hela, 1952). The interrelations between the wind- and current-induced drifts are even more complicated in the Baltic Sea basin where the wind direction frequently varies (Soomere, 2001). Wave effects (Stokes drift) are usually much smaller than

the wind impact but they may in extreme cases become even larger. Similarly to the wind field, wave properties are highly variable in time in the Baltic Sea and the direct wave impact on the drift can be modelled to some extent as a random disturbance to the trajectories of pollutant parcels (Viikmäe et al., 2013). Spatial distributions of the long-term probability for a coastal hit of a realistic oil spill and the time it takes for the spill to reach a coast described in Murawski and Nielsen (2013) are qualitatively similar to the corresponding distributions of nearshore hits and particle age in Andrejev et al. (2011). The impact of seasonally varying wind-induced drift, however, gives rise to substantially different appearances of these distributions for different seasons (Murawski and Nielsen, 2013).

The use of the field of currents to simulate the first approximation of the full drift of surface tracers in high-resolution models (Lončar et al., 2012; Meier and Höglund, 2012), is the best option in many occasions. For example, favourable conditions exist in the Gulf of Finland during a large part of the spring and early summer when the wind is fairly weak (below 5 m/s) (Mietus, 1998), surface waves are very low and a very thin uppermost mixed layer (with a depth of a few metres) stably overlies a sharp pycnocline (Leppäranta and Myrberg, 2009). This framework is also useful during the ice season (up to six months in some years in the Gulf of Finland; Sooäär and Jaagus, 2007) when the wave motion is absent and the wind impact only becomes evident through the ice drift. This setup is of clear value for improving the understanding of the possibilities of practical use of the intrinsic dynamics of currents to preventively reduce the costs of accidents at sea (Soomere and Quak, 2007). It also has an obvious potential for the quantification of the specific role of surface currents in the dynamics of any objects or substances in the surface layer, for example, for search-and-rescue purposes (e.g., Melsom et al., 2012), especially under low wind and old, smooth swells.

The commonly used approach to manage current-driven transport of pollution or important objects is to have ready quick remedial action plans (e.g., Keramitsoglou et al., 2003; Kostianoy et al., 2008, among many others). Another approach is to build a preventive maritime planning strategy; for instance, the optimisation of the shipping routes (Schwehr and McGillivray, 2007) to account for the effect that an accident or release of an object would incur before it actually happens. An area that is highly vulnerable to possible releases of adverse impacts from ship traffic is the nearshore, which usually has the greatest ecological value. While the probability of the hits of open ocean coasts by pollution released from a ship can be reduced by shifting shipping routes farther offshore, the problem for narrow bays, such as the Gulf of Finland, is how to minimise the probability of hitting any coast. A natural way to address this issue is by means of quantification of the offshore areas in terms of their ability to serve a danger to the coastal environment if pollution happened in these areas (Soomere et al., 2010, 2011a).

A convenient way to address this problem is to use statistical analysis of a large number of Lagrangian trajectories of test particles representing the potential pollution passively carried by surface currents. The use of Lagrangian trajectories for solving different environmental problems is becoming increasingly popular. This approach has been used, for example, in studies of current-driven transport of various substances such as water masses with specific properties (Meier, 2007), pollution (Soomere et al., 2011a), suspended matter (Segsneider and Sündermann, 1988), radioactive contamination (Periañez, 2004) and marine debris (Maximenko et al., 2011). Such analysis also allows identification and visualisation of several properties of currents that cannot be extracted directly from the current fields (Soomere et al., 2011c). The results obviously depend to a certain extent on the choice of the underlying velocity fields (Andrejev et al., 2011) as well as on the governing parameters for the trajectory calculations such as the initial location of test particles released into the sea, the duration of single trajectory simulations, and the number of trajectories involved for each calculation session (Viikmäe et al., 2010).

Most of the existing studies into the quantification of offshore domains with respect to their ability to supply environmental risks to the nearshore have focused on the construction of the spatial distributions of quantities characterising the relevant environmental risks for any part of the coast. In other words, the alongshore variability of the probability that pollution will reach the coast has been ignored. This variability is, however, decisive in a more realistic case when the 'value' of different coastal sections is different (Delpeche-Ellmann and Soomere, 2013). Analysis of this variability is particularly important in cases when only short sections of the fairway can be adjusted. This is the typical case in narrow basins where the location of the fairway cannot be altered in some places, for example, because of limited depth.

In this paper, we make an attempt to quantify the link between potential sources of pollution along an existing major fairway in the Gulf of Finland and the sections of the nearshore possibly reached by current-driven contaminants. The problem is analysed using the statistics of hits to the nearshore by passive tracers (equivalently, pollution of the above-described kinds or other possibly adverse impacts) stemming from the fairway, with a goal of establishing which parts of the nearshore are hit more frequently than others and whether or not the tracers stem from specific parts of the fairway. The structure of the paper is as follows. We start with a short description of the modelling environment and the requirements for the basic parameters of the calculations such as the width of the nearshore zone, definition of the model fairway and the duration of trajectory calculations. The probability of hits of the current-driven tracers to different parts of the nearshore is analysed next, followed by the quantification of the ability of different sections of the fairway to serve as the initial point of such tracers. Finally, we analyse links between frequently hit nearshore areas and specific points along the fairway.

2. Modelling environment

In this study the 3D velocity fields simulated for 1987–1996, calculated by the Rossby Centre Ocean circulation model (RCO) in the Swedish Meteorological and Hydrological Institute, were used for the reconstruction of trajectories of tracers. The RCO model is a primitive equation circulation model (Meier et al., 2003) that covers the entire Baltic Sea with a spatial resolution of 2×2 nautical miles (nm) and has 41 vertical layers in z -coordinates. We only use the horizontal velocities in the uppermost, surface layer with a thickness of 3 m that are saved with a temporal resolution of 6 h. Details of the model are described in Meier (2001, 2007) and Meier et al. (2003) and shortly depicted in earlier studies into the statistics of current-driven pollution (see Soomere et al., 2011c and references therein).

The model is forced by wind data on the 10 m level, air temperature and specific humidity on the 2 m level, precipitation, cloudiness and sea level pressure fields. It also accounts for the river inflow and water exchange through the Danish Straits. The forcing data is calculated from the ERA-40 re-analysis using a regional atmosphere model with a horizontal resolution of 22 km and a scheme of adjusting the wind properties using simulated gustiness (Höglund et al., 2009; Samuelsson et al., 2011). A comprehensive comparison of the performance of the RCO model in the Gulf of Finland against several other state-of-the-art circulation models is provided in Myrberg et al. (2010). As the RCO model includes a quite sophisticated ice model (Meier et al., 2003), the impact of the presence of ice on the pattern of currents is accounted for. However, the model does not account for the roughness of the lower surface of the ice (caused, e.g., by ridging). The model also captures inertial waves in the gulf. Owing to a coarse temporal resolution of the saved output data (about half of the period of inertial oscillations), the role of these oscillations in the drift of particles is only partially accounted for.

Given the very small internal Rossby radius in the Gulf of Finland, typically 2–4 km (Alenius et al., 2003), the model only resolves a certain part of statistical features of the meso-scale dynamics in this gulf. An exact representation of the location and properties of single eddies,

however, cannot be expected. The dependence of the properties of surface-current-driven transport of tracers from offshore areas to the nearshore on the resolution of the circulation model of the Gulf of Finland was analysed in Andrejev et al. (2011) using an ocean model with a resolution of 2, 1 and 0.5 nautical miles and with otherwise identical setup and forcing data. While some features of current-driven transport (e.g. the exact location of the optimum fairway) were found to be quite sensitive with respect to the model resolution, some other statistical properties of this transport (e.g., the basic features of the underlying distributions of probabilities of nearshore hits and the time it takes tracers to reach the coast) turned out to be very stable after about 3 years of integration. As the pattern of nearshore hits by tracers released along the fairway is largely governed by the latter properties, it is likely that the spatial statistics of hits to the nearshore by tracers is not particularly sensitive with respect to the resolution of the circulation model either. This assumption is supported by the amazing stability of such patterns with respect to random disturbances to tracers' trajectories (Viikmäe et al., 2013).

The current-driven transport of tracers is analysed applying a Lagrangian trajectory model, TRACMASS (de Vries and Döös, 2001; Döös, 1995). It uses pre-computed 3D Eulerian velocity fields to evaluate an approximate path of selected water parcels (equivalently, of an adverse impact with neutral buoyancy). The model relies on an analytical solution of a differential equation for motion that depends on the velocities on the ocean model grid box walls using a linear interpolation of the velocity field both in time and in space.

As we are specifically interested in surface transport patterns, the tracers are locked in the uppermost layer as in Andrejev et al. (2010) and Soomere et al. (2010). The resulting trajectories are, thus, not truly Lagrangian: they represent purely current-driven motion of objects that are slightly lighter than the surrounding water (such as oil in calm conditions) or objects that are confined to the upper layer by other constraints (for example, lost containers).

The circulation models usually prescribe that the velocity component normal to the rigid boundaries (bottom and coast) should vanish in the boundary cells. This feature, although physically correct, constrains the simulated flow to be largely alongshore in the nearshore and in many cases suppresses the cross-shore motions at a distance of a few grid cells. The process of beaching is usually solved either indirectly, for example, by including artificial spreading of the Lagrangian trajectories (Andrejev et al., 2010), local wave- and wind-induced transport (e.g., in the Seatrack Web; Ambjörn, 2007) or by defining a control line for coastal hits at a certain distance from the geographical coast (Broström et al., 2011).

Comprehensive analysis of the reasonable location for such a control line (the model seaward boundary of the nearshore) was performed in Viikmäe et al. (2010) for the trajectories in the combined RCO-TRACMASS model. Different locations of this line were simulated by means of setting it at distances of 1, 2 and 3 grid cells from the coast (called alert zones 1–3, respectively). The starting points of the trajectories were chosen, as in this study, roughly along the major fairway (Fig. 2). The average probability that trajectories would enter zones 1 and 2 during spring and summer months was very low, about 2% and 4%, respectively, and increased up to 20% and 30%, respectively, during windy months (October–February). Such small probabilities suggest that the statistics of hits to the nearshore based on reaching these zones may have quite large uncertainty. The annual average of the probability that trajectories will enter alert zone 3 is about 30%, with monthly mean values around 80% during the windiest seasons (Viikmäe et al., 2010). Based on these estimates, zone 3 (with a width of about 11 km, 331 grid points, Fig. 2) was chosen as a model nearshore.

3. Method

In this paper, trajectories are simulated in the Gulf of Finland by placing tracers on a line that roughly follows the major fairway

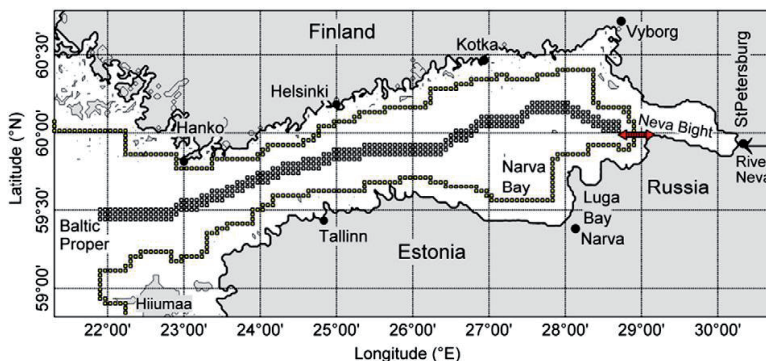


Fig. 2. Initial location of tracers and the border of the nearshore in the Gulf of Finland. The double arrow indicates the separation point of the 'southern' and 'northern' parts of the nearshore.

from the Baltic Proper to Saint Petersburg. In order to mimic the natural spreading of shipping lines, tracers are released in a wider belt covering three model grid cells in the North–South direction (with a width of about 11 km). In each simulation one tracer is released at the centre of each of the 309 grid cells (Fig. 2). The simulations cover the time interval 1987–1996 that includes the interval 1987–1991 used in several previous studies of circulation (Andrejev et al., 2004a,b) and distribution of coastal hits in the Gulf of Finland (Soomere et al., 2010).

An adequate representation of statistical features of transport requires the use of a sufficient number of uncorrelated trajectories. The number of simultaneously calculated independent trajectories is implicitly limited by the number of grid cells used. Namely, trajectories for tracers released in different locations of a single cell reconstructed from modelled velocity data tend to be highly correlated during a long time. The reason is that the trajectory model cannot guess into which direction and how rapidly the real drifter would move under the impact of subgrid processes. A formal solution would be to mimic their contribution towards spreading trajectories in the real ocean. This is usually done by inserting a random disturbance to each trajectory (e.g., Kjellsson and Döös, 2013). Doing so may adjust certain statistical features of large ensembles of trajectories but evidently would not improve the match of simulated trajectories with pathways of real tracers. In other words, improving, e.g., transport speed and dispersion is counterbalanced by a loss of transport direction and possibly other properties (Kjellsson and Döös, 2013).

A better way of increasing the number of trajectories is to repeat the calculations with a certain time lag. As the surface drift speed in the Gulf of Finland is typically 0.1–0.2 m/s (Kõuts et al., 2010) and the current patterns are normally strongly circularly polarised (Lilover et al., 2011), a tracer usually moves only a few kilometres a day from its original location. Therefore, only these trajectories that start at least a couple of days after the previous one (in the case of the 2 nm RCO model) can be treated as independent ones. Thus, the most sensible way to increase the number of trajectories is to improve the spatial resolution of the circulation model or to increase the time period covered by the circulation modelling.

The average time it takes a particle released in the Gulf of Finland to drift to the nearshore (particle age) is about 5 days (Andrejev et al., 2011). For particles released in the central part of the gulf this time is considerably longer, 6–9 days on average. On the one hand, in order to reliably represent the majority of the hits to the nearshore from the points of the fairway in Fig. 2, the duration of trajectories should be at least twice as long as the average particle age for the fairway region. On the other hand, as the probability of nearshore hits rapidly decreases after reaching a maximum value (Viikmäe et al., 2010), the use of very long trajectories would evidently add only a little, if

at all, to the statistics of nearshore hits. Moreover, the use of exceedingly long trajectories would increase the risk of getting subsequent trajectories too close to each other at a certain physical time instant. This would lead to a pair of correlated trajectories. Based on these arguments, we use in this study 20 days long trajectories whereas each new set of trajectories starts with a time lag of 10 days. The calculations were organised as follows (Soomere et al., 2010; Viikmäe et al., 2010). One particle was seeded into the centres of each of the above grid cells at 00:00 on 01 January each year. Their trajectories were calculated until 00:00 on 20 January. New particles were released at the same locations at 00:00 on 10 January and their trajectories were again evaluated during 20 days. The process was repeated until the end of the year. The trajectories for the last release in December were calculated until mid-January of the subsequent year.

Below we only consider such trajectories that enter the nearshore at least once. For each such trajectory, the initial location of the tracer, the point at which the trajectory reaches a nearshore point for the first time and the time elapsed from the release of the tracer (particle age) (Andrejev et al., 2011) are saved. For brevity, we call such events nearshore hits below. Further behaviour of the trajectory is ignored. The total number of time windows used during each 5-year interval was 185 and resulted in 57,165 single trajectories.

4. Results

The monthly number of trajectories and percentages of coastal hits were calculated from the trajectories that started within that month. The number of releases varied to some extent: in January and May new particles were released four times and in February two times. The maximum (84%) and the minimum (5%) amount of the trajectories reached the nearshore in January 1989 and in March 1987, respectively. Following the analysis of properties of net surface transport in different months (Soomere et al., 2011c), we associate the windy season with the period of October–February and the calm season with May–July. The transition months March and April are associated with the windy to calm season and the months August and September with the calm to windy season. The 5-year mean probability that a trajectory would reach the nearshore was 38–50% for the windy season, 25% for the windy to calm (spring) season, 17–18% for the calm season and 25–33% for the calm to windy (autumn) season. Although there was a certain variability in the annual mean probability of nearshore hits (from 25.9% in 1987 to 42% in 1995), the five-year average values (32.9% for 1987–1991 and 34.2% for 1992–1996) insignificantly differed from the average of 33.5% for the entire decade. The resulting data set makes it possible to reveal which sections of the fairway are the most probable sources of coastal

pollution, which nearshore areas get more hits and where the hits are coming from.

It is well known that the short-term variability of Lagrangian transport in the surface layer of the Gulf of Finland is so pronounced that no adequate conclusion can be made based on individual simulations (Viikmäe et al., 2010). For this reason, the results for each time window, both in terms of the source of tracers and frequent places of nearshore hits, were first averaged over at least one month. Thereafter, seasonal and interannual variability in the process was estimated.

4.1. Frequently hit nearshore areas

As the number of releases was the largest in January and May and the percentage of nearshore hits was much higher in January than in May, January was chosen to illustrate the short-term variability of the rate of hits. Considering that the results for individual months are based on a small number of tracers, the monthly mean values of the relevant percentages and the associated patterns are not reliable. Fig. 3 first exemplifies the extensive interannual and seasonal variability of the monthly means. Simulation results for single months (January 1987–1991) still reveal certain repeating features. The north-eastern (NE) nearshore of the gulf from the entrance to the Neva Bight up to Vyborg had constantly a high probability of being hit. In January 1988 a section of the northern (Finnish) nearshore to the east of Helsinki was the most affected one. In all other years the southern (Estonian) nearshore received the majority of hits. The most affected region, slightly to the west of Tallinn, near 24°00'E, extended to the entrance to the Gulf of Finland at 23°30'E and to the east of Tallinn up to 26°30'E in January 1989. Only a short section along the south-eastern (SE) coast of the Gulf of Finland in the Narva Bay region received no hits in all of the months in question (Fig. 3).

The alongshore variation of the frequency of hits was, however, on the same level for different months in question. The typical average number of hits per nearshore point was in the range of 1.5–2 per month (3 or 4 runs). The most frequently hit sections received 9–11 hits, that is, about 5 times as many as the average.

This variability in the transport patterns on a monthly scale was equally strong in a seasonal perspective (Fig. 4). The typical location of the most frequently hit areas during different months largely coincided with those that were hit in January: sections between Hanko and Helsinki (which were frequently hit only during the windy season and

the autumn transitional season), several areas between Tallinn and the Island of Hiiumaa, and the NE nearshore of the Gulf of Finland to the south of Vyborg (the last one received many hits throughout the year, although their number was somewhat smaller in July). These areas received, as expected, the highest number of hits during the windy season and slightly less during both transitional seasons. The nearshore areas less frequently hit were between Helsinki and Kotka, in Narva Bay and also slightly to the west of Narva Bay. Surprisingly, the windy to calm season (represented by March in Fig. 4) did not show frequent hits to the nearshore of Finland; instead, many hits were most likely to occur in areas to the west of Tallinn, between the Estonian mainland and Hiiumaa, and also near the northern part of Hiiumaa. During the calm season there were a few frequently hit areas also between Tallinn and Narva and near Kotka (Fig. 4).

The averaged results for individual years smooth out some of the patterns indicated in Figs. 3 and 4 but still reveal a clear configuration (Fig. 5). As above, the area of most frequent nearshore hits is located in the eastern part of the gulf, to the south of Vyborg, in each year. This is apparently due to the short distance from the fairway to the model nearshore. The results of our model in this area should, however, be interpreted with some care. The 2 nm RCO model might not properly resolve the meso-scale dynamics in this area where the Rossby radius is at places as small as 500 m (Nekrasov and Lebedeva, 2002). Simulations of Andrejev et al. (2004a) suggest that a powerful and persistent flow, possibly partially driven by the voluminous discharge from the River Neva, exists in the sub-surface layer (depths 2.5–7.5 m) from the entrance to the Neva Bight until the longitude of Vyborg. Under many circumstances such an intense flow may entrain the uppermost layer (Gästgifvars et al., 2006), redirect the surface-current-induced transport to the west and in this way implicitly protect that coast against pollution from sources along the fairway.

The model indicates that frequent hits occurred in some years (1988 and 1990, not shown) between Hanko and Helsinki at the northern coast of the gulf while only an average number of hits to this area occurred in other years. Another area frequently receiving a high number of hits (particularly in 1988, 1989 and 1991) was located near the southern coast of the gulf, to the west of Tallinn, around 24°00'E. The region to the east of Helsinki until about 28°30'E is relatively safe with respect to the current-driven impacts stemming from the model fairway. It received a lower than average number of nearshore hits during most of the years whereas only a small area around 28°00'E had an average number of hits. An extensive

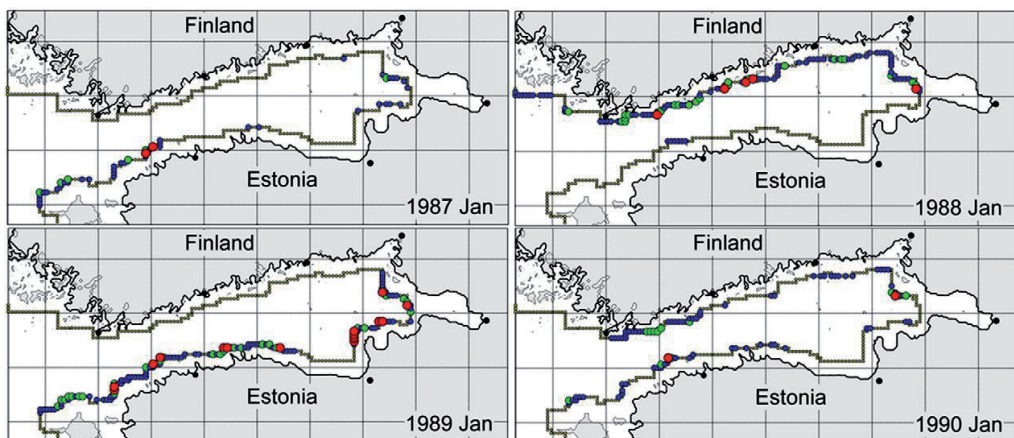


Fig. 3. Inter-annual variability of the most frequently hit domains of the nearshore in the windy season by tracers released in January. The colour code shows the number of hits per point per month. Its 10-year average rate is 0.42 in January and May (4 releases of tracers), 0.21 in February (2 releases) and 0.31 (3 releases of tracers) in all other months. The most frequently hit sections normally received 9–11 hits in January of different years. Grey: sections with no hits, blue: <2 hits, green: 2–5 hits, red: >5 hits.

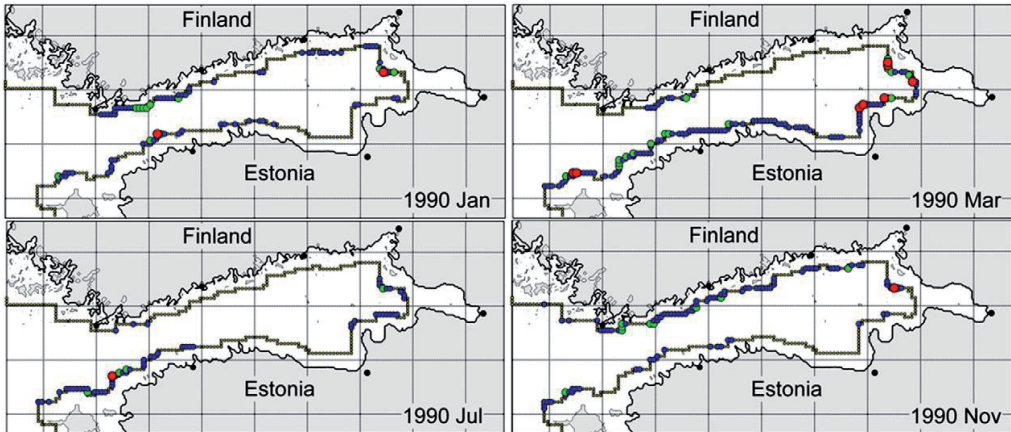


Fig. 4. Seasonal variability of the most frequent hits to the nearshore. Colour code is the same as for Fig. 3.

nearshore stretch between Tallinn and Narva also received a low number of hits during all the years whereas in 1987 the nearshore area of Narva Bay (which is also the most remote from the model fairway) had no hits at all according to the model.

4.2. Spatial and temporal variability and uncertainty of the patterns of hits

The above-described extensive variability of both the spatial pattern of frequently hit nearshore sections and of the number of hits on monthly and seasonal scales is not unexpected because of the high variability in the patterns of currents of the Gulf of Finland (Alenius et al., 1998; Leppäranta and Myrberg, 2009). This raises the question about uncertainties of the resulting estimates, especially in the spatial distribution of the most frequently hit areas. A partial answer to this question can be extracted from the analysis of this variability over longer time intervals and also from a comparison of the results for two different longer periods.

The 5-year pointwise average values of nearshore hits (Fig. 5) exhibit a pattern very similar to the annual average distributions. It reflects an average frequency of hits in the area between Hanko and

Helsinki and also in the area to the west of Tallinn, near the southern coast of the gulf, extending to Hiiumaa. Most frequent hits occurred only in the NW part of Estonia near 24°00'E and in the easternmost part of the gulf, to the south of Vyborg. The northern coast from Helsinki to 28°30'E and the southern coast between Tallinn and Narva, were relatively safe according to the model used.

The temporal variability of the average number of nearshore hits is lower but still considerable on annual scales. The average number of hits per nearshore section per year is 3.76 in 1987–1996 but varies by $-22\%/+25\%$, from 2.9 in 1987 up to 4.7 in 1995. The relevant standard deviation (std) is 0.597 (Fig. 6). This variability, however, rapidly decreases with the increase of the averaging period. Its 5-year averages for 1987–1991 (3.68) and for 1992–1996 (3.83) insignificantly (by less than 2%) differ from the 10-year mean (3.76). This convergence supports the conjecture of Andrejev et al. (2011) that several variables characterising the pattern of surface transport (such as the average probability of hitting the nearshore or the typical time it takes until a hit occurs) converge to their asymptotic values after 3–4 years of simulations.

The alongshore variability of this number, not unexpectedly, remained substantial also in the long-term average apparently because it is mostly determined by geographical conditions and possibly

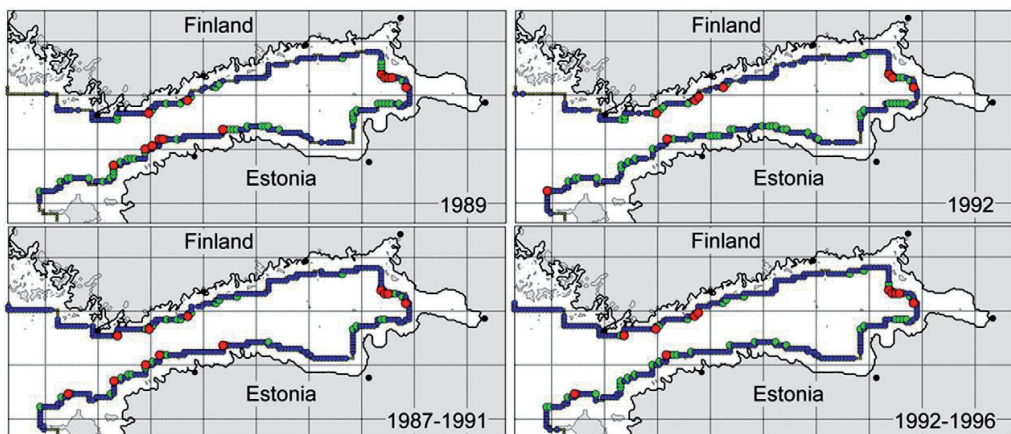


Fig. 5. Annual average map of the most frequent hits to the nearshore in 1989 and 1992, and the 5-year average map of nearshore hits. Grey sections indicate areas with no hits. Blue colour shows sections that received <7 hits/yr (20% of the maximum, about twice as large as the average), green 7–17.5 hits/yr (20–50% of the maximum), red areas where the hit count is >17.5 (>50% of the maximum).

by long-term features of surface transport. While 18 sections had no hits at all during the entire 10-year simulation (30 sections in 1987–1991, 27 sections in 1992–1996), the most frequently hit sections received up to 50 hits a year. The std for alongshore variations of the number of hits was from 4.9 in 1987 to 6.5 in 1989 (Fig. 6). The values of std calculated against the 10-year average of pointwise count of hits were at the same level but varied very little: from 4.75 in 1989 to 4.89 in 1987. This stability of the std over different years may reflect the presence of a persistent structure in the distribution of hits.

The schematic spatial distributions of frequently hit areas in Fig. 5 appear very similar for the periods of 1987–1991, and 1992–1996 and for the entire 10-year interval of 1987–1996. The match of these distributions becomes evident from a comparison of the relevant annual mean number of hits per section (Fig. 7). The locations of the sections receiving the largest number of hits exactly coincide for both 5-year intervals. Moreover, the particular values of the hit count for single points are practically the same for these two intervals (Fig. 7). On average, the count in 1987–1991 exceeds the one in 1992–1996 by 0.15 (which is about 4% of the relevant mean value). The largest pointwise difference is 7.1 at one summit of the triple peak located to the west of Helsinki where the larger value is 17.7. The std of the pointwise difference between the values for the two 5-year intervals is 1.51.

Therefore, the location of the areas that receive the largest number of current-driven hits from the fairway region, found as an average over at least 5 years, is highly persistent. Although the hit counts for individual frequently hit sections may experience quite large variations over different 5-year intervals, the number of hits to these sections is substantially larger than the relevant values for the rest of the nearshore area.

Another possibility for estimating the uncertainty of the performed calculations is to account for only a part of the trajectories. The pattern of frequently hit areas calculated using every second release and averaged over 5 or 10 years was exactly the same as the pattern obtained using the entire set of trajectories. The bias and std of the relevant spatial distributions of the count of hits were even smaller than the presented estimates for the two 5-year intervals.

4.3. Frequent sources of nearshore pollution

Recent studies have revealed a rich family of usually concealed semi-persistent current-driven net surface transport patterns in the modelled circulation of the Gulf of Finland (Soomere et al., 2011c). Although these patterns are highly variable in space and time, their more or less regularly repeating features indicate that they may have a systematic impact, at least in certain seasons, on the current-driven

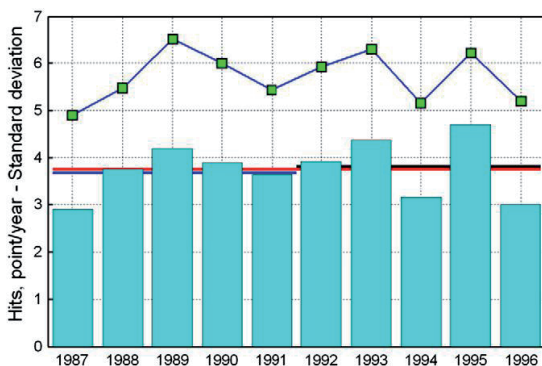


Fig. 6. Interannual variability (bars), five-year mean (blue 1987–1991 and black 1992–1996) and 10-year mean (red) of the average number of coastal hits per year, and standard deviation of the alongshore variation of the number of coastal hits for each year (squares).

transport from the fairway region to the nearshore. The complexity and anisotropy of such patterns makes it complicated to establish their direct impact in dynamical sense. Their presence, at least in the model results, suggests that different sections of the fairway may play different roles in the formation of the pattern of nearshore pollution. More generally, it is most likely that the probability that different fairway sections can serve as a starting point of tracers substantially varies along the major fairway from the Baltic Proper to the ports in the eastern part of the gulf (cf. Andrejev et al., 2011). Differently from the above, the fairway points are characterised in terms of the frequency with which the tracers released at each point reached the nearshore. Special attention is paid to the points, from which tracers drift to the nearshore more frequently (>30% of the maximum count on the annual scale) than on average. Below we speak about dangerous parts of the fairway, alternatively, about hazardousness, having in mind these points.

Similarly to the above-discussed distributions of the most frequently hit nearshore areas, the potential of different parts of the fairway to serve as starting points of tracers that reach the nearshore substantially varies over different months (Fig. 8), seasons (not shown) and years (Fig. 9). The probability that the released adverse impacts will reach the nearshore is the highest during the windy months (Fig. 8). For example, according to the model, in January 1989 about 84% of the released tracers reached the nearshore. The dangerous points to the west of Tallinn exist mostly during the windy season and during a few other months, for example in April, July and in September.

The results averaged for single years (Fig. 9) reveal a lower but still considerable temporal variability in the hazardousness of the fairway. The particular values of the probability that the released adverse impacts will reach the nearshore vary considerably for different years. For example, in 1988–1989 this probability stemming from a part of the fairway to the west of Tallinn frequently exceeds 60% but is much lower in the other years. Importantly, it reveals a persistent pattern along the fairway (Fig. 9). The relatively dangerous sections near the bayhead of the Gulf of Finland and to the south of Vyborg are evident in all years and seasons and during most of the months (Figs. 8 and 9). Only the width of the dangerous part of the fairway to the south of Vyborg changes seasonally, being the widest from September to December (Fig. 8). The least danger comes from the section of the fairway between longitudes 25°E and 27°30'E.

The annual average time (equivalent to particle age introduced in Andrejev et al., 2011 and called so below) it takes for the tracers released at different points of the fairway to reach the nearshore shows a matching pattern. Its details also reveal extensive short-term (monthly and seasonal, not shown) variability, the level of which is considerably smaller on the annual scale (Fig. 10). The fairway section in the widest part of the gulf between Tallinn and Narva has the longest modelled particle age. Its large values (>15 days on average¹) also appeared in a section of the fairway from the entrance to the gulf almost until the mainland of Estonia (in 1987 even from the entrance to the

¹ Note that this estimate is calculated using the particle age of 20 days for all released particles that have not entered the nearshore at all during a particular simulation. Therefore, the average time of the drift of tracers to a particular section of the nearshore (e.g., the time corresponding to the largest probability of hits) may be considerably shorter (Viikmäe et al., 2010). This feature is associated with a somewhat specific nature of the water or particle age. Differently from, e.g., the mass of a water parcel, the particle age (similarly to the water age) is not an additive quantity and thus may be derived in many conceivable ways (Deleersnijder et al., 2001). We assume that all released tracers have a constant and equal mass and an equal weight in calculation of the average age. The calculation of the 'true' value of the age involves, strictly speaking, evaluation of improper integrals over infinite integration time of the model. Under the natural assumption that these integrals converge (this question is out of the scope of this study), truncation in a reasonably long time is expected to give a proper estimate of the age. This is one of the reasons for the choice of the 20 days long integration period, which is twice longer than in the preceding studies (Andrejev et al., 2011; Soomere et al., 2011b). A choice of the truncation is a common issue in studies into water age. Regrettably, detailed information about how exactly the truncation has been implemented is usually not provided. Still, particles that have not left the area of interest by the end of integration are often assumed to be of the age equal to the integration time (e.g. Andrejev et al., 2004b).

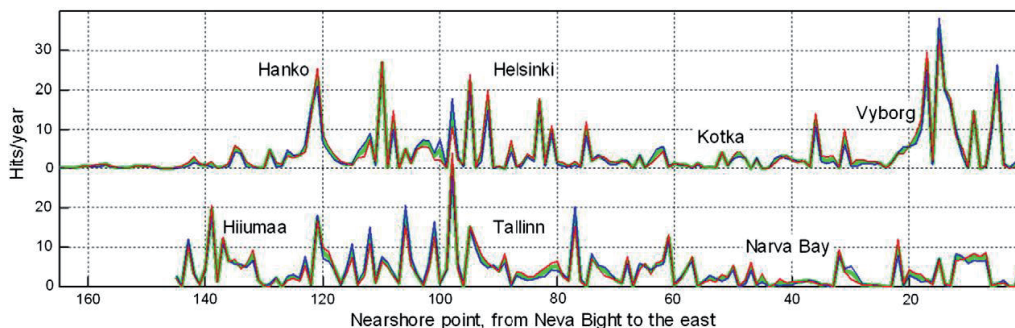


Fig. 7. Pointwise annual mean number of hits in 1987–1991 (blue), 1992–1996 (red) and 1987–1996 (green). The upper triplet of lines reflects the northern nearshore of the Gulf of Finland (Fig. 2) and the lower triplet, southern nearshore. The separation point is marked by a double arrow in Fig. 2.

gulf until the Narva Bay area). Generally, sections of the fairway that are the remotest from the coast provide a low level of danger to the nearshore also in terms of particle age. A section possibly providing a larger level of danger (particle age 10–15 days) is in the narrowest part of the gulf, between Tallinn and Hanko, but extends almost to Hiiumaa in some years. Another section of the fairway posing a greater threat to the nearshore is located in the easternmost part of the gulf, to the south of Vyborg. A small part of this section is characterised by quite fast (<10 days on annual average) current-driven transport of the released tracers to the nearshore.

Analysis of the probabilities of the coastal hits and the particle age suggests that the fairway can be divided into four parts. Overall, a short section of the fairway near the bayhead of the Gulf of Finland, to the south of Vyborg, should be considered as highly dangerous with respect to the current-driven drift of various impacts to the nearshore (Figs. 9, 10) as any contaminant or object placed in the uppermost layer of the sea in this section has a high chance to rapidly drift to the nearshore. This threat is enhanced by the predominance of south-western winds in this area. Another relatively dangerous section is located in the narrow part of the gulf slightly to the west of Tallinn. It takes, on average, 10–15 days (less than 10 days in a smaller section near Vyborg) for the current-driven tracers stemming from these parts of the fairway to reach the nearshore. The less dangerous parts are the sections from Narva to Tallinn and to the west of the mainland of Estonia (extending to the Baltic Proper) from where the drift time to the nearshore is 15–20 days (Fig. 10).

The most frequently affected nearshore area is a short section to the south of Vyborg (Fig. 5). Relatively frequent hits occur to the southern coast of the gulf, in a short section to the north of Luga Bay (Fig. 2), at selected points near the northernmost tip of Estonia and along almost the entire NW coast of Estonia to the west of Tallinn. The northern nearshore of the gulf, except for short sections between Helsinki and Hanko, has generally a lower probability of being hit by tracers released along the fairway.

4.4. Connections of sources and places of hits

Finally, we analyse possible connections between the most frequently hit nearshore areas and the release sites of tracers in different parts of the fairway. As such connections are irrelevant for areas that are infrequently hit, the analysis is only performed from the viewpoint of most frequently hit nearshore areas, namely sections for which the annual number of hits exceeded 60% of the maximum count for at least one of the ten years 1987–1996. The maximum count for individual years varied more or less synchronously with the average rate at which the released particles reached the nearshore, from 32 in 1994 to 49 in 1989. The use of such a relative criterion to some extent levels off the interannual variations of the total number of hits.

Such nearshore areas (total 43, Fig. 11) form a subset of relatively frequently hit areas depicted in Figs. 5 and 7 that seem to be the most endangered by adverse impacts released in the vicinity of the major

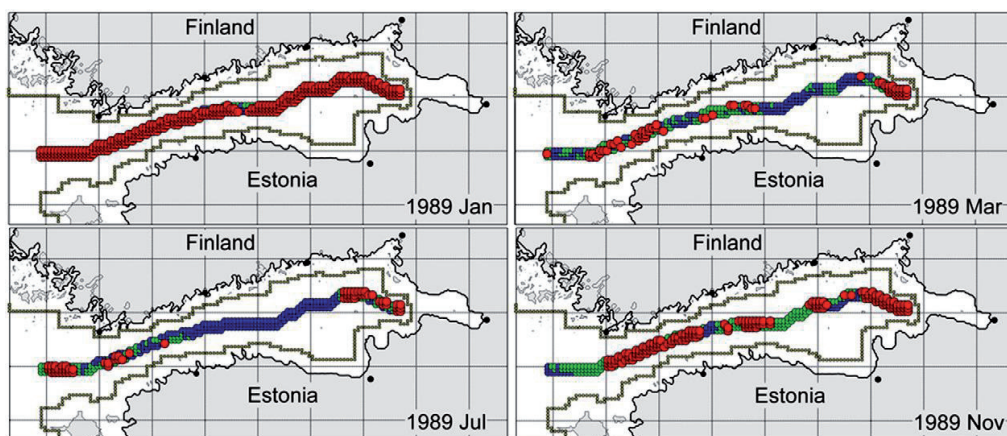


Fig. 8. Seasonal variability of the percentage of released particles reaching the nearshore. Blue: fairway points from where <30% of the released particles reached the nearshore, green: 30–60%, red: >60%.

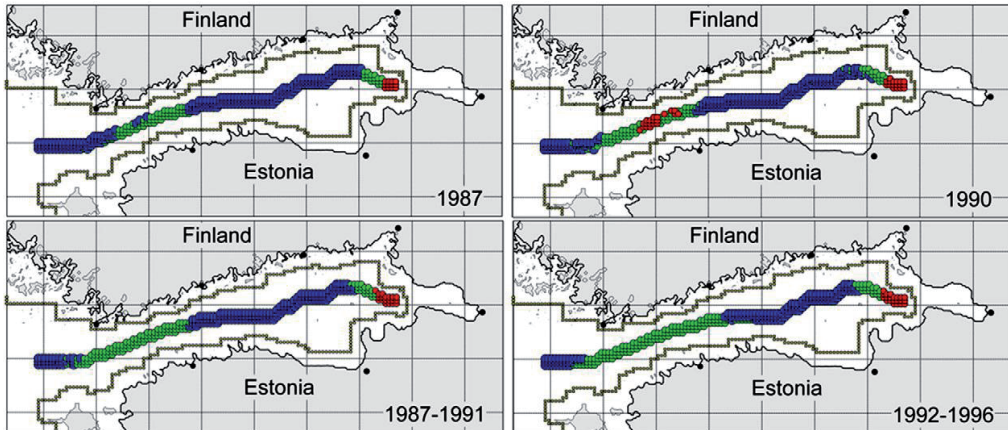


Fig. 9. Interannual variations of the percentage of released particles reaching the nearshore. Colour code is the same as for Fig. 8.

fairway and further transported by surface currents. Most sections of this subset had a largely varying number of hits in different years. Importantly, as a rule, these hits stem from quite different fairway points. Therefore, our simulations did not reveal any persistent pattern of interconnections occurring on the annual basis between potential sources of current-driven tracers or different floating objects and points where they come close to the coast. Such patterns may, though, exist for certain seasons and/or weather patterns. This also means that it is generally not possible to establish, at least using the model at our disposal, where these objects originate from.

There were, however, nine sections of the nearshore that frequently received a massive number of hits by tracers released in relatively small parts of the fairway (Fig. 11). These sections were identified by considering the nearshore areas that received at least 60% of the annual maximum number of hits in any three years out of five consecutive years (1987–1991 or 1992–1996). Five of them were evident in both 5-year intervals.

An area close to the northern coast of the gulf, between Hanko and Helsinki, was predominantly hit by tracers originating in the northernmost sections of the fairway at $24^{\circ}00'E$, $24^{\circ}30'E$ and $25^{\circ}30'E$. An area at the southern coast near $24^{\circ}00'E$ mostly received particles originating in a section of the fairway from $23^{\circ}30'E$ to $24^{\circ}30'E$.

Particles hitting the area in the easternmost part of the gulf, to the south of Vyborg, mostly originated in a fairway section between $28^{\circ}00'E$ and $29^{\circ}00'E$. Finally, a small nearshore area to the NW of Hiiiumaa was hit by tracers stemming from a section of the fairway directly to the north of this area.

5. Discussion and conclusions

The presented attempt to quantify the link between the potential release locations of adverse impacts (the source of which is assumed to be ship traffic along the existing major fairway) in the Gulf of Finland and the sections of the nearshore impacted by the current-driven drift of these impacts has mostly led to intuitively evident results. However, it has also highlighted several interesting aspects of the problem of potential threats to the environment from ship traffic in this basin.

Not surprisingly, the level of danger from the major fairway from the Baltic Proper to Saint Petersburg is roughly inversely proportional to the distance of this fairway from the nearest coast. A short section in the eastern part of the gulf, to the south of Vyborg apparently has the largest potential in terms of impacting the nearshore. Another

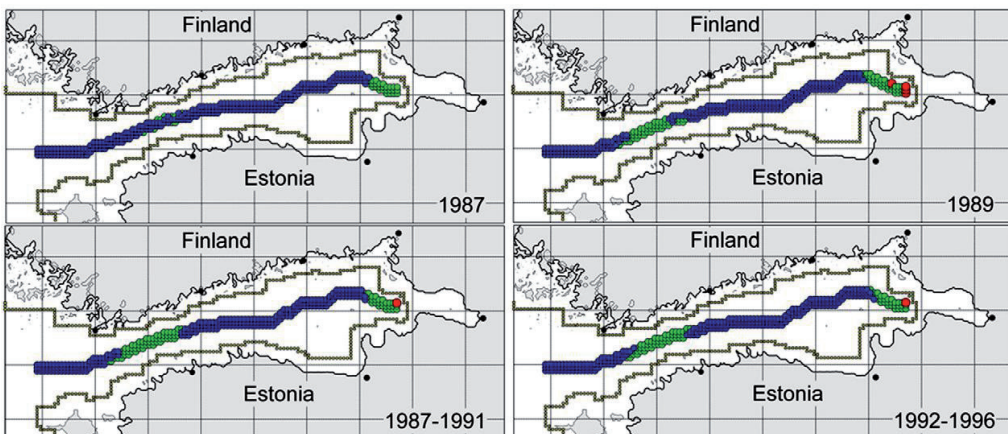


Fig. 10. Average pollution age for different sections of the fairway. Blue: 16–20 days, green: 10–15 days, red: 1–9 days.

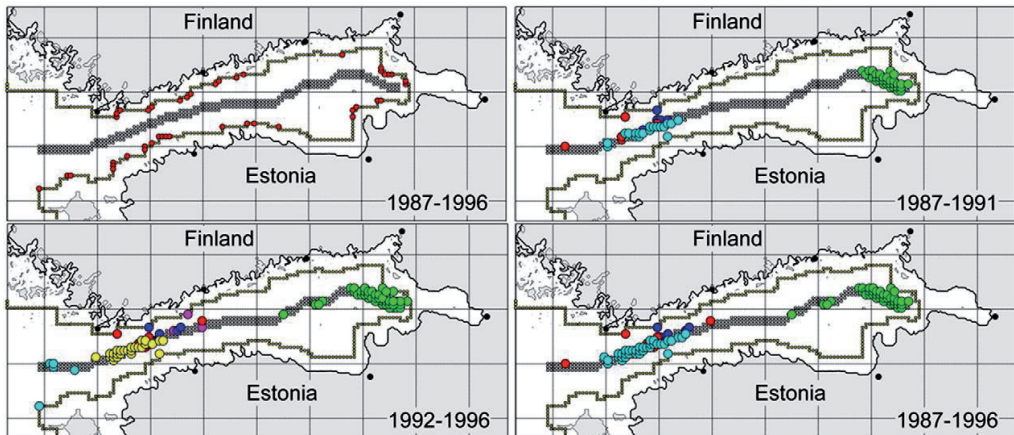


Fig. 11. Upper left panel: Most frequently hit nearshore areas (red; >60% of the annual maximum number of hits at least in three model years out of 1987–1991 or 1992–1996). Other panels: interconnections between the above most frequently hit areas and the origin of the particles. The link between the nearshore areas and the origin is depicted using the same colour.

section with a relative high potential for such an impact exists slightly to the west of Tallinn.

It also seems natural that the most frequently hit nearshore areas are located in relatively narrow parts of the gulf where the drift time of potential adverse impacts from the fairway to the nearshore is comparatively short. The north-eastern nearshore of the gulf, from the entrance to the Neva Bight up to Vyborg, evidently has a persistently high probability of being hit. The nearshore areas between Hanko and Helsinki are frequently hit during most of the months. A similar frequently hit nearshore area seems to exist at the north-western coast of Estonia, between Tallinn and Hiiu. The safest nearshore areas are between Helsinki and Kotka and to the east of Tallinn up to Narva Bay.

The results reveal a considerable interannual and seasonal variability of the distributions of the analysed parameters. Its magnitude substantially exceeds an analogous level in the variations in the semi-persistent patterns of currents (Soomere et al., 2010) or in the location of the optimum fairway (Andrejev et al., 2011). This variability becomes evident already in terms of the percentage of the hits to the nearshore among the released tracers, the monthly values of which vary from 84% during the windy season down to 5% in the calm season.

The nearshore area at the north-eastern bayhead of the Gulf of Finland, to the south of Vyborg, was frequently hit almost all the time. On the one hand, the small internal Rossby radius (Nekrasov and Lebedeva, 2002) and the associated complexity of the hydrodynamics of this area evidently give rise to a high meso-scale activity. Although the resulting system of motions is probably not perfectly reproduced by the used model, the high level of meso-scale motions becomes evident in the modelled current fields as relatively intense cross-shore transport in this region during certain seasons (see Fig. 9 of Soomere et al., 2011c). This feature evidently contributes to the massive number of hits of the nearshore by tracers released along adjacent sections of the fairway. On the other hand, the overall counter-clockwise circulation of the Gulf of Finland (Alenius et al., 1998) merges in this area with the westward flow partially supported by the voluminous runoff from the River Neva (Andrejev et al., 2004a). The resulting persistent flow to the west may suppress the cross-shore transport and naturally protect this coastal section from pollution. A much higher-resolution study is necessary to properly resolve processes in this area.

The probabilities of a hit to the nearshore by an adverse impact released in different parts of the major fairway shed some light on how

dangerous different parts of the fairway are in terms of a drift of tracers from these sections to the nearshore. Most of the time in a year, a highly dangerous part evidently exists near the bayhead of the Gulf of Finland, to the south of Vyborg. Interestingly, the northernmost points of the model fairway provide a clearly greater danger during certain months while all the points at the given latitude provided a comparable level of danger from September to December. This suggests that even a small shift of the shipping line in the north–south direction may considerably change the probability of current-driven coastal pollution. This conjecture matches a similar conclusion of the current-driven tracers from the fairway to the marine protected areas in the Gulf of Finland (Delpeche-Ellmann and Soomere, 2013). Another part of the fairway posing a high threat to the nearshore apparently exists from slightly to the west of Tallinn to almost Hiiu. The safest section of the fairway is between Tallinn and Narva.

The performed simulations also revealed certain frequently hit nearshore areas, which were hit by particles originating in specific sections of the fairway. A few nearshore areas between Hanko and Helsinki were hit by particles originating in quite different fairway sections. Other three similar areas (an area to the south of Vyborg, a section of the NW coast of Estonia and the nearshore of Hiiu) were mostly hit by tracers stemming from the adjacent sections of the fairway. Still, the simulations did not reveal any long-term pattern of current-driven interconnections between specific parts of the fairway and single nearshore areas. This result may be expected as the circulation in the Gulf of Finland has extensive spatio-temporal variability. Such patterns may, however, exist during certain seasons and/or weather conditions but more data is necessary for their identification and analysis.

Acknowledgements

This study was a part of the BONUS+ project BalticWay, which attempted to propose ways to reduce pollution risks in the Baltic Sea by smart placing of human activities. The research was partially supported by the targeted financing by the Estonian Ministry of Education and Research (grant no. SF0140007s11), the Estonian Science Foundation (grant no. 9125) and by the European Union through the Mobilis grant MIT63 and the European Regional Development Fund (Centre of Excellence for Non-linear Studies CENS and the project 'Science-based forecast and quantification of risks to properly and timely react to hazards impacting Estonian mainland, air space,

water bodies and coasts' TERIKVANT). Comments and suggestions from three anonymous referees have been of great help towards improving the manuscript.

References

- Alenius, P., Myrberg, K., Nekrasov, A., 1998. Physical oceanography of the Gulf of Finland: a review. *Boreal Environ. Res.* 3, 97–125.
- Alenius, P., Nekrasov, A., Myrberg, K., 2003. The baroclinic Rossby–radius in the Gulf of Finland. *Cont. Shelf Res.* 23, 563–573.
- Alhimenko, A., Bolshev, A., Yakovlev, A., Klevanny, K., Liukkonen, S., 1997. Modelling oil pollution under ice cover. In: Chung, J.S., Frederking, R.M.W., Saeki, H., Bekker, A.T. (Eds.), Proceedings of the Seventh (1997) International Offshore and Polar Engineering Conference, pp. 594–601.
- Ambjörn, C., 2000. Modelling of trajectory and fate of spills. In: Rodriguez, G.R., Brebbia, C.A., PerezMartell, E. (Eds.), Environmental Coastal Regions III Environmental Studies Series, 5, pp. 33–40.
- Ambjörn, C., 2007. Seatrack Web, forecasts of oil spills, a new version. *Environ. Res. Eng. Manag.* (Aplinkos tyrimai, inžinerija ir vadyba) 3 (41), 60–66.
- Ambjörn, C., 2008. Seatrack Web forecasts and backtracking of oil spills – an efficient tool to find illegal spills using AIS. 2008 IEEE/OES US/EU-Baltic International Symposium, Tallinn, Estonia, May 27–29, 2008. IEEE, pp. 168–176.
- Andrejev, O., Myrberg, K., Alenius, P., Lundberg, P.A., 2004a. Mean circulation and water exchange in the Gulf of Finland – a study based on three-dimensional modelling. *Boreal Environ. Res.* 9, 1–16.
- Andrejev, O., Myrberg, K., Lundberg, P.A., 2004b. Age and renewal time of water masses in a semi-enclosed basin – application to the Gulf of Finland. *Tellus* 56A, 548–558.
- Andrejev, O., Sokolov, A., Soomere, T., Värvi, R., Viikmäe, B., 2010. The use of high-resolution bathymetry for circulation modelling in the Gulf of Finland. *Estonian J. Eng.* 16, 187–210.
- Andrejev, O., Soomere, T., Sokolov, A., Myrberg, K., 2011. The role of the spatial resolution of a three-dimensional hydrodynamic model for marine transport risk assessment. *Oceanologia* 53 (1–1T), 309–334.
- Aps, R., Herkül, K., Kotta, J., Kotta, I., Kopti, R., Leiger, R., Mander, U., Suursaar, Ü., 2009. Bayesian inference for oil spill related Net Environmental Benefit Analysis. In: Brebbia, C.A., Benassai, B., Rodriguez, G.R. (Eds.), Coastal Processes, pp. 235–246.
- Ardhuin, F., Marié, L., Rascale, N., Forget, P., 2009. Observation and estimation of Lagrangian, Stokes and Eulerian currents induced by wind and waves at the sea surface. *J. Phys. Oceanogr.* 39, 2820–2838.
- Brevik, Ø., Allen, Arthur A., Maisondieu, C., Roth, J.C., 2011. Wind-induced drift of objects at sea: the leeway field method. *Appl. Ocean Res.* 33 (2), 100–109.
- Broström, G., Carrasco, A., Hole, L.R., Dick, S., Janssen, F., Mattsson, J., Berger, S., 2011. Usefulness of high resolution coastal models for operational oil spill forecast: the Full City accident. *Ocean Sci.* 7, 805–820.
- Chang, Y.L., Oey, L., Xu, F.H., Lu, H.F., Fujisaki, A., 2011. 2010 oil spill: trajectory projections based on ensemble drifter analyses. *Ocean Dyn.* 61 (6), 829–839.
- de Vries, P., Döös, K., 2001. Calculating Lagrangian trajectories using time-dependent velocity fields. *J. Atmos. Ocean. Technol.* 18, 1092–1101.
- Deissenberg, C., Gurman, V., Rymina, E., Tsiirlin, A., 2001. An empirically tractable model of optimal oil spills prevention in Russian sea harbours. *Int. J. Environ. Pollut.* 15 (3), 301–309.
- Deleersnijder, E., Campin, J.-M., Delhez, E.J.M., 2001. The concept of age in marine modelling. I. Theory and preliminary model results. *J. Mar. Syst.* 28, 229–267.
- Delpêche-Elmann, N.C., Soomere, T., 2013. Investigating the marine protected areas most at risk of current-driven pollution in the Gulf of Finland, the Baltic Sea, using a Lagrangian transport model. *Mar. Pollut. Bull.* 67 (1–2), 121–129.
- Döös, K., 1995. Inter-ocean exchange of water masses. *J. Geophys. Res.* 100, C13499–C13514.
- Elofsson, K., 2010. The costs of meeting the environmental objectives for the Baltic Sea: a review of the literature. *Ambio* 39 (1), 49–58.
- Fingas, M.F., 2011. Buoys and devices for oil spill tracking. Proceedings of the 34th AMOP Technical Seminar on Environmental Contamination and Response. Environment Canada, Ottawa, pp. 213–228.
- Gästgifvars, M., Ambjörn, C., Funkquist, L., 2002. Operational modelling of the trajectory and fate of spills in the Baltic Sea. Proceedings of the 25th Arctic and Marine Oil-spill Program (AMOP) Technical Seminar. Environment Canada, Calgary, Canada, pp. 1115–1129.
- Gästgifvars, M., Lauri, H., Sarkanen, A.-K., Myrberg, K., Andrejev, O., Ambjörn, C., 2006. Modelling surface drifting of buoys during a rapidly-moving weather front in the Gulf of Finland, Baltic Sea. *Estuar. Coast. Shelf Sci.* 70, 567–576.
- Gottinger, H.W., 2001. Econometric modelling, estimation and policy analysis of oil spill processes. *Int. J. Environ. Pollut.* 15 (3), 333–363.
- Gucma, L., 2008. Evaluation of oil spills in the Baltic Sea by means of simulation model and statistical data. In: Soares, C.G., Kolev, P.N. (Eds.), Maritime industry, ocean engineering and coastal resources. 12th International Congress of the International Maritime Association of the Mediterranean, Varna, Bulgaria, September 02–06, 2007. (Proceedings and Monographs in Engineering Water and Earth Sciences). Int. Maritime Assoc. Mediterranean, vols. 1–2, pp. 1153–1159.
- Hela, I., 1952. Drift currents and permanent flow. *Soc. Sci. Fennica Comm. Phys-Math.* XVI (14) (Helsinki), 27 pp.
- HELCOM, 2009. In: Stankiewicz, M., Vlasov, N. (Eds.), Ensuring Safe Shipping in the Baltic. Helsinki Commission, Helsinki (18 pp.).
- Höglund, A., Meier, H.E.M., Broman, B., Kriez, E., 2009. Validation and Correction of Regionalised ERA-40 Wind Fields over the Baltic Sea using the Rossby Centre Atmosphere Model RCA3.0. Rapport Oceanografi No. 97. Swedish Meteorological and Hydrological Institute, Norrköping, Sweden (29 pp.).
- IMO, 2007. Particularly Sensitive Sea Areas. International Maritime Organisation, London.
- Johannessen, J.A., Le Traon, P.-Y., Robinson, I., Nittis, K., Bell, M.J., Pinardi, N., Bahurel, P., 2006. Marine environment and security for the European area – toward operational oceanography. *Bull. Am. Meteorol. Soc.* 87 (8), 1081–1088.
- Kachel, M.J., 2008. Particularly Sensitive Sea Areas. Hamburg Studies on Maritime Affairs, 13. Springer (376 pp.).
- Keramitsoglou, I., Cartalis, C., Kassomenos, P., 2003. Decision support system for managing oil spill events. *Environ. Manag.* 32 (2), 290–298.
- Kjellsson, J., Döös, K., 2013. Surface drifters and model trajectories in the Baltic Sea. *Boreal Environ. Res.* 17 (6), 447–459.
- Kostianoy, A.G., Litovchenko, K.T., Lebedev, S.A., Stanichny, S.V., Pichuzhkina, O.E., 2005. Operational satellite monitoring of oil spill pollution in the northeastern Baltic Sea. Oceans 2005 Europe International Conference, Brest, France, June 20–23, 2005. IEEE, pp. 182–183.
- Kostianoy, A.G., Ambjörn, C., Soloviev, D.M., 2008. Seatrack Web: a numerical tool to protect the Baltic Sea Marine Protected Areas. IEEE/OES US/EU-Baltic International Symposium, Tallinn, Estonia, May 27–29, 2008. IEEE, pp. 7–12.
- Köuts, T., Verjovkina, S., Lagema, P., Raudsepp, U., 2010. Use of lightweight on-line GPS drifters for surface current and ice drift observations. 2010 IEEE/OES US/EU-Baltic International Symposium, Riga, Latvia, August 25–27, 2010. IEEE (10 pp.).
- Lavrova, O., Bocharova, T., Kostianoy, A., 2006. Satellite radar imagery of the coastal zone: slicks and oil spills. In: Marcal, A. (Ed.), Global Developments in Environmental Earth Observation from Space, 25th Symposium of the European-Association-of-Remote-Sensing-Laboratories (EARSeL), University of Porto, Oporto, Portugal, June 06–11, 2005, pp. 763–771.
- Leppäranta, M., Myrberg, K., 2009. Physical Oceanography of the Baltic Sea. Springer Praxis, Berlin–Heidelberg–New York (378 pp.).
- Lilover, M.-J., Pavelson, J., Köuts, T., 2011. Wind forced currents over shallow Naissaar Bank in the Gulf of Finland. *Boreal Environ. Res.* 16 (Suppl. A), 164–174.
- Lončar, G., Leder, N., Paladini, M., 2012. Numerical modelling of an oil spill in the northern Adriatic. *Oceanologia* 54 (2), 143–173.
- Maximenko, N., Hafner, J., Niiler, P., 2011. Pathways of marine debris derived from trajectories of Lagrangian drifters. *Mar. Pollut. Bull.* 65 (1–3), 51–62.
- Meier, H.E.M., 2001. On the parameterization of mixing in three-dimensional Baltic Sea models. *J. Geophys. Res.* 106, C30997–C31016.
- Meier, H.E.M., 2007. Modeling the pathways and ages of inflowing salt- and freshwater in the Baltic Sea. *Estuar. Coast. Shelf Sci.* 74 (4), 610–627.
- Meier, H.E.M., Höglund, A., 2012. Environmentally safe areas and routes in the Baltic proper using Eulerian tracers. *Mar. Pollut. Bull.* 64 (7), 1375–1385.
- Meier, H.E.M., Döschner, R., Faxén, T., 2003. A multiprocessor coupled ice-ocean model for the Baltic Sea: application to salt inflow. *J. Geophys. Res.* 108 (C8) (Art. No. 3273).
- Melson, A., Counillon, F., LaCasce, J.H., Bertino, L., 2012. Forecasting search areas using ensemble ocean circulation modelling. *Ocean Dyn.* 62, 1245–1257.
- Mietus, M., 1998. The climate of the Baltic Sea Basin. (co-ordinator) Marine Meteorology and Related Oceanographic Activities, Report No. 41. World Meteorological Organisation, Geneva (64 pp.).
- Murawski, J., Nielsen, J.W., 2013. Applications of an oil drift and fate model for fairway design. In: Soomere, T., Quak, E. (Eds.), Preventive Methods for Coastal Protection: Towards the Use of Ocean Dynamics for Pollution Control. Springer, pp. 376–415.
- Myrberg, K., Ryabchenko, V., Isave, A., Vankevich, R., Andrejev, O., Bendtsen, J., Eichense, A., Funkquist, L., Inkalta, A., Neelov, I., Rasmus, K., Rodriguez Medina, M., Raudsepp, U., Passenkov, J., Söderkvist, J., Sokolov, A., Kuosa, H., Anderson, T.R., Lehmann, A., Skogen, M.D., 2010. Validation of three-dimensional hydrodynamic models in the Gulf of Finland based on a statistical analysis of a six-model ensemble. *Boreal Environ. Res.* 15 (5), 453–479.
- Nekrasov, A.V., Lebedeva, I.K., 2002. Estimation of baroclinic Rossby radii in Luga-Koporye region. *BFU Res. Bull.* 4–5, 89–93.
- Pahlke, H., 1985. Physikalische Grundlagen der mechanischen Ölbehandlung. Teil 3: Verhalten von Öllachen auf Wasser. Umweltforschungsplan des Bundesministers des Inneren, Forschungsbericht 12023 204/01 (185 pp., in German).
- Periañez, R., 2004. A particle-tracking model for simulating pollutant dispersion in the Strait of Gibraltar. *Mar. Pollut. Bull.* 49, 613–623.
- Reed, M., Aamo, O.M., 1994. Real time oil spill forecasting during an experimental oil spill in the Arctic ice. *Spill Sci. Technol. Bull.* 1, 69–77.
- Samuelsson, P., Jones, C.G., Willén, U., Ullerstig, A., Gollvik, S., Hansson, U., Jansson, C., Kjellström, E., Nikulin, G., Wyser, K., 2011. The Rossby Centre regional climate model RCA3: model description and performance. *Tellus A* 63, 4–23.
- Schwehr, K.D., McGillivray, P.A., 2007. Marine ship Automatic Identification System (AIS) for enhanced coastal security capabilities: an oil spill tracking application. Proceedings of the 2007 OCEANS Conference, Vancouver, Canada, September 29–October 04, 2007. IEEE, pp. 1131–1139.
- Segsneider, J., Sündermann, J., 1988. Simulating large scale transport of suspended matter. *J. Mar. Syst.* 14, 81–97.
- Soõäär, J., Jaagus, J., 2007. Long-term variability and changes in the sea ice regime in the Baltic Sea near the Estonian coast. *Proc. Estonian Acad. Sci. Eng.* 13, 189–200.
- Soomere, T., 2001. Extreme wind speeds and spatially uniform wind events in the Baltic Proper. *Proc. Estonian Acad. Sci. Eng.* 7, 195–211.
- Soomere, T., Quak, E., 2007. On the potential of reducing coastal pollution by a proper choice of the fairway. *J. Coast. Res. Spec. Issue* 50, 678–682.
- Soomere, T., Viikmäe, B., Delpêche, N., Myrberg, K., 2010. Towards identification of areas of reduced risk in the Gulf of Finland. *Proc. Estonian Acad. Sci.* 59, 156–165.

- Soomere, T., Andrejev, O., Myrberg, K., Sokolov, A., 2011a. The use of Lagrangian trajectories for the identification of the environmentally safe fairways. *Mar. Pollut. Bull.* 62, 1410–1420.
- Soomere, T., Berezovski, M., Quak, E., Viikmäe, B., 2011b. Modelling environmentally friendly fairways using Lagrangian trajectories: a case study for the Gulf of Finland, the Baltic Sea. *Ocean Dyn.* 61, 1669–1680.
- Soomere, T., Delpeche, N., Viikmäe, B., Quak, E., Meier, H.E.M., Döös, K., 2011c. Patterns of current-induced transport in the surface layer of the Gulf of Finland. *Boreal Environ. Res.* 16 (Suppl. A), 49–63.
- Tufte, L., Trieschmann, O., Hunsäenger, T., Barjenbruch, U., 2004. Spatial analysis and visualization of oil spill monitoring results of the North Sea and Baltic Sea. In: Ehlers, M., Posa, F., Kaufmann, H.J., Michel, U., DeCarolis, G. (Eds.), *Proceedings of the Conference on Remote Sensing for Environmental Monitoring, GIS Applications and Geology IV*, Maspalomas, Spain, September 14–16, 2004. *Proceedings of the Society of Photo-Optical Instrumentation Engineers (SPIE)*, 5574, pp. 90–99.
- Uiboupin, R., Raudsepp, U., Sipelgas, L., 2008. Detection of oil spills on SAR images, identification of polluters and forecast of the slicks trajectory. *IEEE/OES US/EU-Baltic International Symposium*, Tallinn, Estonia, May 27–29, 2008. *IEEE*, pp. 270–274.
- Vandenbulcke, L., Beckers, J.-M., Lenartz, F., Barth, A., Poulain, P.-M., Aidonidis, M., Meyrat, J., Arduin, F., Tonani, M., Fratianni, C., Torrisi, L., Pallela, D., Chiggiato, J., Tudor, M., Book, J.W., Martin, P., Peggion, G., Rixen, M., 2009. Super-ensemble techniques: application to surface drift prediction. *Prog. Oceanogr.* 82 (3), 149–167.
- Verjovkina, S., Raudsepp, U., Kõuts, T., Vahter, K., 2010. Validation of Seatrack Web using surface drifters in the Gulf of Finland and Baltic Proper. *2010 IEEE/OES US/EU-Baltic International Symposium*, Riga, Latvia, August 25–27, 2010. *IEEE* (7 pp.).
- Viikmäe, B., Soomere, T., Viidebaum, M., Berezovski, M., 2010. Temporal scales for transport patterns in the Gulf of Finland. *Estonian J. Eng.* 16, 211–227.
- Viikmäe, B., Torsvik, T., Soomere, T., 2013. Impact of horizontal eddy-diffusivity on Lagrangian statistics for coastal pollution from a major marine fairway. *Ocean Dyn.* 63 (5), 589–597.
- Wang, K., Lepparanta, M., Gästgifvars, M., Vainio, J., 2007. A comparison of drift between sea ice and oil spills in the Baltic Sea: the runner 4 case. In: Yue, Q.J., Ji, S.Y. (Eds.), *19th International Conference on Port and Ocean Engineering under Arctic Conditions (POAC 2007)*, Dalian Univ. Technology, Dalian, Peoples Republic of China, June 27–30, 2007. *Recent Development of Offshore Engineering in Cold Regions*, pp. 847–854.

Paper G

Viikmäe B., Torsvik T. and Soomere T. 2013. Impact of horizontal eddy-diffusivity on Lagrangian statistics for coastal pollution from a major marine fairway. *Ocean Dynamics*, 63(5), 589–597.

Impact of horizontal eddy diffusivity on Lagrangian statistics for coastal pollution from a major marine fairway

Bert Viikmäe · Tomas Torsvik · Tarmo Soomere

Received: 30 November 2012 / Accepted: 2 April 2013 / Published online: 26 April 2013
© Springer-Verlag Berlin Heidelberg 2013

Abstract Lagrangian trajectory methods are often applied as deterministic transport models, where transport is due strictly to advection without taking into account stochastic elements of particle dispersion, which raises questions about validity of the model results. The present work investigates the impact of horizontal eddy diffusivity for a case study of coastal pollution in the Gulf of Finland, where the pollutants are assumed to originate from a major fairway and are transported to the coast by surface currents. Lagrangian trajectories are calculated using the TRACMASS model from velocity fields calculated by the Rossby Centre circulation model for 1982 to 2001. Three cases are investigated: (1) trajectory calculation without eddy diffusivity, (2) stochastic modelling of eddy diffusivity with a constant diffusion coefficient and (3) stochastic modelling of eddy diffusivity with a time- and space-variable diffusion coefficient. It is found that the eddy diffusivity effect increases the spreading rate of initially closely packed trajectories and the number of trajectories that eventually reach the coast. The pattern of most frequently hit coastal sections, the probability of hit to each such section and the time the pollution spends offshore are virtually invariant with respect to inclusion of eddy diffusivity.

Responsible Editor: Martin Verlaan

Based on the presentation “Spatial Pattern of Hits to the Nearshore from a Major Marine Highway in the Gulf of Finland” to the 16th Biennial Workshop of the Joint Numerical Sea Modelling Group (JONSMOD)

This article is part of the Topical Collection on the *16th biennial workshop of the Joint Numerical Sea Modelling Group (JONSMOD) in Brest, France 21–23 May 2012*

B. Viikmäe (✉) · T. Torsvik · T. Soomere
Institute of Cybernetics at Tallinn University of Technology,
Akadeemia tee 21,
12618 Tallinn, Estonia
e-mail: bert@ioc.ee

Keywords Hydrodynamic modelling · Lagrangian transport · Statistics of currents · Baltic Sea · Pollution transport · Pollution control · Ship routing · Smagorinsky diffusion

1 Introduction

Lagrangian trajectory methods offer a convenient, and increasingly popular, framework for the study of flow-driven transport problems in the marine environment. They are used for applications such as the transport of fish eggs and larvae (Mariani et al. 2010), toxic algae (Havens et al. 2010), suspended particulate matter (Gräwe and Wolff 2010), oil pollution (Korotenko et al. 2004; Chrastansky and Callies 2009), or marine litter (Yoon et al. 2010), among others. Analysing transport by tracking individual particles over time provides several advantages compared to Eulerian tracer concentration methods, including the ability to backtrack particle trajectories to a specific place of origin and to easily extract measures depending on time integrated properties of individual agents. In many cases, perhaps in particular for simulations of ocean drift (de Vries and Döös 2001; Döös 1995), Lagrangian trajectories are calculated as a pure advection process which implicitly assumes that the velocity field gives a true representation of the flow at all relevant spatial and temporal scales. However, in practical applications, the velocity vectors represent the average flow characteristics over some spatial and temporal scales, in which case the disregard for subgrid-scale processes in the Lagrangian trajectory calculations is a controversial issue.

It is well known that the horizontal dispersion of substances floating on the sea surface is not only the result of molecular processes, but is enhanced by the effects of shearing and straining on length scales ranging from millimetres to kilometres and also normally involves the direct wind and

wave impact on objects and substances on the sea surface. This process not only leads to spreading of clusters of initially closely packed single tracers but may also substantially modify the trajectories of floating objects. Observations of horizontal diffusivity have traditionally been summarized in diffusion diagrams (Stommel 1949; Okubo 1971), which have demonstrated that the effective horizontal diffusivity varies with respect to the characteristic length scale L of the observations. For limited ranges of length scales, the effective horizontal diffusivity can be approximated by a power law L^P , where the power P is close to $4/3$ for small scales and is reduced to approximately 1.1 for large scales. A similar scale dependence of dispersion (but with somewhat different power laws) was recently demonstrated for surface drifters in the test area (Gulf of Finland) used in this study (Soomere et al. 2011d). A further complication of the problem is due to the fact that shearing and straining effects are not uniformly distributed in the ocean. This has led to the development of non-linear lateral diffusion models such as the Smagorinsky model (Smagorinsky 1963), which accounts for local deformations in the velocity field.

Particle diffusion can be modelled by using a random walk technique (Hunter et al. 1993; Visser 1997), formulated in such a way that properties of individual motion can be related to advection–diffusion-like equations governing the evolution of a continuous tracer field (Dimou and Adams 1993; Visser 2008). When applied to large-scale motion, the application of such diffusion models inevitably requires some form of parameterization of the eddy diffusivity. The horizontal eddy diffusivity associated with turbulent horizontal dispersion can vary over a few orders of magnitude in coastal environments, from approximately $0.1 \text{ m}^2/\text{s}$ up to about $10 \text{ m}^2/\text{s}$ (Sundermeyer and Ledwell 2001; Bogucki et al. 2005). A previous study of Lagrangian trajectories in the Baltic Sea region (Döös and Engqvist 2007) applied two different values for horizontal eddy diffusivity, 5 and $20 \text{ m}^2/\text{s}$, and found a slightly higher correlation between Lagrangian trajectories and tracer measurements when using the lower diffusion coefficient value.

There exist a number of recent studies where statistics of current-driven surface transport is presented, dealing with different adverse substances in the surface layer of the ocean (Korotenko et al. 2004; Chrastansky and Callies 2009; Havens et al. 2010; Yoon et al. 2010, and others). A series of studies have specifically focused on the approximate solution of an inverse problem related to oil spill propagation, investigating the risk of pollution from potential ship accidents to reach different parts of the coastal zone, with the goal of identifying the regions where it is safer to travel in terms of minimising either the coastal pollution (Soomere et al. 2010, 2011a, b, c; Meier and Höglund 2012) or the impact to the marine protected areas (Delpeche-Ellmann and Soomere 2013). These studies rely on the calculation of Lagrangian trajectories

for passive tracers, where the displacement is due exclusively to advection within numerically modelled velocity fields. The presence of subgrid-scale processes eventually modifies the particle trajectories. While on shorter time scales and for relatively small basins of regular shape this modification apparently does not considerably affect the statistics of large ensembles of trajectories, for longer time scales (exceeding the typical turnover time of synoptic eddies), the distortions of the trajectories may be large enough to affect the entire transport patterns. Such distortions may have significant influence on the solutions for the optimum location of the fairway (Meier and Höglund 2012), the “corridor” for safe operation (Soomere et al. 2011b), place for refuge for ships in distress or the stress to the marine protected areas (Delpeche-Ellmann and Soomere 2013), or the equiprobability line that divides the potential costs of accidents between the opposite coasts (Soomere et al. 2010).

The present study focuses on the effect that the inclusion of subgrid-scale motions may have on the transport patterns estimated from large sets of the purely advective Lagrangian trajectories. It is natural to assume that the effect of inclusion of such motions, for example, in terms of horizontal eddy diffusivity, will considerably impact single Lagrangian trajectories. It is, however, unclear whether or how strongly the resulting statistics is affected. In the present paper, the focus is on the simulated transport of various substances and pollution in the uppermost layer of the sea from a major fairway in the Gulf of Finland to the coastal regions north and south of the fairway. The aim is to estimate how large an impact the eddy diffusivity is likely to have on previous results of coastal risk assessment.

2 Modelling environment

The 3D velocity fields simulated for 1982–2001, provided by the Swedish Meteorological and Hydrological Institute, were used in this study for calculations of trajectories of potential adverse impacts. The Rossby Centre Ocean circulation model (RCO) was used to calculate the Eulerian velocity fields. This model has a horizontal grid resolution of 2×2 nautical miles (nmi), which is considered acceptable with regard to meso-scale dynamics in the open part of the Baltic Sea (Meier et al. 2003; Meier 2007). Typical values of the internal Rossby radius in the Gulf of Finland are 2–4 km (Alenius et al. 2003); hence, this implementation of the RCO model is barely eddy permitting for the area of interest (cf. Albreten and Røed 2010), and an accurate representation of mesoscale eddies cannot be expected. The model uses 41 vertical z -coordinate levels, where the thickness of the vertical layers varies between 3 m close to the surface and 12 m at 250-m depth. A time step splitting scheme is used, with the choice of 150 s for

the baroclinic and 15 s for the barotropic time step. The RCO model is a Bryan–Cox–Semtner primitive equation circulation model following Webb et al. (1997) with a free surface (Killworth et al. 1991) and open boundary conditions (Stevens 1991) in the northern Kattegat. It includes an advanced sea ice model (Meier et al. 2003), which accounts for the influence of sea ice on the surface currents. However, the model does not account for the roughness of the lower surface of the ice (e.g. ridging). A turbulence closure scheme of the k - ϵ type with flux boundary conditions is used to parameterize subgrid-scale mixing to include the effect of a turbulence-enhanced layer due to breaking surface gravity waves (Meier 2001). A flux-corrected, monotonicity-preserving transport scheme following Gerdes et al. (1991) is embedded. No explicit horizontal diffusion is applied.

The model is forced with 10 m wind, 2 m air temperature, 2 m specific humidity, precipitation, total cloudiness and sea level pressure fields from a regionalization of the ERA-40 re-analysis over Europe using a regional atmosphere model with a horizontal resolution of 25 km (Samuelsson et al. 2011). As the atmospheric model tends to underestimate wind speed extremes, to improve the wind statistics, the wind is adjusted using simulated gustiness (Samuelsson et al. 2011). To calculate the air–sea fluxes over open water and over sea ice, standard bulk formulae are used. For further details of the model set-up and an extensive validation of the model output, we refer the reader to Meier (2001, 2007) and Meier et al. (2003).

The RCO model provides a variety of outputs, but for the Lagrangian trajectory analysis of surface layer transport, we only employ the horizontal velocity fields in the uppermost layer that is responsible for advection due to currents in the water sheet at depths 0–3 m. The output is stored once in 6 h to keep the size of output information at a reasonable level. A comprehensive comparison of the performance of the RCO model in the Gulf of Finland against several other state-of-the-art circulation models is provided in Myrberg et al. (2010).

The current-driven paths of single passive tracers (representing, e.g. certain adverse impacts on the sea surface) are analysed with the use of a Lagrangian trajectory model, TRACMASS (Döös 1995; de Vries and Döös 2001). The model accepts pre-computed 3D Eulerian velocity fields as input data and computes particle advection at any point within the computational domain at any given time instance by using local linear interpolation of the velocity field in both space and time. As we are specifically interested in surface transport patterns, the test particles are locked in the uppermost layer as in Soomere et al. (2010) and Andrejev et al. (2010). The resulting trajectories are therefore not exactly representative for truly passive, neutrally buoyant tracer particles, but represent current-driven motion of objects that are slightly lighter than the surrounding water (e.g. oil in otherwise calm conditions, or lost containers).

3 Method

Lagrangian particle trajectories are simulated for particles seeded along a line covering three model grid cells (6 nmi or about 11 km) in the north–south direction that roughly follows the major fairway from the Baltic Proper to Saint Petersburg (Fig. 1). Trajectories are calculated over several days (Soomere et al. 2010; Viikmäe et al. 2010), and the coordinates of the instantaneous trajectory points are saved every 6 h. The resulting trajectories evidently depend on the update time interval for the input current velocity data as well as on the temporal resolution of the trajectory calculation scheme. Previous experience with non-diffusive TRACMASS simulations has shown that simulated particle patches disperse much slower than real drifters (Jönsson et al. 2004; Engqvist et al. 2006; Döös and Engqvist 2007; Döös et al. 2008). This is to be expected since the particles are transported by velocity fields that are steady over the update time interval and do not contain information about subgrid-scale turbulent motions. In order to obtain more realistic particle dispersion, a stochastic eddy diffusivity term is included in the Lagrangian model. The analysis involves three different datasets of trajectories: (1) non-diffusive simulation, (2) particle diffusion with a constant value horizontal diffusion coefficient and (3) particle diffusion with a horizontal diffusion coefficient which is variable in time and space, calculated by the Smagorinsky model.

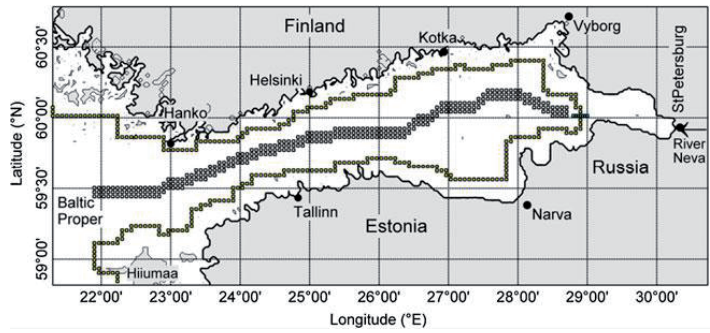
3.1 Spatial and temporal properties

Particles were seeded at the centre of each of the 309 grid cells along the fairway, and trajectories were calculated for time windows of 20 days. Particles were released on the first day of each month, with subsequent simulations following at 5-day intervals, giving a total of six runs per month (with time windows sometimes extending to the middle of the following month). The final analysis only includes trajectories that at some time enter the nearshore region (Fig. 1) within the 20-day simulation time window. For each such trajectory, the initial location of the tracer, the point at which the trajectory reaches a nearshore point for the first time and the time elapsed from the release of the tracer (particle age) (Andrejev et al. 2011) are saved. These events are called nearshore hits. The total number of time windows used during the 20-year simulation was 1,440 and resulted in 444,960 single trajectories.

3.2 Particle diffusion

Particle diffusion is modelled as a random walk process, where a random displacement is added to the trajectory position at each time step Δt in the simulation. The scheme was introduced in TRACMASS by Levine (2005) and applied recently by Döös et al. (2011). The horizontal

Fig. 1 Initial location of tracer particles and the border of the three-grid-cell-wide nearshore region in the Gulf of Finland. The “southern” and “northern” parts of the nearshore are separated at 60°N in the eastern part of the model area



displacements x_d and y_d are stochastic variables calculated by

$$x_d = \sqrt{-4A_H \Delta t \log(1 - q_1)} \cos(2\pi q_2), \tag{1}$$

$$y_d = \sqrt{-4A_H \Delta t \log(1 - q_1)} \sin(2\pi q_2), \tag{2}$$

where A_H is the horizontal eddy diffusion coefficient, and q_1 and q_2 are uniformly distributed random numbers between 0 and 1. The added horizontal displacement relative to the original position of the particle is

$$r_H = \sqrt{x_d^2 + y_d^2} = \sqrt{-4A_H \Delta t \log(1 - q_1)}. \tag{3}$$

The horizontal constant eddy diffusion coefficient A_H was set to 5 m²/s which, based on results from previous studies (Döös and Engqvist 2007), is a reasonable value for the Gulf of Finland.

The uniform eddy diffusivity model presented above provides a simple but rather crude representation of subgrid-scale turbulent effects. A slightly more elaborate representation of the eddy diffusivity is achieved by allowing the eddy diffusion coefficient to vary in space and time. A simple scheme was proposed by Smagorinsky (1963):

$$A_H = \lambda \Delta x \Delta y \left[\left(\frac{\partial u}{\partial x} - \frac{\partial v}{\partial y} \right)^2 + \left(\frac{\partial u}{\partial y} + \frac{\partial v}{\partial x} \right)^2 \right]^{\frac{1}{2}}, \tag{4}$$

where u and v denote the zonal and meridional velocity components, Δx and Δy are the zonal and meridional grid increments, respectively, and λ is an adjustment factor. The Smagorinsky formula makes the diffusion coefficient dependent on the deformation of the velocity field, introducing stronger diffusion where the deformation is large. The adjustment factor λ is typically set to a constant value in the range 0.05 to 0.2 (Haidvogel and Beckmann 1999), and a constant value of 0.05 has been used in the following analysis.

The use of a spatially variable eddy diffusion coefficient requires modification of the original displacement Eqs. (1) and

(2). Visser (2008) showed that a random walk particle tracking model would tend to accumulate particles in areas with low diffusivity, violating the principle that a uniform distribution should be maintained in a diffusive process. An additional drift term depending on the gradient of the eddy diffusion coefficient is required in order to maintain consistency with the diffusion equation (Visser 2008; Brickman and Smith 2002; Gräwe 2011; Shah et al. 2011). This is accomplished by modifying the displacement equations

$$x_d = \sqrt{-4A_H \Delta t \log(1 - q_1)} \cos(2\pi q_2) + \frac{\partial A_H}{\partial x} \Delta t, \tag{5}$$

$$y_d = \sqrt{-4A_H \Delta t \log(1 - q_1)} \sin(2\pi q_2) + \frac{\partial A_H}{\partial y} \Delta t. \tag{6}$$

Note that the original Eqs. (1) and (2) are retained as a special case when the eddy diffusion coefficient is constant.

4 Results

The effect of eddy diffusivity on the statistics of trajectories can be quantified by analysing spreading of patches of particles. A simple test case was constructed in order to illustrate this effect for particle trajectories in the Gulf of Finland. Particles were seeded within four box areas, called patches below, consisting of 5 × 5 grid cells, with a cluster of four particles seeded within each grid cell, altogether 400 particles (Fig. 2a). Trajectories were simulated over a time window of 4 days, starting from April 17, 1987, which covers a period with unusually strong variability in the surface current field. The maximum separation among the four particle clusters within each grid cell was calculated at the end of the simulation run.

Panels b, c and d of Fig. 2 show the maximum separation distance within each cluster of four particles seeded within single grid cells. There is a clear difference between results without eddy diffusivity, where the maximum separation was in the range of 1–4 km, and the results which included

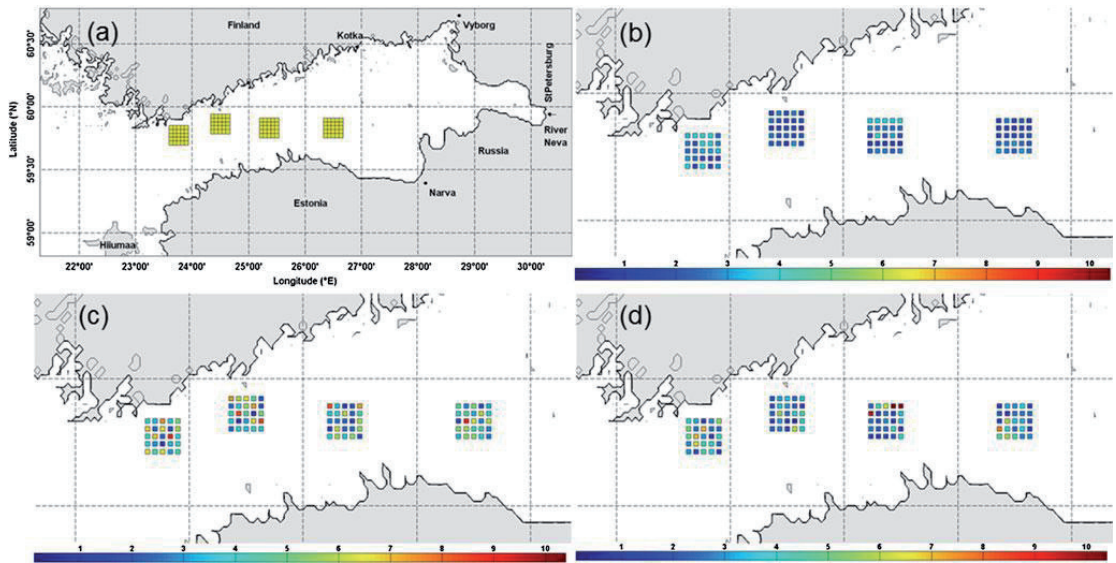


Fig. 2 The figure panels show the four patches of particle seeding areas **(a)** and the maximum particle separation for each four-particle cluster seeded within a grid cell for the three different methods: **b** no eddy diffusivity, **c**

eddy diffusivity with a constant diffusion coefficient, **d** eddy diffusivity with a time- and space-variable diffusion coefficient. The grid cell colour corresponds to a distance as shown by the *colour bar* [km]

particle diffusion, where the maximum separation was in the range of 1–10 km. While there may be some coherent structures that lead to large separation distances in the non-diffusive case, the separation distance is highly variable even between neighbouring grid cells when eddy diffusivity is included, especially for the constant eddy diffusivity.

The mean separation distance within each of the four patches is given in Table 1. The largest separation distance is in patch 1, regardless of model method, which corresponds to a region with locally strong surface currents. The inclusion of constant eddy diffusivity increased the maximum particle separation by roughly a factor of two. The variance in separation distance is about 0.6–1.2 km without eddy diffusivity in different patches and increases even more, to about 1.9–2.4 km with constant eddy diffusivity. The Smagorinsky model, which resulted in slightly smaller separation distances than the constant diffusivity case, may have equally large variability in regions with strong velocity field deformation, but comes closer to the non-diffusive results in less dynamic areas. Figure 3 shows the spatial variability of

the Smagorinsky diffusion coefficient at a single time instance. There is considerable variability due to velocity field deformations, but the strong responses are confined to localized patches. In most of the model area, the Smagorinsky diffusion coefficient is close to the selected constant diffusion coefficient value of 5 m²/s. Results in Fig. 3 represent an extreme event, and in most cases, the maximum values and variability of the Smagorinsky eddy diffusion coefficient would be considerably lower.

4.1 Frequently hit nearshore areas: non-diffusive case

Lagrangian trajectories of particles seeded along the fairway (Fig. 1) have been calculated for the period 1982–2001, with six simulations per month, giving a total of 1,440 simulation runs. The following analysis is based on annually averaged percentages of coastal hits. Interannual variability of the monthly mean patterns of transport has been discussed in Viikmäe and Soomere (Spatial pattern of current-driven hits to the nearshore from a major marine highway in the Gulf of Finland. *J Marine Syst.*, *submitted*).

Table 1 Mean values of maximum particle separation distance for each of the four patches, numbered from west to east

	Patch 1	Patch 2	Patch 3	Patch 4
No diffusion	1.9±1.2 km	1.4±0.9 km	1.8±1.0 km	1.4±0.6 km
Constant diffusion	3.0±2.2 km	2.9±2.4 km	2.6±2.0 km	2.8±1.9 km
Smagorinsky diffusion	2.4±1.8 km	1.9±1.5 km	2.3±2.4 km	2.2±1.6 km

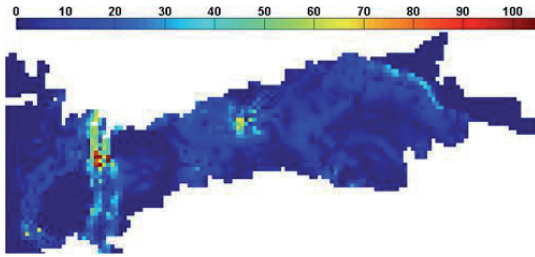


Fig. 3 Spatial variation of the Smagorinsky horizontal eddy diffusion coefficient

Figure 4 shows areas of high coastal hit probability for a few selected years. The north-eastern (NE) nearshore of the gulf, from the entrance to the Neva Bight up to Vyborg, had constantly a large probability of being hit. During almost all the years from 1982 to 2001, the most frequently hit nearshore areas (marked by red circles) of the southern coast were slightly to the west of Tallinn, near 24°00'E. In 1983, 1995 and 1997, this region extends to the entrance of the Gulf of Finland at 22°00'E and in 1989, 1991, 1993 and 1997 to the east of Tallinn up to 25°30'E and even to 25°50'E. The northern coast received hits mostly between Hanko and Helsinki and to the NE nearshore of the gulf, from the entrance to the Neva Bight up to Vyborg. The coastal region between Hanko and Helsinki had a few (one to four) frequently hit nearshore points during most of the years, except in 1985, 1989 and 1994, when this region received only a low (blue circles) or medium (green circles) number of hits.

The area near the entrance to the Neva Bight up to Vyborg was frequently hit during all the years. The area to

Table 2 Total number of nearshore hits calculated with different methods

Method	Total number of nearshore hits (1982–2001)	Percent of the total number of single trajectories
No diffusion	142,052	31.92
Constant diffusion	149,853	33.68
Smagorinsky diffusion	149,315	33.56

the west of Tallinn received a high number of hits during almost all the years from 1982 to 2001, except 1985 and 1986. The nearshore region to the east of Tallinn, reaching almost to 26°00'E, had most frequent hits in 1989, 1991, 1993 and 1997. The less frequently hit coastal areas were between Helsinki and Kotka for the northern coast and for the southern coast Narva Bay and also slightly to the west of Narva Bay. In 1987, 1996 and 1998–2000, Narva Bay had almost no hits. The highest number of frequently hit nearshore areas (11–13 nearshore points) occurred in 1983, 1993, 1995 and 1997, and the lowest number (three to four nearshore points) occurred in 1985, 1986, 1987 and 1994 (Fig. 4).

4.2 The effect of particle diffusion on coastal hits

Simulations presented in the previous section were repeated using the particle diffusion model with constant and Smagorinsky diffusion coefficients. In spite of the substantial changes to the statistics of spreading of initially closely located tracers, the differences in the total number of

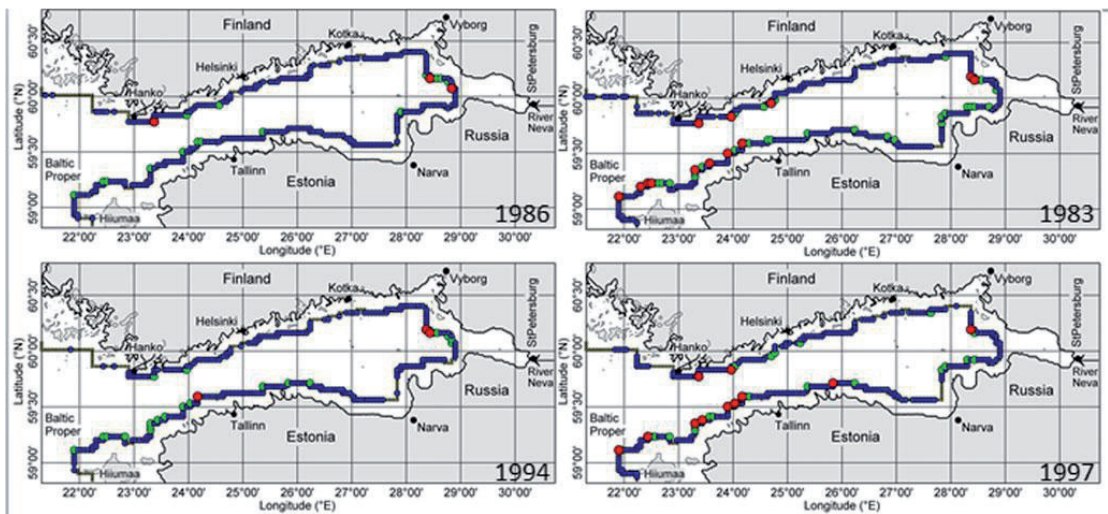
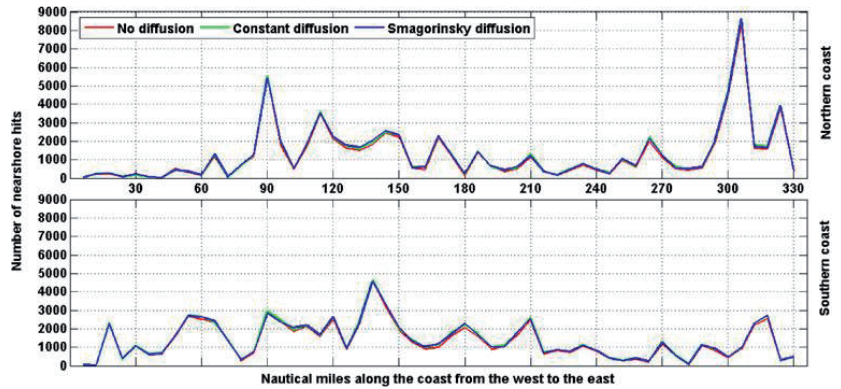


Fig. 4 The years with the lowest number of frequently hit nearshore areas (three nearshore points, left panels) and the years with the highest number (11–13 nearshore points, right panels)

Fig. 5 The most frequently hit nearshore areas averaged for the period 1982–2001 for the northern (*upper panel*) and southern coast (*lower panel*) of the Gulf of Finland. The *x*-axis is the distance along the coast [nmi], from the west of the gulf, near Hanko in the north and Hiiumaa in the south, to the eastern end of the gulf, near River Neva



nearshore hits for 1982–2001 calculated with all three methods were found to be less than 2 % (Table 2).

The distribution of coastal hits along the northern and southern coastlines of the Gulf of Finland averaged over 20 years (Fig. 5) confirms that the main features of this distribution almost do not change when eddy diffusivity is included into the model. It is interesting to note that the regions where the results of purely advective simulations depart from those obtained using the eddy diffusivity model are not primarily at the extremes. In other words, the rate of hits to the regions that are extremely exposed to or completely sheltered from coastal hits remains unchanged, and small variations only occur in regions that receive a moderate level of coastal hits. A possible interpretation of this result is that the eddy diffusivity contributes to pushing particles into less dominant parts of the coastal currents, but the count of hits at sections corresponding to peaks in Fig. 5 is not reduced since the total number of coastal hits increases.

4.3 Probability and time for nearshore hits

The number of coastal hits over the 20-year period 1982–2001 ranged from a minimum of 21 % (4,700 trajectories) in 1985 to a maximum of 42 % (9,400 trajectories) in 1995. Figure 6 shows the variation in coastal hits per year and the annual average time (called particle age below) for the particles to drift from the source area until the coast. The mean value of coastal hits for the entire 20-year period was 31.9 %. The 5-year average values (29.6 % for 1982–1986; 32.5 % for 1987–1991; 34 % for 1992–1996; 31.5 % for 1997–2001) do not seem to indicate any long-term trend.

The mean particle age for nearshore hits for the 1982–2001 simulation period was 16–18 days, with the highest value in 1985 and the lowest in 1995. The mean value for 1982–2001 was 17 days (Fig. 6). The effect of eddy diffusivity is thus to very slightly increase the number of coastal hits by about 1–2 % in single years and to reduce the average time it takes for particles to reach the coast, by less

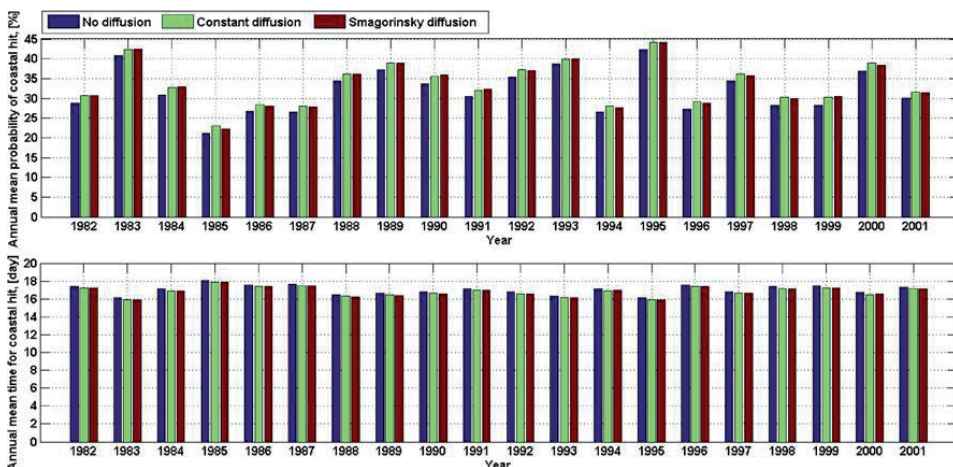


Fig. 6 The annual mean nearshore hit probabilities (*upper panel*) and annual mean particle age for nearshore hits (*lower panel*) for 1982–2001

than 0.5 days. The simulated results with eddy diffusivity follow closely the non-diffusive results for each year. It is clear that the interannual variability is significantly larger than the variability caused by eddy diffusivity for these coastal hits results.

5 Discussion and concluding remarks

The inclusion of a classical representation of the impact of subgrid-scale processes, as expected, had considerable impact on the spreading of Lagrangian trajectories and, consequently, on several key properties of the statistics of transport. Clear modifications exist for the statistics of purely advective transport in terms of the spreading rate and the increase in the average distance of the tracers from their release site. Interestingly, several other statistical properties of the transport were almost insensitive with respect to the presence or absence of subgrid-scale processes. Most importantly, the statistics of the transport of the tracers to the coastal areas and of the time it took until the tracer reached the nearshore remained essentially unchanged. In addition, the spatial pattern of frequently hit coastal areas remains practically the same after the inclusion of eddy diffusivity.

Although random velocity components are often included in Lagrangian trajectory models to represent the effects of diffusion, the actual effect of the diffusion component is often not reported. Döös and Engqvist (2007) reported on the impact of diffusion with respect to the average age of particles within a specific region. In such case, where the random walk process may easily move a particle from one grid cell to the neighbour, the local diffusion can have significant impact in prolonging or shortening the residence time. However, since the velocity field in which the particles are advected is relatively smooth, due to limitations of the underlying ocean model, the general direction of movement is only slightly influenced by a random jump from one grid cell to the next. In a locally homogeneous velocity field, the long-term drift of particles is not significantly influenced by diffusion. Therefore, the sensitivity to particle diffusion mostly comes into consideration when particles are in the immediate vicinity of the coastal zone. This can explain why the maxima of coastal hits do not shift when particle diffusion is included. However, we do see evidence of a slightly higher coastal hit frequency in the less exposed regions where, in the absence of a velocity vector directed to the coast, particle diffusion contributes to displace particles towards the coast.

It should be noted that adding anisotropic disturbances (surface waves, wind) may result in a shift of the peak of the probability distribution along the coast. Chrastansky and Callies (2009) suggested to add an extra wind-induced drift component of 1.8 % of the 10-m wind, but did not report on

the impact of this wind-induced drift component on the final results. Correlations between mean sea level pressure fields and particle advection to five coastal target areas were found to be significant for some areas in the winter season and insignificant for the summer season, so a general conclusion about the direct wind input effect could not be drawn. For our study area in the Gulf of Finland, we have not had high-resolution wind data available to include a wind-induced drift component in our model and have therefore not undertaken a study of this effect.

The stability of the results with respect to horizontal diffusion nevertheless suggests that the distributions of the probability of coastal hits and the time it takes for the tracer (or pollution) to reach the coast (Soomere et al. 2011a) are generally insensitive with respect to the nature of subgrid processes and are basically defined by large-scale and mesoscale advection, the main features of which can be replicated using ocean models of moderate resolution. Moreover, this result suggests that the pattern of coastal areas that are frequently hit by adverse impacts (pollution, litter) from the offshore is also largely invariant with respect to the details of the Lagrangian transport models and the methods of accounting for subgrid-scale processes. Another implicit consequence from the presented results is that the estimates for the basin-wide distribution of the probabilities of coastal hits by surface-driven pollution and the time it takes for the pollution to reach the coast (Andrejev et al. 2011; Soomere et al. 2011c) apparently are also largely invariant with respect to the way of accounting for the impact of subgrid processes.

Acknowledgments This work, motivated by the BONUS+ project BalticWay, was supported by the European Union through the Mobilitas grant MTT63 and through support to the Estonian Centre of Excellence for Non-linear Studies (CENS) from the European Regional Development Fund, targeted financing by the Estonian Ministry of Education and Research (grant SF0140007s11) and the Estonian Science Foundation (grant no. 9125). We are grateful to Anders Höglund (SMHI) who extracted and prepared the RCO model data.

References

- Albretsen J, Røed LP (2010) Decadal simulations of mesoscale structures in the northern North Sea/Skagerrak using two ocean models. *Ocean Dyn* 60:933–955
- Alenius P, Nekrasov A, Myrberg K (2003) The baroclinic Rossby-radius in the Gulf of Finland. *Cont Shelf Res* 23:563–573
- Andrejev O, Sokolov A, Soomere T, Värvi R, Viikmäe B (2010) The use of high resolution bathymetry for circulation modelling in the Gulf of Finland. *Estonian J Eng* 16:187–210
- Andrejev O, Soomere T, Sokolov A, Myrberg K (2011) The role of the spatial resolution of a three-dimensional hydrodynamic model for marine transport risk assessment. *Oceanologia* 53(1-TI):309–334
- Bogucki DJ, Jones BH, Carr M-E (2005) Remote measurements of horizontal eddy diffusivity. *J Atm Ocean Technol* 22:1373–1380

- Brickman D, Smith PC (2002) Lagrangian stochastic modelling in coastal oceanography. *J Atmos Oceanic Tech* 19:83–99
- Chrastansky A, Callies U (2009) Model-based long-term reconstruction of weather-driven variations in chronic oil pollution along the German North Sea coast. *Mar Pollut Bull* 58:967–975
- de Vries P, Döös K (2001) Calculating Lagrangian trajectories using time-dependent velocity fields. *J Atmos Ocean Technol* 18:1092–1101
- Delpeche-Ellmann NC, Soomere T (2013) Investigating the marine protected areas most at risk of current-driven pollution in the Gulf of Finland, the Baltic Sea, using a Lagrangian transport model. *Mar Pollut Bull*. doi:10.1016/j.marpolbul.2012.11.025
- Dimou K, Adams E (1993) A random-walk, particle tracking model for well-mixed estuaries and coastal waters. *Estuar Coast Shelf Sci* 37:99–110
- Döös K (1995) Inter-ocean exchange of water masses. *J Geophys Res* 100:C13499–C13514
- Döös K, Engqvist A (2007) Assessment of water exchange between a discharge region and the open sea—a comparison of different methodological concepts. *Estuar Coast Shelf Sci* 74:585–597
- Döös K, Nycander J, Coward AC (2008) Lagrangian decomposition of the Deacon Cell. *J Geophys Res* 113, C07028
- Döös K, Ruppel V, Brodeau L (2011) Dispersion of surface drifters and model-simulated trajectories. *Ocean Model* 39:301310
- Engqvist A, Döös K, Andrejev O (2006) Modeling water exchange and contaminant transport through a Baltic coastal region. *Ambio* 35:435–447
- Gerdes R, Köberle C, Willebrand J (1991) The influence of numerical advection schemes on the results of ocean general circulation models. *Clim Dyn* 5:211–226
- Gräwe U, Wolff J-O (2010) Suspended particulate matter dynamics in a particle framework. *Envir Fluid Mech* 10:21–39
- Gräwe U (2011) Implementation of high-order particle-tracking schemes in a water column model. *Ocean Model* 36:80–89
- Haidvogel DB, Beckmann A (1999) Numerical ocean circulation modeling. Imperial College Press, London, 344 pp
- Havens H, Luther ME, Meyers SD, Heil CA (2010) Lagrangian particle tracking of a toxic dinoflagellate bloom within the Tampa Bay estuary. *Mar Pollut Bull* 60:2233–2241
- Hunter JR, Craig PD, Phillips HE (1993) On the use of random walk models with spatially variable diffusivity. *J Comp Phys* 106:366–376
- Jönsson B, Lundberg P, Döös K (2004) Baltic sub-basin turnover times examined using the Rossby Centre Ocean Model. *Ambio* 23:257–260
- Killworth P, Stainforth D, Webb D, Paterson S (1991) The development of a free-surface Bryan-Cox-Semtner ocean model. *J Phys Oceanogr* 21:1333–1348
- Korotenko KA, Mamedov RM, Kontar AE, Korotenko LA (2004) Particle tracking method in the approach for prediction of oil slick transport in the sea: modelling oil pollution resulting from river input. *J Marine Syst* 48:159–170
- Levine RC (2005) Changes in shelf waters due to air-sea fluxes and their influence on the Arctic Ocean circulation as simulated in the OCCAM global ocean model. PhD thesis, University of Southampton, Faculty of Engineering Science and Mathematics, School of Ocean and Earth Science, 225 pp
- Mariani P, MacKenzie BR, Iudicone D, Bozec A (2010) Modelling retention and dispersion mechanisms of bluefin tuna eggs and larvae in the northwest Mediterranean Sea. *Prog Oceanogr* 86:45–58
- Meier HEM (2001) On the parameterization of mixing in three-dimensional Baltic Sea models. *J Geophys Res* 106:C30997–C31016
- Meier HEM (2007) Modeling the pathways and ages of inflowing salt- and freshwater in the Baltic Sea. *Estuar Coast Shelf Sci* 74(4):610–627
- Meier HEM, Höglund A (2012) Environmentally safe areas and routes in the Baltic Proper using Eulerian tracers. *Mar Pollut Bull* 64:1375–1385
- Meier HEM, Dööscher R, Faxén T (2003) A multiprocessor coupled ice-ocean model for the Baltic Sea: application to salt inflow. *J Geophys Res* 108(C8):3273
- Myrberg K, Ryabchenko V, Isaev A, Vankevich R, Andrejev O, Bendtsen J, Erichsen A, Funkquist L, Inkala A, Neelov I, Rasmus K, Rodriguez Medina M, Raudsepp U, Passenko J, Söderkvist J, Sokolov A, Kuosa H, Anderson TR, Lehmann A, Skogen MD (2010) Validation of three-dimensional hydrodynamic models in the Gulf of Finland based on a statistical analysis of a six-model ensemble. *Boreal Environ Res* 15(5):453–479
- Okubo A (1971) Oceanic diffusion diagrams. *Deep-Sea Res* 18:789–802
- Samuelsson P, Jones CG, Willén U, Ullerstig A, Gollvik S, Hansson U, Jansson C, Kjellström E, Nikulin G, Wyser K (2011) The Rossby Centre regional climate model RCA3: model description and performance. *Tellus A* 63:4–23
- Shah SHAM, Heemink AW, Deleersnijder E (2011) Assessing Lagrangian schemes for simulating diffusion on non-flat isopycnal surfaces. *Ocean Model* 39:351–361
- Soomere T, Viikmäe B, Delpeche N, Myrberg K (2010) Towards identification of areas of reduced risk in the Gulf of Finland. *Proc Estonian Acad Sci* 59:156–165
- Soomere T, Andrejev O, Myrberg K, Sokolov A (2011a) The use of Lagrangian trajectories for the identification of the environmentally safe fairways. *Mar Pollut Bull* 62:1410–1420
- Soomere T, Berezovski M, Quak E, Viikmäe B (2011b) Modelling environmentally friendly fairways using Lagrangian trajectories: a case study for the Gulf of Finland, the Baltic Sea. *Ocean Dyn* 61:1669–1680
- Soomere T, Delpeche N, Viikmäe B, Quak E, Meier HEM, Döös K (2011c) Patterns of current-induced transport in the surface layer of the Gulf of Finland. *Boreal Environ Res* 16(Suppl A):49–63
- Soomere T, Viidebaum V, Kalda J (2011d) On dispersion properties of surface motions in the Gulf of Finland. *Proc Estonian Acad Sci* 60(4):269–279
- Smagorinsky J (1963) General circulation experiments with the primitive equations. *Mon Wea Rev* 91(3):99–164
- Stevens DP (1991) A numerical ocean circulation model of the Norwegian and Greenland Seas. *Prog Oceanogr* 27(3–4):365–402
- Stommel H (1949) Horizontal diffusion due to oceanic turbulence. *J Marine Res* 8:199–255
- Sundermeyer MA, Ledwell JR (2001) Lateral dispersion over the continental shelf: analysis of dye release experiments. *J Geophys Res* 106(5):9603–9621
- Viikmäe B, Soomere T, Viidebaum M, Berezovski M (2010) Temporal scales for transport patterns in the Gulf of Finland. *Estonian J Eng* 16:211–227
- Visser AW (1997) Using random walk models to simulate the vertical distribution of particles in a turbulent water column. *Marine Ecol Progr Series* 158:275–281
- Visser AW (2008) Lagrangian modelling of plankton motion: from deceptively simple random walks to Fokker-Planck and back again. *J Marine Syst* 70:287–299
- Webb DJ, Coward AC, de Cuevas BA, Gwilliam CS (1997) A multiprocessor ocean circulation model using message passing. *J Atmos Oceanic Technol* 14:175–183
- Yoon J-H, Kawano S, Igawa S (2010) Modeling of marine litter drift and beaching in the Japan Sea. *Mar Pollut Bull* 60:448–463

**DISSERTATIONS DEFENDED AT
TALLINN UNIVERSITY OF TECHNOLOGY ON
CIVIL ENGINEERING**

1. **Heino Mölder.** Cycle of Investigations to Improve the Efficiency and Reliability of Activated Sludge Process in Sewage Treatment Plants. 1992.
2. **Stellian Grabko.** Structure and Properties of Oil-Shale Portland Cement Concrete. 1993.
3. **Kent Arvidsson.** Analysis of Interacting Systems of Shear Walls, Coupled Shear Walls and Frames in Multi-Storey Buildings. 1996.
4. **Andrus Aavik.** Methodical Basis for the Evaluation of Pavement Structural Strength in Estonian Pavement Management System (EPMS). 2003.
5. **Priit Vilba.** Unstiffened Welded Thin-Walled Metal Girder under Uniform Loading. 2003.
6. **Irene Lill.** Evaluation of Labour Management Strategies in Construction. 2004.
7. **Juhan Idnurm.** Discrete Analysis of Cable-Supported Bridges. 2004.
8. **Arvo Iital.** Monitoring of Surface Water Quality in Small Agricultural Watersheds. Methodology and Optimization of Monitoring Network. 2005.
9. **Liis Sipelgas.** Application of Satellite Data for Monitoring the Marine Environment. 2006.
10. **Ott Koppel.** Infrastruktuuri arvestus vertikaalselt integreeritud raudtee-ettevõtja korral: hinnakujunduse aspekt (Eesti peamise raudtee-ettevõtja näitel). 2006.
11. **Targo Kalamees.** Hygrothermal Criteria for Design and Simulation of Buildings. 2006.
12. **Raido Puust.** Probabilistic Leak Detection in Pipe Networks Using the SCEM-UA Algorithm. 2007.
13. **Sergei Zub.** Combined Treatment of Sulfate-Rich Molasses Wastewater from Yeast Industry. Technology Optimization. 2007.
14. **Alvina Reihan.** Analysis of Long-Term River Runoff Trends and Climate Change Impact on Water Resources in Estonia. 2008.
15. **Ain Valdmann.** On the Coastal Zone Management of the City of Tallinn under Natural and Anthropogenic Pressure. 2008.
16. **Ira Didenkulova.** Long Wave Dynamics in the Coastal Zone. 2008.
17. **Alvar Toode.** DHW Consumption, Consumption Profiles and Their Influence on Dimensioning of a District Heating Network. 2008.
18. **Anneli Kuu.** Biological Diversity of Agricultural Soils in Estonia. 2008.
19. **Andres Tolli.** Hiina konteinerveod läbi Eesti Venemaale ja Hiinasse tagasisaadetavate tühjade konteinerite arvu vähendamise võimalused. 2008.
20. **Heiki Onton.** Investigation of the Causes of Deterioration of Old Reinforced Concrete Constructions and Possibilities of Their Restoration. 2008.

21. **Harri Moora.** Life Cycle Assessment as a Decision Support Tool for System optimisation – the Case of Waste Management in Estonia. 2009.
22. **Andres Kask.** Lithohydrodynamic Processes in the Tallinn Bay Area. 2009.
23. **Loreta Kelpšaitė.** Changing Properties of Wind Waves and Vessel Wakes on the Eastern Coast of the Baltic Sea. 2009.
24. **Dmitry Kurennoy.** Analysis of the Properties of Fast Ferry Wakes in the Context of Coastal Management. 2009.
25. **Egon Kivi.** Structural Behavior of Cable-Stayed Suspension Bridge Structure. 2009.
26. **Madis Ratassepp.** Wave Scattering at Discontinuities in Plates and Pipes. 2010.
27. **Tiia Pedusaar.** Management of Lake Ülemiste, a Drinking Water Reservoir. 2010.
28. **Karin Pachel.** Water Resources, Sustainable Use and Integrated Management in Estonia. 2010.
29. **Andrus Räämet.** Spatio-Temporal Variability of the Baltic Sea Wave Fields. 2010.
30. **Alar Just.** Structural Fire Design of Timber Frame Assemblies Insulated by Glass Wool and Covered by Gypsum Plasterboards. 2010.
31. **Toomas Liiv.** Experimental Analysis of Boundary Layer Dynamics in Plunging Breaking Wave. 2011.
32. **Martti Kiisa.** Discrete Analysis of Single-Pylon Suspension Bridges. 2011.
33. **Ivar Annus.** Development of Accelerating Pipe Flow Starting from Rest. 2011.
34. **Emlyn D.Q. Witt.** Risk Transfer and Construction Project Delivery Efficiency – Implications for Public Private Partnerships. 2012.
35. **Oxana Kurkina.** Nonlinear Dynamics of Internal Gravity Waves in Shallow Seas. 2012.
36. **Allan Hani.** Investigation of Energy Efficiency in Buildings and HVAC Systems. 2012.
37. **Tiina Hain.** Characteristics of Portland Cements for Sulfate and Weather Resistant Concrete. 2012.
38. **Dmitri Loginov.** Autonomous Design Systems (ADS) in HVAC Field. Synergetics-Based Approach. 2012.
39. **Kati Kõrbe Kaare.** Performance Measurement for the Road Network: Conceptual Approach and Technologies for Estonia. 2013.
40. **Viktoria Voronova.** Assessment of Environmental Impacts of Landfilling and Alternatives for Management of Municipal Solid Waste. 2013.
41. **Joonas Vaabel.** Hydraulic Power Capacity of Water Supply Systems. 2013.
42. **Inga Zaitseva-Pärnaste.** Wave Climate and its Decadal Changes in the Baltic Sea Derived from Visual Observations.